

Methods and Protocols
in Food Science

Springer Protocols

Hector Koolen *Editor*

Mass Spectrometry for Food Analysis

 Humana Press

METHODS AND PROTOCOLS IN FOOD SCIENCE

Series Editor
Anderson S. Sant'Ana
University of Campinas
Campinas, Brazil

For further volumes:
<http://www.springer.com/series/16556>

Methods and Protocols in Food Science series is devoted to the publication of research protocols and methodologies in all fields of food science.

Volumes and chapters will be organized by field and presented in such way that the readers will be able to reproduce the experiments in a step-by-step style. Each protocol will be characterized by a brief introductory section, followed by a short aims section, in which the precise purpose of the protocol will be clarified.

Mass Spectrometry for Food Analysis

Edited by

Hector Koolen

Amazonas State University, Manaus, Brazil

 Humana Press

Editor

Hector Koolen
Amazonas State University
Manaus, Brazil

ISSN 2662-950X ISSN 2662-9518 (electronic)
Methods and Protocols in Food Science
ISBN 978-1-0716-2106-6 ISBN 978-1-0716-2107-3 (eBook)
<https://doi.org/10.1007/978-1-0716-2107-3>

© The Editor(s) (if applicable) and The Author(s), under exclusive license to Springer Science+Business Media, LLC, part of Springer Nature 2022

This work is subject to copyright. All rights are solely and exclusively licensed by the Publisher, whether the whole or part of the material is concerned, specifically the rights of translation, reprinting, reuse of illustrations, recitation, broadcasting, reproduction on microfilms or in any other physical way, and transmission or information storage and retrieval, electronic adaptation, computer software, or by similar or dissimilar methodology now known or hereafter developed.

The use of general descriptive names, registered names, trademarks, service marks, etc. in this publication does not imply, even in the absence of a specific statement, that such names are exempt from the relevant protective laws and regulations and therefore free for general use.

The publisher, the authors and the editors are safe to assume that the advice and information in this book are believed to be true and accurate at the date of publication. Neither the publisher nor the authors or the editors give a warranty, expressed or implied, with respect to the material contained herein or for any errors or omissions that may have been made. The publisher remains neutral with regard to jurisdictional claims in published maps and institutional affiliations.

This Humana imprint is published by the registered company Springer Science+Business Media, LLC, part of Springer Nature.

The registered company address is: 1 New York Plaza, New York, NY 10004, U.S.A.

Series Preface

The *Methods and Protocols in Food Science* series is devoted to the publication of research protocols and methodologies in all fields of food science. The series is unique as it includes protocols developed, validated, and used by food and related scientists as well as theoretical bases are provided for each protocol. Aspects related to improvements, adaptations, and further developments in the protocols may also be approached.

The *Methods and Protocols in Food Science* series aims to bring the most recent developments in research protocols in the field as well as very well-established methods. As such the series targets undergraduates, graduates, and researchers in the field of food science and correlated areas. The protocols documented in the series will be highly useful for scientific inquiries in the field of food sciences, presented in such a way that the reader will be able to reproduce the experiments in a step-by-step style.

Each protocol is characterized by a brief introductory section, followed by a short aims section, in which the precise purpose of the protocol is clarified. Then, an in-depth list of materials and reagents required for employing the protocol is presented, followed by comprehensive and step-by-step procedures on how to perform that experiment. The next section brings the dos and don'ts when carrying out the protocol, followed by the main pitfalls faced and how to troubleshoot them. Finally, template results are presented and their meaning/conclusions addressed.

The *Methods and Protocols in Food Science* series will fill an important gap, addressing a common complaint of food scientists, regarding the difficulties in repeating experiments detailed in scientific papers. With this, the series has a potential to become a reference material in food science laboratories of research centers and universities throughout the world.

Campinas, Brazil

Anderson S. Sant'Ana

Preface

The analytical technique mass spectrometry (MS), since its conception and commercial availability in the early 1940s, has been applied to analyze foodstuff, especially for the identification of the chemical composition and as quality control technique. During its evolution, the technique passed through a wide range of developments in new ionization techniques, mass analyzers, detectors, hyphenation with chromatography, and data processing. The achievement of new commercially available instruments diversified the application possibilities of MS, especially in food science. Those achievements were possible due to breakthrough scientific findings, such as gas-phase studies on organic molecules of food interest, studies with metals and the first applications of laser ionizations expanded the possibilities for food science. In particular, the development of the electrospray ionization technique by John B. Fenn in the 1980s, which enabled the coupling with liquid chromatography and made possible the ionization of large molecules, was remarkable. At that time, iconically his colleagues commented that Fenn “made elephants fly,” and since then, those “elephants” have been flying, enabling the analysis of protein-rich foods. Moreover, in the last 20 years, several MS developments expanded even more the range of applications in food science with the development of ambient ionization sources and miniaturized devices, creation of orbitraps and its hybrids, coupling MS with ion mobility spectroscopy and data processing with molecular networking.

Despite being so applicable, the technique possesses a long list of instrumental arrangements and acronyms that makes the understanding in inexperienced students and scientists difficult. Moreover, sometimes, the protocols of MS applications in food analysis are not clear and/or available, thus making proper reproductions difficult. Moreover, the demand of more concise publications precludes the appointment of key procedures that are essential for a good MS reproducibility. The relevance of protocol handbooks relies on those biases, addressing questions, mainly of young students.

Therefore, the aim of this book is to summarize handful of protocols involving mass spectrometry and its associated techniques applied to food sciences and correlated areas. The handbook covers from micro- to macronutrients analysis in foods of different origin, in which several possibilities of mass spectrometry, as the sole analytical platform or as a detection mode in combination with chromatography. Part I will describe relevant protocols of consolidated mass spectrometry-related methodologies, covering direct injection, matrix-assisted laser desorption ionization (MALDI), gas chromatography (uni- and bidimensional) coupled to MS, liquid chromatography coupled to MS, and inductively coupled plasma mass spectrometry (ICP-MS). Next, the book will describe protocols with relatively new and/or emerging mass spectrometry techniques, such as paper spray mass spectrometry, traveling wave ion mobility mass spectrometry, supercritical fluid chromatography coupled to mass spectrometry, and data processing using molecular networks (Part II). All of those applied in the bioprospection search for contaminants and quality control of fruits, vegetables, animal protein, olive oil, coffee, tea, beer, milk, lactic bacteria, and emerging food ingredients (e.g., crickets).

My ambition is to offer the readers not only a comprehensive and updated collection of state-the-of-art methodologies and models for food analysis, but also to encourage more people to use any kind of mass spectrometry technique to tackle questions in food science and/or related to this field.

Manaus, Brazil

Hector Koolen

Contents

<i>Series Preface</i>	<i>v</i>
<i>Preface</i>	<i>vii</i>
<i>Contributors</i>	<i>xiii</i>

PART I CONSOLIDATED MS-BASED TECHNIQUES

1 Mass Fingerprinting for High-Throughput Analyses of Food: Authentication and Quality Control	3
<i>Tzitziki González-Rodríguez, Héctor A. Peniche-Pavía, Jhonathan Pazmiño-Arteaga, and Robert Winkler</i>	
2 MALDI-MS Application for Food Control	17
<i>Igor Pereira, Bijay Banstola, Kelin Wang, Fabrizio Donnarumma, Kermit K. Murray, and Boniek Gontijo Vaz</i>	
3 MALDI-TOF-Mass Spectrometry: Sample Preparation Protocols for Meat and Milk Products	23
<i>Jörg Rau, Martin Dyk, Olivera Wenninger, and Ekkehard Hiller</i>	
4 Comprehensive Identification of Plant Polyphenols by LC-MS	31
<i>Álvaro Fernández-Ochoa, María de la Luz Cádiz-Gurrea, and Antonio Segura Carretero</i>	
5 Quantitative Determination of Antioxidant Compounds in Fruits Using Liquid Chromatography Tandem Mass Spectrometry	43
<i>Giovana Anceski Bataglioni</i>	
6 Development of an Ultraperformance Liquid Chromatography-Mass Spectrometry Method to Determine Sterols in Olive Oils	61
<i>María Jesús Lerma-García, Miriam Beneito-Cambra, Ernesto Francisco Simó-Alfonso, and José Manuel Herrero-Martínez</i>	
7 A Workflow for Lipid Annotation in Coffee Samples by Liquid Chromatography-Mass Spectrometry	71
<i>Ana Carolina R. Silva, Rafael Garrett, and Claudia M. Rezende</i>	
8 A Novel HPLC-Based Method with LC-Electrospray MS for Analysis of Polyethylene Glycol in Various Foods	89
<i>Jubee Park and Chan Lee</i>	
9 Application of UHPLC-HRMS/MS for the Analysis of Beta-Casomorphin 5 and 7 in Milk	109
<i>Duc Doan Nguyen, Francesco Buseti, and Stuart Keith Johnson</i>	
10 Identification of Oligopeptides by Ultra-High-Pressure Liquid Chromatography Coupled with Quadrupole-Orbitrap Ultra-High-Resolution Mass Spectrometry	121
<i>Mingjie Chen, Feng Zhao, and Naixing Ye</i>	

11	Database Construction Strategies for Proteome Measurement of Novel Food Ingredients	133
	<i>Sophia Escobar-Correas, Utpal Bose, James A. Broadbent, Angéla Jubász, and Michelle L. Colgrave</i>	
12	Lipidomics Study of Fishes Using Hydrophilic Interaction Chromatography and Mass Spectrometry	145
	<i>Qing Shen, Xina Yu, Pei Luo, Pingya Wang, Qiaoling Zhao, Jie Liao, and Xiaofang Zhu</i>	
13	Detection of Aroma Compounds in Food by Gas Chromatography-Mass Spectrometry/Olfactometry	157
	<i>Nina Buck, Bianca Lok, and Philipp Denk</i>	
14	Solid-Phase Microextraction and Comprehensive Two-Dimensional Gas Chromatography for Food Analysis	173
	<i>Andre Cunha Paiva, Juliana Crucello, Victor Hugo Cavalcanti Ferreira, and Leandro Wang Hantao</i>	
15	Identification of Lactic Acid Bacteria in Food Matrices by High-Resolution Nano-LC-ESI MS/MS	193
	<i>Mariangela Valletta, Angela Chambery, and Rosita Russo</i>	

PART II EMERGING MS-BASED TECHNIQUES

16	Acetylcholinesterase (ACHE) and α -Glucosidase Inhibitory Assay by Effect-Directed Analysis on High Performance Thin-Layer Chromatography Coupled to Mass Spectrometry	213
	<i>Mario Aranda, Jonathan Carrasco, and Karem Henríquez</i>	
17	Application of Paper Spray Ionization for Preliminary Amazonian Berry Fruits Components Identification	219
	<i>Luiz Paulo Moraes de Oliveira, Débora de Sena Raposo, Luciana dos Santos Ipiranga Rodrigues, Silvio Oliveira Assunção Junior, Francinaldo Araujo da Silva-Filho, Bruna Ribeiro de Lima, Emmanoel Vilaça Costa, Afonso Duarte Leão de Souza, Hector Henrique Ferreira Koolen, and Felipe Moura Araujo da Silva</i>	
18	Analysis of Food Components by MALDI Imaging Mass Spectrometry: Sample Preparation for Identification of Peptides in Dry-Cured Ham	225
	<i>Dina Rešetar Maslov</i>	
19	Modern Tools in Food Chemical Characterization Using Mass Spectrometry Data and Molecular Networking: Revisiting the Study Case of Solanaceae Family	245
	<i>Celio Fernando Figueiredo Angolini and Ana Paula Aparecida Pereira</i>	
20	Traveling Wave Ion Mobility-Mass Spectrometry to Address Chemical Food Safety Issues	259
	<i>Maykel Hernández-Mesa, Gaud Dervilly, and Bruno Le Bizec</i>	
21	Determination Method of Acrylamide in Beverages and Foods by Supercritical Fluid Chromatography/Tandem Mass Spectrometry	281
	<i>Tosbiaki Yoshioka, Yoshihiro Izumi, and Takeshi Bamba</i>	

22 Application of Bubbling Extraction Coupled to Gas Chromatography Mass Spectrometry in Food Analysis 293
Yuanji Gao, Lei He, Lijuan Zhao, and Quan He

23 Aroma Analysis by Proton Transfer Reaction-Mass Spectrometry 307
Jonathan Beauchamp, Franco Biasioli, and Patrick Silcock

Index 321

Contributors

- CELIO FERNANDO FIGUEIREDO ANGOLINI • *Center for Natural and Human Sciences, University of ABC (UFABC), Santo André, Brazil*
- MARIO ARANDA • *Laboratorio de Investigación en Fármacos y Alimentos, Departamento de Farmacia, Facultad de Química y de Farmacia, Pontificia Universidad Católica de Chile, Santiago, Chile*
- SILVIO OLIVEIRA ASSUNÇÃO JUNIOR • *Metabolomics and Mass Spectrometry Research Group, Superior School of Health Sciences, University of the State of Amazonas, Manaus, Brazil*
- TAKESHI BAMBA • *Division of Metabolomics, Medical Institute of Bioregulation, Kyushu University, Fukuoka, Japan*
- BIJAY BANSTOLA • *Department of Chemistry, Louisiana State University, Baton Rouge, LA, USA*
- GIOVANA ANCESKI BATAGLION • *Department of Chemistry, Federal University of Amazonas, Manaus, Brazil*
- JONATHAN BEAUCHAMP • *Department of Sensory Analytics and Technologies, Fraunhofer Institute for Process Engineering and Packaging IVV, Freising, Germany*
- MIRIAM BENEITO-CAMBRA • *Department of Analytical Chemistry, Faculty of Chemistry, University of Valencia, Burjassot, Spain*
- FRANCO BIASIOLI • *Sensory Quality Unit, Edmund Mach Foundation, San Michele all'Adige, Italy*
- UTPAL BOSE • *CSIRO Agriculture and Food, St Lucia, QLD, Australia; Australian Research Council Centre of Excellence for Innovations in Peptide and Protein Science, School of Science, Edith Cowan University, Joondalup, WA, Australia*
- JAMES A. BROADBENT • *CSIRO Agriculture and Food, St Lucia, QLD, Australia*
- NINA BUCK • *Department of Sensory Analytics and Technologies, Fraunhofer Institute for Process Engineering and Packaging IVV, Freising, Germany; Department of Chemistry and Pharmacy, Friedrich-Alexander-Universität Erlangen-Nürnberg, Erlangen, Germany*
- FRANCESCO BUSETTI • *ChemCentre of WA, Perth, WA, Australia*
- JONATHAN CARRASCO • *Laboratorio de Investigación en Fármacos y Alimentos, Departamento de Farmacia, Facultad de Química y de Farmacia, Pontificia Universidad Católica de Chile, Santiago, Chile*
- ANGELA CHAMBERY • *Department of Environmental, Biological and Pharmaceutical Sciences and Technologies, University of Campania "Luigi Vanvitelli", Caserta, Italy*
- MINGJIE CHEN • *College of Life Sciences, Henan Key Laboratory of Tea Plant Biology, Xinyang Normal University, Xinyang, Henan, People's Republic of China*
- MICHELLE L. COLGRAVE • *CSIRO Agriculture and Food, St Lucia, QLD, Australia; Australian Research Council Centre of Excellence for Innovations in Peptide and Protein Science, School of Science, Edith Cowan University, Joondalup, WA, Australia*
- EMMANOEL VILAÇA COSTA • *Department of Chemistry, Federal University of Amazonas, Manaus, Brazil*
- JULIANA CRUCELLO • *Institute of Chemistry, University of Campinas, Campinas, Brazil*
- FELIPE MOURA ARAUJO DA SILVA • *Analytical Center, Multidisciplinary Support Center, Federal University of Amazonas, Manaus, Brazil*

- FRANCINALDO ARAUJO DA SILVA-FILHO • *Analytical Center, Multidisciplinary Support Center, Federal University of Amazonas, Manaus, Brazil*
- MARÍA DE LA LUZ CÁDIZ-GURREA • *Department of Analytical Chemistry, Faculty of Sciences, University of Granada, Granada, Spain; Research and Development of Functional Food Centre (CIDAF), Health Science Technological Park, Granada, Spain*
- BRUNA RIBEIRO DE LIMA • *Analytical Center, Multidisciplinary Support Center, Federal University of Amazonas, Manaus, Brazil*
- PHILIPP DENK • *Department of Sensory Analytics and Technologies, Fraunhofer Institute for Process Engineering and Packaging IVV, Freising, Germany*
- LUIZ PAULO MORAIS DE OLIVEIRA • *Analytical Center, Multidisciplinary Support Center, Federal University of Amazonas, Manaus, Brazil*
- GAUD DERVILLY • *LABERCA, Oniris, INRAE, Nantes, France*
- DÉBORA DE SENA RAPOSO • *Metabolomics and Mass Spectrometry Research Group, Superior School of Health Sciences, University of the State of Amazonas, Manaus, Brazil*
- AFONSO DUARTE LEÃO DE SOUZA • *Department of Chemistry, Federal University of Amazonas, Manaus, Brazil*
- FABRIZIO DONNARUMMA • *Department of Chemistry, Louisiana State University, Baton Rouge, LA, USA*
- LUCIANA DOS SANTOS IPIRANGA RODRIGUES • *Metabolomics and Mass Spectrometry Research Group, Superior School of Health Sciences, University of the State of Amazonas, Manaus, Brazil*
- MARTIN DYK • *Chemical and Veterinary Analysis Agency Stuttgart (CVUAS), Fellbach, Germany*
- SOPHIA ESCOBAR-CORREAS • *CSIRO Agriculture and Food, St Lucia, QLD, Australia; Australian Research Council Centre of Excellence for Innovations in Peptide and Protein Science, School of Science, Edith Cowan University, Joondalup, WA, Australia*
- ÁLVARO FERNÁNDEZ-OCHOA • *Department of Analytical Chemistry, Faculty of Sciences, University of Granada, Granada, Spain; Max Delbrück Center for Molecular Medicine in the Helmholtz Association (MDC), Berlin, Germany; Berlin Institute of Health Metabolomics Platform at the Charite, Berlin, Germany*
- YUANJI GAO • *College of Chemistry and Materials Science, Sichuan Normal University, Chengdu, People's Republic of China*
- RAFAEL GARRETT • *Metabolomics Laboratory (LabMeta-LADETEC), Institute of Chemistry, Federal University of Rio de Janeiro, Rio de Janeiro, Brazil*
- TZITZIKI GONZÁLEZ-RODRÍGUEZ • *Department of Biotechnology and Biochemistry, Center for Research and Advanced Studies (CINVESTAV), Irapuato, Mexico*
- LEANDRO WANG HANTAO • *Institute of Chemistry, University of Campinas, Campinas, Brazil*
- LEI HE • *College of Chemistry and Materials Science, Sichuan Normal University, Chengdu, People's Republic of China*
- KAREM HENRÍQUEZ • *Laboratorio de Biotecnología y Genética de Alimentos, Departamento de Ciencia y Tecnología de los Alimentos, Facultad de Farmacia, Universidad de Concepción, Concepción, Chile*
- QUAN HE • *Department of Chemistry, Zhejiang University, Hangzhou, People's Republic of China*
- MAYKEL HERNÁNDEZ-MESA • *Department of Analytical Chemistry, Faculty of Sciences, University of Granada, Granada, Spain; Laboratory for the Study of Residues and Contaminants in Foods (LABERCA), ONIRIS, Nantes, France*

- JOSÉ MANUEL HERRERO-MARTÍNEZ • *Department of Analytical Chemistry, Faculty of Chemistry, University of Valencia, Burjassot, Spain*
- EKKEHARD HILLER • *Chemical and Veterinary Analysis Agency Stuttgart (CVUAS), Fellbach, Germany*
- VICTOR HUGO CAVALCANTI FERREIRA • *Institute of Chemistry, University of Campinas, Campinas, Brazil*
- YOSHIHIRO IZUMI • *Division of Metabolomics, Medical Institute of Bioregulation, Kyushu University, Fukuoka, Japan*
- STUART KEITH JOHNSON • *School of Molecular and Life Sciences, Faculty of Science and Engineering, Curtin University, Perth, WA, Australia*
- ANGÉLA JUHÁSZ • *Australian Research Council Centre of Excellence for Innovations in Peptide and Protein Science, School of Science, Edith Cowan University, Joondalup, WA, Australia*
- HECTOR HENRIQUE FERREIRA KOOLEN • *Metabolomics and Mass Spectrometry Research Group, Superior School of Health Sciences, University of the State of Amazonas, Manaus, Brazil*
- BRUNO LE BIZEC • *LABERCA, Oniris, INRAE, Nantes, France*
- CHAN LEE • *Department of Food Science and Technology, Chung-Ang University, Anseong, Republic of Korea*
- MARÍA JESÚS LERMA-GARCÍA • *Department of Analytical Chemistry, Faculty of Chemistry, University of Valencia, Burjassot, Spain*
- JIE LIAO • *Zhejiang Huacai Testing Technology Co., Ltd., Shaoxing, China*
- BIANCA LOK • *Department of Sensory Analytics and Technologies, Fraunhofer Institute for Process Engineering and Packaging IVV, Freising, Germany; Department of Chemistry and Pharmacy, Friedrich-Alexander-Universität Erlangen-Nürnberg, Erlangen, Germany*
- PEI LUO • *State Key Laboratories for Quality Research in Chinese Medicines, Faculty of Pharmacy, Macau University of Science and Technology, Macau, People's Republic of China*
- DINA REŠETAR MASLOV • *Laboratory of Proteomics, Internal Diseases Clinic, Faculty of Veterinary Medicine, University of Zagreb, Zagreb, Croatia*
- KERMIT K. MURRAY • *Department of Chemistry, Louisiana State University, Baton Rouge, LA, USA*
- DUC DOAN NGUYEN • *Faculty of Food Science and Technology, Vietnam National University of Agriculture, Trau Quy, Hanoi, Vietnam*
- ANDRÉ CUNHA PAIVA • *Institute of Chemistry, University of Campinas, Campinas, Brazil*
- JUHEE PARK • *Department of Food Science and Technology, Chung-Ang University, Anseong, Republic of Korea*
- JHONATHAN PAZMIÑO-ARTEAGA • *Group of Drug Stability, Cosmetics and Food Analysis, University of Antioquia, Medellín, Colombia; La Salada Research Group, SENA National Apprenticeship Service, Caldas, Antioquia, Colombia*
- HÉCTOR A. PENICHE-PAVÍA • *Department of Biotechnology and Biochemistry, Center for Research and Advanced Studies (CINVESTAV), Irapuato, Mexico*
- ANA PAULA APARECIDA PEREIRA • *Department of Food and Nutrition, Faculty of Nutrition, Federal University of Mato Grosso, Cuiabá, Brazil*
- IGOR PEREIRA • *Institute of Chemistry, Federal University of Goiás, Goiânia, Brazil; Department of Chemistry, Louisiana State University, Baton Rouge, LA, USA*
- JÖRG RAU • *Chemical and Veterinary Analysis Agency Stuttgart (CVUAS), Fellbach, Germany*

- CLAUDIA M. REZENDE • *Aroma Analysis Laboratory, Institute of Chemistry, Federal University of Rio de Janeiro, Rio de Janeiro, Brazil*
- ROSITA RUSSO • *Department of Environmental, Biological and Pharmaceutical Sciences and Technologies, University of Campania “Luigi Vanvitelli”, Caserta, Italy*
- ANTONIO SEGURA CARRETERO • *Department of Analytical Chemistry, Faculty of Sciences, University of Granada, Granada, Spain; Research and Development of Functional Food Centre (CIDAF), Health Science Technological Park, Granada, Spain*
- QING SHEN • *Collaborative Innovation Center of Seafood Deep Processing, Zhejiang Province Joint Key Laboratory of Aquatic Products Processing, Institute of Seafood, Zhejiang Gongshang University, Hangzhou, People’s Republic of China; State Key Laboratories for Quality Research in Chinese Medicines, Faculty of Pharmacy, Macau University of Science and Technology, Macau, People’s Republic of China*
- PATRICK SILCOCK • *Department of Food Science, University of Otago, Dunedin, New Zealand*
- ANA CAROLINA R. SILVA • *Aroma Analysis Laboratory, Institute of Chemistry, Federal University of Rio de Janeiro, Rio de Janeiro, Brazil; Metabolomics Laboratory (LabMeta-LADETEC), Institute of Chemistry, Federal University of Rio de Janeiro, Rio de Janeiro, Brazil*
- ERNESTO FRANCISCO SIMÓ-ALFONSO • *Department of Analytical Chemistry, Faculty of Chemistry, University of Valencia, Burjassot, Spain*
- MARIANGELA VALLETTA • *Department of Environmental, Biological and Pharmaceutical Sciences and Technologies, University of Campania “Luigi Vanvitelli”, Caserta, Italy*
- BONIEK GONTIJO VAZ • *Institute of Chemistry, Federal University of Goiás, Goiânia, Brazil*
- KELIN WANG • *Department of Chemistry, Louisiana State University, Baton Rouge, LA, USA*
- PINGYA WANG • *Zhoushan Institute for Food and Drug Control, Zhoushan, China*
- OLIVERA WENNINGER • *Chemical and Veterinary Analysis Agency Stuttgart (CVUAS), Fellbach, Germany*
- ROBERT WINKLER • *Department of Biotechnology and Biochemistry, and UGA-Langebio, Center for Research and Advanced Studies (CINVESTAV), Irapuato, Mexico*
- NAIXING YE • *College of Horticulture, Fujian Agriculture and Forestry University, Fuzhou, People’s Republic of China*
- TOSHIAKI YOSHIOKA • *Analytical Science Laboratories, Asahi Quality & Innovations, LTD., Moriya, Japan*
- XINA YU • *Collaborative Innovation Center of Seafood Deep Processing, Zhejiang Province Joint Key Laboratory of Aquatic Products Processing, Institute of Seafood, Zhejiang Gongshang University, Hangzhou, People’s Republic of China*
- FENG ZHAO • *College of Pharmacy, Fujian University of Traditional Chinese Medicine, Fuzhou, People’s Republic of China*
- LIJUAN ZHAO • *College of Chemistry and Materials Science, Sichuan Normal University, Chengdu, People’s Republic of China*
- QIAOLING ZHAO • *Zhoushan Institute for Food and Drug Control, Zhoushan, China*
- XIAOFANG ZHU • *Shaoxing Shanzhou Testing Technology Co., Ltd., Shaoxing, China*

Part I

Consolidated MS-Based Techniques



Chapter 1

Mass Fingerprinting for High-Throughput Analyses of Food: Authentication and Quality Control

Tzitziki González-Rodríguez, Héctor A. Peniche-Pavía,
Jhonathan Pazmiño-Arteaga, and Robert Winkler

Abstract

Mass fingerprinting is a fast and straightforward approach for analyzing the chemical composition of biological materials. This chapter details how to generate mass fingerprints from diverse food sources, from the extraction of metabolites to data analysis, using different mass spectrometry (MS) methods. We cover four high-throughput ionization techniques for MS: Direct liquid-introduction electrospray ionization (DLI-ESI), low-temperature plasma (LTP) ionization, matrix-assisted laser desorption/ionization time-of-flight (MALDI-ToF), and leaf spray (LS). Further, we describe data visualization with clustering methods and data mining.

Key words Chemical profiles, Mass fingerprinting, Direct analysis, Clustering, Classification, Data mining

1 Introduction

Mass spectrometry (MS) provides information about the chemical composition of complex samples and is therefore widely used in food analysis. Typical MS applications include the trace analysis for agrochemicals and contaminants [1, 2] and the determination of macronutrients and nutraceutical compounds [3, 4]. Recently, consumers also demonstrate increased awareness of additional criteria such as authenticity and sustainability of products, which also can be addressed with MS strategies [5–7].

Conventional food analysis with MS uses gas or liquid chromatography for reducing the complexity of mixtures [5, 7, 8]. In contrast, direct and ambient ionization methods skip this pre-separation step [9, 10]. Mass fingerprinting (MSF) has lower analytical performance than chromatography-based methods because of ion suppression and overlapping signals [8, 11]. But sample handling and manipulation steps are reduced, which results

in a drastically increased sample throughput [12–14]. MSF spectra contain more information than MS spectra after chromatographic separation [15].

High-resolution mass analyzers and fragmentation studies distinguish compounds with similar masses in MSF [16, 17]. Further, adequate data processing workflows excavate relevant data from noisy data sets and make MSF a valuable sample classification tool [8, 18].

In this chapter, we present four MSF methods:

1. In direct liquid-introduction electrospray ionization (DLI-ESI) MS, extracted samples are introduced directly to the mass spectrometer after minimum preparation [14, 15]. The soft ionization technique is suitable for polar metabolites and multiply charged proteins that are in the range of 50–2000 m/z [19, 20], mainly reporting protonated molecules $[M + H]^+$ and adducts $[M + X]^+$ in positive mode, and de-protonated molecules $[M - H]^-$ in negative mode [21].
2. Low-temperature plasma (LTP) is an ambient ionization method for the direct analysis of solid, liquid, and gaseous samples without any pre-treatment [9]. Different degrees of ionization and fragmentations are possible depending on the used discharge gas and operating parameters [22]. Compared to ESI, less polar compounds are detectable, and the molecular weight range is reduced ($<500 m/z$) [12, 13]. LTP MS is a fast method (~ 20 s per sample) and ideal for high-throughput screening.
3. Matrix-assisted laser desorption/ionization time-of-flight (MALDI-ToF) MS instruments are popular for their fast analysis of solid samples and high analytical resolution in a broad weight range (from 200 to several KDa) [23]. Besides whole proteins and peptides, hydrophobic compounds such as lipids can also be measured [24, 25]. The detectable molecule classes and the analytical parameters depend strongly on the sample preparation, which requires the co-crystallization with a chemical matrix [26].
4. Leaf spray (LS) is one of the most recent ambient MS applications. A high electrical potential is applied directly to a leaf or another plant tissue. Its endogenous sap generates an electrospray-like ionization that can be introduced into the mass spectrometer [27]. LS allows real-time studies of a living organism's chemical profile with multiple applications such as detection of agrochemical residues in vegetables and fruits [28, 29] and determination of poisonous compounds [30].

Interpretation and visualization of data are fundamental for every mass spectrometry experiment. This task is often the most time-consuming step and critical for the interpretation of the

results. This area's advance is pushed forward by an active community developing open-source software tools and workflows for MS data analysis [31].

Here, we explain how to process mass spectra for producing plots that visualize differences between sample groups. We demonstrate the visualization and comparison of MSF data sets with hierarchical cluster analysis (HCA), principal component analysis (PCA), and the building of predictive classification models with the Random Forest algorithm.

2 Materials

2.1 Biological Material

Here, we explain in detail how to generate metabolite fingerprints from different biological sources and MS platforms:

1. For Subheading 3.1, we utilized lyophilized maize leaves (*see* Notes 1 and 2).
2. For Subheading 3.2, we employed liquor samples (tequila and mezcal) and fresh jalapeño chilies for in vivo experiments.
3. For Subheading 3.3, we used unroasted coffee beans.
4. For Subheading 3.4, we used fresh maize leaves.

2.2 DLI-ESI MS

2.2.1 Sample Preparation

1. Methanol, HPLC grade (Sigma-Aldrich, St. Louis, MO, US).
2. Ultrapure water (Water system Milli-Q[®] Q-Gard 1, Merck, Darmstadt, DE).
3. Formic acid (Fermont, Monterrey, MX).
4. 2.0 mL polypropylene microtubes (Eppendorf[®], Hamburg, DE).
5. 0.2 μm nylon membrane filters (MilliporeSigma[™], Burlington, MA, US).
6. Pipettes and proper tips for handling organic solvents.
7. Equipment:
 - Mixer mill (Model MM 301, Retsch GmbH, DE).
 - Vortex (Model G560, Scientific Industries Inc., US).
 - Ultrasonic bath (Model 1510, 80W, Branson, Danbury, CT, US).
 - Centrifuge (Model 5427R, Eppendorf[®], Hamburg, DE).

2.2.2 Mass Analyzer

1. LCQ-Fleet ion trap MS (Thermo Scientific, Waltham, MA, US).
2. Installation for mass spectrometer:
 - Single syringe pump, Fisherbrand[™] (Fisher Scientific, Waltham, MA, US).

- Nitrogen gas generator (Peak Scientific, Glasgow, UK).
- UPS Security Plus (Powervar™, Waukegan, IL, US).
- SV40 BI oil-sealed pump (SOGEVAC®, Leybold, Export, PA, US).

2.3 LTP MS

2.3.1 Sample Preparation

1. Scalpel.
2. Microscope slide and adhesive tape.
3. 2.0 mL HPLC glass vials (Waters™, Milford, MA, US).

2.3.2 Desorption/Ionization Probe

1. 3D-printed LTP ionization probe [32].
2. AIMS power supply (Kuturabi SA de CV, Irapuato, MX).
3. Optional (for improving the desorption): Continuous wave (CW) UV laser, 405 nm (Fermion III Series, Micro Laser Systems Inc.), and plano-convex lens (Edmund Optics, NJ, US) for focusing [33].
4. Helium gas (technical grade) supply, with flow regulator (Swagelok, OH, USA).

2.3.3 Sampling Platform

1. Open LabBot for sample movement and mounting the UV laser, a lens holder, and the LTP probe [34].

2.3.4 Mass Analyzer

1. LCQ-Fleet ion trap MS with ambient adaptation (Thermo Scientific, Waltham, MA, US).

2.4 MALDI-ToF MS

2.4.1 Sample and Matrix Preparation

1. n-Hexane (EMSURE®, Merk).
2. Benzine (Petroleum ether 35–60 °C; JT Baker®).
3. Chloroform (EMPARTA®, Merk).
4. Methanol, HPLC grade (Sigma-Aldrich, St. Louis, MO, US).
5. 2,5-dihydroxybenzoic acid (Supelco®, St. Louis, MO, US).
6. Acetonitrile (LiChrosolv®, Merk).
7. 2.0 mL HPLC glass vials (Waters, Milford, MA, US).
8. 5 mL polypropylene tubes (Eppendorf®, Hamburg, DE).
9. Pipettes and tips proper for handling organic solvents.
10. 0.2 µm nylon membrane filters (MilliporeSigma™, Burlington, MA, US).
11. Nitrogen gas (Grade 5.0).
12. Stainless steel MALDI sample plates (Bruker Daltonics, Bremen, Germany).

2.4.2 Mass Analyzer

1. Autoflex III smartbeam MALDI-ToF MS (Bruker Daltonics, Bremen, Germany).

2.5 Leaf Spray MS

2.5.1 Sample Preparation

1. Scalpel or scissors (*see Note 11*).
2. Methanol, HPLC grade (Sigma-Aldrich, St. Louis, MO, US).
3. Pipettes and proper tips for handling organic solvents.

2.5.2 Sampling Platform

1. Laboratory stand.
2. Alligator clips.
3. AIMS power supply (Kuturabi SA de CV, Irapuato, MX).

2.5.3 Mass Analyzer

1. LCQ-Fleet ion trap MS with ambient adaptation (Thermo Scientific, Waltham, MA, US).

3 Methods

3.1 DLI-ESI MS

3.1.1 Sample Preparation

1. Prepare the extraction solvent: dissolve pure methanol with ultrapure water (80:20 *v/v*) containing 0.1% formic acid. Calculate and prepare enough solution for the extraction of all samples.
2. Grind the lyophilized tissue to homogeneity. For this step, we recommend ball milling. A very fine powder with the lowest amount of water is critical to have an optimum extraction.
3. Weigh 10 mg of ground material into a 2 mL microtube. It is essential to use high-quality polypropylene tubes because some solvents can dissolve plastics and contaminate the sample and the mass spectrometer.

3.1.2 Metabolite Extraction

1. Add 1 mL of extraction solvent to the tube with the biological material (ensure its correct labeling). Close the tubes, ensuring that no evaporation will take place during extraction.
2. After adding the solvent, mix them thoroughly in a Vortex mixer.
3. Place the tubes in an ultrasonic bath at maximum frequency for 15 min at 10 °C.
4. Centrifuge at 4 °C and $10,000 \times g$ for 10 min.
5. Filter with 0.2 μm pore size filters. Extracts can be kept at -20 °C for less than 24 h.

3.1.3 Analytical Procedure

1. There are two options for injecting the extracts directly into the ESI probe: an external syringe pump [14] or an autosampler (*see Note 4*) [13].
2. Here, we explain using an external syringe pump for direct injection to an LCQ-Fleet ion trap mass spectrometer.
3. Open Thermo Tune Plus for LCQ control (Xcalibur™ 3.0 Qual Browser).

4. Set the following parameters: capillary temperature 280 °C, tube lens 115 V, capillary, and spray voltage to 3 V and 4.5 V, respectively.
5. Set the flow rate to 10 $\mu\text{L}/\text{min}^{-1}$.
6. Acquire the mass spectra in the positive mode in a range of 100–1250 m/z after the signal stabilization.
7. Use extraction solvent as the blank solution to acquire the reference mass spectrum.

3.2 LTP MS

3.2.1 Sample

Preparation: Solids

1. Cut material with a scalpel to prepare a coarse mixture.
2. Put the sample on the microscope glass slide.

3.2.2 Sample

Preparation: Liquids

1. Liquid samples such as liquors do not need any preparation. The samples are filled into a glass vial and placed directly in front of the LTP probe (*see Note 6*).

3.2.3 Analytical

Procedure

1. Mount the 3D-LTP probe at an angle of 45° to the sample surface.
2. Mount the laser at an angle of 90° to the sample surface; focus the laser.
3. Set the helium flow for the LTP probe to 0.1 L/min.
4. Set the LTP probe's power supply to a voltage of 7 kV and a frequency of 10 kHz.
5. For MS, select positive ion mode for an m/z range of 50–500.
6. Set the capillary temperature set to 200 °C, and the capillary voltage set to 55 V.
7. Set the tube lens voltage set to 25 V.
8. Spectra are acquired in a full scan and continuous mode.
9. Food samples can be attached directly to a glass slide using double-sided adhesive tape.

3.3 MALDI-ToF MS

3.3.1 Sample Extraction

1. Freeze the green coffee beans with liquid nitrogen for 5 min.
2. Grind coffee beans in a mixer mill to a fine powder.
3. Weight 2 g of the powder in a polypropylene tube.
4. Add 5 mL of 1:1 (v/v) hexane/benzine solution.
5. Mix on a Vortex for 5 min.
6. Transfer the tube to an ultrasound sonication bath (frequency 40 kHz; 80 W) for 30 min at 10 °C.
7. Filter the extract through the membrane filters.
8. Transfer the filtrate to a glass vial of known weight.

9. Remove the solvent by drying with nitrogen gas.
10. Determine the quantity of coffee oil.

3.3.2 Sample and Matrix Preparation

1. Transfer 10 mg of coffee oil into a 10 mL volumetric flask.
2. Dissolve with chloroform/methanol 2:1 (*v/v*). 3b. For the MALDI matrix, dissolve 200 mg of 2,5-dihydroxybenzoic acid in 10 mL of acetonitrile.

3.3.3 Analytical Procedure

1. Mix the green coffee oil solution and MALDI matrix in a ratio of 1:1.
2. Place 1.0 μL of the mixture on a sample plate made of polished steel using a dried droplet method.
3. Set the following settings: 337 nm nitrogen laser, an acceleration voltage of 20 kV in positive mode.
4. Acquired spectra in reflectron mode within a mass range of 550–1600 *m/z*. Use five single laser shots per sample.
5. For more details, go to [25] and *see* **Note 8**.

3.4 Leaf Spray MS

3.4.1 Sample Preparation

1. Cut the leaf or plant tissue into an isosceles triangle shape (*see* **Note 11**).

3.4.2 Analytical Procedure

1. Place the sample into the alligator clip and mount it on the laboratory holder.
2. Adjust the stand arm and the alligator clip to position the tissue in line with the MS inlet, approximately 5–10 mm (*see* **Note 12**).
3. Turn on the mass analyzer in collection data mode (before applying high voltage).
4. Power on the AIMS power supply and optimize the voltage for the best ionization (4–6 kV).
5. Add methanol directly to the leaf if needed (*see* **Note 13**).
6. Acquire data when the signal stabilizes.

3.5 Data Analysis

The example data set was generated from maize leaves extracts, analyzed by DLI-ESI MS. The data set and R script for data processing and statistical analysis are available from https://github.com/tzi-ki/maize_data.

3.5.1 Mass Spectra Visualization

1. Download the data set [35].
2. Convert the raw data files to the HUPO standard .mzML using the ProteoWizard MS Convert Tool: <http://proteowizard.sourceforge.net/download.html> [36]. In this example, the data set is already in the proper format.

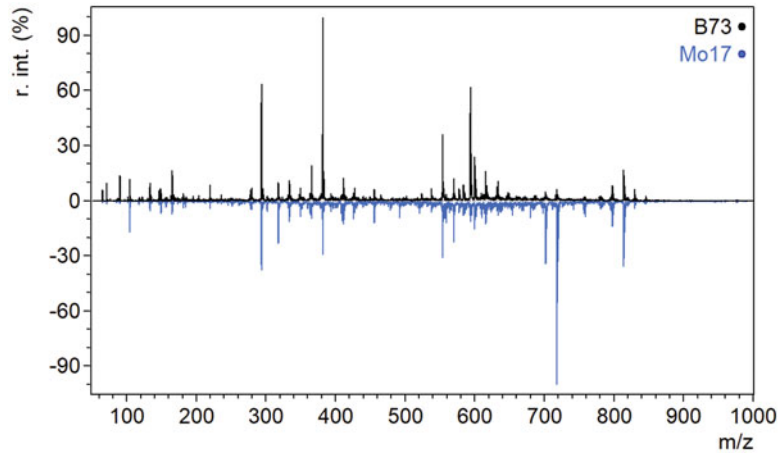


Fig. 1 Comparison of mass spectra of maize leaf extracts acquired with DLI-ESI MS. The maize inbred lines B73 (top, black) and Mo17 (bottom, blue) show clear differences in their mass fingerprints

3. To visualize and compare mass spectra from different samples, download and execute mMass (<http://www.mmass.org>) [37].
4. Select a file: File> Open> B73_L(1).mzML> Open.
5. Select all scans and click Open selected.
6. To sum up, all scans, go to Processing> Math Operations> Sum all visible> Apply.
7. Right-click the Combined spectra (in the left panel) and customize (color, name, etc.).
8. Repeat previous steps for another sample (e.g., Mo17_L(1).mzML).
9. Right-click the last combined spectra and select Flip Spectrum (Fig. 1).

3.5.2 Data Pre-processing

1. Open the script MSF_DataAnalysis (https://github.com/tziki/maize_data/blob/master/MSF_DataAnalysis.md).
2. Follow the instructions outlined in it:
3. Set the working directory in the R environment to the data location.
4. Install the R packages needed for MS analysis: MALDIquant and MALDIquantForeign [18, 38].
5. Import the .mzML data into the R workspace.
6. Sum scans for each independent spectrum.
7. Calibrate and normalize intensity using the total ion current (TIC).
8. Estimate the signal-to-noise ratio and detect peaks from the spectra.

9. Pick and bin peaks.
10. Generate the feature matrix with the complete m/z and intensity values.
11. Export the feature matrix for subsequent statistical analysis.

3.5.3 Statistical Analysis and Visualization

Heatmap and Hierarchical Clustering Analysis (HCA)

1. Install the R packages pheatmap and factoextra.
2. Execute the function pheatmap to visualize the default heatmap.
3. Optimize parameters for visualization (e.g., color key, size of letters).
4. Set the matrix distance and the linkage method for hierarchical clustering analysis (HCA) (*see Note 9*).
5. Optional: See Subheading 4.4.3 to learn how to select the most important variables.
6. Plot the heatmap (Fig. 2).

Principal Component Analysis

1. Use k -means to define the interest clusters, $k = 2$ groups (centers argument).
2. Create the PCA object using the feature matrix.
3. Plot the PCA to visualize your clusters in two dimensions (Fig. 3).

3.5.4 Data Mining: Random Forest

1. Install the R package rattle [39].
2. Open the GUI typing rattle() into the R command line.
3. Import the feature matrix generated in Subheading 3.5.2, using the R data option within the Data tab. Click Execute to load your data set. In the provided script, this R data is named IonFrame.
4. Click the Model tab and select Forest. Click Execute to build a Random Forest model. For identifying the features with predictive power for sample classification, generate a random forest model with 500 tree decisions or more. The algorithm ranks the most important variables for classification based on the mean decrease Gini index.

4 Notes

1. Freshly harvested plant tissue should be rapidly submerged into liquid nitrogen to stop the metabolism.
2. For further recommendations for growing plant material, harvest, and sampling storage, *see* reference [40].
3. For exploratory non-targeted metabolomics, we recommend beginning with pure methanol or methanol/water solutions

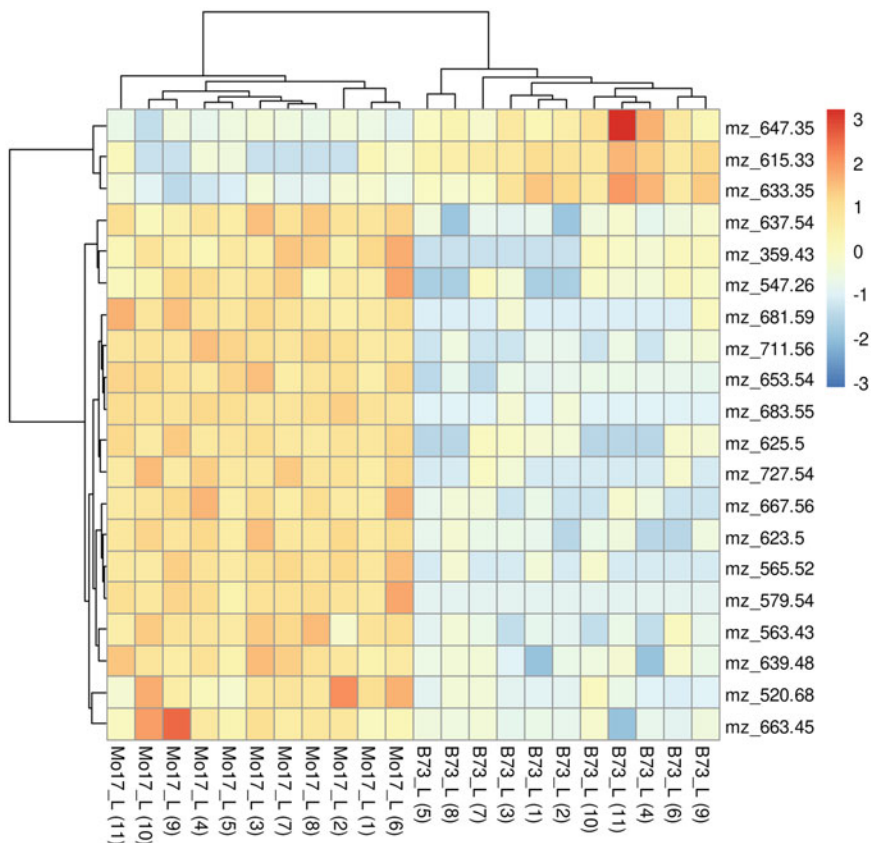


Fig. 2 Heatmap with hierarchical clustering analysis (HCA) of two varieties of maize. Eleven individual samples were measured for each genotype, and 20 variables were selected. The two inbred lines of maize are separated. The rows represent the features, and columns represent the different samples. The color represents intensity: red for higher and blue for lower intensities. The dendrograms represent the hierarchical relationship between the samples and variables

(e.g., 2:1); in both cases, acidified with 0.1% formic acid. All solvents should be LC-MS grade. Some studies, such as lipidomics experiments, may require the separation of polar from non-polar compounds. For those cases, a liquid-liquid extraction using a mixture of water: methanol: chloroform (1:2:0.8), or similar is possible [41].

4. In the case of using an autosampler (Accela 600 autosampler, Thermo Scientific), inject all samples three times in random order, with a loop filling of 10 μL . Do not use any column. Employ a gradient method to reduce the carry-over of samples between injections at a 100 $\mu\text{L}/\text{min}$ flow rate. Start with 0.5% methanol for 3 min, then 100% methanol for 1 min, and finally 0.5% for 2 min.
5. Clean the cone after 20 samples to avoid ion suppression.

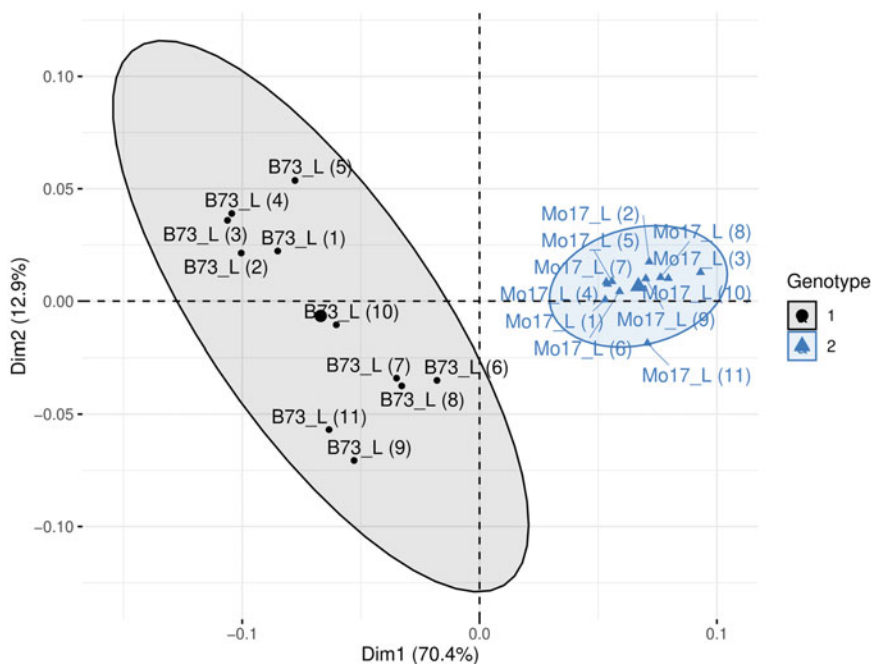


Fig. 3 Principal Component Analysis (PCA) with the k -means algorithm for clustering. Each cluster represents a distinct maize genotype: Black cluster—B73; blue cluster—Mo17

6. Samples from fruit juice or with a high sugar content should be diluted to 1:10 or 1:50 with the solvent mix to avoid ion suppression and the clogging of the ESI probe's needle.
7. Calibrate the mass analyzers before measurements.
8. The samples are analyzed on three different days for MALDI-ToF MS to even out differences in sample extraction, co-crystallization, and measurements.
9. For clustering analyses, the distance measure between samples and the linkage method for defining the cluster distance need to be defined. From our experience, we recommend “correlation” as the distance measure and “complete” as the linkage method.
10. Random Forest (RF) analysis can be used as a simple and efficient filter for variables. High-ranking important variables (m/z features) obtained from RF analysis are more likely to be relevant.
11. The biological sample must have a sharp tip to generate an appropriate spray (if you are analyzing, e.g., stems, roots, grains, or fruits).
12. Ensure that the metal clip with the sample is appropriate to the MS inlet to avoid an electric arc or an electric discard.

13. Plants with high water content do not require the addition of any organic solvent. The choice of solvent with different polarities offers the opportunity to extract and ionize different compounds from the same sample.

Acknowledgments

The project was funded by the CONACyT Fronteras project 2015-2/814 and the bilateral grant CONACyT-DFG 2016/277850. T. G.-R. and H.A.P.-P. acknowledge their CONACyT scholarships. We thank Leonardo Soto Rodríguez for testing the data analysis script.

Conflict of Interest *R.W. is the co-inventor of the patent “Non-thermal plasma jet device as source of spatial ionization for ambient mass spectrometry and method of application” (WO 2014/057409) and shareholder of the company KUTURABI SA de CV.*

References

1. Wiley JS, García-Reyes JF, Harper JD et al (2010) Screening of agrochemicals in food-stuffs using low-temperature plasma (LTP) ambient ionization mass spectrometry. *Analyst* 135:971–979. <https://doi.org/10.1039/b919493b>
2. Pizzo JS, Galuch MB, Santos PDS et al (2019) Determination of coconut oil adulteration with soybean oil by direct infusion electrospray ionization mass spectrometry. *J Braz Chem Soc* 30:1468–1474. <https://doi.org/10.21577/0103-5053.20190042>
3. Mo S, Dong L, Hurst WJ, van Breemen RB (2013) Quantitative analysis of phytosterols in edible oils using APCI liquid chromatography-tandem mass spectrometry. *Lipids* 48: 949–956. <https://doi.org/10.1007/s11745-013-3813-3>
4. Calvano CD, Monopoli A, Loizzo P et al (2013) Proteomic approach based on MALDI-TOF MS to detect powdered milk in fresh cow’s milk. *J Agric Food Chem* 61: 1609–1617. <https://doi.org/10.1021/jf302999s>
5. Ellis DI, Brewster VL, Dunn WB et al (2012) Fingerprinting food: current technologies for the detection of food adulteration and contamination. *Chem Soc Rev* 41:5706–5727. <https://doi.org/10.1039/C2CS35138B>
6. Laursen KH, Bontempo L, Camin F, Roßmann A (2016) Chapter 9—advances in isotopic analysis for food authenticity testing. In: Downey G (ed) *Advances in food authenticity testing*. Woodhead Publishing, Sawston, pp 227–252
7. Medina S, Pereira JA, Silva P et al (2019) Food fingerprints—a valuable tool to monitor food authenticity and safety. *Food Chem* 278: 144–162. <https://doi.org/10.1016/j.foodchem.2018.11.046>
8. Ren J-L, Zhang A-H, Kong L, Wang X-J (2018) Advances in mass spectrometry-based metabolomics for investigation of metabolites. *RSC Adv* 8:22335–22350. <https://doi.org/10.1039/C8RA01574K>
9. Martínez-Jarquín S, Winkler R (2017) Low-temperature plasma (LTP) jets for mass spectrometry (MS): ion processes, instrumental set-ups, and application examples. *TrAC Trends Anal Chem* 89:133–145. <https://doi.org/10.1016/j.trac.2017.01.013>
10. Gan H-H, Soukoulis C, Fisk I (2014) Atmospheric pressure chemical ionisation mass spectrometry analysis linked with chemometrics for food classification—a case study: geographical provenance and cultivar classification of monovarietal clarified apple juices. *Food Chem* 146: 149–156. <https://doi.org/10.1016/j.foodchem.2013.09.024>
11. Koulman A, Cao M, Faville M et al (2009) Semi-quantitative and structural metabolic phenotyping by direct infusion ion trap mass spectrometry and its application in genetical metabolomics. *Rapid Commun Mass*

- Spectrom 23:2253–2263. <https://doi.org/10.1002/rcm.4142>
12. Gamboa-Becerra R, Montero-Vargas JM, Martínez-Jarquín S et al (2017) Rapid classification of coffee products by data mining models from direct electrospray and plasma-based mass spectrometry analyses. *Food Anal Methods* 10:1359–1368. <https://doi.org/10.1007/s12161-016-0696-y>
 13. Martínez-Jarquín S, Moreno-Pedraza A, Cázarez-García D, Winkler R (2017) Automated chemical fingerprinting of Mexican spirits derived from: agave (tequila and mezcal) using direct-injection electrospray ionization (DIESI) and low-temperature plasma (LTP) mass spectrometry. *Anal Methods* 9: 5023–5028. <https://doi.org/10.1039/c7ay00793k>
 14. Garcia-Flores M, Juarez-Colunga S, Garcia-Casarrubias A et al (2015) Metabolic profiling of plant extracts using direct-injection electrospray ionization mass spectrometry allows for high-throughput phenotypic characterization according to genetic and environmental effects. *J Agric Food Chem* 63:1042–1052. <https://doi.org/10.1021/jf504853w>
 15. Goodacre R, Vaidyanathan S, Bianchi G, Kell DB (2002) Metabolic profiling using direct infusion electrospray ionisation mass spectrometry for the characterisation of olive oils. *Analyst* 127:1457–1462. <https://doi.org/10.1039/B206037J>
 16. Madalinski G, Godat E, Alves S et al (2008) Direct introduction of biological samples into a LTQ-Orbitrap hybrid mass spectrometer as a tool for fast metabolome analysis. *Anal Chem* 80:3291–3303. <https://doi.org/10.1021/ac7024915>
 17. Draper J, Lloyd AJ, Goodacre R, Beckmann M (2013) Flow infusion electrospray ionisation mass spectrometry for high throughput, non-targeted metabolite fingerprinting: a review. *Metabolomics* 9:4–29. <https://doi.org/10.1007/s11306-012-0449-x>
 18. Gibb S, Strimmer K (2012) MALDIquant: a versatile R package for the analysis of mass spectrometry data. *Bioinformatics* 28: 2270–2271. <https://doi.org/10.1093/bioinformatics/bts447>
 19. Jardine I (1990) Electrospray ionization mass spectrometry of biomolecules. *Nature* 345: 747–748. <https://doi.org/10.1038/345747a0>
 20. Winkler R (2010) ESIprot: a universal tool for charge state determination and molecular weight calculation of proteins from electrospray ionization mass spectrometry data. *Rapid Commun Mass Spectrom* 24:285–294
 21. Fenn J, Mann M, Meng C et al (1989) Electrospray ionization for mass spectrometry of large biomolecules. *Science* 246:64–71. <https://doi.org/10.1126/science.2675315>
 22. Harper JD, Charipar NA, Mulligan CC et al (2008) Low-temperature plasma probe for ambient desorption ionization. *Anal Chem* 80:9097–9104. <https://doi.org/10.1021/ac801641a>
 23. Clark CM, Costa MS, Sanchez LM, Murphy BT (2018) Coupling MALDI-TOF mass spectrometry protein and specialized metabolite analyses to rapidly discriminate bacterial function. *Proc Natl Acad Sci U S A* 115: 4981–4986. <https://doi.org/10.1073/pnas.1801247115>
 24. Calvano CD, Zambonin CG (2013) MALDI-Q-TOF-MS ionization and fragmentation of phospholipids and neutral lipids of dairy interest using variable doping salts. *Adv Dairy Res* 1:1–8
 25. Pazmiño-Arteaga JD, Chagolla A, Gallardo-Cabrera C, et al (2019) Screening for green coffee with sensorial defects due to aging during storage by MALDI-ToF mass fingerprinting. *Food Anal Methods*, 12. <https://doi.org/10.1007/s12161-019-01485-9>
 26. Karas M, Bachmann D, Bahr U, Hillenkamp F (1987) Matrix-assisted ultraviolet laser desorption of non-volatile compounds. *Int J Mass Spectrom Ion Process* 78:53–68. [https://doi.org/10.1016/0168-1176\(87\)87041-6](https://doi.org/10.1016/0168-1176(87)87041-6)
 27. Liu J, Wang H, Cooks RG, Ouyang Z (2011) Leaf spray: direct chemical analysis of plant material and living plants by mass spectrometry. *Anal Chem* 83:7608–7613. <https://doi.org/10.1021/ac2020273>
 28. Pereira I, Rodrigues SRM, de Carvalho TC et al (2016) Rapid screening of agrochemicals by paper spray ionization and leaf spray mass spectrometry: which technique is more appropriate? *Anal Methods* 8:6023–6029. <https://doi.org/10.1039/C6AY01154C>
 29. Malaj N, Ouyang Z, Sindona G, Cooks RG (2012) Analysis of pesticide residues by leaf spray mass spectrometry. *Anal Methods* 4: 1913–1919. <https://doi.org/10.1039/C2AY25222H>
 30. Tadjimukhamedov FK, Huang G, Ouyang Z, Cooks RG (2012) Rapid detection of urushiol allergens of toxicodendron genus using leaf spray mass spectrometry. *Analyst* 137: 1082–1084. <https://doi.org/10.1039/C2AN16077C>
 31. Winkler R (2020) Processing metabolomics and proteomics data with open software: a

- practical guide, 1st edn. Royal Society of Chemistry, Cambridge
32. Martínez-Jarquín S, Moreno-Pedraza A, Guillén-Alonso H, Winkler R (2016) Template for 3D printing a low-temperature plasma probe. *Anal Chem* 88:6976–6980. <https://doi.org/10.1021/acs.analchem.6b01019>
 33. Moreno-Pedraza A, Rosas-Román I, Garcia-Rojas NS et al (2019) Elucidating the distribution of plant metabolites from native tissues with laser desorption low-temperature plasma mass spectrometry imaging. *Anal Chem* 91: 2734–2743. <https://doi.org/10.1021/acs.analchem.8b04406>
 34. Rosas-Román I, Ovando-Vázquez C, Moreno-Pedraza A et al (2020) Open LabBot and RmsiGUI: community development kit for sampling automation and ambient imaging. *Microchem J* 152:104343. <https://doi.org/10.1016/j.microc.2019.104343>
 35. González-Rodríguez T (2020) Mass spectra of leaf extracts from maize
 36. Kessner D, Chambers M, Burke R et al (2008) ProteoWizard: open source software for rapid proteomics tools development. *Bioinformatics* 24:2534–2536. <https://doi.org/10.1093/bioinformatics/btn323>
 37. Strohal M, Kavan D, Novák P et al (2010) mMass 3: a cross-platform software environment for precise analysis of mass spectrometric data. *Anal Chem* 82:4648–4651. <https://doi.org/10.1021/ac100818g>
 38. Gibb S, Franceschi P (2019) MALDIquant-Foreign: import/export routines for ‘MALDIquant’
 39. Williams GJ (2009) Rattle: a data mining GUI for R. *R J* 1:45–55
 40. Biais B, Bernillon S, Deborde C et al (2012) Precautions for harvest, sampling, storage, and transport of crop plant metabolomics samples. *Methods Mol Biol* 860:51–63. https://doi.org/10.1007/978-1-61779-594-7_4
 41. Creydt M, Arndt M, Hudzik D, Fischer M (2018) Plant metabolomics: evaluation of different extraction parameters for nontargeted UPLC-ESI-QTOF-mass spectrometry at the example of white *Asparagus officinalis*. *J Agric Food Chem* 66:12876–12887. <https://doi.org/10.1021/acs.jafc.8b06037>



Chapter 2

MALDI-MS Application for Food Control

Igor Pereira, Bijay Banstola, Kelin Wang, Fabrizio Donnarumma, Kermit K. Murray, and Boniek Gontijo Vaz

Abstract

Matrix-assisted laser desorption and ionization mass spectrometry (MALDI-MS) is a fast, reliable, and accurate tool to guarantee food control in terms of pesticide distribution and microbiological contamination. In this chapter, we describe an interesting protocol to determine the distribution of the fungicide imazalil in apples using MALDI-MS which enables to visualize the penetration of chemical into fruit over the time. Images of apple slices showed the penetration depth of imazalil up to 7 days. The protocol described here is a valuable tool to fast fruit screening attempting food control.

Key words MALDI-MS, Food control, Apple, Fungicide

1 Introduction

Food containing threatening microorganisms such as bacteria, viruses, parasites, and chemical residues is causing hundreds of diseases, including cancer. According to WHO, around 600 million, 10% of people worldwide have sick after eating contaminated food, and approximately 420,000 die every year. In addition, US\$ 110 billion is wasted each year in productivity and medical expenses resulting from unsafe food in low- and middle-income countries [1]. Therefore, food control is vital to many aspects of human life, including support to national economies, trade, and tourism.

Foodstuff chemical analysis related to examining authentication and detecting fraud is complicated due to the complexity and diversity of matrices and the miscellaneous and unknown processes [2]. Mass spectrometry (MS) plays an important role in the high-throughput analysis aiming detection and quantification of organic molecules [3]. Usually, food control has been performed by using gas chromatography coupled to mass spectrometry (GC-MS) [4] and liquid chromatography coupled to mass spectrometry (LC-MS) [5]. Both techniques demonstrate excellent analytical

performance, but sometimes need extensive sample preparation protocols.

Matrix-assisted laser desorption ionization mass spectrometry (MALDI) is a powerful MS tool that allows fast, reliable, and accurate detection of food issues [3]. Among MS methods, MALDI has exhibited a remarkable ability to scrutinize food samples looking forward to chemical fingerprints to ensure safety and authentication, guaranteeing such a food control [6]. MALDI-MS is a soft ionization technique producing monocharged ions with low internal energy at low pressure ($\cong 10^{-6}$ mbar) and the absence of extensive fragmentation. To perform MALDI analysis, a sample is embedded in the matrix in vast excess. The laser strikes the sample mixed with the matrix and is absorbed mainly through the matrix, thereby evaporating, bringing intact analyte molecules into the gas phase. Through this procedure, ions (mainly $[M + H]^+$ and $[M + Na]^+$) are released by the matrix top emerging charged analyte molecules.

Most of MALDI applications dedicated to food control have concerned the analysis of milk and dairy products, oils, fish and seafood, vegetables, fruit, meat, and, to a minor extent, a few other categories [7]. Nearly all of the works have been dedicated to evaluating food quality and detection of adulterations, while just a few applications have been committed to researching the distribution of spatial localization of chemical pesticides on food. Here, we describe a simple protocol using MALDI to examine fruits, exemplified here by apple, in an attempt to determine some prohibited pesticide residue [3].

2 Materials and Protocols

2.1 Materials

1. Acetonitrile, HPLC grade from Thermo-Fisher (Waltham, MA, US).
2. Fluoroacetic Acid (FA) from Thermo-Fisher (Waltham, MA, US).
3. Trifluoroacetic Acid (TFA) from Thermo-Fisher (Waltham, MA, US).
4. α -cyano-4-hydroxycinnamic acid (CHCA) from Sigma-Aldrich (St. Louis, MO, USA).
5. Ultra-pure water produced in house.
6. Plain glass microscope slides from Thermo-Fisher (Waltham, MA, US).
7. Indium tin oxide (ITO) microscope slides from Bruker Daltonics (Bremen, Germany).

8. Imazalil was purchased from MedChem Express (Monmouth Junction, NJ, USA).
9. Fuji apples were purchased from a local supermarket.
10. 4 L Glass recipient.
11. Pipettes and proper tips for handling organic solvents.

2.2 Sample Preparation

1. 12 apples were submerged for 2 min in a 4 L glass containing 2 L of a 1000 ppm aqueous solution of imazalil.
2. The control group was not treated.
3. The apples were stored at room temperature for 0, 1, 4, and 7 days [45, 46].
4. On each day, 4 apples (3 containing imazalil and 1 control) were removed and cut into 0.2 mm thick sections (one slice for each apple) using a vibratome (Vibratome 1500, Ted Pella, Redding, CA, USA) and mounted on ITO glass slides.
5. The apple slices were dried under vacuum for 15 min before sampling.
6. The same approach was used for laser ablation experiments, but plain glass slides were used without vacuum drying before sampling.
7. The apple slices were sampled 5 min after being cut.

2.3 MALDI-MS

1. UltrafleXtreme (Bruker Daltonics, Bremen, Germany).
2. A 10 mg/mL solution of CHCA in 1:1 H₂O/ACN containing 0.1% TFA was used as matrix.
3. The matrix was sprayed on the slides using a home-built pneumatic nebulizer (*see Note 1*).
4. The matrix was sprayed at a distance of 8 cm from the apple section and 14 spray cycles of 20 s each were used. (*see Note 2*).
5. MALDI mass spectra were recorded using a tandem time-of-flight mass spectrometer (UltrafleXtreme, Bruker, Bremen, Germany).
6. The instrument is equipped with a 355 nm Nd:YAG laser operating at a repetition rate of 1 kHz.
7. The section surface was irradiated with 1000 laser shots and a step size of 200 μm in the positive ion linear mode.
8. The intensity of protonated imazalil (m/z 297) was used for imaging (Fig. 1).
9. After data acquisition, images were reconstructed using the FlexImaging software (Bruker) (Fig. 2).

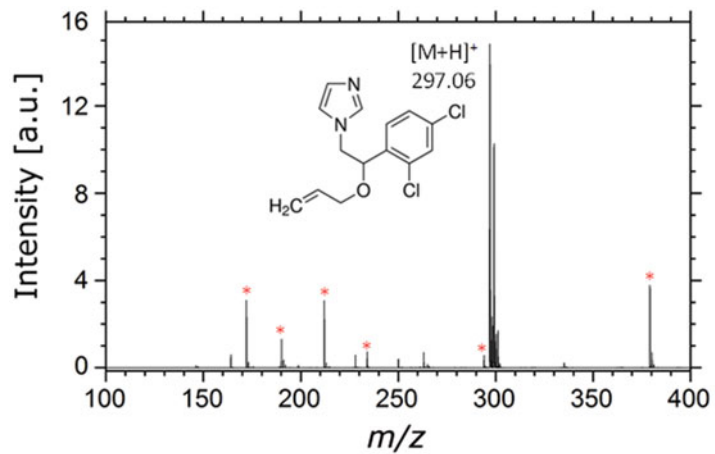


Fig. 1 MALDI mass spectrum obtained from the application of 1 μL of a 1000 ppm imazalil (m/z 297.06 $[\text{M} + \text{H}]^+$) solution on an apple slice. CHCA peaks are labeled with red asterisks (with permission from [3])

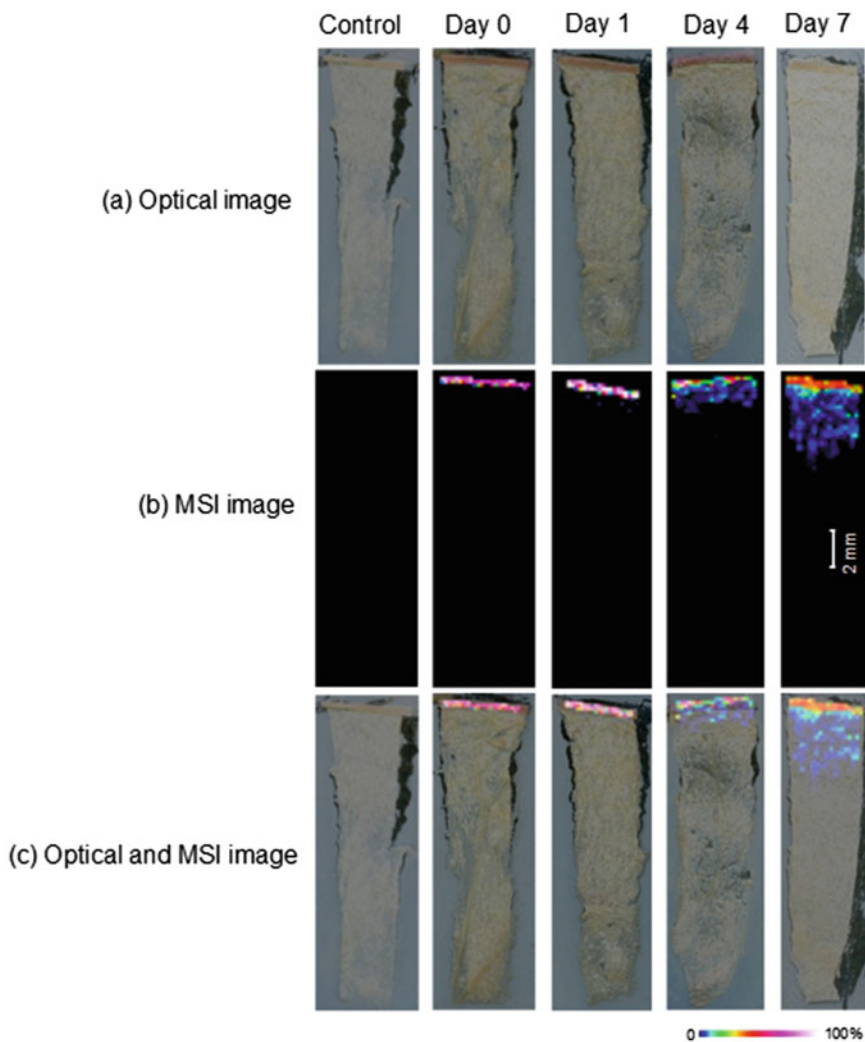


Fig. 2 Penetration analysis of imazalil (m/z 297.04 $[\text{M} + \text{H}]^+$) in apples by MALDI imaging on Day 0, 1, 4, and 7 after dipping application of imazalil: (a) optical image of apple slices; (b) MALDI imaging of imazalil; (c) merged optical and MALDI imaging image (with permission from [3])

3 Notes

1. The flow rate of the solution was 100 $\mu\text{L}/\text{min}$, and the nitrogen gas pressure was 70 kPa (10 PSI).
2. The matrix was allowed to dry for 1 min between each spray cycle.

Acknowledgments

This material is based upon work supported by the National Science Foundation under Grant No. CHE-1709526. IP gratefully acknowledges support from the Brazilian Federal Agency for Support and Evaluation of Graduate Education (CAPES) under PDSE program—88881.132855/2016-01.

References

1. WHO (2019) Food safety, <https://www.who.int/news-room/factsheets/detail/food-safety>. Accessed May 2021
2. Aung MM, Chang YS (2014) Traceability in a food supply chain: safety and quality perspectives. *Food Control* 39:172–184. <https://doi.org/10.1016/j.foodcont.2013.11.007>
3. Pereira I, Bastola B, Wang K et al (2019) Matrix-assisted laser desorption ionization imaging and laser ablation sampling for analysis of fungicide distribution in apples. *Anal Chem* 91: 6051–6056. <https://doi.org/10.1021/acs.analchem.9b00566>
4. Sharma D, Nagpal A, Pakade YB et al (2010) Analytical methods for estimation of organophosphorus pesticide residues in fruits and vegetables: a review. *Talanta* 82:1077–1089. <https://doi.org/10.1016/j.talanta.2010.06.043>
5. Masiá A, Suarez-Varela MM, Llopis-Gonzalez A et al (2016) Determination of pesticides and veterinary drug residues in food by liquid chromatography-mass spectrometry: a review. *Anal Chim Acta* 936:40–61. <https://doi.org/10.1016/j.aca.2016.07.023>
6. Spengler B (2015) Mass spectrometry imaging of biomolecular information. *Anal Chem* 87: 64–82. <https://doi.org/10.1021/ac504543v>
7. Zambonin C (2021) Mass spectrometry applications for food fraud detection. *Appl Sci* 11: 3374. <https://doi.org/10.3390/app11083374>



MALDI-TOF-Mass Spectrometry: Sample Preparation Protocols for Meat and Milk Products

Jörg Rau, Martin Dyk, Olivera Wenninger, and Ekkehard Hiller

Abstract

Matrix-assisted laser desorption/ionization time-of-flight mass spectrometry (MALDI-TOF-MS) is widely used for species determination of microbes by analyzing their protein pattern. Additional applications for species identification in food of animal origin, such as meat or milk products, have been developed recently. For these purposes, standardized sample preparations are helpful to build compatible mass pattern containing databases. We compile sample preparation procedures here that have proven successful.

Key words MALDI-TOF-MS, Food fraud, Species identification

1 Introduction

The importance of mass spectrometry-based methodologies that utilize the proteome of samples is increasing in food analysis. Matrix-assisted laser desorption/ionization time-of-flight mass spectrometry (MALDI-TOF-MS) is used routinely in a number of laboratories for species determination of microbes. However, the technology also opens up a broad range of further applications, especially in species identification of protein-rich food of animal and plant origin.

The MALDI-TOF-MS workflow comprises several steps, consisting of sampling to provide the protein-containing material of interest, appropriate sample preparation to extract and clean the protein-fraction, measurement in the MALDI-TOF-MS with suitable basic device setup, and comparison of the sample mass spectrum obtained with reference spectra stored in a database.

This last-mentioned appropriate database of reference spectra of known species is the key for a reliable identification and conducting a standardized sample preparation for the respective application is the necessary basis. For microorganisms, manufacturers already offer extensive database collections of reference spectra,

which are usually based on sample extraction protocols and which are similar across manufacturers. In contrast, the development of own supplements for other topics is of increasing importance for many users. This applies especially for multidisciplinary working groups in institutions with overlapping objectives, or in institutions aspiring dual use of existing MALDI-TOF-MS systems to increase the workload of existing equipment. In the area of food analysis, the examination of pathogenic microorganisms or hygiene parameters is extended by application of databases for combating food fraud [1]. Examples include the differentiation of animal species in fish, other seafood, insects, skeletal muscle meat, or cheese [2–6].

One of the most challenging tasks when developing an identification method using MALDI-TOF-MS is the extraction of proteins and peptides from the sample material. These methods should be easy to use, rapid, and inexpensive.

Usually, the instrument manufacturers suggest several established sample preparation procedures for analysis of microorganisms, such as bacteria and filamentous fungi [7, 8]. Other specialized protocols have been published, e.g., for highly pathogenic bacteria or Mycobacteria [9, 10]. Beyond microbiology, suitable sample preparation procedures are necessary, which are also the basis for the development of specific reference databases for food analysis [11]. For analysis of food of animal origin, we provide sample preparation methods for which most experience is available from the development of MALDI-TOF-MS databases of skeletal muscle meat and cheese, as well as from their application in the daily routine of food control [5, 6]. The protocols are based on existing procedures described in literature with modifications or enhancements that have proven successful in daily practice. These and further preparation protocols were collected in the form of short protocols on the MALDI User Platform “MALDI-UP” (<https://maldi-up.ua-bw.de>) [12]. A comprehensive collection of reference spectra and single spectra generated by using these protocols is also available for exchange on the MALDI-UP-homepage. This should facilitate the exchange of similarly created spectra between MALDI-users for mutual benefit [13].

2 Materials

All relevant regulations to ensure chemical safety in the workplace must be obeyed. Follow all waste disposal regulations when disposing waste materials with care. Prepare all solutions using ultrapure water (prepared by purifying deionized water) and analytical grade reagents. Always use chemicals of the highest purity available, e.g., HPLC or LC-MS grade. Prepare and store all reagents at room temperature (unless otherwise indicated).

1. 1.5 mL and 2.0 mL reaction tubes and tips.
2. Silica beads (e.g., 0.1 mm diameter).
3. Micro-pestle, fitted for the tubes used.
4. Spatula in different dimensions.
5. Small beaker.
6. *Only for the separation of butter plasm:*
 - (a) Special glass tube ca. 2.2 cm diameter, ca. 12 cm length, open on both sides, with one rubber and one cork stopper.
 - (b) Refrigerator (10 °C).
 - (c) Heating chamber/drying chamber (for ca. 70 °C).
7. Benchtop centrifuge.
8. Centrifuge with centrifuge tubes and temperature control.
9. Heating block.
10. MALDI sample target, type is depending on the MALDI-TOF-MS instrument (e.g., steel-plate).
11. Demineralized water.
12. Acetic acid (diluted to 50%).
13. OS solvent (acetonitrile 50%, water 47.5%, and trifluoroacetic acid 2.5%) (*see Note 1*).
14. HCCA matrix solution: α -cyano-4-hydroxycinnamic acid solution saturated, dissolved in OS solvent (*see Note 2*).

3 Methods

3.1 Protocol for Meat Products

This protocol for meat was based on the short description by Post and Dikler (2010) and was further adapted [14, 15]. It was used to create and validate a reference database for skeletal muscle meat [5].

3.1.1 Samples

Suitable not exclusively for the following types of samples: Muscle meat of mammals, birds, and reptiles in natural form—raw, frozen, or heated (cooked, grilled)—also applicable for offal, such as liver and kidney (*see Note 3*).

This protocol is not suitable for strongly ripened, autolyzed meat samples, and not for ripened or cured products because the maturation process causes significant changes in the protein pattern. Similarly, highly processed meat products with mixed composition, such as sausages, are unsuitable for direct automated pattern-based identification, even if mass spectra could be obtained by this sample preparation.

3.1.2 *Extraction*

1. Add silica beads (about 5 mm high) to a 1.5 mL reaction tube.
2. Add 100–200 μL OS.
3. Add about 3 mm^3 muscle tissue (*see Note 4*).
4. Homogenize/grind the sample using a micro-pestle.
5. Mix thoroughly by vortexing for 10–20 s.
6. Centrifuge at 12,000–14,000 $\times g$ (RCF) in a benchtop centrifuge for 2 min.
7. Pipet 1 μL supernatant onto a target sample spot (*see Note 5*).
8. As soon as the sample spot has dried, overlay the sample with 1 μL HCCA matrix solution (to prevent oxidation reactions leading to peak shifting).
9. Allow the sample spot to air-dry before analysis (*see Note 6*).

3.1.3 *Measurement*

For measurement in the MALDI-TOF-mass spectrometer, the same instrument settings and mass ranges (e.g., m/z 2000–20,000 Dalton) can be used for common applications in microbiology (*see Notes 7 and 8*).

3.2 Protocol for Milk Products

3.2.1 *Samples*

Suitable not exclusively for the following types of samples: milk, milk products e.g., yogurt or cheese—raw, frozen, or heated (cooked, baked) (*see Note 9*). For butter, the separation of fat and the protein-containing aqueous fraction is preceded.

In milk products with mixed composition made from milk of two animal species, good mass spectra can usually be obtained by this sample preparation. Depending on the composition of the database and the evaluation system (algorithm) used, it is possible to identify the animal species that has the greatest protein proportion in the milk product.

For butter, the water fraction is separated prior to further precipitation.

For pure milk, it is necessary to precipitate the proteins (mostly casein), start with **step 3.2.2**.

For yogurt or (fresh-) cheese (already “precipitated” casein), start with **step 3.3.4**.

3.2.2 *Separation of Fat (for Milk) (see Note 10)*

1. Add about 30 mL milk to a 50 mL centrifuge tube.
2. Centrifuge at 2,000 $\times g$ (RCF) and 8 °C for 12 min.
3. To carefully remove the fat, decant the liquid into a small beaker; the fat should cling to the wall of the centrifuge tube and is to be discarded.

3.2.3 *Separation of Fat (for Butter Plasm)*

1. Butter should be refrigerated (max. 15 °C).
2. Close the glass tube with one stopper.

3. Press the open side of the glass tube into the butter until it is ca. 75% full.
4. Close the tube with the cork stopper.
5. With the rubber stopper at the bottom, melt for 3–4 h at ca. 70 °C (*see Note 11*).
6. After melting the butter and settling the serum in the bottom of the glass tube, place it in the refrigerator (ca. 10 °C; 3–4 h or overnight).
7. Butter plasm is collected by removing the rubber stopper on the bottom and sampling of the aqueous phase.

Adapted from Norm DIN 10349:2004–2010 [16].

3.2.4 Precipitation of Casein

1. Add a few drops of dilute acetic acid to the skimmed milk.
2. Heat the liquid to 40–45 °C (e.g., in a heating block) for at least 15 min until enough casein precipitates.

3.2.5 Separation of Casein and Whey

1. Transfer the liquid with the precipitate to 1.5 mL reaction tubes.
2. Centrifuge at 12,000–14,000 $\times g$ (RCF) in a benchtop centrifuge for 2 min.
3. Discard the supernatant (= whey) and merge the pellets (= casein) (*for mare milk: see Note 12*).

3.2.6 Washing

1. Add 1 mL aqua dest. and stir with a spatula.
2. Centrifuge at 12,000–14,000 $\times g$ (RCF) in a benchtop centrifuge for 2 min.
3. Discard the supernatant.

All further steps were used for precipitated milk, yogurt, butter, or (fresh) cheese.

3.2.7 Organic Solvent Extraction Procedure (with Spatula)

1. Transfer a small amount (about 3 mm³) of the sample to a 1.5 mL tube.
2. Add 200 μ L OS.
3. Homogenize by stirring with a spatula.
4. Mix thoroughly by vortexing for 10–20 s.
5. Centrifuge at 12,000–14,000 $\times g$ (RCF) in a benchtop centrifuge for 2 min.
6. Pipet 1 μ L supernatant onto a target sample spot (we recommend spotting the supernatant in duplicate or triplicate).

7. As soon as the sample spot has dried, overlay the sample with 1 μL HCCA matrix solution (to prevent oxidation reactions leading to peak shifting).
8. Allow the sample spot to air-dry before analysis.

3.2.8 Measurement

For measurement in the MALDI-TOF-mass spectrometer, the same instrument settings and mass ranges (e.g., m/z 2000–20,000 Dalton) can be used as for common applications in microbiology.

4 Notes

1. OS can be stored at room temperature for a couple of weeks without further issues. Fresh preparations are recommended to avoid evaporation of the volatile components.
2. Either purchase from your MALDI system provider or prepare according to the manufacturer's recommendations. The storage conditions are also usually specified from the manufacturer of the MALDI system. If the suspension color changes, it must be remade.
3. Measure or freeze the meat samples as soon as possible to prevent protein oxidation or degradation that possibly results in uncontrolled m/z -signal shifting. Freezing at $-20\text{ }^{\circ}\text{C}$ prevents or reduces the aging effects for years [5].
4. For the best results, use material from the inner part of the tissue to avoid possible surface oxidation and contamination. Fresh pieces of meat can be easily cut with a small pair of scissors. Avoid layers of fat or visible connective tissue. Meat samples from frozen material can be obtained using a wood-drill (3.5 mm diameter) and a standard cordless screwdriver.
5. We recommend spotting the supernatant on two or three spot positions to obtain duplicate or triplicate measurements.
6. Good crystallization is often indicated in the light by the formation of a uniform spot surface.
7. In our experience, the instrument settings recommended by the manufacturer for the identification of microorganisms are also suitable for the recording of meat spectra.
8. It is absolutely necessary to follow the manufacturer's calibration routines and instrument accuracy checks for the MALDI-TOF-MS system. Poorly calibrated MS often result in insufficient match with the reference databases used.
9. Measure or freeze the milk product samples as soon as possible to prevent protein oxidation or degradation that possibly

results in uncontrolled m/z -signal shifting. Freezing at -20°C prevents or reduces the aging effects [6].

10. This step can be skipped for milk with an especially low-fat content, e.g., mare milk.
11. Place the tube in a beaker.
12. For mare milk you will need the content of about six tubes (mare or donkey milk does not contain as much casein as other milk types). Less tubes are required for other milk types.

References

1. Pavlovic M, Huber I, Busch U (2020) MALDI-TOF MS profiling-based identification of food components. In: Reference module in food science, pp 1–5. <https://doi.org/10.1016/B978-0-08-100596-5.22767-4>
2. Stahl A, Schöder U (2017) Development of a MALDI-TOF-MS-based protein fingerprint database of common food fish allowing fast and reliable identification of fraud and substitution. *J Agric Food Chem* 65:7519–7527. <https://doi.org/10.1021/acs.jafc.7b02826>
3. Stephan R, Johler S, Oesterle N, Näumann G, Voge G, Pflüger V (2014) Rapid and reliable species identification of scallops by MALDI-TOF mass spectrometry. *Food Control* 46: 6–9. <https://doi.org/10.1016/j.foodcont.2014.04.047>
4. Ulrich S, Kühn U, Biermaier B, Piacenza N, Schwaiger K, Gottschalk C, Gareis M (2017) Direct identification of edible insects by MALDI-TOF mass spectrometry. *Food Control* 76:96–101. <https://doi.org/10.1016/j.foodcont.2017.01.010>
5. Rau J, Hiller E, Männig A, Dyk M, Wenninger O, Stoll P, Wibbelt G, Schreiter P (2021) Animal species identification of meat using MALDI-TOF MS. *Aspects of Food Control and Animal Health* 14:1–12. <https://ejournal.cvuas.de/issue202114.asp>
6. Rau J, Korte N, Dyk M, Wenninger O, Schreiter P, Hiller E (2020) Rapid animal species identification of feta and mozzarella cheese using MALDI-TOF mass-spectrometry. *Food Control* 117:107349. <https://doi.org/10.1016/j.foodcont.2020.107349>
7. Pranada AB, Schwarz G, Kostrzewa M (2016) Maldi biotyping for microorganism identification in clinical microbiology. In: Cramer R (ed) *Advances in MALDI and laser-induced soft ionization mass spectrometry*. Springer International Publishing Switzerland, Cham, pp 197–222. https://doi.org/10.1007/978-3-319-04819-2_11
8. van Belkum A, Welker M, Pincus D, Charrier JP, Girard V (2017) Matrix-assisted laser desorption ionization time-of-flight mass spectrometry in clinical microbiology: what are the current issues? *Ann Lab Med* 37:475–483. <https://doi.org/10.3343/alm.2017.37.6.475>
9. Lasch P, Nattermann H, Stämmler M, Grunow R, Bannert N, Appel B, Naumann D (2008) MALDI-TOF mass spectrometry compatible inactivation method for highly pathogenic microbial cells and spores. *Anal Chem* 80:2026–2034. <https://doi.org/10.1021/ac701822j>
10. Alcolea-Medina A, Fernandez MTC, Montiel N, Luzón García MP, Delamo Sevilla C, North N, Martínez Lirola MJ, Wilks M (2019) An improved simple method for the identification of mycobacteria by MALDI-TOF MS (matrix-assisted laser desorption-ionization mass spectrometry). *Sci Rep* 9: 20216. <https://doi.org/10.1038/s41598-019-56604-7>
11. Spielmann G, Huber I, Maggipinto M, Haszprumar G, Busch U, Pavlovic M (2018) Comparison of five preparatory protocols for fish species identification using MALDI-TOF MS. *Eur Food Res Technol* 244:685–694. <https://doi.org/10.1007/s00217-017-2983-2>
12. Dyk M, Wenninger O, Guckert C, Fuchs J, Wind C, Hiller E, Schreiter P, Rau J (2020) Collection of sample preparation protocols for MALDI-TOF MS based identification of meat, dairy products, fish and insects. *Aspects of Food Control and Animal Health* 13:1–13. <https://doi.org/10.48414/aspects2020/13>
13. Rau J, Eisenberg T, Männig A, Wind C, Lasch P, Sting R (2016) MALDI-UP—an internet platform for the exchange of MALDI-TOF mass spectra—user guide for <http://mal-di-up.ua-bw.de/>. *Aspects of Food Control and Animal Health* 2016(1):

- 1–17. https://ejournal.cvuas.de/docs/cvuas_ejournal_201601.pdf
14. Post A, Dikler S (2010) Identification of fish species by protein profiling using MALDI-TOF mass spectrometry. Poster FACSS 2010: 583
15. Stoll P, Rau J (2015) Tierartendifferenzierung von Fleisch mittels MALDI-TOF MS; 44. Deutscher Lebensmittelchemikertag 14. Karlsruhe. https://maldi-up.ua-bw.de/docs/CVUAS_Stoll_Rau_Tierarten_MALDITOFMS_20150914.pdf
16. DIN 10349:2004–2010 (2004) Determination of pH of butter plasm—Bestimmung des pH-Wertes im Butterplasma [German]



Comprehensive Identification of Plant Polyphenols by LC-MS

Álvaro Fernández-Ochoa, María de la Luz Cádiz-Gurrea, and Antonio Segura Carretero

Abstract

The study of plant phenolic compounds has increased during the last decades due to their bioactive properties as well as their structural variability. This advance has been possible thanks to the development of advanced analytical techniques such as mass spectrometry, chromatographic techniques, and nuclear magnetic resonance. In addition, the development of software and databases has played a fundamental role in advancing the chemical characterization of these compounds. In this chapter, we present a protocol for the comprehensive identification of phenolic compounds based on liquid chromatography (reverse-phase mode) coupled to high-resolution mass spectrometry, which has been the most widely used technique to study this type of compounds. Furthermore, a data processing methodology based on open software and databases is detailed in this protocol.

Key words Polyphenols, Phenolic compounds, Mass spectrometry, Liquid chromatography, Characterization, Identification, Bioactive compounds, Open-source software

1 Introduction

Phenolic compounds are a class of chemical compounds that have attracted great interest in the scientific community in recent decades. This fact is due to their wide structural diversity as well as the multiple bioactive biological activities that have been described for them [1–3].

Most phenolic compounds, also known as polyphenols, have a common basic skeleton formed by an aromatic ring with one or more hydroxyl substituents. These compounds make up one of the most numerous and widely distributed groups of substances in the plant kingdom, with more than 10,000 different structures currently known [4]. These are a group of compounds synthesized from the secondary metabolism of plants through various pathways such as shikimic acid, acetate, phenylpropanoid, and flavonoid

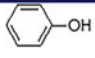
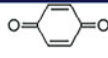
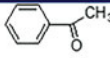
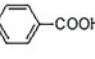
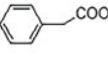
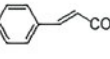
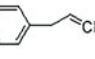
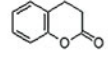
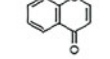
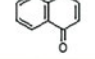
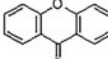
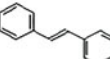
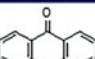
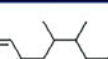
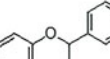
Simple phenols	Phenols		Benzo-quinones		Aceto-phenones	
	Benzoic acids		Phenylacetic acids		Cynamic acids	
	Phenyl-propenes		Coumarins Isocoumarins		Chromones	
	Naphtho-quinones					
Polyphenols	Lignin	Highly cross-linked aromatic polymer	Xanthenes		Stilbenes	
	Antra-quinones		Lignans Neolignans		Hydrolyzable tannins	Heterogeneous polymer formed by phenolic acids and simple sugars
	Flavonoids	Subfamilies: Flavandiol, Flavanol, Dihydrochalcone, Proanthocyanidin/Condensed tannin, anthocyanidin, Isoflavonoid, dihydroflavonol, biflavonol, flavanol, aurone, flavone, chalcone, flavanone.				

Fig. 1 Main families of phenolic compounds

pathways [5]. Based on their chemical structure, phenolic compounds can be classified into different families; the main ones are shown in Fig. 1.

The analytical methodology for the analysis of phenolic compounds has evolved over time, going from simple spectrophotometric determinations, which determine the total content, to its identification and quantification through the use of high-resolution analytical techniques [2]. These techniques, such as nuclear magnetic resonance (NMR) and mass spectrometry (MS), which is usually coupled to chromatographic techniques (liquid chromatography (LC), gas chromatography (GC), and capillary electrophoresis (CE)), have played an important role in the phytochemical characterization of phenolic compounds [6]. In addition, these techniques are also currently applied to study other characteristics of these compounds, such as their bioavailability or metabolism, through metabolomic approaches and nutritional intervention trials [6].

The recent development of analytical techniques is making it possible to have instruments with greater sensitivity and resolution, which allow the identification and quantification of phenolic compounds present in low concentrations, with high accuracy and precision [7, 8]. Among all the analytical techniques, LC-MS has been the most widely used for the phytochemical characterization of phenolic compounds [6]. Furthermore, tandem mass spectrometry (MS/MS) [9], software development, and increase in open-source MS/MS libraries (e.g., MassBank Europe [10], MoNA—

MassBank of North America [11]), databases (e.g., FooDB [12], HMDB [13], LIPID MAPS [14], PlantCyc [15]), and in silico fragmentation tools (e.g., MS-FINDER [16], MetFrag [17]) have been of great importance for the comprehensive characterization of polyphenols by LC-MS.

In this chapter, we present a qualitative characterization protocol for phenolic compounds based on LC-MS/MS [18]. In addition, we present a data-processing pipeline based on open-source software and databases, so that it can be applied by users of different LC-MS/MS instruments.

2 Materials

All chemicals and solvents used have to be of HPLC-MS analytical grade. All processes and solutions can be carried out at room temperature unless otherwise mentioned.

2.1 Chemicals

1. Methanol, LC-MS analytical grade.
2. Acetic acid (Sigma-Aldrich, Steinheim, Germany).
3. Ultrapure water purified by a Milli-Q system from Millipore (Bedford, MA, USA).
4. Leucine Enkephalin (Waters reference material), or other mass calibrants depending on the conditions of each LC-MS instrument.

2.2 Mobile Phases

1. Mobile phase A is an aqueous acetic acid (0.5%) solution. Mobile phase B is methanol. Both mobile phases must be sonicated for 15 min before being used in the LC-MS. Purge the LC system when you are going to start using the mobile phases (*see Note 1*).

2.3 LC-MS Materials

1. An ultrahigh-performance liquid chromatography (UHPLC) system coupled to a high-resolution mass spectrometer (HRMS) with electrospray ionization (ESI) (*see Note 2*): Chromatographic separation can be performed on a reversed-phase C18 column (e.g., 1.8 μm , 4.6 \times 150 mm, or similar). Pre-columns of the same packing and/or prefilters should also be used.

2.4 Software

1. The LC-HRMS data processing can be carried out by the different commercial software of the instrument's own brand (e.g., MassLynx (Waters), Qualitative Data Analysis (Agilent), Data Analysis (Bruker Daltonics)). For MS^E data collected by Waters instruments, it is recommended to use Symphony software for data conversion. In order to make this protocol as accessible as possible, the data-processing pipeline is based on

open-source software such as msConvert [19], MZmine 2.0 [20], and SIRIUS [21]. These tools can be downloaded from the following websites:

2. msConvert: <http://proteowizard.sourceforge.net/download.html>.
3. MZmine 2.0: <http://mzmine.github.io/>.
4. SIRIUS: <https://bio.informatik.uni-jena.de/software/sirius/>.

3 Methods

3.1 Extract Solution Preparation

1. A dry extract rich in phenolic compounds should be dissolved in methanol to a concentration of 5 mg/L (*see Notes 3–5*).
2. The extract solution should be vortexed to achieve complete dissolution (*see Note 6*).
3. Next, the extract should be centrifuged at 14,800 rpm during 15 min.
4. Take the supernatant and filter it through a 0.20 mm filter before transferring it to the HPLC vials.
5. Keep the prepared samples at $-20\text{ }^{\circ}\text{C}$ until the analytical stage.
6. A blank sample should be prepared in order to detect signals that are not from the plant of interest. Ideally, this sample should be prepared from the beginning of the extraction process, using the same experimental conditions but without the plant sample.

3.2 LC Method

1. Use an injection volume of 5 μL .
2. The following gradient of these mobile phases can be used in order to achieve an efficient separation: 0.0 min [A:B 100:0], 5.0 min [A:B 75:25], 20.0 min [A:B 61:39], 30.0 min [A:B 40:60], 38 min [A:B 0:100], and 46.0 min [A:B 100:0] (*see Notes 7 and 8*). The starting conditions should be kept at the end of the method for at least 5 min.
3. Set the mobile-phase flow at 0.4 mL/min.
4. Use a column temperature of $25\text{ }^{\circ}\text{C}$.
5. Use a sequence consisting of multiple blanks at the beginning and end of the analysis. Ideally, inject at least three replicates per sample to ensure reproducibility of the analyses. If different types of extracts are going to be analyzed, run blank samples between them to avoid possible carryover peaks.

3.3 MS Method

1. Make sure that the equipment is correctly calibrated (according to the manuals of each MS instrument) before starting its use.
2. Use a negative ionization mode (*see Note 9*).

Table 1
MS parameters

MS parameters	
<i>m/z</i> range	50–1200 <i>m/z</i>
Mode	Centroid
Cone voltage	30 V
Capillary voltage	−2.2 kV
Desolvation temperature	500 °C
Desolvation gas flow	700 L/h
Cone gas flow	50 L/h
Source temperature	100 °C
Scan duration	0.1 s
Resolution	20,000 FWHM

3. Table 1 details the main MS parameters.
4. The MS^E acquisition is based on using two parallel scan functions by rapid switching, in which one scan is operated at low collision energy in the gas cell (4 eV) and the other at an elevated collision energy (MS^E energy linear ramp: from 20 to 60 eV) (*see Note 10*).
5. Leucine Enkephalin is injected continuously during the analysis for mass calibration at a concentration of 300 ng/mL (*see Note 11*).

3.4 Data Conversion

1. In order to be able to read the data in the open-source data-processing software, it is necessary to transform the data format into an adequate format (.mzML or .mzXML). For that purpose, use msConvertGUI software [19] (*see Notes 12 and 13*).
2. The signals from both MS¹ and MS² levels must be extracted. Figure 2 shows schematically how to use this software in a simple way.

3.5 Peak Detection

1. Use the Automated Data Analysis Pipeline (ADAP) for pre-processing mass spectrometry data [22]. Table 2 details the parameters for the data-processing pipeline, which are described below.
2. Import the .mzML or .mzXML data files from the blanks and extract samples to the MZmine software (“Raw data methods” → “Raw data import”).
3. Detect masses from the mass spectra (“Raw data methods” → “Feature detection” → “Mass detection”). Select MS¹-level

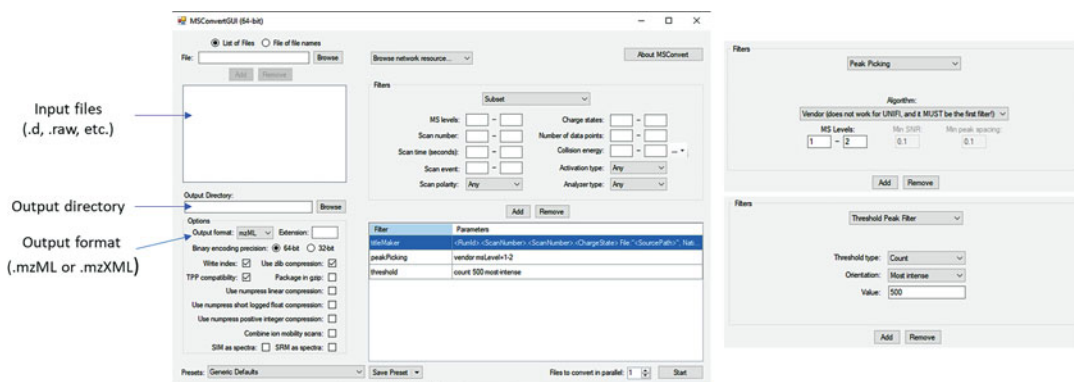


Fig. 2 Scheme of msConvert software

Table 2
MZmine parameters for peak detection

Mass detection	MS level	1
	Mass detector	Centroid
	Noise level	1.0 E3
	MS level	2
	Mass detector	Centroid
	Noise level	1.0 E2
ADAP chromatogram builder	MS level	1
	Min n° of scans	9
	Group intensity threshold	1.0 E3
	Min highest intensity	1.0 E4
	<i>m/z</i> tolerance	10 ppm
Chromatogram deconvolution	Algorithm	Wavelets (ADAP)
	S/N threshold	50
	S/N estimator	Intensity window SN
	Min feature height	5 E4
	Coefficient/area threshold	110
	Peak duration range	0.05–0.3
	RT wavelet range	0–0.30
	<i>m/z</i> range for MS ² scan pairing	0.002 Da
	RT range for MS ² scan pairing	0.05 min
Isotopic peak grouper	<i>m/z</i> tolerance	10 ppm
	Retention time (RT) tolerance	0.02 min
	Maximum charge	2
	Representative isotope	Most intense
Alignment	Algorithm	Join aligner
	<i>m/z</i> tolerance	10 ppm
	Weight for <i>m/z</i>	3
	RT tolerance	0.02 min
	Weight for RT	1
Gap filling	Intensity tolerance	25%
	<i>m/z</i> tolerance	10 ppm
	RT tolerance	0.02 min

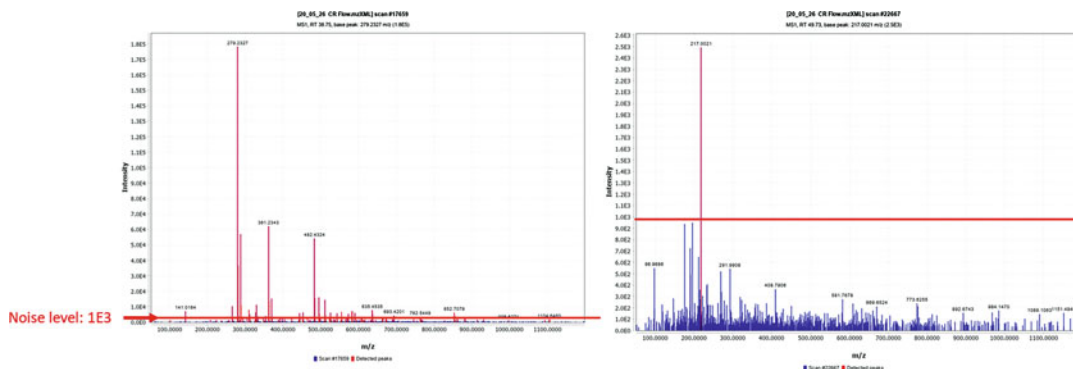


Fig. 3 Examples of MS¹ scans for noise-level inspection

scans from all raw data files. Click on mass detector “centroid” selecting a noise level of 1.0 E3. Repeat this step for the MS²-level scans using a lower noise level (1.0 E2) (Fig. 3, *see Note 14*).

4. Run the ADAP chromatogram builder method using the parameters suggested in Table 2 (*see Notes 15 and 16*) (“Raw data methods” → “Feature detection” → “ADAP chromatogram builder”).
5. Run the ADAP feature detection method using the parameters suggested in Table 2 (*see Note 15*) (“Feature list methods” → “Feature detection” → “Chromatogram deconvolution”).
6. Group the signals corresponding to isotopes using the function “Isotopic peak grouper” (“Feature list methods” → “Isotopes” → “Isotopic peak grouper”).
7. Use the alignment function to align the detected features between different samples (“Feature list methods” → “Alignment” → “Join aligner”).
8. We also recommend using the function “gap filling” especially when using replicates or samples of similar plant extracts (“Feature list methods” → “Gap filling” → “Peak finder, multithreaded”).
9. Click on “aligned feature list” to see the results. These results can be exported in a .csv file (“Feature list methods” → “Export/import” → “Export to .csv file”).
10. Identify the signals from the blank and remove them from the results matrix (*see Note 17*).
11. Predict the molecular formula of detected compounds using the SIRIUS function in MZmine. Use a m/z tolerance of 10 ppm, and $[M-H]^-$ as ionization type. Select 5 candidates return (“Feature list methods” → “Identification” → “SIRIUS structure prediction”). Although SIRIUS can be used within

the MZmine environment, we recommend exporting the data and using SIRIUS software independently, for a better performance and visualization (see next Subheading 3.6). To export the results for SIRIUS, export the MS² scans of the compounds of interest in a .mgf format (“Select scans” → Right click on “Export Scan”) or use the “Export to SIRIUS” function to export all scans together (“Feature list methods” → “Export/import” → “Export to SIRIUS”).

3.6 Compound Identification

1. Open SIRIUS and import the .mgf files exported in Subheading 3.5, **step 11** (click on “Import compound” for individual spectra or on “Import” for multiple compounds). When the MS² files are imported, verify that the precursor mass has been assigned correctly or correct it manually.
2. Click on “Compute All” to run the molecular formula prediction and structure elucidation steps (click on “SIRIUS” and “CSI:FingerID,” selecting “All included DBs”).
3. In “Sirius overview” tab, the results will be displayed (Fig. 4). Select the molecular formula with the highest “Sirius Score” as the potential candidate whenever it makes biological sense. In the mass spectrum, you will be able to see the MS fragments that can be explained for the predicted formula (signals in green). A hierarchical structure tree with all the fragments is also shown on the display.

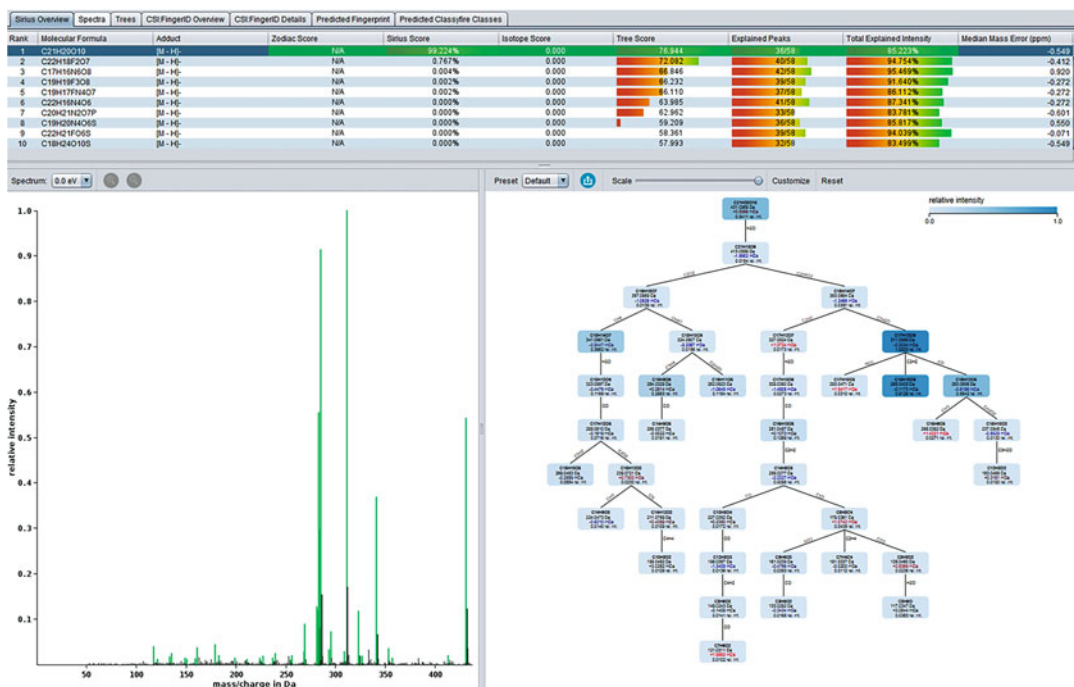


Fig. 4 Example of results obtained by SIRIUS software

4. Click on the “CSI:FinderID Details” tab to see the structural elucidation results. For phenolic compounds from plants, we recommend selecting the candidates with a highest percentage described in the libraries “Natural Products,” “PlantCyc,” “HMDB,” “GNPS,” and “KEGG.”
5. Although you can select the first highest ranked candidate as potential compound, we recommend selecting the first ones and comparing them with experimental MS/MS databases (MassBank Europe [10], MoNA—MassBank of North America [11]) or bibliographic data (*see* Notes 18 and 19).
6. Another tool to aid identification that is currently increasing in popularity is GNPS. You can export the data directly from MZmine to import it into GNPS (“Feature list methods” → “Export/import” → “Export to GNPS”). For more information on the use of this platform, we recommend reading the GNPS documentation [23].

4 Notes

1. The volumes of mobile phases to prepare depend on the number of extract samples to be analyzed in each particular study.
2. This protocol is based on an ACQUITY UPLC H-Class System (Waters, Milford, MA, USA) coupled to a QTOF-MS (SYNAPT G2, Waters Corp., Milford, MA, USA). This protocol can be easily adapted to other UHPLC systems. If using HPLC equipment, consider the maximum pressure of the instrument to select the column or modify the gradient accordingly.
3. Since the extract could be obtained by different extraction techniques (e.g., solid maceration, supercritical fluid extraction, microwave-assisted extraction, ultrasound-assisted extraction) [24], the solvent to dissolve it can vary. We recommend using the same solvent composition as that used in the extraction process (i.e., the solvent composition before the solvent drying-down process).
4. Given the photosensitivity of some phenolic compounds [25], all extract solution preparation should be carried out with protection from light. Tophaceous glass materials and HPLC vials should be used, or use protection by aluminum foil.
5. Depending on the composition and concentration of the original extract, the starting concentration value of 5 mg/L can be modified. We consider this value as a good starting point, and depending on the preliminary results, it might be more appropriate to use an extract with a higher or lower concentration. It is important not to use very high starting concentrations so as not to saturate the MS detector signal.

6. In case the complete dissolution of the extract is not achieved, use ultrasound for a few minutes to facilitate the dissolution process.
7. The gradient proposed in this protocol can be applied in both HPLC and UHPLC instruments. However, for UHPLC instruments, it could be cut to a duration of about 10–15 minutes maintaining the proportions.
8. The gradient proposed in this protocol can be basic to make a general phenolic profiling of a plant sample. If the sample to be analyzed is enriched in a particular phenolic family, we suggest that the gradient be optimized to improve the separation of those specific compounds.
9. If there is possibility of resources, we also recommend analyzing the samples using a positive ionization mode.
10. Although the parameters of an MS^E method are detailed, the rest of the protocol can be followed with another conventional MS/MS method.
11. This information is from specific calibration method of the QTOF/MS (SYNAPT G2, Waters Corp., Milford, MA, USA) instrument. Use the calibration method established in the manuals of each MS instrument.
12. For MS^E data collected by Waters instruments, we recommend to use Symphony software for data conversion.
13. Use a filter to remove noise signals, so the size of the files will be smaller (Fig. 2).
14. The noise level can vary between instruments and also depend on the experimental conditions. Click on “show preview” and check several MS¹ scans to visually inspect the noise level (Fig. 3).
15. The parameters presented in Table 2 should be optimized for each particular instrument. You can use the “Show preview” option to view the results of the parameters selected in each stage.
16. A retention time filter can be used for the last region of the chromatogram corresponding to the cleaning and equilibration of the LC system (e.g., last 5–10 min).
17. Use a fold change (area extract samples/area blanks) cutoff of 10.
18. Even if the data are compared with the MS/MS databases or bibliography, characterization at 100% efficiency cannot be guaranteed until the data is compared with that of a chemical standard. This point is very important in the case of isomers that have similar MS/MS spectra (especially stereoisomers). We recommend following the levels of identification proposed by the Metabolomics Standard for this task [26].

19. These identification tools are currently oriented to MS/MS spectra acquired in data-dependent acquisition mode. For independent data acquisition such as MS^E spectra, the results must be analyzed carefully. These tools may not be able to correctly predict the molecular formula and/or structure of the compound, especially when several compounds are co-eluting. For these cases, it is necessary to use previously data-independent MS/MS deconvolution strategies (for example: MS-DIAL pipeline) [27].

References

1. Del Rio D, Rodriguez-Mateos A, Spencer JPE et al (2013) Dietary (poly)phenolics in human health: structures, bioavailability, and evidence of protective effects against chronic diseases. *Antioxid Redox Signal* 18:1818–1892. <https://doi.org/10.1089/ars.2012.4581>
2. Tsao R (2010) Chemistry and biochemistry of dietary polyphenols. *Nutrients* 2:1231–1246
3. Han X, Shen T, Lou H (2007) Dietary polyphenols and their biological significance. *Int J Mol Sci* 8:950–988. <https://doi.org/10.3390/i8090950>
4. Bravo L, Sources D, Significance N (2009) Polyphenols: chemistry, dietary sources, metabolism, and nutritional significance. *Nutr Rev* 56:317–333. <https://doi.org/10.1111/j.1753-4887.1998.tb01670.x>
5. Patil VM, Masand N (2018) anticancer potential of flavonoids: chemistry, biological activities, and future perspectives. In: *Studies in natural products chemistry*
6. Fernández-Ochoa Á, Leyva-jiménez FJ, De la Luz Cádiz-Gurrea M et al (2021) The role of high-resolution analytical techniques in the development of functional foods. *Int J Mol Sci* 22:3220. <https://doi.org/10.3390/ijms22063220>
7. Zhang A, Sun H, Wang X (2018) Mass spectrometry-driven drug discovery for development of herbal medicine. *Mass Spectrom Rev* 37:307–320. <https://doi.org/10.1002/mas.21529>
8. Levy AJ, Oranzi NR, Ahmadireskety A et al (2019) Recent progress in metabolomics using ion mobility-mass spectrometry. *TrAC Trends Anal Chem* 116:274–281. <https://doi.org/10.1016/J.TRAC.2019.05.001>
9. Kind T, Tsugawa H, Cajka T et al (2018) Identification of small molecules using accurate mass MS/MS search. *Mass Spectrom Rev*
10. MassBank Europe, High Quality Mass Spectral Database. <https://massbank.eu/MassBank/>. Accessed 30 May 2021
11. MoNA - MassBank of North America. <https://mona.fiehnlab.ucdavis.edu/>. Accessed 30 May 2021
12. FoodDB. www.fooddb.ca. Accessed 30 May 2021
13. Wishart DS, Feunang YD, Marcu A et al (2018) HMDB 4.0: The human metabolome database for 2018. *Nucleic Acids Res* 46:D608–D617. <https://doi.org/10.1093/nar/gkx1089>
14. Schmelzer K, Fahy E, Subramaniam S, Dennis EA (2007) The lipid maps initiative in lipidomics. *Methods Enzymol* 432:171–183. [https://doi.org/10.1016/S0076-6879\(07\)32007-7](https://doi.org/10.1016/S0076-6879(07)32007-7)
15. Plant Metabolic Network (PMN). www.plantcyc.org. Accessed 30 May 2021
16. Tsugawa H, Kind T, Nakabayashi R et al (2016) Hydrogen rearrangement rules: Computational MS/MS fragmentation and structure elucidation using MS-FINDER software. *Anal Chem*. <https://doi.org/10.1021/acs.analchem.6b00770>
17. Ruttkies C, Schymanski EL, Wolf S et al (2016) MetFrag relaunched: incorporating strategies beyond in silico fragmentation. *J Cheminform* 8:3. <https://doi.org/10.1186/s13321-016-0115-9>
18. De la Luz Cádiz-Gurrea M, Pinto D, Delerue-Matos C, Rodrigues F (2021) Olive fruit and leaf wastes as bioactive ingredients for cosmetics—a preliminary study. *Antioxidants* 10:1–18. <https://doi.org/10.3390/antiox10020245>
19. Adusumilli R, Mallick P (2017) Data conversion with ProteoWizard msConvert. Humana Press, New York, NY, pp 339–368
20. Pluskal T, Castillo S, Villar-Briones A, Orešič M (2010) MZmine 2: modular framework for processing, visualizing, and analyzing mass spectrometry-based molecular profile data. *BMC Bioinformatics* 11:395. <https://doi.org/10.1186/1471-2105-11-395>

21. Dührkop K, Fleischauer M, Ludwig M et al (2019) SIRIUS 4: a rapid tool for turning tandem mass spectra into metabolite structure information. *Nat Methods* 16:299–302. <https://doi.org/10.1038/s41592-019-0344-8>
22. Du-Lab Team (2019) ADAP user manual, version 4.0.0
23. Aron AT, Gentry EC, McPhail KL et al (2020) Reproducible molecular networking of untargeted mass spectrometry data using GNPS. *Nat Protoc* 15:1954–1991. <https://doi.org/10.1038/s41596-020-0317-5>
24. Ameer K, Shahbaz HM, Kwon JH (2017) Green extraction methods for polyphenols from plant matrices and their byproducts: a review. *Compr Rev Food Sci Food Saf* 16: 295–315
25. Pires FB, Dolwitsch CB, Dal Prá V et al (2017) Qualitative and quantitative analysis of the phenolic content of *Connarus* var. *angustifolius*, *Cecropia obtusa*, *Cecropia palmata* and *Mansoa alliacea* based on HPLC-DAD and UHPLC-ESI-MS/MS. *Rev Bras Farmacogn* 27:426–433. <https://doi.org/10.1016/j.bjp.2017.03.004>
26. Sumner LW, Amberg A, Barrett D et al (2007) Proposed minimum reporting standards for chemical analysis: Chemical Analysis Working Group (CAWG) Metabolomics Standards Initiative (MSI). *Metabolomics* 3(3):211–221. <https://doi.org/10.1007/s11306-007-0082-2>
27. Tsugawa H, Cajka T, Kind T et al (2015) MS-DIAL: data-independent MS/MS deconvolution for comprehensive metabolome analysis. *Nat Methods* 12:523–526. <https://doi.org/10.1038/nmeth.3393>



Quantitative Determination of Antioxidant Compounds in Fruits Using Liquid Chromatography Tandem Mass Spectrometry

Giovana Anceski Bataglion

Abstract

Quantification of antioxidant compounds in fruits is important in many studies of food chemistry, including those regarding the investigation of biological activities and recovery of bioactive compounds from by-products. In this chapter, we describe a protocol for quantitatively determining antioxidant compounds in fruits using LC-MS/MS. Demonstration of the method is shown for different classes of compounds, including phenolic acids (hydroxybenzoic and hydroxycinnamic acids) and flavonoids (flavonols, flavanones, flavan-3-ols, and flavones). The protocol details sample preparation, instrumental analysis, data interpretation, and quantification. Sample preparation involves extraction that is assisted by ultrasound or microwaves followed by a purification step using solid phase extraction. Analyses are carried out using selected reaction monitoring with two transitions for each compound. Two methods of quantification are described: internal standard method and standard addition method. They are both discussed based on the availability of standards, sample number, and matrix effects.

Key words LC-MS/MS, Phenolic compounds, Phenolic acids, Flavonoids, Fruits

1 Introduction

Fruits are rich in various bioactive compounds and represent a valuable component of a healthy diet [1–3]. They are consumed in natura and used in ice-creams, candies, desserts, jams, marmalades, and other fruit preserves. In addition, there has been an increased interest in using by-products from fruit processing as natural additives to improve the quality of food products. In this sense, their use as a functional food and as carriers for nutrients has attracted the attention of food scientists [4]. This interest is due to the biological activities that compounds in fruits have in the human body, such as decreases in total cholesterol, high-density lipoprotein cholesterol, low-density lipoprotein cholesterol, tumor initiation/promotion, platelet aggregation, and eicosanoid synthesis.

Antioxidant and antimutagenic activities are also related to the bioactive compounds contained in fruits; although they occur in small quantities and vary widely in chemical structure and function [1–3, 5–8]. In fruits, phenolic molecules are reported as the main bioactive compounds responsible for providing a number of health benefits [3].

Phenolic compounds are characterized by the presence of at least one aromatic ring with one or more hydroxyl functional groups attached. As a result, they can vary from simple phenolic acids to complex oligomers such as procyanidins and condensed tannins. Phenolic compounds can be classified regarding their water solubility or in two main groups, flavonoids and non-flavonoids, which are then divided into subgroups. In the group containing the non-flavonoids, phenolic acid is the most important subgroup of phytochemicals in fruits. Phenolic acids are essentially derivatives of benzoic and cinnamic acids. Flavonoids can be classified into seven subgroups: flavonols, flavones, isoflavones, flavanones, anthocyanidins, flavanols, and flavanol [3, 9]. The phenolic composition in fruits varies considerably, with a special contribution of flavonols, flavan-3-ols, anthocyanins, and hydroxycinnamic and hydroxybenzoic acids [3]. Additionally, phenolic compounds can exist in their glycosylated forms or esterified with gallic acid, as epigallocatechin [3, 9]. The structural diversity of phenolic compounds associated with their low concentrations and complexity of food matrices are reasons for requiring sensitive and selective techniques for both qualitative and quantitative analyses [10].

Most analytical methods for determining phenolic compounds are based on liquid chromatography with detection based on spectrophotometric and/or mass spectrometric techniques. Several configurations are reported for liquid chromatography coupled to mass spectrometry, including the most recent developments in both techniques [3, 10]. Regarding the separation technique, the conventional high performance liquid chromatography (usually with columns with particle size of 5 μm) has been enhanced to become ultra-high performance liquid chromatography (columns with particle size lower than 2 μm). Improved resolution, higher peak efficiency, shorter retention times, narrower peaks, lower detection/quantification limits, and reduced solvent consumption are considered the main advantages of using sub-2 μm columns. Regarding mass spectrometry, single low-resolution analyzers have been replaced to tandem and/or high-resolution instruments. Tandem mass spectrometry using a triple quadrupole is mostly used for quantitative purposes. Improved selectivity and signal-to-noise ratio, lower detection/quantification limits, and the variety of experiments are considered the main advantages of triple quadrupole tandem mass spectrometry [10].

Methods for determining phenolic compounds in fruits usually require steps such as lyophilization, extraction, purification, analysis, and quantification. Usually, the freeze-dried powder is subjected to solid-liquid extraction, which can be assisted by ultrasound or microwaves [9, 11, 12]. The extraction of phenolic compounds has been performed using different solvents, with a mixture of ethanol: water (80:20, v/v) being considered a good composition for obtaining phenolic acids and flavonoids. Depending on the matrix, a purification step is carried out via solid phase extraction (SPE) using a variety of adsorbents and sizes [9, 13, 14]. In general, C18 adsorbents present good recoveries for flavonoids, whereas the polymeric ones give good results for both flavonoids and phenolic acids. Chromatographic separation is predominantly carried out in reversed-phase mode (C18 columns) using acidified water and organic solvent (methanol or acetonitrile) as phases A and B, respectively [3, 10]. Electrospray ionization (ESI) in the negative ion mode is the most common choice for both flavonoids and phenolic acids. For quantitative purposes, using triple quadrupole, selected reaction monitoring (SRM) is preferable [10, 15]. Quantification of phenolic compounds in fruits has been performed using different strategies. Like for other complex matrices, standard addition and internal standard methods are preferable to the external calibration method [10].

In this chapter, we describe a protocol for determining phenolic compounds in fruits using LC-MS/MS. In detail, we present the steps of sample preparation, optimization of spectrometric parameters, analysis and quantification.

2 Materials

2.1 Equipment

1. Analytical balance.
2. Centrifuge.
3. Lyophilizer.
4. Vortex mixer.
5. Water purification system.
6. Ultrasonic bath or microwave system.
7. Nitrogen gas evaporator (*see Note 1*).
8. Liquid chromatograph coupled to a tandem mass spectrometer with its own pump and gas supply (*see Note 2*).
9. Single syringe infusion pump.

2.2 Supplies and Chromatography Accessories

1. Glass centrifuge tube (*see Note 3*).
2. Glass syringe (*see Note 3*).
3. Glass vials (2.0 mL) with Teflon cap for chromatographic analysis.

4. Volumetric glass flasks (*see Note 3*).
5. Glass Pasteur pipettes (*see Note 3*).
6. Vacuum filtration system (47 mm, 300 mL funnel, 1000 mL receiving flask).
7. Vacuum manifold for SPE.
8. Micropipettes and tips.
9. Membrane filters of 0.2 μm (*see Note 4*).
10. Syringe filters of 0.22 or 0.45 μm (*see Note 4*).
11. C18 column (*see Note 5*).
12. SPE cartridges (*see Note 6*).

2.3 Chemicals, Solvents, and Gases

1. Standards of antioxidant compounds, such as phenolic acids (hydroxycinnamic and hydroxybenzoic acids) and flavonoids (flavonols, flavanones, flavan-3-ols, and flavones) (*see Table 1 and Note 7*).
2. Isotope-labeled internal standards, at least one for the phenolic acids and another for the flavonoids (*see Note 7*).
3. Acetonitrile (ACN, LC-MS grade), methanol (MeOH, LC-MS grade), ethanol (EtOH, LC-MS grade), and formic acid (FA, LC-MS grade).
4. Ultrapure water with resistivity of 18.2 M Ω .cm.
5. Nitrogen gas for drying extracts.

2.4 Standard Solutions and Mobile Phase

1. Individual stock solutions: Each standard (analytes and internal standards) is individually dissolved in EtOH to prepare stock solutions at 1.0 mg/mL (*see Note 8*).
2. Individual intermediate solutions: Each stock solution is diluted to yield an intermediate solution at 5.0 $\mu\text{g/mL}$ (*see Note 9*).
3. Working solutions: Individual solutions of 0.5 $\mu\text{g/mL}$ (500 ng/mL) for optimization of instrumental parameters are prepared from intermediate solutions by diluting them ten times (*see Note 10*).
4. Mixed solution A: Prepare one mixed solution at 5.0 $\mu\text{g/mL}$ from all individual analyte solutions (*see Note 9*).
5. Mixed solution B: Prepare one mixed solution at 5.0 $\mu\text{g/mL}$ from all individual isotope-labeled standard solutions (*see Note 9*).
6. Mixed solution C: Prepare one mixed solution at 0.5 $\mu\text{g/mL}$ from the mixed solution A by diluting it ten times (*see Note 11*).
7. Calibration curve using the internal standard method: Prepare solutions of different concentrations of analytes and equal

Table 1
Common antioxidant compounds and their retention times, precursor ions and product ions

Compound	Retention time	[M – H] ⁻	Fragments	Fragments for SRM
Pyrogallol	0.61	125	69,79,81,97	79,69
Quinic acid	0.72	191	85,93,111,127	85,93
Gallic acid	0.81	169	79,107,125	125,79
Homogentisic acid	0.91	167	108,123	123,108
Protocatechuic acid	1.37	153	81,91,93,109,	109,91
4-Hydroxybenzoic acid	2.52	137	93	93
2,5-Dihydroxybenzoic acid	2.53	153	81,109	109,81
(+)-Catechin	4.42	289	245,203,123, 125,109	245,125
(-)-Epicatechin	4.59	289	109,123,125,245	125,109
Bergenin	4.64	327	192,207,234,249	192,207
(-)-Epigallocatechin	4.85	305	125,167,179,219	125,179
Caffeic acid	5.26	179	87,107,135	135,107
Vanillic acid	5.31	167	108,152	152,108
Chlorogenic acid	5.33	353	85,161,191	191,85
Syringic acid	6.02	197	121,123,138,153	121,153
(-)-Epigallocatechin gallate	6.63	457	125,169,305	169,305
Ethyl Gallate	6.57	197	78,97,124,169	124,169
Ellagic acid	6.79	301	145,185,201,229	185,145
<i>p</i> -Coumaric acid	6.96	163	93,119	119
Ferulic acid	7.45	193	117,134,149,178	117,134
(-)-Epicatechin gallate	7.52	441	125,169,271,289	169,289
Sinapinic acid	7.65	223	149,164,179,193	149,164
Propyl gallate	8.08	211	78,124,169	124,169
Myricetin	8.15	317	107,121,151,179	151,179
Isovitexin	8.24	431	269,283,311,341	311,341
Naringenin	8.24	579	271	271
Hesperidin	8.33	609	301	301
Rutin	8.47	609	301	301
Diosmin	8.65	607	301	301
Quercetin	8.89	301	107,121,151,179	121,151
Cinnamic acid	8.96	147	103	103
Hesperetin	9.53	301	164,174,199,215	164,215
Luteolin	9.61	285	93,133,151,	133,107

(continued)

Table 1
(continued)

Compound	Retention time	[M – H] [–]	Fragments	Fragments for SRM
Kaempferol	9.88	285	93,117,159,185,	93,185
Apigenin	9.97	269	117,149,151	117,151
Isorhamnetin	10.00	315	117,149,151	107,151

Table 2
Calibration curves based on internal standard method

Analyte concentration (ng/mL)	Aliquot of mixed solution (μL)	Aliquot of internal standard solution (μL)	Water (μL)
10	20 ^a	100 ^b	880
25	50 ^a	100 ^b	850
50	100 ^a	100 ^b	800
75	150 ^a	100 ^b	750
100	200 ^a	100 ^b	700
250	50 ^c	100 ^b	850
500	100 ^c	100 ^b	800
750	150 ^c	100 ^b	750
1000	200 ^c	100 ^b	700

^aMixed solution C with analytes at 0.5 μg/mL

^bMixed solution B with internal standards at 5.0 μg/mL. The final concentration of internal standards is constant at 0.5 μg/mL

^cMixed solution A with analytes at 5.0 μg/mL

concentrations of internal standards. Suggested concentrations for analytes: 10, 25, 50, 75, 100, 250, 500, 750, and 1000 ng/mL. Suggested concentration for internal standards: 500 ng/mL. Table 2 shows mixing volumes for calibration curve solutions (*see Note 12*). Calibration curve using the standard addition method is discussed below.

8. Mobile phase A: Water acidified with FA (0.1%, v/v) (*see Note 13*).
9. Mobile phase B: MeOH.
10. Wash solvent: MeOH.
11. Seal wash solvent: MeOH.

2.5 Samples

1. Fruits of interest may be purchased in supermarkets, open air markets, from street vendors, or may be collected directly from a tree that grows naturally or in orchards. This protocol can also be applied to fruit juices though with slight modifications.

3 Methods

3.1 LC-MS/MS Analysis

1. Each individual solution at 500 ng/mL is injected into a mass spectrometer using a syringe pump at a flow rate of 5.0 $\mu\text{L}/\text{min}$ (*see Note 14*).
2. First, identify the m/z value for the precursor ion $[M - H]^-$ in the full scan spectrum obtained in the negative ion mode (*see Note 15*). Table 1 lists such values for common antioxidant compounds.
3. Once the precursor ion has been visualized, change the operation mode to product ion scan experiment and identify the major fragments for each compound (*see Note 15*). Table 1 lists the values for common antioxidant compounds.
4. Change the operation mode to SRM (MRM, multiple reaction monitoring, in some software), set at least two transitions (precursor ion > product ion) for each compound and optimize them regarding CE and other voltages (*see Note 16*). Table 1 lists two possible transitions for common antioxidant compounds.
5. Once the previous steps have been done for all compounds, the transitions and their respective parameters are put together in a single method file. Additionally, the syringe pump is disconnected from the mass spectrometer, and an LC system is coupled to it.
6. Set the ESI parameters as suggested by the user's manual for the flow rate used (*see Note 17*).
7. Connect a C18 column and use water acidified with FA (0.1%, v/v) as mobile phase A and MeOH as mobile phase B (*see Note 13*).
8. Set the LC gradient profile as follows: 0–1 min (5% B), 1–4 min (5–60% B), 4–7 min (60–70% B), 7–10 min (70–100% B), 10–12 min (100% B), 12–13 min (100–5% B), 13–15 min (5% B) (*see Note 18*).
9. Other LC parameters, such as flow rate (0.45 mL/min) and injection volume (5.0 μL), need to be set.
10. Put vials containing the blank and individual standard solutions into the autosampler chamber, and run them to verify retention time, peak shape, and purity of compounds (*see Note 19*).

11. Put vials containing the blank, mixed standard solutions and samples into the autosampler chamber and run them to construct calibration curves and quantify the analytes in the fruits.

3.2 Sample Preparation

3.2.1 Extraction

1. Wash fruits with water to eliminate contaminants and dust.
2. Weigh the fruits before removing any parts or before lyophilization.
3. Seed and peel may be removed depending on the species and the study objectives. Cut the fruits or use a food processor/blender to obtain small pieces. Then, freeze the material in a proper recipient to lyophilizing it at a later time.
4. Lyophilize the pieces of fruits (whole or pulp) while protecting them from light using aluminum foil.
5. Weigh the freeze-dried fruits and calculate the percentage of water.
6. Macerate the freeze-dried powder in a pistil and mortar.
7. Place about 1.0 g of freeze-dried fruit in a glass tube (*see Note 20*).
8. For quantification purposes using the internal standard method, they are added into fruit samples before the extraction procedure. Surrogate solution (mixed solution B with internal standards at 5.0 µg/mL; 100 µL) is added to the freeze-dried fruit before extraction. Alternatively, the analyst may choose the method of standard addition for quantification purposes. In this case, several extractions are done using fruit samples spiked with different quantities of analytes, as shown in Table 3 (*see Notes 7 and 21*).
9. Add 5.0 mL of an EtOH/water solution (80:20, v/v) to the freeze-dried extract, and then the mixture is mixed in a vortexer (*see Note 22*).
10. The mixture is subjected to extraction of the antioxidant compounds, which may be assisted by microwaves or ultrasound (*see Note 23*).
11. After releasing the phenolic compounds from the solid matrix, the mixture is centrifuged at $2264 \times g$ for 5 min.
12. Collect the supernatant with a glass Pasteur pipette and transfer it to a glass tube. Repeat extraction following the procedure previously described.
13. Supernatants are pooled and the solvent evaporated with a gentle stream of nitrogen gas to eliminate EtOH, and then lyophilized (*see Note 24*). Weigh the dried extract.
14. The raw extract without purification may be analyzed. In addition, a clean-up step using SPE cartridges (C18 or polymeric adsorbents) may improve quantitative results (*see Note 25*).

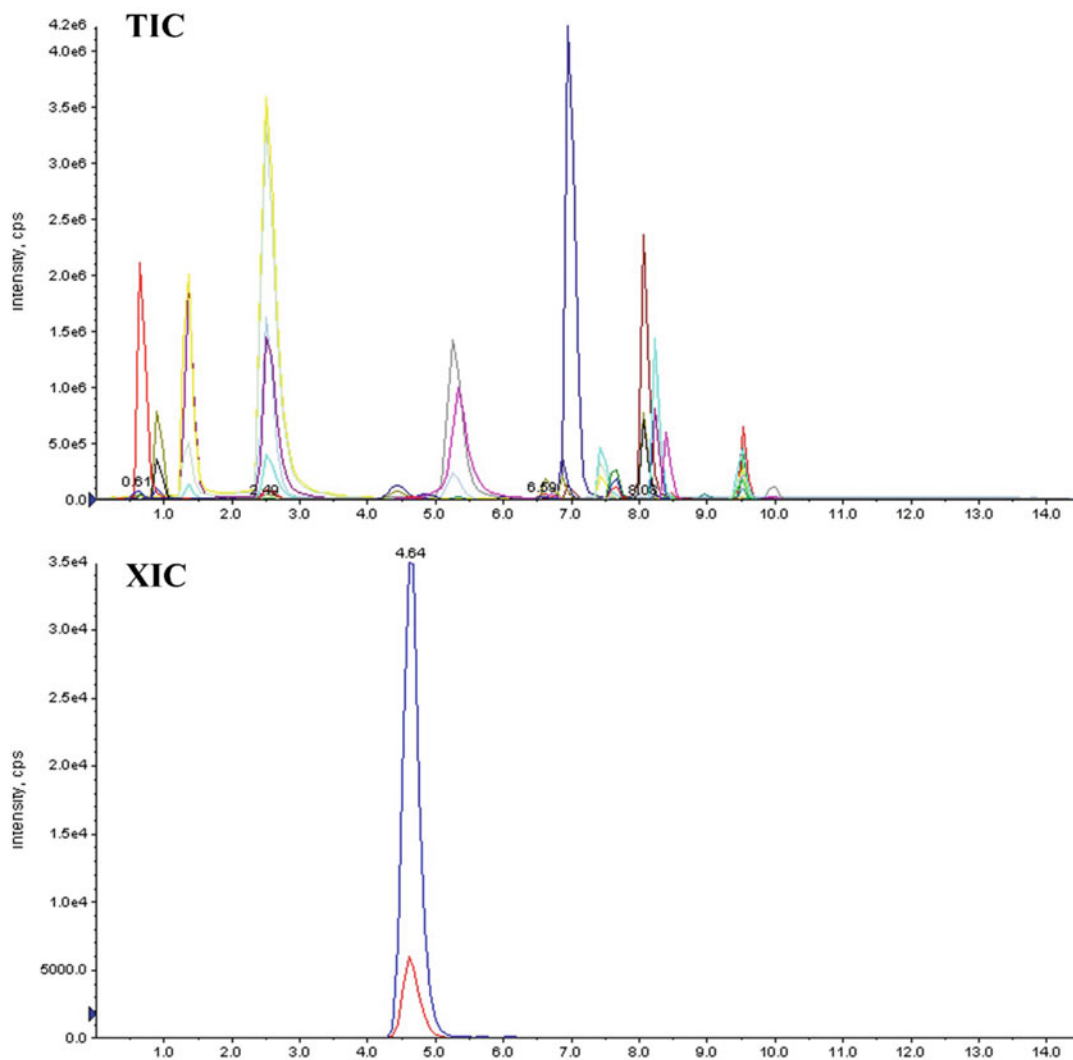


Fig. 1 Total ion chromatogram (TIC) and extracted ion chromatogram (XIC) for bergenin

15. For instrumental analysis, redissolve the dried extract with 200 μL of MeOH, add 800 μL de water and, then filter it through a 0.22 or 0.45 μm filter to remove particles before injection.
16. Transfer the filtered sample solution to glass vials (2.0 mL) and proceed to LC-MS/MS analysis. Occasionally, the concentrations of some compounds in the extract solution may be too high (outside of calibration curve range), thus dilution needs to be carried out.

3.3 Data Processing

Figure 1 shows the total ion chromatogram (TIC) and the extracted ion chromatogram (XIC) for an antioxidant compound (bergenin).

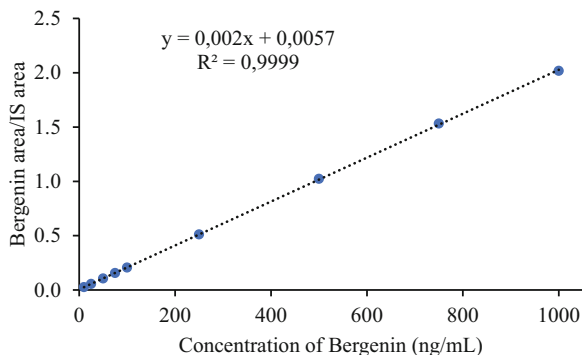


Fig. 2 Curve calibration for bergenin based on internal standard method

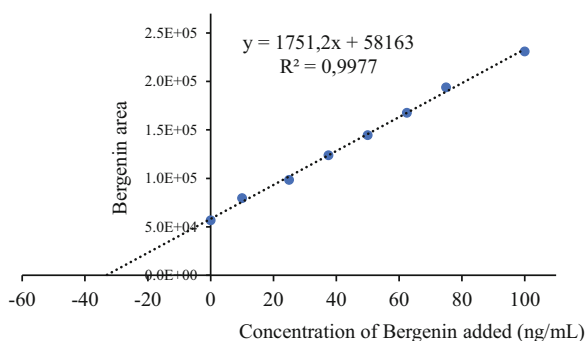


Fig. 3 Curve calibration for bergenin based on standard addition method

1. For standard solutions, identify each analyte and internal standard by referring to the transitions and retention times of the standards (*see* Fig. 1 and Table 1).
2. For samples, identify each analyte by comparing its retention time and transitions to those of the standards (*see* **Note 26**).
3. Follow instructions 4–6 and 7–8 for internal standard and standard addition methods, respectively.
4. Internal standard method: Integrate the peak for each analyte and internal standard in the solutions with different concentrations in order to construct calibration curve (*see* Fig. 2 and Table 2).
5. Internal standard method: Construct the calibration curve by plotting the ratio of the analyte signal to the internal standard signal as a function of the analyte standard concentration. The curve equation is used to calculate the analyte concentration in unknown samples (*see* **Note 27**, *see* Fig. 2 and Table 2).
6. Internal standard method: Integrate the peak for each analyte and internal standard in the sample solutions and calculate the ratio of the analyte signal to the internal standard signal. This

Table 3
Calibration curve based on internal addition method

Analyte concentration added (ng/mL)	Aliquot of mixed solution (μL) ^a
0	0
10	20
25	50
37.5	75
50	100
62.5	125
75	150
100	200

^aMixed solution C with analytes at 0.5 $\mu\text{g}/\text{mL}$

ratio is considered the y of the curve equation to find the analyte concentration (*see* Fig. 2 and Table 2).

7. Standard addition method: Integrate the peak for each analyte in the solutions from extractions with different additions of the standards (*see* Fig. 3 and Table 3).
8. Standard addition method: Construct the calibration curve by plotting the analyte signal as a function of the concentration added to the sample. The x-intercept gives the concentration of the analyte in the sample without spiking the standards (*see* **Note 28**, *see* Fig. 3 and Table 3).
9. Consider the appropriate calculations and/or dilutions to express concentration of the analyte as I) mass/mass of extract, II) mass/mass of dried fruit, III) mass/mass of fresh fruit (*see* **Note 29**).

4 Notes

1. A nitrogen gas evaporator may be a homemade one made with a glass Pasteur pipette coupled to a hose and a support to fix tubes containing samples.
2. Herein, demonstrations were based on results obtained using an 1200 Series HPLC system with a quaternary pump (Agilent Technologies, Santa Clara, USA) coupled to a 4000 Q-Trap system (Applied Biosystems Sciex, Foster City, USA) with an ESI source. Data acquisition and processing were executed using Analyst 1.6.3 (Applied Biosystems Sciex, Foster City, USA).

3. Solvent may leach compounds out of ordinary plastic tubes, thus contaminating samples and resulting in high noise baseline. Therefore, glass tubes or plastic of high quality should be used.
4. Membrane and syringe filters of nylon, PTFE (hydrophobic and hydrophilic) or PVDF. For columns with a particle size lower than 3 μm , 0.22 μm filters are preferable.
5. Herein, a Kinetex C18 column (particle size of 2.6 μm , length of 50 mm, and internal diameter of 2.1 mm) (Phenomenex, Aschaffenburg, Germany) was used. If possible, choose a C18 end-capped column with particle size lower than 3 μm .
6. SPE cartridges (C18 or polymeric adsorbents) may be used in a clean-up step. Usually, C18 provides good recoveries for flavonoid aglycones, whereas adsorbents based on polystyrene-divinylbenzene-*N*-vinylpyrrolidone copolymers yield good recoveries for both phenolic acids and flavonoids. Cartridges of 200 mg are typically used.
7. Other similar compounds (phenolic acids, flavonoids—aglycones, and glycosylated and esterified derivatives) may be included in the method. Ideally, an isotope-labeled internal standard should be used for each analyte, which is often impossible. Instead, one isotope-labeled internal standard may be used for each compound class for evaluating recovery. Another possibility is using one of the available compounds as internal standard. Its absence in the sample is indispensable. Thus, a preliminary analysis of the sample without any addition is done. The compounds that were not detected in that previous analysis may be chosen as internal standards for the following ones. In addition, the analyst may choose not to use any internal standard and quantify compounds using the standard addition method (*see* **Note 21**).
8. For instance, a mass of 10 mg of the standard is weighed and transferred to a 10 mL volumetric glass flask, which is then completed with solvent up to the volumetric mark to obtain a concentration of 1.0 mg/mL. For the isotope-labeled internal standards, a quantity of 1.0 mg is usually available for purchase. Some flavonoid aglycone standards are difficult to dissolve in EtOH. Therefore, a minimum amount of a less polar solvent is required to dissolve the solid before the addition of EtOH. Store all solutions at $-20\text{ }^{\circ}\text{C}$ to avoid photolysis, oxidation, and solvent evaporation.
9. Use the dilution equation ($C_1 V_1 = C_2 V_2$), where C_1 is the initial concentration, V_1 is the initial volume, C_2 is the final concentration, and V_2 is the final volume. For instance, an aliquot of 25 μL of the stock solution is transferred to a

5.0 mL volumetric flask, then it is completed with MeOH up to the volumetric mark to yield a concentration of 5.0 $\mu\text{g}/\text{mL}$.

10. Use the dilution equation again. For instance, an aliquot of 100 μL of the intermediate solution is transferred to a 2.0 mL glass vial. Add 900 μL of MeOH to yield a concentration of 0.5 $\mu\text{g}/\text{mL}$. This solution volume is usually enough to optimize instrumental parameters. Depending on equipment sensitivity and molecule ionization efficiency, a more diluted solution may be required.
11. Transfer an aliquot of 500 μL of the mixed solution A to a 5.0 mL volumetric flask, and then complete it with MeOH up to the volumetric mark to yield a concentration of 0.5 $\mu\text{g}/\text{mL}$.
12. Considering C_1 as the concentration of the mixed solution A or C and V_2 of 1.0 mL, use the dilution equation to calculate V_1 , which is the aliquot needed to prepare solutions with C_2 of 10, 25, 50, 75, 100, 250, 500, 750, and 1000 ng/mL . Table 2 shows the mixing volumes of the calibration curve solutions. Such a wide range of concentration is due to the high variability of the concentrations found for phenolic compounds in fruits.
13. Preparation of the mobile phase A: Measure out 999 mL of ultrapure water and transfer it to a glass bottle. Add 1 mL of FA to it. Prepare a fresh mobile phase before use. Filter it through 0.2 or 0.45 μm membrane filter using a vacuum system and, then degas it in ultrasonic bath for 10 min. Use inline filters in HPLC solvent bottles.
14. MS/MS optimization is individually carried out for each compound from the working solution of 500 ng/mL . Depending on equipment sensitivity and molecule ionization efficiency, a more diluted solution may be required. Optimization from the individual standard is recommended because there are analytes that have the same molecular mass. In addition, the fragmentation of phenolic compounds is very similar, and this may occur in the source, creating several possibilities of interferences. Before starting the optimization, make sure the mass analyzers are calibrated.
15. Using a syringe pump with a flow rate of 5.0 $\mu\text{L}/\text{min}$, source parameters may be set as suggested by the equipment user manual. Herein, the following ESI parameters were set in the negative ion mode: ion spray voltage at 4.0 kV, nebulizer gas at 20 psi, and curtain gas at 10 psi. For full scan experiments, set a scan range of mass at m/z 100 to 700 (or according to analyte mass). For product ion scan experiments, set the m/z of the precursor ion in the first mass analyzer and set a scan range of mass in the third one—from m/z 50 to a value that ensures that you see $[\text{M} - \text{H}]^-$ in the spectrum. Additionally, vary collision energy (CE) automatically or manually to ensure a proper

spectrum—low intensity for the precursor ion and high intensity for the product ions.

16. It is strongly recommended that more than one precursor ion > product ion transition is monitored to demonstrate the specificity of the quantitative analysis. If it is possible, choose product ions that are not derived from common losses, such as CO₂ and H₂O. At the same time, choose the most abundant product ions. If in doubt, set more than two transitions in order to decide afterwards which one will be discharged. Automatically or manually optimize the MS voltages as CE, CXP, DP, and EP. The election of the quantifier and qualifier transitions is based on their intensity. Usually, the highest one is elected as the quantifier transition.
17. When the MS is connected to the LC, source parameters need to be adjusted for the new flow rate. Because the optimum values differ for each equipment, optimization of the source parameters must be done. At first, preliminary analyses can be done using values suggested in the equipment user manual. Herein, the following MS parameters were set in the negative ion mode: ion spray voltage at 4.0 kV, heater gas at 40 psi, nebulizer gas at 45 psi, curtain gas at 12 psi, and ion spray temperature at 550 °C.
18. Some adjustment in the elution gradient may be required depending on the column used. The chromatographic method should contain washing and equilibration steps to ensure reproducibility of the next runs in the same sequence. When working on the reversed-phase mode, the phenolic compounds are eluted according to molecule polarity and size. Thus, phenolic acids commonly elute before flavonoid aglycones. Table 1 shows the retention times of analytes under the chromatographic conditions described herein. It is not necessary that all compounds be completely separated, except those with the same precursor and product ions such as the protocatechuic/gentisic acids, (+)-catechin/(−)-epicatechin, kaempferol/luteolin, and hesperidin/quercetin pairs.
19. Purge each device to ensure air bubbles have been removed from the pipeline before analysis. Then, download the method parameters and ensure the column is well equilibrated before analysis of the standard solutions or samples. Run some blank injections to ensure a stable baseline and reproducible retention times.
20. Ideally, the phenolic compounds should be immediately extracted after lyophilization. Similarly, the chromatographic analyses should be done immediately after extraction. If this is not possible, the freeze-dried extract must be stored at −20 °C to avoid photolysis and oxidation.

21. The choice between internal standard and standard addition methods is based on the availability of isotope-labeled standards, sample matrix, and the number of samples. For studies with one or few samples, the standard addition method is an attractive option to correct matrix effects and for obtaining proper quantification. If this quantification method is chosen, extractions are done from fruit samples spiked with different quantities of analytes. Furthermore, it is necessary to analyze the non-spiked sample to determine the original concentrations of analytes. Thus, 0, 20, 50, 75, 100, 125, 150, and 200 μL of mixed solution C with analytes at 0.5 $\mu\text{g}/\text{mL}$ are added to the freeze-dried fruit before extraction.
22. The analyst may choose other values for fruit mass and solvent volume. Consider the proportion of 5 mL/g of freeze-dried fruit.
23. For ultrasound-assisted extraction, use a frequency of 20–40 kHz at 40 °C for 15 min, protect the mixture from the light with aluminum foil. For microwave-assisted extraction, use a power level of 100 W at 40 °C for 15 min.
24. Regulate the pressure of the gas cylinder to avoid losses of compounds caused by solution splashing.
25. Similar concentrations of phenolic compounds are found for raw and purified extracts in some fruits. However, raw extracts for some fruits show a relevant matrix effect. In this case, a clean-up using SPE cartridges may help to eliminate interferences. Usually, C18 provides good recoveries for flavonoid aglycones, whereas polymeric adsorbents yield good recoveries for both phenolic acids and flavonoids. It is important to check the general instructions provided by the supplier for the conditioning and equilibration steps. Herein, we described a protocol for a clean-up using a 200 mg cartridge with a sorbent based on polystyrene-divinylbenzene-*N*-vinylpyrrolidone copolymers. The cartridge is first conditioned by rinsing it with 3 mL of methanol and is equilibrated with 3 mL of water acidified with FA (0.1%, v/v). The extract (redissolved in a minimum amount of MeOH ($\approx 250 \mu\text{L}$) and diluted in 5 mL of water acidified with FA) is loaded in the cartridge. Then, it is washed with 3 mL of water acidified with FA to remove sugars and other polar interferences. The retained phenolic compounds are eluted with 5 mL of MeOH. The extract is evaporated to dryness with a gentle stream of nitrogen gas until dry.
26. It is important to verify the ratio for the transitions monitored for confirming the identity of phenolic compounds. Thus, compare the peak area ratio between the transitions ($A_{\text{qualifier transition}}/A_{\text{quantifier transition}}$) found in sample with that observed

in the standard solution. Considering that fragmentation in tandem instruments is highly reproducible, a substantial change in this ratio indicates chemical interference in at least one of the transitions.

27. The calibration curve based on the internal standard method yields a model described by the following mathematical equation: $y = a + bx$, where y is the instrument response (peak area), b represents the slope (sensitivity), a is the intercept (background), and x represents the corresponding concentration (*see* Fig. 1).
28. The calibration curve based on standard addition method yields a model described by the following mathematical equation: $y = a + bx$. The point at $x = 0$ is the reading of the sample without the addition of standards (original concentration), whereas the other points are the reading after spiking increasing quantities of standards. Thus, the value on the x-axis at which $y = 0$, x-intercept, is the concentration of analyte in the sample without spiking (*see* Fig. 2).
29. The x-value found using the curve equation is the concentration of analyte in the vial (analyzed solution). If any dilution was done, use the following equation: $C_{\text{concentrated extract}} = C_{\text{diluted extract}} \times \frac{V_f}{V_i}$, where volume ratio is the dilution factor used. If no dilution was done, the concentration obtained using calibration curve is equal to the concentration of extract solution. For expressing concentration in analyte mass/extract mass, use the following equation: $C_{\text{analyte/extract mass}} = C_{\text{extract solution}} \times \frac{V_{\text{solution}}}{m_{\text{extract}}}$, where m_{extract} is the mass of extract and V_{solution} is the volume of solvent used for redissolving it. For expressing the concentration in analyte mass/dried fruit mass, use the following equation: $C_{\text{analyte/dried fruit mass}} = C_{\text{analyte/extract mass}} \times \frac{m_{\text{extract}}}{m_{\text{dried fruit}}}$, where m_{extract} is the mass of extract obtained after extraction from a certain mass of dried fruit ($m_{\text{dried fruit}}$). For expressing the concentration in analyte mass/fresh fruit mass, use the following equation: $C_{\text{analyte/fresh fruit mass}} = C_{\text{analyte/dried fruit mass}} \times \frac{m_{\text{dried fruit}}}{m_{\text{fresh fruit}}}$, where $m_{\text{dried fruit}}$ is the mass of material obtained after lyophilization of a certain mass of fresh fruit ($m_{\text{fresh fruit}}$).

References

1. Heleno SA, Martins A, Queiroz MJRP, Ferreira ICFR (2015) Bioactivity of phenolic acids: metabolites versus parent compounds: a review. *Food Chem* 173:501–513. <https://doi.org/10.1016/j.foodchem.2014.10.057>
2. Sun C et al (2020) Anti-diabetic effects of natural antioxidants from fruits. *Trends Food Sci Technol*. <https://doi.org/10.1016/j.tifs.2020.07.024>
3. Haminiuk CWI, Maciel GM, Plata-Oviedo MSV, Peralta RM (2012) Phenolic compounds in fruits—an overview. *Int J Food Sci Technol* 47:2023–2044. <https://doi.org/10.1111/j.1365-2621.2012.03067.x>

4. Majerska J, Michalska A, Figiel A (2019) A review of new directions in managing fruit and vegetable processing by-products. *Trends Food Sci Technol* 88:207–219. <https://doi.org/10.1016/j.tifs.2019.03.021>
5. Kris-Etherton PM et al (2002) Bioactive compounds in foods: their role in the prevention of cardiovascular disease and cancer. *Am J Med* 113:71–88. [https://doi.org/10.1016/S0002-9343\(01\)00995-0](https://doi.org/10.1016/S0002-9343(01)00995-0)
6. Ahangarpour A, Sayahi M, Sayahi M (2019) The antidiabetic and antioxidant properties of some phenolic phytochemicals: a review study. *Diabetes Metab Syndr Clin Res Rev* 13: 854–857. <https://doi.org/10.1016/j.dsx.2018.11.051>
7. Pap N et al (2021) Berry polyphenols and human health: evidence of antioxidant, anti-inflammatory, microbiota modulation, and cell-protecting effects. *Curr Opin Food Sci*. <https://doi.org/10.1016/j.cofs.2021.06.003>
8. Roleira FMF et al (2015) Plant derived and dietary phenolic antioxidants: anticancer properties. *Food Chem* 183:235–258. <https://doi.org/10.1016/j.foodchem.2015.03.039>
9. Alara OR, Abdurahman NH, Ukaegbu CI (2021) Extraction of phenolic compounds: a review. *Curr Res Food Sci* 4:200–214. <https://doi.org/10.1016/j.crf.2021.03.011>
10. Motilva MJ, Serra A, Macià A (2013) Analysis of food polyphenols by ultra high-performance liquid chromatography coupled to mass spectrometry: an overview. *J Chromatogr A* 1292:66–82. <https://doi.org/10.1016/j.chroma.2013.01.012>
11. Kumar K, Srivastav S, Sharanagat VS (2021) Ultrasound assisted extraction (UAE) of bioactive compounds from fruit and vegetable processing by-products: a review. *Ultrason Sonochem* 70:105325. <https://doi.org/10.1016/j.ultsonch.2020.105325>
12. Dzah CS et al (2020) The effects of ultrasound assisted extraction on yield, antioxidant, anti-cancer and antimicrobial activity of polyphenol extracts: a review. *Food Biosci* 35:100547. <https://doi.org/10.1016/j.fbio.2020.100547>
13. Antolovich M, Prenzler P, Robards K, Ryan D (2000) Sample preparation in the determination of phenolic compounds in fruits. *Analyst* 125:989–1009. <https://doi.org/10.1039/B000080I>
14. Ćirić A, Prosen H, Jelikić-Stankov M, Durević P (2012) Evaluation of matrix effect in determination of some bioflavonoids in food samples by LC-MS/MS method. *Talanta* 99: 780–790. <https://doi.org/10.1016/j.talanta.2012.07.025>
15. Bataglion GA, Da Silva FMA, Eberlin MN, Koolen HHF (2015) Determination of the phenolic composition from Brazilian tropical fruits by UHPLC-MS/MS. *Food Chem* 180: 280–287. <https://doi.org/10.1016/j.foodchem.2015.02.059>



Development of an Ultrapformance Liquid Chromatography–Mass Spectrometry Method to Determine Sterols in Olive Oils

María Jesús Lerma-García, Miriam Beneito-Cambra,
Ernesto Francisco Simó-Alfonso, and José Manuel Herrero-Martínez

Abstract

A protocol to determine sterols from olive oils by ultrapformance liquid chromatography (UPLC) coupled to mass spectrometry (MS) detection has been described in this chapter. First, sterols were extracted from olive oils by oil saponification, liquid–liquid extraction of non-saponifiable fraction using diethyl ether, and separation of the sterol fraction by thin layer chromatography. Next, sterols were separated by UPLC and identified by MS. The described UPLC-MS method was able to separate sterols in less than 5 min, being possible to quantify them by linear regression. Therefore, the sterol contents established by applying this methodology could be used for olive oil authentication.

Key words Sterol, Olive oil, Ultrapformance liquid chromatography, Mass spectrometry, Authentication

1 Introduction

Olive oil is a highly appreciated product characterized by its high nutritional value, excellent organoleptic properties, and health benefits [1]. These characteristics are related to olive oil composition: although it is mainly composed by triacylglycerols, the presence of other compounds (such as phenolic compounds, tocopherols, and sterols, among others) is very important from this point of view. Sterols (also known as phytosterols) are bioactive compounds present in the non-saponifiable fraction of vegetable oils and fats. In addition to its demonstrated nutritional value, several health benefits such as reduction of blood cholesterol contents and decrease of cardiovascular risk of coronary heart disease [2, 3] have been also associated with its ingestion.

Sterol profile is characteristic of each type of oil, but it is also dependent of fruit or *seed* quality, environmental conditions (agronomic and climatic), oil extraction method, refining practice, genetic variety of the fruit, etc [4]. For this reason, the development of rapid and reliable methods to determine sterols in oils (which is extensible to other sterol-rich foods) is of great importance from the point of view of authentication and quality of the product.

Different analytical techniques have been previously employed to determine sterols present in vegetable oils. Among them, gas chromatography (GC) with both flame ionization and mass spectrometry (MS) detectors has been mainly used [5], jointly high-performance liquid chromatography (HPLC)-MS. The main disadvantage of GC methodologies is the need of using thermally stable columns and the derivatization process needed to detect the aforementioned analytes. To overcome these handicaps, HPLC-MS could be alternatively used. However, the introduction of ultraperformance liquid chromatography (UPLC) with its advantages needs to be explored since this latter technique reduces analysis time, increases signal-to-noise ratios, and enhances peak resolution when compared to conventional HPLC methods [6].

In this chapter, a method for the extraction and determination of sterols from olive oils using ultraperformance liquid chromatography coupled to mass spectrometry detection has been described. The chromatographic method here described was able to separate (in less than 5 min), identify different sterols present in the olive samples (of which there are not standards available) and quantify them as a fingerprint for olive oil authentication.

2 Materials

Prepare all solutions using ultrapure water and analytical-grade reagents (unless indicated otherwise). Prepare and store all reagents and solutions at room temperature (unless indicated otherwise). Diligently follow all waste disposals regulations when disposing waste materials.

2.1 Olive Oil Saponification

1. Potassium hydroxide ethanolic solution ca. 2 M. Weigh 130 g of potassium hydroxide (minimum titre 85%) in a glass beaker. Add 200 mL of distilled water using a graduated cylinder to dissolve the solid. Add ethanol to a volume of 1 L. Store at room temperature in well-stoppered dark glass bottles (*see Note 1*).

2.2 Liquid-Liquid Extraction of the Non-saponifiable Fraction

1. Diethyl ether.
2. Anhydrous sodium sulfate.

2.3 Separation of the Sterol Fraction

1. Glass plates (20 × 20 cm) for thin layer chromatography (TLC), coated with silica gel without fluorescent indicator (0.25 mm plate thickness).
2. Plate-developing chamber (20 × 20 cm).
3. Potassium hydroxide ethanolic solution 0.2 M. Weigh 13 g of potassium hydroxide (minimum titre 85%) in a glass beaker. Add 20 mL of ultrapure water using a graduated cylinder. Add ethanol to a volume of 1 L. Store at room temperature in well-stoppered dark glass bottles (*see Note 1*).
4. Chloroform.
5. N-hexane (HPLC-grade).
6. Diethyl ether (HPLC-grade).
7. 2,7-dichlorofluorescein 0.2% (m/v) in ethanol. Weigh 0.2 g of 2,7-dichlorofluorescein in a glass beaker. Add 100 mL ethanol and few drops of potassium hydroxide ethanolic solution 0.2 M. Introduce the resulting solution into a sprayer.

2.4 Sterol Standard Stocks

1. Individual sterol standard solutions. Prepare a stock standard solution of 500 $\mu\text{g mL}^{-1}$ for each one of the following commercially available sterols: β -sitosterol (mixture containing 75% β -sitosterol and 10% campesterol), ergosterol, stigmasterol, cholesterol, and lanosterol. For this purpose, weigh 5 mg of the corresponding standard and dissolve it with 2-propanol up to 10 mL using a 10 mL volumetric flask. Store at $-20\text{ }^{\circ}\text{C}$ until use.
2. Sterol test mixture (50 $\mu\text{g mL}^{-1}$ each, except β -sitosterol and campesterol which concentration is 38 and 5 $\mu\text{g mL}^{-1}$, respectively). Take 500 μL of the corresponding sterol standard solution using a pipette, and transfer them into a 5 mL volumetric flask. Adjust volume up to 5 mL using 2-propanol. Store at $-20\text{ }^{\circ}\text{C}$ until use.

2.5 UPLC-MS Analysis

1. Mobile phase A (ACN containing 0.01% (v/v) acetic acid). Take 100 μL of acetic acid using a pipette, and add them to 1 L of acetonitrile (LC-MS-grade). Degas mobile phase for 10 min using an ultrasonic bath.
2. Mobile phase B (ultrapure water containing 0.01% (v/v) acetic acid). Take 100 μL of acetic acid using a pipette, and add them to 1 L of ultrapure water previously filtered using a nylon

HPLC mobile phase filtration membrane. Degas mobile phase for 10 min using an ultrasonic bath.

3. AcQuity ultraperformance liquid chromatograph with a binary pump system (Waters, Mildford, MA, USA).
4. Mass spectrometer dotted with single quadrupole detector (SQD) and atmospheric pressure chemical ionization (APCI) source (Waters).
5. AcQuity UPLC BEH C18 column (50 × 2.1 mm, 1.7 μm, Waters).

3 Methods

3.1 Oil Saponification

1. Weigh 5 g oil (with a precision of 0.1 mg) directly into a 250 mL round bottom flask. Add 50 mL of 2 M ethanolic potassium hydroxide solution, fit the reflux condenser, and heat using a heating mantle to gentle boiling for 20 min (*see Note 2*). Next, add 50 mL of ultrapure water from the top of the condenser, take it off, and wait until the solution is cooled to room temperature (*see Note 3*).

3.2 Liquid–Liquid Extraction of the Non-saponifiable Fraction

1. Transfer the solution of the round bottom flask into a 500 mL separating funnel. To transfer quantitatively all the solution, wash the flask several times with ultrapure water portions up to 50 mL.
2. Add 80 mL of diethyl ether to the separating funnel. Shake and invert it vigorously for at least 30 s (*see Note 4*). Wait until a complete separation of the two phases is observed (*see Note 5*).
3. Drain the bottom layer (aqueous phase) to another 500 mL separating funnel, and perform two more extractions using 70 mL diethyl ether.
4. Combine the three diethyl ether extracts in the same separating funnel containing 50 mL ultrapure water. The diethyl ether layer was continuously washed with water until neutral pH (*see Note 6*).
5. After washing water removal, dry the organic layer with anhydrous sodium sulfate (*see Note 7*) and filter the remaining solution into a 250 mL round bottom flask (*see Note 8*), washing the separating funnel and the filter with small amounts of diethyl ether.
6. Using a rotatory evaporator (30 °C), evaporate the solvent until no more of 2 or 3 mL are left. Next, evaporated until dryness using a nitrogen stream, finishing the drying step in an oven at 100 °C for 15 min.

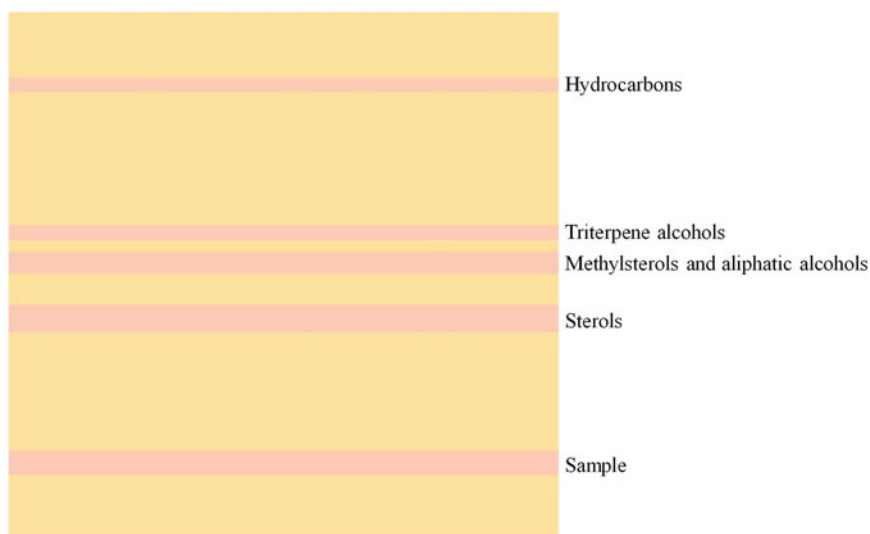


Fig. 1 Unsaponifiable fraction of an olive oil by TLC

3.3 Separation of the Sterol Fraction

1. Preparation of the basic TLC plates. Immerse the silica gel plates in a tray containing 0.2 M potassium hydroxide ethanolic solution (*see Note 9*) for 10 s. Let them dry in a fume cupboard (ca. 2 h) and next place them in an oven at 100 °C for 1 h (*see Note 10*).
2. Place mobile phase (n-hexane:diethyl ether, 60:40 (v/v)) into the plate-developing chamber with a height of ca. 1 cm (*see Note 11*). Close the chamber with its cover and wait at least 30 min in order to achieve liquid-vapor equilibrium.
3. Prepare a solution of the non-saponifiable fraction by solving the residue previously obtained (in Subheading 3.2, **step 6**) with 2 mL chloroform.
4. Draw a thin line across the plate on its lower end (2 cm from the bottom of the plate) (*see Note 12*), and depose uniformly 0.3 mL of the non-saponifiable fraction solution above it using a 100 μ L microsyringe or a microcapillary.
5. Place the prepared TLC plate in the plate-developing chamber, cover the chamber, and leave it undisturbed on your bench top. Let the mobile phase rise up the TLC plate until the solvent is about 1 cm below the top of the plate. Remove the plate from the chamber and allow it to dry under a fume cupboard.
6. Spray lightly and uniformly the TLC plate with a sprayer containing the 0.2% ethanolic 2,7-dichlorofluorescein solution. Leave it to dry. The different types of compounds separated on the TLC plate are shown in Fig. 1.
7. Scrape off the silica gel band containing the sterol fraction using a metal spatula (*see Note 13*).

8. Suspend the scraped silica gel in 10 mL diethyl ether in a glass vial. Filter the suspension under vacuum through a Whatman no. 1 paper using a Büchner funnel. Wash the residue several times with small amounts of diethyl ether. Evaporate the filtrate until dryness using a rotatory evaporator at 30 °C.
9. Dissolve the obtained residue in 500 µL of 2-propanol, and store the solution at –20 °C in injection amber vials until use.

3.4 UPLC-MS Analysis

1. Prepare a calibration series using the sterol test mixture (Sub-heading 2.4, **step 2**) of 0.5, 1, 5, 10, 25, and 50 µg mL⁻¹ (total volume of 2 mL with 2-propanol) and transfer the resulting solutions to injection vials after filtering with nylon syringe filters of 0.22 µm (*see Note 14*).
2. Insert the injection vials into the autosampler.
3. Assemble the analytical column in the column oven and set the oven temperature at 10 °C.
4. Purge and prime the UPLC system with both mobile phase A and B.
5. Set the flow rate at 0.8 mL min⁻¹ and condition the column at 80% mobile phase A and 20% mobile phase B until stable baseline (*see Note 15*).
6. Program mobile phase gradient as follows: linear gradient from 80 to 100% A for 0.5 min, followed by an isocratic elution with 100% A for 4.5 more min. Next, return to initial conditions with 80% mobile phase A for 2 min.
7. Operate the MS spectrometer in APCI positive-ion mode.
8. Acquire MS spectra in both total ion chromatogram (TIC, *m/z* range 300–500) and in selected ion recording (SIR) modes. The *m/z* values monitored for each sterol are indicated in Table 1 (*see Note 16*).
9. Set the ionization source parameters (*see Note 17*) as follows: corona, 4 kV; source temperature, 120 °C; desolvation gas temperature, 400 °C with a flow rate of 750 L/h; individual cone voltage, 30 V.
10. Program and run the standards and samples list including standard/sample name, vial position, injection volume (15 µL), and UPLC-MS method name. An example of the TIC and SIRs obtained for an extra virgin olive oil sample is shown in Fig. 2.
11. Process data using MassLinx 4.1 software and generate a calibration curve for each sterol standard by representing the intensity of each analyte (y-axis) vs concentration (x-axis), using linear regression.

Table 1
Ions observed in the APCI mass spectra of olive oil samples (adapted with permission from ref. [6]. Copyright 2010 American Chemical Society)

Peak no.	Analyte	Ion $[M + H - H_2O]^+$ (m/z)
1	Erythrodiol	425.5
2	Uvaol	425.5
3	Ergosterol	379.5
4	Brassicasterol	381.5
5	Δ^5 -Avenasterol	395.5
6	Cholesterol	369.5
7	Campesterol	383.5
8	Campestanol	385.5
9	Stigmasterol	395.5
10	Clerosterol	395.5
11	$\Delta^{5,24}$ -Stigmastadienol	395.5
12	β -Sitosterol	397.5
13	Δ^7 -Stigmastenol	397.5
14	Sitostanol	399.5

12. Calculate the concentration of sterols found in olive oil sample extracts using the linear regression equation (*see Note 18*).
13. Calculate the percentage of each sterol found in the total sterol fraction of olive oils.

4 Notes

1. It is not advisable to keep it more than 2 days since this solution reacts with atmospheric carbon dioxide.
2. The 20 min counting starts when the solution starts to boil.
3. It is possible to proceed with the protocol with a temperature of ca. 30 °C.
4. It is important to release the pressure generated in the funnel by inverting it and opening the stopcock.
5. In some cases, an emulsion is formed in the interface. It could be eliminated by adding a few drops of ethanol. If there is not an emulsion, but the separation is unclear, it is possible to obtain a clear separation of both phases by performing a soft rotatory shaken of the funnel.

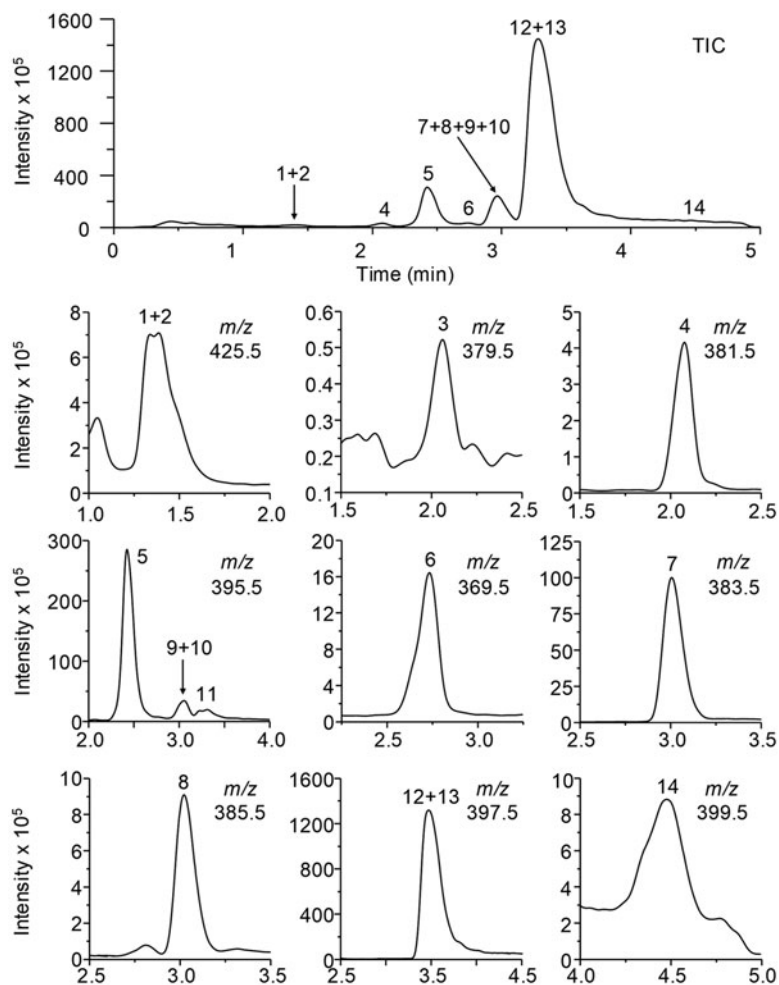


Fig. 2 TIC and SIRs of an extra virgin olive oil sample. Peak identification as indicated in Table 1. (Reprinted with permission from ref. [6]. Copyright 2010 American Chemical Society)

6. pH could be measured using pH indicator paper or by adding to the water layer a few drops of phenolphthalein indicator solution (10 g/L in ethanol). In this latter, washing should be stopped when the water layer was no longer pink.
7. Add anhydrous sodium sulfate until no more aggregation of particles was observed. This proves that all the remaining water is eliminated.
8. Use a conical funnel with filter paper.
9. It is important that the TLC plates are completely immersed into the solution. Then, at least the solution contained in the tray should be of 4 cm height.

10. It is very important to control temperature. If it is higher than 100 °C, the silica gel becomes detached from the glass. Store the basic TLC plates into a desiccator until use, but do not store more than 15 days.
11. Be sure that the mobile phase level is below the starting line of the TLC plate. Otherwise, the spotted sample will dissolve away.
12. Draw the line using a pencil since the ink of a pen could interfere in the separation. Take care not to press so hard with the pencil and not to break the silica gel.
13. In order to also extract triterpene dialcohols (erythrodiol and uvaol), it is necessary to scrape not only sterol band, but also all the silica gel comprised between sample and sterol bands.
14. These calibration solutions are adequate for all sterols considered in the study except for β -sitosterol, which concentration in olive oils is high. Then, additional calibration solutions should be prepared, comprising the 50–250 $\mu\text{g mL}^{-1}$ range. Prepare 100, 150, 200, and 250 $\mu\text{g mL}^{-1}$ solutions and proceed in the same way.
15. A conditioning of 15 min is usually required.
16. For each sterol, the m/z value corresponding to the $[\text{M} + \text{H} - \text{H}_2\text{O}]^+$ was selected since these peaks show higher intensities than the respective $[\text{M} + \text{H}]^+$ peaks [6, 7]. A total of 9 SIR channels, according to Table 1, were monitored. A total of 11 peaks, which corresponded to 14 possible sterols usually present in olive oils, were observed.
17. The optimization of the source parameters for each available sterol standard was automatically performed using Intellistar software (Waters).
18. As there is no possibility to acquire standards for all sterols found (they are not commercial), estimate the concentration of these sterols as follows: use the calibration curve of lanosterol to estimate the concentration of campestanol and sitostanol (due to their similar sensitivity [8]) and to estimate erythrodiol + uvaol content (due to their structural resemblance). Use the calibration curve of β -sitosterol to estimate the concentration of the rest of compounds (brassicasterol, Δ^5 -avenasterol, and $\Delta^{5,24}$ -stigmastadienol) [6].

Acknowledgments

Work supported by Grant RTI2018-095536-BI00 funded by MCIN/AEI/10.13039/501100011033 and by “ERDF A way of making Europe”, by the “European Union”.

References

1. Owen RW, Giacosa A, Hull WE, Haubner R, Wurtel G, Spiegelhalter B, Bartsch H (2000) Olive oil consumption and health: the possible role of antioxidants. *Lancet Oncol* 1:107–112. [https://doi.org/10.1016/S1470-2045\(00\)00015-2](https://doi.org/10.1016/S1470-2045(00)00015-2)
2. Piironen V, Lindsay DG, Miettinen TA, Toivo J, Lampi AM (2000) Plant sterols: biosynthesis, biological function and their importance to human nutrition. *J Sci Food Agric* 80: 939–966. [https://doi.org/10.1002/\(SICI\)1097-0010\(20000515\)80:7<939::AID-JSFA644>3.0.CO;2-C](https://doi.org/10.1002/(SICI)1097-0010(20000515)80:7<939::AID-JSFA644>3.0.CO;2-C)
3. Perona JS, Cabello-Moruno R, Ruiz-Gutierrez V (2006) The role of virgin olive oil components in the modulation of endothelial function. *J Nutr Biochem* 17:429–445. <https://doi.org/10.1016/j.jnutbio.2005.11.007>
4. Lerma-García MJ, Concha-Herrera V, Herrero-Martínez JM, Simó-Alfonso EF (2009) Classification of extra virgin olive oils produced at La Comunitat Valenciana according to their genetic variety using sterol profiles established by high-performance liquid chromatography with mass spectrometry detection. *J Agric Food Chem* 57: 10512–10517. <https://doi.org/10.1021/jf902322c>
5. Cercaci L, Passalacqua G, Poerio A, Rodriguez-Estrada MT, Lercker G (2007) Composition of total sterols (4-desmethyl-sterols) in extravirgin olive oils obtained with different extraction technologies and their influence on the oil oxidative stability. *Food Chem* 102:66–76. <https://doi.org/10.1016/j.foodchem.2006.01.062>
6. Lerma-García MJ, Simó-Alfonso EF, Mendez A, Liberia JL, Herrero-Martínez JM (2010) Fast separation and determination of sterols in vegetable oils by ultraperformance liquid chromatography with atmospheric pressure chemical ionization mass spectrometry detection. *J Agric Food Chem* 58:2771–2776. <https://doi.org/10.1021/jf9043887>
7. Segura-Carretero A, Carrasco-Pancorbo A, Cortacero S, Gori A, Cerretani L, Fernández-Gutiérrez A (2008) A simplified method for HPLC-MS analysis of sterols in vegetable oil. *Eur J Lipid Sci Technol* 110:1142–1149. <https://doi.org/10.1002/ejlt.200700237>
8. Lu B, Zhang Y, Wu X, Shi J (2007) Separation and determination of diversiform phytosterols in food materials using supercritical carbon dioxide extraction and ultraperformance liquid chromatography atmospheric pressure chemical ionization-mass spectrometry. *Anal Chim Acta* 588:50–63. <https://doi.org/10.1016/j.aca.2007.01.067>



A Workflow for Lipid Annotation in Coffee Samples by Liquid Chromatography-Mass Spectrometry

Ana Carolina R. Silva, Rafael Garrett, and Claudia M. Rezende

Abstract

Lipids in coffee are not only precursors for flavor and volatile compounds, but also considered essential for brew taste and body. They account for around 7–15% of the dry bean weight in both Arabica and Robusta green coffee beans and include different subclasses, such as triacylglycerols (TAG), phospholipids (PL), and β -*N*-alkanoyl-5-hydroxytryptamides. Due to this fraction relevance, our work provides a protocol to analyze lipids in coffee samples by liquid chromatography-high resolution tandem mass spectrometry (LC-HRMS/MS). An open-source metabolomics software is used for feature detection, data alignment, and lipid annotation.

Key words Coffee, LC-MS, Lipidomics, Lipid extraction, MTBE

1 Introduction

Lipids are key constituents involved in numerous biological functions in vegetables, such as cell growth, signaling, differentiation, and energy storage [1, 2]. While the lipid fraction reported in green Arabica coffee beans is between 15 and 17% of dry bean weight, in Robusta coffees it is about 7–10% [3], including different subclasses: triacylglycerols (TAG) (around 75%), esterified diterpenes (18%), free diterpenes and fatty acids (1.0%), sterols (4.7%), tocopherols (0.1%), phospholipids (PL) (0.4%), and β -*N*-alkanoyl-5-hydroxytryptamides (C-5HT) (0.8%). Whereas most of these lipids are located in the endosperm region of green beans, the C-5HTs are observed in the waxy layer that covers the beans [3].

The composition of coffee fatty acids has already been used to discriminate post-harvesting processes, coffee bean variety, and growing location [4–6]. Meanwhile, diterpenes have been associated with higher quality coffees [7]. Phospholipids—phosphatidylcholine (PC), phosphatidylinositol (PI), phosphatidylethanolamine (PE), and lysophosphatidylcholine

(LPC)—have been identified not only in Arabica but also in Robusta coffees [8–11]. A drop in PC and PE content when humidity and temperature were increased during storage of Arabica coffee beans has been described in the literature [8].

Lipids in coffee are precursors for flavor and volatile compounds, which are considered essential for brew taste and body [12, 13]. The milled beans used in coffee beverage preparation might differ in terms of coffee species, grinding, and roast degree. Therefore, depending on the brewing method, the amount of lipids may change significantly [12–15]. For instance, filtered coffees have a lower amount of lipids than non-filtered ones, and it is because most of the lipids are retained by the filter paper [12, 15]. Thus, in non-filtered brews (e.g., espresso) lipids improve texture perception. Yet, not only free and esterified diterpenes but also phospholipids are present in higher concentrations in espresso coffees than other brew types [12–16]. Also, C-5HTs are related to stomach irritation caused by coffee beverage consumption in sensitive people [17].

Due to the complexity of the coffee lipid fraction, it is crucial to use comprehensive and powerful techniques to unveil and explore its composition. Liquid chromatography coupled to high-resolution mass spectrometry (LC-HRMS) is one of the most suitable techniques for analyzing complex mixtures due to its higher throughput, enhanced separation, and reliable detection of a large number of lipids from distinct subclasses in the same extraction and analytical method [18, 19].

Some steps are vital when considering to profile the lipid fraction in coffee comprehensively. It includes proper sample extraction, separation by liquid chromatography, ionization by electrospray ionization, detection by high-resolution mass spectrometry, and data processing for lipid annotation. Liquid chromatography separation enhances lipid discrimination and detection, while tandem HRMS experiment allows confident lipid structure annotation via precursor/fragment spectra [2, 19]. Because each step may influence the outcomes, the workflow should be adapted according to each sample type.

Here, we described a protocol for coffee samples analysis that allows extensive lipid coverage using LC-HRMS/MS and open-source software for feature detection, data alignment, and compound annotation [20].

2 Materials

2.1 Equipments

1. Calibrated pipettes of 20–200 μL , 100–1000 μL .
2. Vortex mixer.
3. Centrifuge for 2.0 mL tubes.

4. Nitrogen evaporator.
5. Ultrasonic bath.
6. Digital weighing scale.
7. UHPLC system coupled to a high-resolution mass spectrometer using an electrospray ion source.

2.2 Reagents

1. Solvents for sample preparation: methanol LC-MS grade (MeOH), methyl *tert*-butyl ether HPLC grade (MTBE), and deionized water (H₂O).
2. Solvents for LC-HRMS analysis: deionized water, acetonitrile, and isopropanol LC-MS grade.
3. Mobile-phase modifiers: formic acid and ammonium formate LC-MS grade.
4. Mixture of deuterated lipid standards: Splash Lipidomix Mass Spectrometry Standard from Avanti Polar Lipids: (15:0–18:1 (d7)PC 150.6 µg/mL; 15:0–18:1 (d7)PE 5.3 µg/mL; 15:0–18:1 (d7)PS (Na Salt) 3.9 µg/mL; 15:0–18:1 (d7)PG (Na Salt) 26.7 µg/mL; 15:0–18:1 (d7)PI (NH₄ Salt) 8.5 µg/mL; 15:0–18:1 (d7)PA (Na Salt) 6.9 µg/mL; 18:1(d7) LysoPC 23.8 µg/mL; 18:1(d7) LysoPE 4.9 µg/mL; 18:1(d7)Chol Ester 329 µg/mL; 18:1(d7)MAG 1.8 µg/mL; 15:0–18:1(d7) DAG 8.8 µg/mL; 15:0–18:1(d7)-15:0TAG 52.8 µg/mL; d18:1–18:1(d9)SM; Cholesterol (d7) 98.4 µg/mL) (*see Note 1*).

2.3 Coffee Samples

1. Green (raw) Arabica coffee beans.
2. Green Arabica coffee beans must be ground using a mill and passed over a 40-mesh sieve (0.5 mm pore size).
3. Keep the milled coffee beans in an amber tube away from light until analysis.

2.4 Supplies

1. 1.5 or 2.0 mL centrifuge tubes.
2. Pipette tips for organic solvents, such as acetonitrile, methanol, isopropanol, and methyl *tert*-butyl ether.
3. Glass vials (2.0 mL volume).
4. Proper caps for vials, depending on the LC specification.
5. Acquity UPLC CSH C₁₈ column (150 mm × 2.1 mm; 2.5 µm) (Waters, Milford, MA, USA).
6. Acquity UPLC CSH C₁₈ VanGuard pre-column (5 mm × 2.1 mm; 2.5 µm) (Waters, Milford, MA, USA).

2.5 LC and Sample Solvents

1. Sample reconstitution solvent: isopropanol:acetonitrile:water (2:1:1, v/v).
2. Mobile phase A: acetonitrile:water (60:40, v/v) with 10 mM ammonium formate and 0.1% formic acid (*see Note 2*).

3. Mobile phase B: isopropanol:acetonitrile (90:10 v/v) with 10 mM ammonium formate and 0.1% formic acid.
4. Column wash solvent C: acetonitrile 100%.
5. Column wash solvent D: isopropanol:acetonitrile:water (60:20:20 v/v).

3 Methods

3.1 Lipid Extraction

1. The lipid extraction for coffee samples is based on the Matyash method [21, 22]. At least triplicate extractions must be performed.
2. Weigh 15 mg of the milled coffee in a 2.0 mL centrifuge tube using a digital weighing scale (*see Note 3*).
3. A blank extraction sample must be performed in the same way as the coffee sample but using 15 μL of H_2O instead of a milled coffee sample in a 2.0 mL centrifuge tube.
4. Add 50 μL of Splash Lipidomix mixture into the centrifuge tube containing 15 mg of milled coffee beans and into the blank centrifuge tube.
5. Add 100 μL of methanol into the centrifuge tube containing the milled coffee beans and the Splash Lipidomix.
6. Vortex the centrifuge tube for 30 s.
7. Add 500 μL of MTBE into the centrifuge tube containing milled coffee beans, splash Lipidomix, and methanol.
8. Vortex the centrifuge tube for 30 s.
9. Add 125 μL of deionized water into the centrifuge tube containing milled coffee beans, splash Lipidomix, methanol, and MTBE.
10. Place the centrifuge tube in an ultrasonic bath for 15 min.
11. Incubate the centrifuge tube containing milled coffee beans, Splash Lipidomix, methanol, MTBE, and deionized water in a refrigerator at 4 °C for 10 min.
12. After 10 min, remove the centrifuge tube from the refrigerator and centrifuge the tube at $9000 \times g$ for 15 min. After this, there should be two layers: the inferior aqueous phase and the superior organic phase. The lipids are in the superior organic phase.
13. Collect 400 μL of the superior organic phase to another centrifuge tube, using a calibrated pipette (*see Note 4*).
14. Dry the organic phase (lipids) under nitrogen flow.
15. Store the samples at -20 °C until analysis (*see Note 5*).

3.2 LC-HRMS/MS Analysis

1. Reconstitute the dried lipid extract with 500 μL of 2:1:1 isopropanol:acetonitrile:water. Transfer the lipid extract to an LC vial and cap the vial.
2. Prepare a pooled quality control (QC) sample by mixing a small amount of each sample into the same LC vial and analyze it throughout the sequence (*see* **Note 6**).
3. Equilibrate the LC column at 45 °C with starting percentages of mobile phases A and B (40% B). Wait until the pressure is stable to start the analysis. Pressure should be within the range of 400–500 bar at the beginning of each run.
4. Create an instrument sequence following the order: solvent blank, extraction blank, at least 5 pooled QCs for conditioning the system, a pooled QC for data analysis, and a randomized batch of coffee samples [23].
5. LC solvent flow, injection volume, and temperature: 0.450 mL/min, 45 °C, and 5 μL .
6. Apply the following LC gradient: 0–2.0 min 40% B; 2.0–2.1 min 43% B; 2.1–12.0 min 50% B; 12.0–12.1 min 54% B; 12.1–18.0 min 70% B; 18.0–18.1 min 99% B; 18.1–25.0 min 40% B [24, 25].
7. The acquisition method for an Orbitrap mass spectrometer (QExactive Plus model, Thermo Fisher Scientific) is described here. The following parameters should be used in positive ion mode: spray voltage at 3.9 kV, sheath gas and auxiliary nitrogen pressure at 45 and 20 arbitrary units, respectively, capillary and heater temperatures at 320 °C and 400 °C, respectively. For negative-ESI mode, use the spray voltage of 3.6 kV.
8. Full-scan MS conditions should be used with polarity switching (if possible) following calibration of the instrument: S-lens RF level at 70 eV, a resolution of 35.00 full width at half maximum (FWHM) with automatic gain control (AGC) of 1×10^6 ions, maximum injection time of 150 ms, and scanning range from m/z 140 to 2000 Da. Data is acquired in profile mode.
9. Fragmentation of ions should be obtained using data-dependent acquisition (ddMS²-top3). Ions are isolated using a 1.2 amu window, and isolation is triggered using an intensity threshold of 1×10^6 , isotope exclusion on, and dynamic exclusion of 10 s. Ions are fragmented by HCD using NCE of 30 for ESI (–) and 35 for ESI (+) with a resolution of 17,500 FWHM with AGC of 1×10^5 ions and maximum injection time of 50 ms (*see* **Note 7**).
10. Run the sequence applying these LC-HRMS/MS conditions.

3.3 LC-HRMS/MS Data Analysis

3.3.1 Data Analysis of .Raw Files on Xcalibur Qual Browser

1. Open the .raw files on Xcalibur Qual Browser or other software for data analysis.
2. Total ion chromatograms for green Arabica coffee lipids should have a similar profile to Fig. 1. The elution order is based on the unsaturation degree and carbon-chain length of fatty acyl moieties [18, 24].
3. Inspect the files to see if all deuterated standards were extracted correctly, keeping a constant retention time and peak area across samples. Ensure they have a standard deviation below 20% for the peak areas and below 10% for retention time drift. Figures 2 and 3 show the extracted ion chromatogram (EIC) for each deuterated standard from Splash Lipidomix.

3.3.2 LC-HRMS/MS Data Processing Using the MS-DIAL Software

Conversion of .Raw Files to an Analysis Base File (ABF)

1. Because MS-DIAL works with the Analysis Base File (ABF) format, the first step is to download the freely available file converter to the vendor's format. The program accepts the main LC-MS vendor formats [20].
2. Using a web browser, go to <https://www.reifycs.com/AbfConverter/index.html> and download the file converter according to your operating system.
3. Extract the files from the zip folder.
4. To start a new conversion, double click "AnalysisBaseFileConverter.exe".
5. Drag and drop the .raw files into the Analysis Base File Converter. By default, the converted files will be saved in the same folder as the original .raw files. To save into another folder, click Browse and choose a location.
6. To start the process, click "Convert". The ABF files will be used to process the data on MS-DIAL software.

Starting a Project in MS-DIAL Software

1. Using a web browser, go to <http://prime.psc.riken.jp/compms/msdial/main.html> and download the latest version of MS-DIAL.
2. Extract the files from the zip folder and double click on "MSDIAL.exe" to start a project.

Starting a Project

3. Open the software, go to "File" and click on "New Project".
4. To choose a project file path, click on "Browse", which needs to be the same folder containing ABF files.
5. Go to ionization type and click on "soft ionization (LC/MS, LC/MS/MS, or precursor-oriented GC/MS/MS)".
6. Go to Separation type and click on "Chromatography (GC, LC, CE, SFC)".

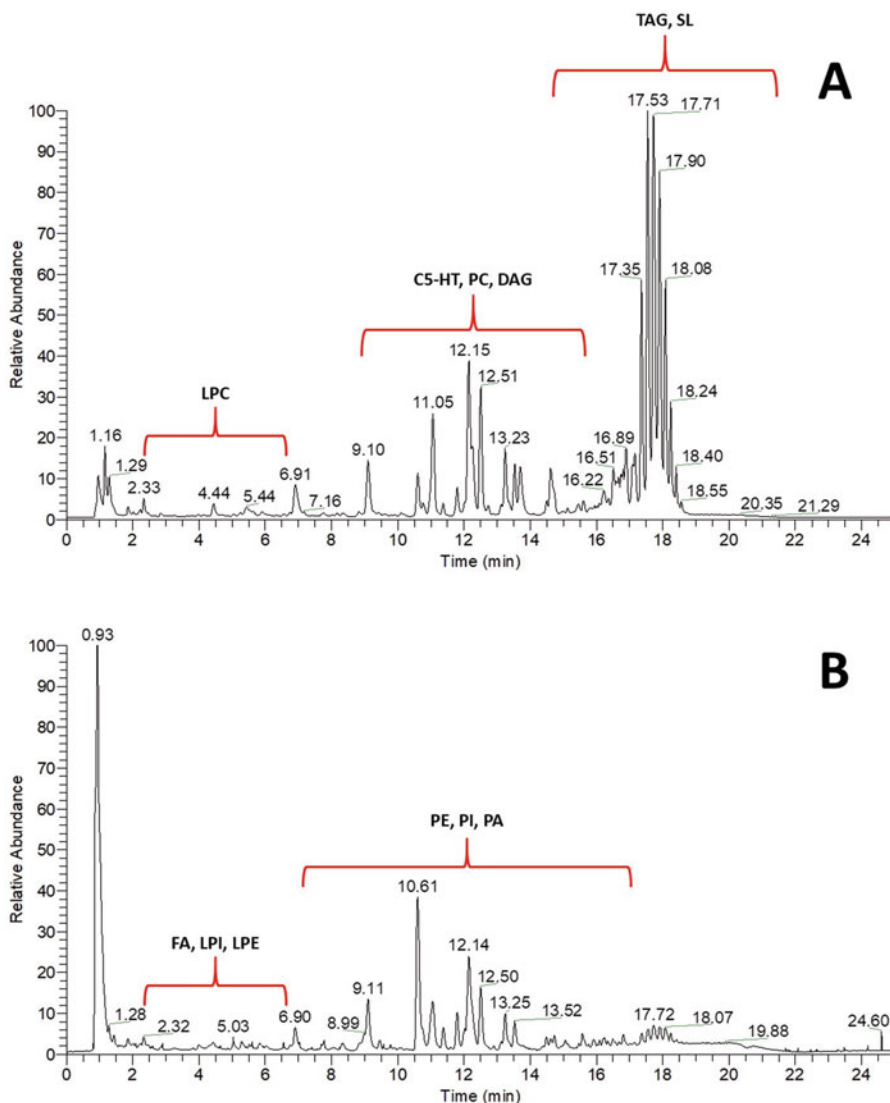


Fig. 1 LC-HRMS total ion chromatogram (TIC) of lipids from green Arabica coffee beans using the CSH C₁₈ column. **(a)** positive electrospray ion mode and **(b)** negative electrospray ion mode. *LPC* lysophosphatidylcholine, *PC* phosphatidylcholine, *C5-HT*^β *N*-alkanoyl-hydroxytryptamides, *DG* diacylglycerol, *TG* triacylglycerol, *SL* sterol lipids, *FA* fatty acids, *LPI* lysophosphatidylcholine, *LPE* lysophosphatidylethanolamines, *PE* phosphatidylethanolamine, *PI* phosphatidylinositol, *PA* phosphatidic acid

7. Go to MS method type and click on “Conventional LC/MS or data-dependent MS/MS” (see **Note 8**).
8. Go to Data type (MS1) and Data type (MS/MS) and click on “Profile data” for both (see **Note 9**).
9. You must create one project for each electrospray ion mode. Go to Ion mode and click on “Positive ion mode” or “Negative ion mode”.

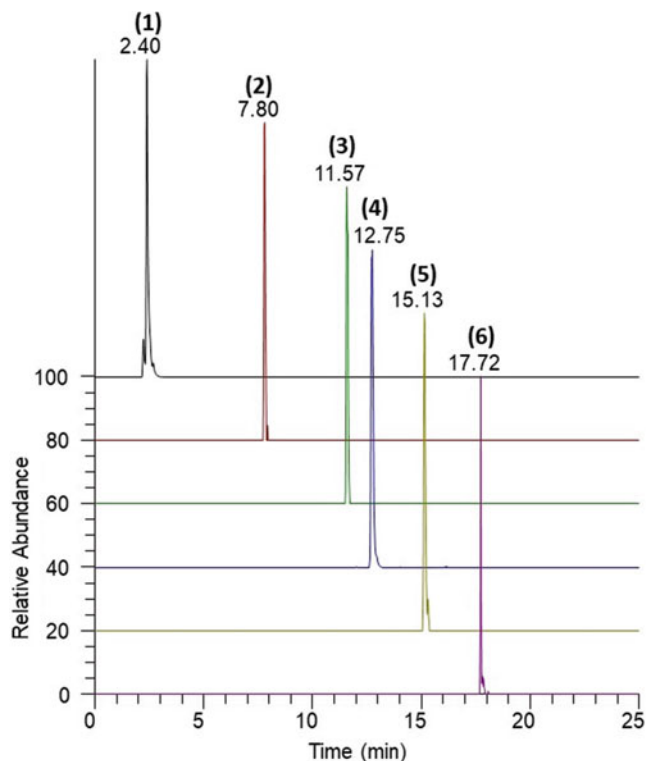


Fig. 2 Extracted ion chromatograms (EIC) of deuterated standards in the positive ion mode from LC-HRMS analysis using a CSH C₁₈ column. (1) 18:1(d7) Lyso PC; (2) 18:1(d7) Chol Ester; (3) Cholesterol (d7); (4) 15:0–18:1(d7) PC; (5) 15:0–18:1 (d7) DAG; (6) 15:0–18:1(d7)-15:0 TAG

10. Go to Target omics and click on “Lipidomics”.
11. Click on “Next” to go to “New project window”.

Importing ABF Files

12. Click on “Browse” and select ABF files. Here, you can select the type of sample (Sample, Standard, QC, and Blank).
13. The Class ID will be the different groups of samples that you have. For instance, if you analyzed coffees from different geographical regions, each region can be a Class ID.
14. The analyst can also include the batch information, analytical order, and sample injection volumes in this step.
15. Once it is all filled, click “Next” to go to “Analysis parameter setting”. Each tab is detailed below.

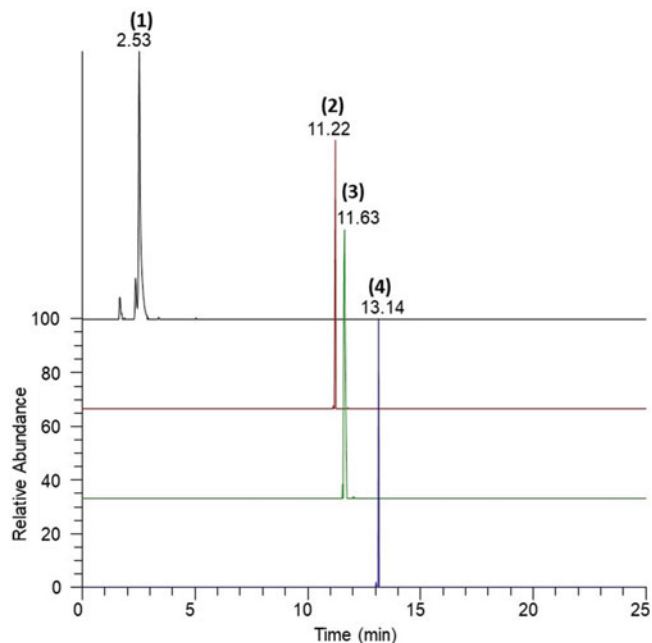


Fig. 3 Extracted ion chromatograms (EIC) of deuterated standards in the negative ion mode from LC-HRMS analysis using a CSH C₁₈ column. (1) 18:1(d7) Lyso PE; (2) 15:0–18:1(d7) PI (NH₄ Salt); (3) 15:0–18:1(d7) PG (Na Salt); (4) 15:0–18:1(d7) PE

Analysis Parameter Setting

Data collection

1. Set 0.005 Da as MS1 tolerance and 0.025 Da as MS2 tolerance (*see Note 10*).
2. Set 0 min as Retention Time Begin and 25 min as Retention Time End from the LC method.
3. Set 140 as MS1 Mass range begin and 2000 Da as MS1 Mass range end.
4. Set 140 as MS/MS Mass range begin and 2000 Da as MS/MS Mass range end.
5. Set 1 as the Maximum charged number.
6. If you are using a personal quadcore configuration computer, use 2 as threads. Refer to the MS-DIAL tutorial for more information.

Peak detection

1. Set 500,000 as Minimum peak height.
2. Set 0.1 Da as Mass slice width.
3. Apply Linear Weighted Moving Average as Smoothing method.

4. Set 3 and 5 as smoothing level and Minimum peak width, respectively.
5. Peaks from column or solvent can be specified in the “Exclusion list”.

MS2Dec

1. Set 0.4 as sigma window value and 10 as MS/MS abundance cut-off.
2. Set true for “Exclude after precursor ion”.
3. Set 0.5 for “Keep the isotopic ions until” and Set true for “Keep the isotopic ions w/o MS2Dec”.

Identification

1. In the MSP file, click “Select” to choose the solvent type (HCOONH₄ for formate ammonium and HCCOONH₄ for acetate ammonium).
2. Select specific lipid classes for identification.
3. In “Retention time tolerance” set 100 or larger to ignore the use of retention time comparison to the MSP database.
4. Set 0.005 Da to “Accurate mass tolerance (MS1)” and 0.1 Da to “Accurate mass tolerance (MS2)”.
5. Set 80% to “Identification score cut off” (*see Note 11*).

Adduct

1. In positive ion mode set true for [M + H]⁺, [M + Na]⁺, [M + NH₄]⁺, [M + H - H₂O]⁺.
2. In negative ion mode set true for [M - H]⁻, [M + HCOO]⁻, [M - H - H₂O]⁻.

Alignment

1. A result name will be automatically generated.
2. If the data has a quality control (QC), specify one QC file in the “Reference file”.
3. Set 0.05 min as “Retention time tolerance” and 0.015 Da as “MS1 tolerance”.
4. Keep 0.5 for both Retention time and MS1 factor.
5. If the experiment has a blank, set true for “Remove based on blank information”.
6. Set 0 in the “Peak count filter” and in “N% detected in at least one group”, set 50% to detect peaks in at least half of the samples in the same group.
7. Set true for “Keep ‘identified’ metabolite features”, “Keep ‘annotated (without MS2)’ metabolite features”.
8. Set false for “Gap filling by compulsion”.

Data Processing

Data Analysis and Interpretation

1. When data processing is finished, double click on the alignment file in the Alignment navigator window.
2. In “Peak spot navigator” check Ref. matched to see the identified lipids using MS/MS spectra.
3. Go to alignment spot viewer and click on “show ion table”. A summary table with identified lipids can be shown from this button.
4. Eliminate the compounds with a mass error above 8 ppm.

Lipid Annotation in Positive Ion Mode

Check the fragmentation pattern for each class in positive ion mode from Table 1 and the similarity between experimental and theoretical representatives MS/MS spectra, as shown in Fig. 4. Briefly, two types of adducts are observed for LPC and PC, $[M + H]^+$ and $[M + Na]^+$. The main product ions generated from the $[M + H]^+$ precursors are loss of water ($[M + H - H_2O]^+$) and protonated phosphocholine (m/z 184.07) [26, 27]. Fragments from the fatty acyl units are present in low abundance. Therefore, product ions from $[M + Na]^+$ adducts are used to annotate PC and LPC. The major fragments are loss of phosphocholine ($[M + Na - 183]^+$) and esterified fatty acyl group ($[M + Na - R_xCO_2H]^+$) [26, 27]. Acylglycerols, such as DAG and TAG are neutral lipids and have no

Table 1

Characteristic fragments and fatty acyl identification fragments of the main lipid classes found in coffee samples in LC-HRMS positive ion mode

Lipid class	Precursor ion	Characteristic fragment	Fatty acyl identification fragments
TAG	$[M + NH_4]^+$	–	$[M + NH_4 - (R_1CO_2H + 17)]^+$, $[M + NH_4 - (R_2CO_2H + 17)]^+$, $M + NH_4 - (R_3CO_2H + 17)]^+$
DAG	$[M + NH_4]^+$	–	$[M + NH_4 - (R_1CO_2H + 17)]^+$, $[M + NH_4 - (R_2CO_2H + 17)]^+$
LPC	$[M + H]^+$	m/z 184.0739 protonated phosphocholine	$[M + H]^+$
PC	$[M + Na]^+$	m/z 146.9817 sodiated phosphate	$[M + Na - R_1CO_2H]^+$,
		$[M + Na - 183]^+$ loss of phosphocholine	$[M + Na - R_2CO_2H]^+$
C5-HT	$[M + H]^+$	m/z 160.0748 (serotonin), m/z 177.1021 (serotonin + NH_3)	$[M + H]^+$

LPC lysophosphatidylcholine, PC phosphatidylcholine, DAG diacylglycerol, TAG triacylglycerol, C-5HT^βN-alkanoyl-hydroxytryptamide, R_1 fatty acid chain, R_2 fatty acid chain

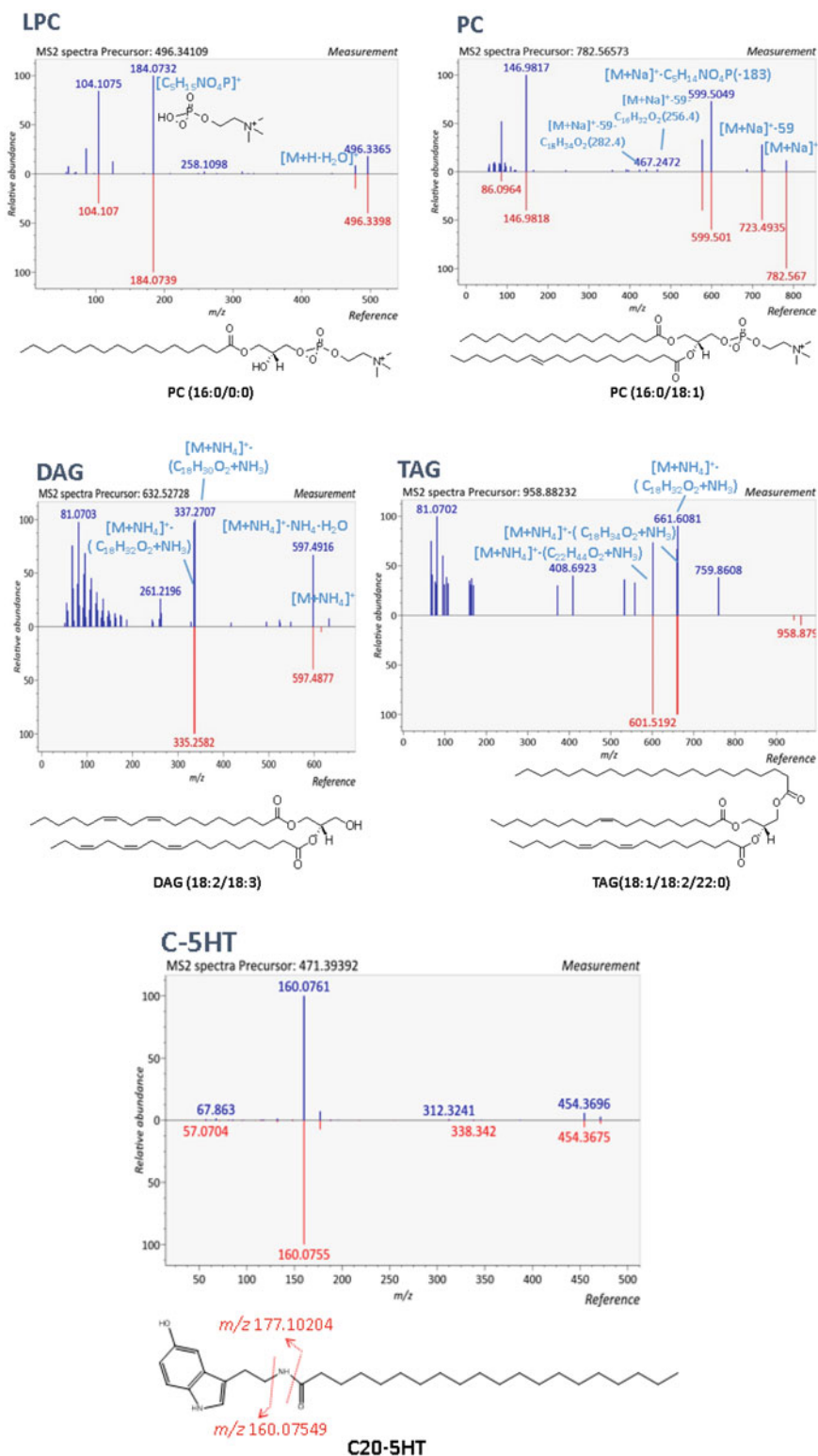


Fig. 4 Experimental (blue) and theoretical (red) representative MS/MS spectra in positive ESI mode for LPC, PC, DAG, TAG, and C-5HT classes. *LPC* lysophosphatidylcholine, *PC* phosphatidylcholine, *DAG* diacylglycerol, *TAG* triacylglycerol, *C-5HT* β *N*-alkanoyl-hydroxytryptamide

electrostatic charge in solution, so $[M + Na]^+$ and $[M + NH_4]^+$ adduct ions are observed. Generally, product ions from $[M + NH_4]^+$ are used to identify these compounds since ammonium ions present in the mobile phase are sprayed at the ESI source. Putative identification of these compounds is based on the high accurate precursor m/z values and fragments from the fatty acyl moiety $[M + NH_4 - (R_xCO_2H + 17)]^+$ [26].

*Lipid Annotation in
Negative Ion Mode*

Phospholipids as LPE, PI, and PE are identified as $[M-H]^-$ adducts. The MS/MS spectra of these lipids show fragments from the lipid head group (e.g., m/z 241.01 from phosphatidylinositol) and fragments of fatty acyl moiety ($[R_xCO_2]^-$). PC and LPC can be identified in negative ion mode as $[M + HCOO]^-$ ions [26, 27]. The fragmentation pattern for each class in negative ion mode can be checked in Table 2. The similarity between experimental and theoretical representatives MS/MS spectra for specific classes in Fig. 5.

Table 2
Characteristic fragments and fatty acyl identification fragments of main lipid classes found in coffee samples in LC-HRMS negative ion mode

Lipid class	Precursor ion	Characteristic fragment	Fatty acyl identification fragments
LPE	$[M - H]^-$	m/z 140.0118 deprotonated phosphoethanolamine	m/z R_1
		m/z 196.0375 glycerophosphoethanolamine anion	
LPI	$[M - H]^-$	m/z 241.0119 deprotonated inositol phosphate	m/z R_2
PI	$[M - H]^-$	m/z 241.0119 deprotonated inositol phosphate	$[M - H - R_1CH_2CO_2H]^-$, $[M - H - R_2CH_2CO_2H]^-$, m/z R_1 , m/z R_2
PA	$[M - H]^-$	m/z 152.9953 (glycerol 3-phosphate after loss of H_2O)	$[M - H - R_1CH_2CO_2H]^-$, $[M - H - R_2CH_2CO_2H]^-$
			m/z R_1 , m/z R_2
PE	$[M - H]^-$	m/z 140.0118, deprotonated phosphoethanolamine	$[M - H - R_1CH_2CO_2H]^-$, $[M - H - R_2CH_2CO_2H]^-$, m/z R_1 , m/z R_2
		m/z 196.0375, glycerophosphoethanolamine anion	

LPI lysophosphatidylinositol, *LPE* lysophosphatidylethanolamine, *PA* phosphatidic acid, *PI* phosphatidylinositol, *PE* phosphatidylethanolamine, R_1 fatty acid chain, R_2 fatty acid chain

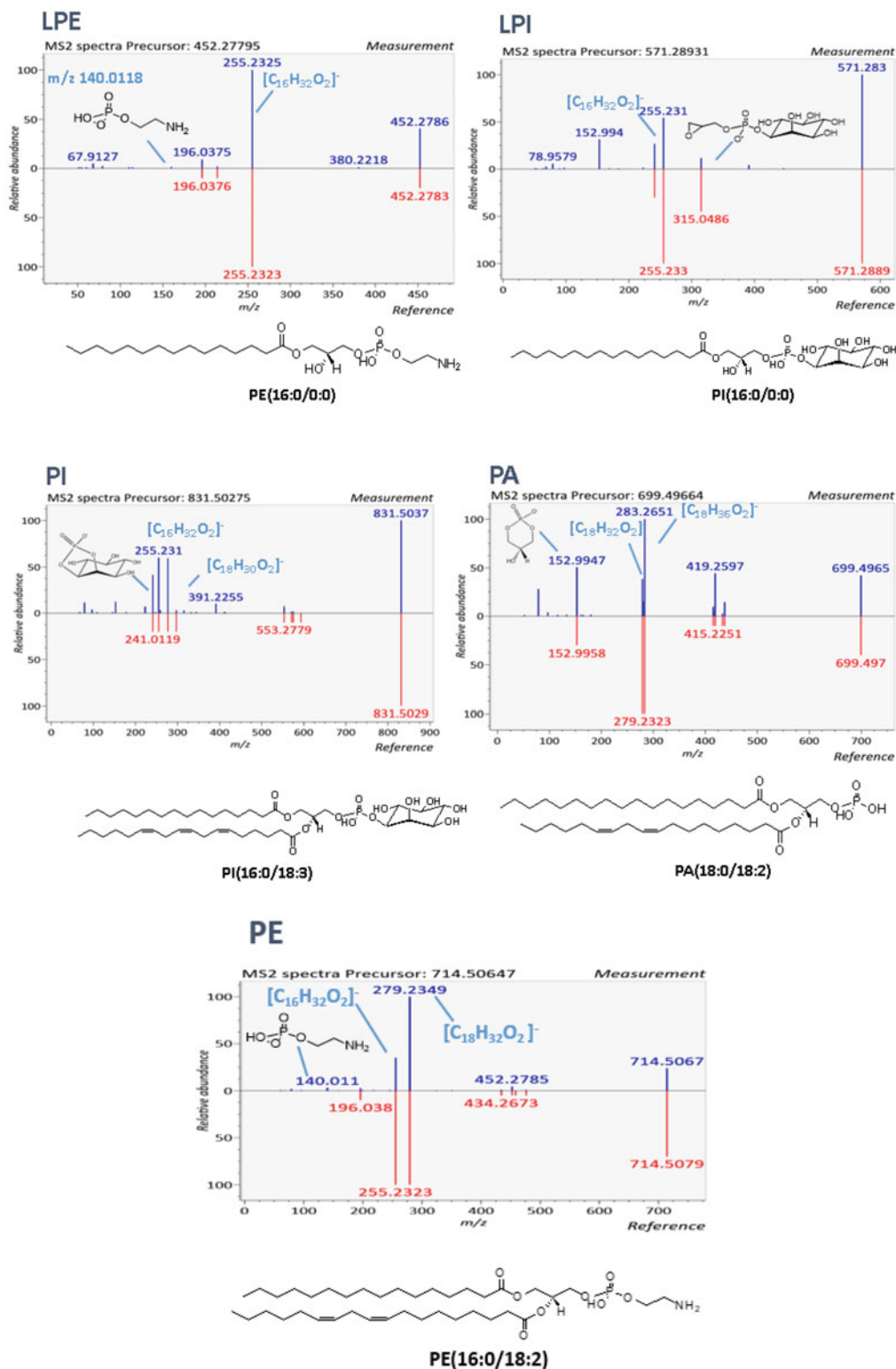


Fig. 5 Experimental (blue) and theoretical (red) representative MS/MS spectra in negative ESI mode for LPI, LPE, PI, PA, and PE classes. *LPI* lysophosphatidylinositol, *LPE* lysophosphatidylethanolamine, *PA* phosphatidic acid, *PI* phosphatidylinositol, *PE* phosphatidylethanolamine

4 Notes

1. Equisplash Lipidomix can also be used as a mixture of the deuterated internal standard instead of Splash Lipidomix. Furthermore, other internal standards representing classes of compounds also found in the coffee lipid fraction can be used.
2. One liter of mobile phase requires 0.63 g of ammonium formate and 1.0 mL of formic acid.
3. The lipid extraction can be performed for coffee beverages as well. In this case, 400 μL of it can be used. Do not add water and follow the procedure described in Subheading 3.1.
4. To increase the lipid yield, a re-extraction can be done using 200 μL of 10:3:2.5 (v/v/v) MTBE/MeOH/H₂O. Then, the organic phases must be combined before being evaporated.
5. The lipids are stable for two to four freeze-thaw cycles when stored at $-80\text{ }^{\circ}\text{C}$ [2, 28].
6. The combination of aliquots of all samples is called pooled quality control (QC), and it is used to verify the system stability and correct systematic measurement bias [25, 28].
7. The acquisition method described is for a Q Exactive Plus mass spectrometer (Thermo Fisher Scientific). Whether other systems are used, please check the best conditions in the literature.
8. If Data-Independent Analysis (DIA) or All Ion Fragmentation (AIF) are used instead of DDA (Data-Dependent Analysis), click in one of the respective options in MS Method Type for MS-DIAL data processing.
9. When using other LC-MS systems or mzML converted files, check if the data type is in Centroid or profile mode.
10. Please refer to the MS-DIAL tutorial when other LC-MS systems are used.
11. It is possible to create a table with the following information to find the internal standards in data efficiently: Name, m/z (MZ), retention time (RT), Adduct, InChiKey, Formula, Smiles, and Ontology. An example for PC 15:0_18:1(d7) is showed below. Save the table as .txt. Go to Advanced in the "Identification" tab, and select this .txt file. Set 100 min to "Retention time tolerance", 0.01 Da as "Accurate mass tolerance", and 80% to "Identification score cut off".

Name PC 15:0_18:1(d7)

RT 12.75

MZ 775.59531

Adduct [M + Na]⁺

InChiKey

ZEWLKXMNQOCOQ-GCHPQBSENA-N
Formula C41H73D7NO8P

Smiles [C@](COP(=O)([O])OCC[N+](C)(C)C)([H])(OC(CCCCCC/C=C\CCCCC([2H])([2H])C([2H])([2H])C([2H])([2H])=O)COC(CCCCCCCCC)=O

Ontology PC

References

- Alves MA, Lamichhane S, Dickens A et al (2021) Systems biology approaches to study lipidomes in health and disease. *Biochim Biophys Acta Mol Cell Biol Lipids* 1866:158857. <https://doi.org/10.1016/j.bbalip.2020.158857>
- Züllig T, Trötz Müller M, Köfeler HC (2020) Lipidomics from sample preparation to data analysis: a primer. *Anal Bioanal Chem* 412: 2191–2209. <https://doi.org/10.1007/s00216-019-02241-y>
- Ahmad R, Ahmad N, AlOthman F et al (2020) Extraction of methyl xanthines and their UHPLC–DAD determination in consumable beverages used in Eastern province of Saudi Arabia. *Biomed Chromatogr* 34:1–12. <https://doi.org/10.1002/bmc.4712>
- de Souza Gois Barbosa M, Dos Santos Scholz MB, Kitzberger CSG, de Toledo Benassi M (2019) Correlation between the composition of green Arabica coffee beans and the sensory quality of coffee brews. *Food Chem* 292: 275–280. <https://doi.org/10.1016/j.foodchem.2019.04.072>
- Speer K, Kölling-Speer I (2019) Lipids. In: Farah A (ed) *Coffee production, quality and chemistry*, 1st edn. Royal Society of Chemistry, London
- Garrett R, Schmidt EM, Pereira LFP et al (2013) Discrimination of arabica coffee cultivars by electrospray ionization Fourier transform ion cyclotron resonance mass spectrometry and chemometrics. *LWT Food Sci Technol* 50:496–502. <https://doi.org/10.1016/j.lwt.2012.08.016>
- Villarreal D, Laffargue A, Posada H et al (2009) Genotypic and environmental effects on coffee (*Coffea arabica* L.) bean fatty acid profile: impact on variety and origin chemometric determination. *J Agric Food Chem* 57: 11321–11327. <https://doi.org/10.1021/jf902441n>
- Amorim ACL, Hovell AMC, Pinto AC et al (2009) Green and roasted Arabica coffees differentiated by ripeness, process and cup quality via electrospray ionization mass spectrometry fingerprinting. *J Braz Chem Soc* 20:313–321. <https://doi.org/10.1590/S0103-50532009000200017>
- Novaes FJM, Oigman SS, de Souza ROMA et al (2015) New approaches on the analyses of thermolabile coffee diterpenes by gas chromatography and its relationship with cup quality. *Talanta* 139:159–166. <https://doi.org/10.1016/j.talanta.2014.12.025>
- Dussert S, Davey M, Laffargue A, Doubeau S, Swennen R, Etienne H (2006) Oxidative stress, phospholipid loss and lipid hydrolysis during drying and storage of intermediate seeds. *Physiol Plant* 127:192–204. <https://doi.org/10.1111/j.1399-3054.2006.00666.x>
- Zhou L, Khalil A, Bindler F et al (2013) Effect of heat treatment on the content of individual phospholipids in coffee beans. *Food Chem* 141:3846–3850. <https://doi.org/10.1016/j.foodchem.2013.06.056>
- Xu L, Lao F, Xu Z et al (2019) Use of liquid chromatography quadrupole time-of-flight mass spectrometry and metabolomic approach to discriminate coffee brewed by different methods. *Food Chem* 286:106–112. <https://doi.org/10.1016/j.foodchem.2019.01.154>
- Anagbogu CF, Zhou J, Olasupo FO et al (2021) Lipidomic and metabolomic profiles of *Coffea canephora* L. beans cultivated in southwestern Nigeria. *PLoS One* 16:1–16. <https://doi.org/10.1371/journal.pone.0234758>
- Cowan AK (2006) Phospholipids as plant growth regulators. *Plant Growth Regul* 48: 97–109. <https://doi.org/10.1007/s10725-005-5481-7>
- Mamode Cassim A, Gouguet P, Gronnier J et al (2019) Plant lipids: key players of plasma membrane organization and function. *Prog Lipid Res* 73:1–27. <https://doi.org/10.1016/j.plipres.2018.11.002>

16. Rubach M, Lang R, Seebach E et al (2012) Multi-parametric approach to identify coffee components that regulate mechanisms of gastric acid secretion. *Mol Nutr Food Res* 56: 325–335. <https://doi.org/10.1002/mnfr.201100453>
17. Cordoba N, Fernandez-Alduenda M, Moreno FL, Ruiz Y (2020) Coffee extraction: a review of parameters and their influence on the physicochemical characteristics and flavour of coffee brews. *Trends Food Sci Technol* 96:45–60. <https://doi.org/10.1016/j.tifs.2019.12.004>
18. Moeenfarid M, Silva JA, Borges N et al (2015) Quantification of diterpenes and their palmitate esters in coffee brews by HPLC-DAD. *Int J Food Prop* 18:2284–2299. <https://doi.org/10.1080/10942912.2014.933351>
19. Moeenfarid M, Erny GL, Alves A (2016) Variability of some diterpene esters in coffee beverages as influenced by brewing procedures. *J Food Sci Technol* 53:3916–3927. <https://doi.org/10.1007/s13197-016-2378-6>
20. Cajka T, Fiehn O (2014) Comprehensive analysis of lipids in biological systems by liquid chromatography-mass spectrometry. *Trends Anal Chem* 61:192–206
21. Tsugawa H, Ikeda K, Takahashi M et al (2020) A lipidome atlas in MS-DIAL 4. *Nat Biotechnol* 38:1159–1163. <https://doi.org/10.1038/s41587-020-0531-2>
22. Matyash V, Liebisch G, Kurzchalia TV et al (2008) Lipid extraction by methyl-tert-butyl ether for high-throughput lipidomics. *J Lipid Res* 49:1137–1146. <https://doi.org/10.1194/jlr.D700041-JLR200>
23. Silva ACR, da Silva CC, Garrett R, Rezende CM (2020) Comprehensive lipid analysis of green Arabica coffee beans by LC-HRMS/MS. *Food Res Int* 137:109727. <https://doi.org/10.1016/j.foodres.2020.109727>
24. Broadhurst D, Goodacre R, Reinke SN et al (2018) Guidelines and considerations for the use of system suitability and quality control samples in mass spectrometry assays applied in untargeted clinical metabolomic studies. *Metabolomics* 14:1–17. <https://doi.org/10.1007/s11306-018-1367-3>
25. Zalloua P, Kadar H, Hariri E et al (2019) Untargeted mass spectrometry lipidomics identifies correlation between serum sphingomyelins and plasma cholesterol. *Lipids Health Dis* 18:1–10. <https://doi.org/10.1186/s12944-018-0948-5>
26. Gil A, Zhang W, Wolters JC et al (2018) One- vs two-phase extraction: re-evaluation of sample preparation procedures for untargeted lipidomics in plasma samples. *Anal Bioanal Chem* 410:5859–5870. <https://doi.org/10.1007/s00216-018-1200-x>
27. Xu T, Hu C, Xuan Q, Xu G (2020) Recent advances in analytical strategies for mass spectrometry-based lipidomics. *Anal Chim Acta* 1137:156–169. <https://doi.org/10.1016/j.aca.2020.09.060>
28. Murphy RC, Axelsen PH (2011) Mass spectrometric analysis of long-chain lipids. *Mass Spectrom Rev* 30:579–599. <https://doi.org/10.1002/mas>



A Novel HPLC-Based Method with LC-Electrospray MS for Analysis of Polyethylene Glycol in Various Foods

Juhee Park and Chan Lee

Abstract

Various types of polymers, such as gums, chitosan, carrageenan, and polydextrose, are used as additives in the food industry. Among these additives, polyethylene glycol (PEG), also called Macrogol, can be used to wrap food and preserve the quality and stability of the foods. PEG is also used as an antifoaming agent, thickener, emulsifier, glazing agent, and a carrier in various foods. PEG products used as food additives have molecular weights between 200 and 9500 g/mol, and an analytical method that can simultaneously analyze the levels of PEGs with a wide range of molecular weights is required to meet food regulations. Polymer analysis is generally conducted using high-performance liquid chromatography (HPLC), infrared (IR) spectroscopy, nuclear magnetic resonance (NMR) spectroscopy, mass spectrometry (MS), and pyrolysis gas chromatography-mass spectrometry (Py-GC/MS). Here, we present an advanced HPLC method to analyze all PEG products utilized in diverse foods, with proper extraction methods for different food matrices. In addition, PEG peaks obtained from HPLC analysis were further verified using liquid chromatography-electrospray ionization tandem mass spectrometry (LC-ESI-MS/MS) with the observed m/z of PEG ions, which results in the formation of charge-neutral polymer adducts $[M + n\text{NH}_4]^{n+}$ with NH_4^+ , as well as protonated species $[M + n\text{H}]^{n+}$ (n : charge state). This new method generates reliable results that can be easily employed in PEG analysis.

Key words Polyethylene glycol, High-performance liquid chromatography, Evaporative light scattering detector, Liquid chromatography tandem mass spectrometry, Polymer, Food additive, Antifoaming agent, Carrier, Thickener, Emulsifier, Glazing agent

1 Introduction

Natural and synthetic polymers, such as gum, chitosan, carrageenan, polydextrose, polyethylene glycol (PEG), and polyvinyl alcohol acetate, can be used as food additives. With respect to chemical composition, they are characterized by the presence of repeating units of monomers and a broad molecular weight distribution [1]. Among these polymers, a PEG product called Macrogol, in the molecular weight range of 200–9500 g/mol, is used as an antifoaming agent, emulsifier, glazing agent, carrier, and

thickener in various types of foods [2]. PEGs present in foods generally do not have detrimental effects on human health [3]. Therefore, they can be safely used to maintain food quality and stability and be used as protective materials for food preservation. PEG products are also widely used as medical, chemical, and biological additives for other purposes. As various PEG products have industrial applications, an appropriate method capable of analyzing PEGs is required in accordance with the regulations governing its use. Particularly, analysis of PEGs present in foods is essential for maintaining food quality and controlling food safety.

To date, polymers have been analyzed using techniques, such as chromatography, infrared spectroscopy, nuclear magnetic resonance spectroscopy, ultraviolet visible spectroscopy, and mass spectrometry [4]. Recently, pyrolysis-GC/MS, a method in which a pyrolysis device is connected to a mass spectrometer, has gained attention as an analytical tool for polymers [5]. In this method, the polymer is directly inserted into the pyrolysis source device, and the pyrolyzed products are analyzed using GC/MS. Among the reported methods, mass spectrometry with matrix-assisted laser desorption/ionization (MALDI) and electrospray ionization (ESI) are considered the most powerful tools for PEG analysis. ESI is increasingly being recognized as a more appropriate method for the analysis of PEGs than MALDI because it is easier to use for CID MS/MS studies and can be easily coupled to liquid separation methods [6]. Furthermore, the liquid separation method combined with ESI can determine the number of functional groups in a polyol and polyol mixture, including PEGs [7], even though ESI is associated with complexities such as multiple charging and stricter solvent requirements during separation than MALDI in general. In addition, ESI in conjunction with tandem mass spectrometry (MS/MS) can elucidate more detailed structural properties of polymers [8]. A notable feature of ESI-MS analysis is the formation of various ions with different charges. The mass-to-charge (m/z) ratio of the ion envelope often overlaps fully or partially with the next charged state. Another feature of note is the production of adducts with cations, such as NH_4^+ , Na^+ , and K^+ , as well as the formation of protonated species $[\text{M} + n\text{H}]^{n+}$ [9]. Therefore, ESI mass spectrometry requires a close examination of the ionized ions in the analysis.

Several mass spectrometric methods have been reported for the analysis of PEGs. Electrospray droplet impact/secondary ion mass spectrometry (EDI/SIMS) was developed as a new ionization method to analyze polystyrene (PS) and PEG [10]. Desorption electrospray ionization (DESI)-orbitrap mass spectrometry (MS) was employed as a new tool for the characterization of various synthetic polymers, including PEGs (range, 500 g/mol to >20,000 g/mol) [11]. Even though these mass spectrometric methods are able to analyze PEGs, none of these can simultaneously analyze all PEG products with molecular weights between

200 and 9500 in food, except for our recently reported method that uses high-performance liquid chromatography (HPLC) and liquid chromatography (LC)-ESI-MS/MS [12]. However, this new method has limitations with respect to analysis of foods because it is optimized only for food supplement tablets [12], and only MS data in the form of protonated species $[M + Na^+ + H_3O_{n-1}^+]$ (n : charged state of product ion) have been reported. Therefore, we describe new pretreatment methods for HPLC analysis to verify the peaks using LC-ESI-MS/MS to analyze PEGs in food supplement tablets and other food categories, such as gums, candy, and drinks. Furthermore, additional analytical MS data have been generated for wide applications, in which the m/z of PEG ions are analyzed not only in the form of protonated species $[M + nH]^{n+}$ (n : charge state), but also in the form of other adducts such as $[M + nNH_4]^{n+}$, which are often generated in MS analysis.

2 Materials

2.1 Chemicals

1. The analytical standard for PEGs includes a wide range of molecular weights (g/mol). PEG 300, 400, 600, 2000, 4000, 6000, and 8000 can be used for the simultaneous analysis of PEGs (Table 1, *see Note 1*).
2. Organic reagents should be handled using nitrile gloves. All reagents should be prepared using deionized water. Methanol should be HPLC grade. Reagents should be stored at room temperature.
3. HPLC instrumentation: 1100 or 1200 Series HPLC system (Agilent, Santa Clara, CA) with a binary LC pump, well-plate autosampler with temperature control, and column oven (Table 2).
4. Organic reagents should be handled using nitrile gloves. All mobile phases are HPLC grade and stored at room temperature.

2.2 Supplies

1. Amber (2.0 mL) and WrtOn vials with PTFE/RS screw caps (Agilent Technologies, Santa Clara, CA, USA) for HPLC analysis.
2. Amber (2.0 mL) and WrtOn vials with PTFE/SIL-bonded septa pre-slit screw caps (Agilent Technologies, Santa Clara, CA, USA) for LC-ESI-MS/MS analysis.
3. C8 column, YMC-Triart C8, 4.6 mm I.D. \times 150 mm, S-5, 12 nm, (YMC, Japan).
4. Syringe (1-cc; Korea Vaccine Co., Ltd., Seoul, Korea).
5. Syringe filter (0.2 μ m pore size and 13-mm diameter; WhatmanTM, Whatman International Ltd., Midstone, England).

Table 1
PEG suppliers

Analytical standard	Vendor
Polyethylene glycol 300	Tokyo Chemical Industry, Tokyo, Japan
Polyethylene glycol 400	Tokyo Chemical Industry, Tokyo, Japan
Polyethylene glycol 600	Tokyo Chemical Industry, Tokyo, Japan
Polyethylene glycol 2000	Tokyo Chemical Industry, Tokyo, Japan
Polyethylene glycol 4000	Tokyo Chemical Industry, Tokyo, Japan
Polyethylene glycol 6000	USP, Rockville, MD, USA
Polyethylene glycol 8000	USP, Rockville, MD, USA

Table 2
Applied mobile phases

Mobile phases	Components
Mobile phase 1	Water (HPLC grade)
Mobile phase 2	Acetonitrile (HPLC grade)
Mobile phase 3	0.1% (v/v) formic acid (LC-MS grade) in water (HPLC grade)
Mobile phase 4	0.1% (v/v) formic acid (LC-MS grade) in acetonitrile (HPLC grade)

2.3 Instruments

2.3.1 Analytical Instrument

1. HPLC and LC-ESI-MS/MS are used to detect PEGs. More details related to the analytical instrument are provided in Table 3.

2.3.2 General Instrument

1. Several instruments are used to prepare the standard solutions and extract PEG from foods. More details related to the analytical instrument are provided in Table 4.

3 Methods

3.1 Quantitative Analysis of PEG in Foods

1. PEGs can be extracted and analyzed in foods as described in steps 1–3. Solvent extraction is used to extract PEG in foods. LC-ESI-MS/MS is used to estimate the size of the polymer in this simultaneous analysis.

3.1.1 Preparation of Analytical Standards

1. Weigh 100 mg of PEG standard in glass tubes with screw caps.
2. Pipette 2 mL of 50% methanol into each glass tube and tightly seal with screw caps.

Table 3
Employed instrumentation

Instrument	Component	Vendor
HPLC	1200 series and 1260 infinity series Degasser Binary pump 1260 Autosampler Thermostatted column compartment Evaporative light scattering detector	Agilent Technologies 1200 series and 1260 Infinity series (San Jose, CA, USA)
LC-ESI-MS/MS	Accela autosampler Accela 600 pump Accela PDA detector LTQ Velos Pro	Thermo Scientific (San Jose, CA, USA) Thermo Fisher Scientific (San Jose, CA, USA)

Table 4
Other instruments utilized

Instrument	Part number	Vendor
Ultrasonic cleaner	3510R-DTH	Branson (Branson Ultrasonics Corporation, Danbury, CT, USA)
Ultrapure water system	PURELAB Chorus 1 Complete	ELGA (High Wycombe, UK)
Vortex mixer	Vortex-Genie 2	Scientific Industries (New York, NY, USA)
Centrifuge	VS-100B	Vision (Daejeon, Korea)
Water bath	SB-1000	Eyela (Tokyo Rikakikai Co., Tokyo, Japan)
Analytical balance	EL204-IC	Mettler-Toledo (Columbus, OH, USA)
Balance	FX-2000i	A&D Company (Tokyo, Japan)

3. Mix the liquid in each tube using a vortex mixer.
4. Pipette 1 mL of PEG standard from each glass tube into a new glass tube.
5. Mix a solution containing 5 molecular weights of PEG using the vortex mixer. This solution contains 10,000 µg/mL of the standard solution.
6. Prepare dilutions of the 10,000 µg/mL standard solution (i.e., 200, 500, 1000, 1500, 2000, and 3000 µg/mL), as shown in Table 5.
7. Store the prepared solutions at 25 °C or transfer them to 2.0 mL amber vials for analysis.

Table 5
PEG's Calibration curve concentrations

Conc. ($\mu\text{g/mL}$)	10,000 $\mu\text{g/mL}$ solution	50% methanol
200	20 μL	980 μL
500	50 μL	950 μL
1000	100 μL	900 μL
1500	150 μL	850 μL
2000	200 μL	800 μL
3000	300 μL	700 μL

8. Seal the vial with a screw cap and slit the screw cap for analysis using HPLC and LC-ESI-MS/MS.

3.1.2 Extraction of PEG from Food

Liquid Food

1. Pipette 3 mL of the liquid sample containing PEG into a 50 mL conical tube.
2. Add 9 mL of 50% methanol in the same tube and seal with a screw cap.
3. Mix the tube vigorously for 3 min.
4. Aspirate 1 mL of the solution using a 1-cc syringe.

High-Fat Food

1. Place a piece of high-fat food sample containing PEG into a 50 mL conical tube.
2. Add 5 mL of 75% methanol in the same tube and seal with a screw cap (*see Note 2*).
3. Mix the tube vigorously for 3 min.
4. Aspirate 1 mL of the solution using a 1-cc syringe (*see Note 3*).

Other Food

1. Place a piece of coated food sample containing PEG into a 50 mL conical tube.
2. Add 5 mL of 50% methanol in same tube and seal with a screw cap.
3. Mix the tube vigorously for 3 min.
4. Aspirate 1 mL of the solution using a 1-cc syringe (*see Note 3*).

3.1.3 Transfer the Extract to the Sample Vial

1. Label the sample vials for identification.
2. Aspirate 1 mL of the extract using a 1-cc syringe. Using a 0.45 μm pore size PVDF syringe filter, filter the extract into a 2.0 mL amber vial.
3. Seal the vial tightly with a screw cap.

3.1.4 HPLC Analysis

This step was used to quantify PEG in foods using HPLC.

1. The standard solutions and samples prepared in **steps 1–3** were placed on the vial tray of the autosampler.
2. The HPLC consisted of a degasser, a binary pump, an autosampler, a thermostatted column compartment, and an evaporative light scattering detector. A YMC-Triart C8 column was equipped with a thermostatted column compartment. Mobile phase 1 and 2 were used as the mobile phase with gradient elution conditions; 0 min, A 80%, B 20%; 7 min, A 55%, B 45%; 14 min, A 45%, B 55%; 15 min, A 80%, B 20%; 20 min, A 80%, B 20%. The flow rate is 1 mL/min, and the sample injection volume is 10 μ L. The thermostatted column compartment was set to 60 °C. ELSD analytical conditions were set as follows: evaporator temperature, 50 °C; nebulizer temperature, 70 °C; N₂ gas flow rate, 1.4 SLM. All settings were processed in the software, which is Agilent ChemStation instrument 1 online. Equilibration of the HPLC column lasted over 30 min with an 80:20 ratio (v/v) of mobile phases 1 and 2 (*see Note 4*).
3. The software, Agilent ChemStation instrument 1 offline, was used for peak integration. Peaks were identified manually, and peak areas were automatically integrated (*see Notes 5 and 6*). Where required, manual integration was employed to estimate the peak area, and the peak areas were inputted into Excel. All the data, including concentrations and peak areas were transformed into logarithmic (base 10) values to verify the linearity of the calibration curve, estimate the value of PEG in food [13], and make it easier to calculate. The calibration curve was plotted as a distributed graph with the logarithmic concentrations and peak areas of the PEG standards. The concentration of PEG in food was estimated by inputting the measured peak area in the equation of the trend line. The obtained logarithmic value could be converted to an exponential value in order to simplify the calculation of the estimated value (*see Note 6*). The HPLC chromatogram of the PEG is shown in Fig. 1.

3.2 Qualitative Analysis of PEG in Foods

3.2.1 LC-ESI-MS/MS Analysis

The following steps were used to identify the PEGs in food using LC-ESI-MS/MS:

1. The prepared vials were placed in a vial tray of the autosampler.
2. The LC-ESI-MS/MS apparatus consisted of an Accela HPLC system (quadruple pump, autosampler, and PDA) and LTQ Velos Pro series. The autosampler was equipped with a YMC-Triart C8 column. Mobile phase 3 and 4 were used as mobile phases with gradient elution conditions described as follows: 0 min, A 80%, B 20%; 7 min, A 55%, B 45%; 14 min, A 45%, B 55%; 15 min, A 80%, B 20%; and 20 min, A 80%, B

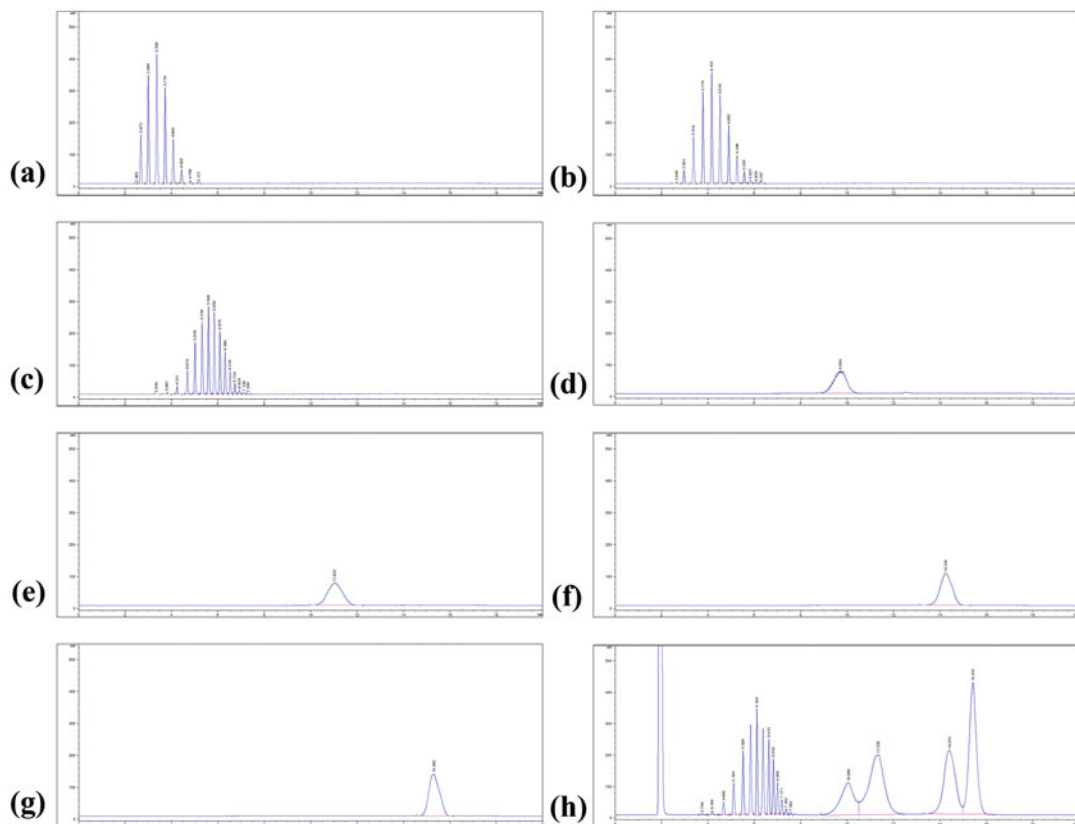


Fig. 1 HPLC chromatograms of PEG standards, PEG 300 (a), 400 (b), 600 (c), 2000 (d), 4000 (e), 6000 (f), 8000 (g), and mixture of PEG spiked in blank matrix (h)

20%. The flow rate was 1 mL/min, and the sample injection volume was 10 μ L. The column temperature was set at 60 $^{\circ}$ C. The ESI source was set to positive ion mode, 5 kV of spray voltage, 275 $^{\circ}$ C of capillary temperature, 35 L/h sheath gas flow, 5 L/h aux gas flow, and 35 V collision energy. All settings were processed using the XcaliburTM software. Equilibration of the HPLC column lasted over 30 min with an 80:20 ratio (v/v) of mobile phases 3 and 4 (*see Note 4*). In addition, LC-ESI-MS/MS was operated in the positive ion mode, and the signal was recorded in the profile mode to observe the characteristics of the charge state (*see Notes 7 and 8*) (Fig. 2).

4 Notes

1. PEG 600 is a colorless liquid that should be stored at 25 $^{\circ}$ C. It easily solidifies when surrounded by cool air, such as from air conditioners and winter air. If liquid PEG 600 gets solidified, it should be incubated at 25 $^{\circ}$ C to enable its conversion into the

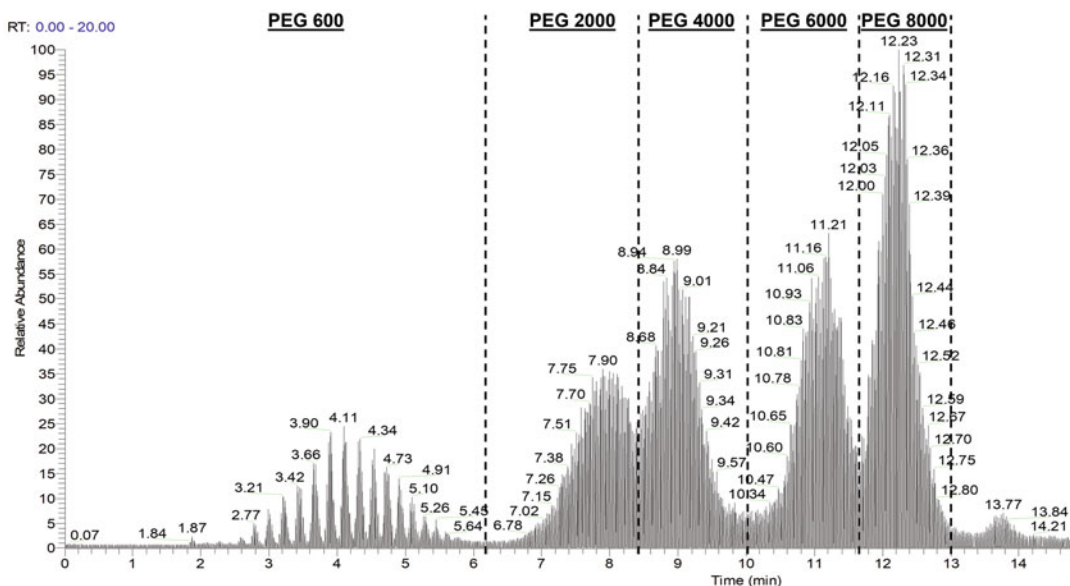


Fig. 2 Total ion chromatograms of the PEG mixtures containing PEG 600, 2000, 4000, 6000, and 8000 in ESI-LC-MS/MS analysis

liquid form. Solidification does not affect product quality or stability.

2. High-fat foods can interfere with the detection of PEG; therefore, 75% methanol is used to prevent such interference. Hexane is generally used to remove fat, but it interferes with the detection of PEG.
3. If the mixed solutions are very chunky, then the solution is centrifuged. The chunky solution is transferred into a 1.5 mL Eppendorf tube and centrifuged at $10,000 \times g$ for 15 s. The supernatant is then collected using a 1-cc syringe.
4. For column equilibrium, mobile phases are retained at an 80:20 ratio (v/v) for at least 30 min. To analyze the PEG stably, the column should be appropriately equilibrated prior to initiation of analysis to detect the target compound. It is recommended that after the analysis, the column should be washed alternately with 5:95 and 95:5 ratios of water and acetonitrile because the PEG elutes out of the column from low to high organic solvent ratio over time.
5. For PEG 600, it is recommended to select the largest peak to calculate the value because of detection of a number of peaks over 10. The peaks of PEG 2000 and 4000, as well as those of PEG 6000 and 8000, are manually split because they partially overlap between PEG 2000 and 4000, and PEG 6000 and 8000.

6. Peaks of PEG with diverse molecular weights are detected in order, and they overlap due to the concordance of molecular weight of PEG products. Polymers such as PEGs are difficult to manufacture with a uniform molecular weight; thus, PEG products are sold with a wide range of molecular weights centered around a single molecular weight marked on the product label. This HPLC analysis method can be employed to quantify PEG with diverse molecular weights in foods. However, to quantify the amount of PEG in food, the molecular weights of PEG available for simultaneous analysis are limited to 600–8000 due to overlapping peaks of PEG 200–600.
7. The monomer of PEG is ethylene glycol (molecular weight, 44.05 ± 0.5). This is observed in the analytical results using LC-ESI-MS/MS, which make it possible to confirm the presence of PEG in the analyzed sample. As the molecular weight of PEG increases, its charged state also increases, and these properties were confirmed in our previous study [12]. Unlike in our previous study, other m/z patterns, such as $[M + nH]^{n+}$ and $[M + nNH_4]^{n+}$ (n : charge state), were investigated in this study. Charge state patterns of 1, 0.5, 0.33, and 0.25 apart in the isotope cluster can be identified through the profile mode in ESI-MS analysis. It is difficult to observe these patterns in the +5 or more charge states due to limitations of the technology; thus, the identification of PEG in the analyte can be estimated by comparing the expected mass values and observed m/z values. The formula used to calculate the expected mass values is as follows:
 - (a) Expected mass values = $(M + n NH_4)/n$ (n : charge state).
 - (b) $M = m(O-CH_2-CH_2) + 2H + O = m \times 44.05 + 2 + 16$ (m : number of ethylene glycol units).
 - (c) The charge states and MS fragments of the PEG standard can be observed using LC-ESI-MS, and more details are provided in Tables 6 and 7.
8. To identify the mass data of PEG, the Xcalibur raw file is opened in the Thermo Xcalibur Qual Browser software. Ranges are selected by pressing and releasing the right mouse button in the chromatogram view (TIC). The scan filter is set as ITMS + p ESI Full ms [50.00–2000.00], and the plot type is set as TIC. An RT at the peak of PEG is chosen. The observed mass fragments are compared with the values shown in Tables 6 and 7. Most of the observed data, including RT, mass fragmentation pattern, and molecular weights, are similar, but can be different from the data described in Tables 6 and 7. This may be caused by the use of different instruments and columns to identify the mass fragments of PEG. However, this limitation in identifying PEGs can be overcome with the use of LC-ESI-MS.

Table 6
Observed MS fragments and charge states of PEG ions; [M + $n\text{NH}_4$] $^{n+}$ (n : charge state)

No.	PEG product	Retention time	Molecular weight	Charge state	Observed MS fragments [M + $n\text{NH}_4$] $^{n+}$ (n : charge state)	
1	PEG 300–400	2.28	238.28	+1	256.17	
2		2.41	282.33	+1	300.09	
3	PEG 300–600	2.57	326.38	+1	344.17	
4		2.78	370.43	+1	388.18	
5		3.00	414.49	+1	432.34	
6		3.21	458.54	+1	476.26	
7		3.46	502.59	+1	520.35	
8		3.66	546.64	+1	564.26	
9		3.88	590.70	+1	608.43	
10		4.13	634.75	+1	652.43	
11		4.32	678.80	+1 → +2	696.52 357.17	
12		4.53	722.85	+1 → +2	740.35 379.26	
13		4.75	766.91	+1 → +2	784.44 401.26	
14		4.94	810.96	+1 → +2	828.52 423.26	
15		5.11	855.01	+1 → +2	572.52 445.26	
16		5.30	899.06	+1 → +2	916.52 467.26	
17		PEG 2000	6.97	1471.74	+2 → +3	753.35 508.26
18			7.08	1515.80	+2 → +3	775.44 522.93
19	7.17		1559.85	+2 → +3	797.44 539.26	
20	7.22		1603.90	+2 → +3	819.44 553.93	
21	7.33		1647.95	+2 → +3	841.52 568.60	
22	7.35		1692.01	+2 → +3	865.94 581.68	
23	7.43		1736.06	+2 → +3	885.52 596.43	
24	7.54		1780.11	+2 → +3	907.52 611.01	
25	7.61		1824.16	+2 → +3	929.44 625.60	
26	7.67		1868.22	+2 → +3	951.61 640.43	
27	7.74		1912.27	+2 → +3	973.52 655.02	
28	7.77		1956.32	+2 → +4	995.52 669.77 508.10	
29	7.85		2000.37	+2 → +4	1017.61 684.43 517.85	
30	7.93		2044.43	+2 → +4	1039.61 700.68 530.10	

(continued)

Table 6
(continued)

No.	PEG product	Retention time	Molecular weight	Charge state	Observed MS fragments [M + $n\text{NH}_4$] ^{r+} (r: charge state)
31		7.98	2088.48	+2 → +4	1061.53 713.68 539.85
32		8.03	2132.53	+2 → +4	1083.61 728.43 550.85
33		8.10	2176.58	+2 → +4	1105.61 743.10 561.85
34	PEG	8.16	2220.64	+2 → +4	1127.69 757.77 574.01
35	2000-4000	8.23	2264.69	+2 → +4	1149.61 772.44 583.85
36		8.28	2308.74	+2 → +4	1171.70 787.19 594.93
37		8.31	2352.79	+2 → +4	1194.11 801.77 606.85
38		8.36	2396.84	+2 → +5	1215.70 816.52 616.93 498.26
39		8.44	2440.90	+2 → +5	1238.11 831.44 628.10 507.01
40	PEG 4000	8.50	2484.95	+2 → +5	1260.28 846.19 639.18 514.51
41		8.55	2529.00	+2 → +5	1282.20 860.85 650.10 523.51
42		8.58	2573.05	+2 → +5	1304.28 875.19 661.18 533.43
43		8.61	2617.11	+2 → +5	1326.20 890.19 672.18 541.35
44		8.63	2661.16	+2 → +5	1348.20 904.86 683.18 550.01
45		8.68	2705.21	+2 → +5	1370.28 919.52 694.18 559.85
46		8.71	2749.26	+2 → +5	1392.78 934.52 705.35 567.76
47		8.73	2793.32	+2 → +5	1414.79 949.19 716.18 576.60
48		8.76	2837.37	+2 → +5	1436.20 964.19 727.35 585.35
49		8.81	2881.42	+2 → +5	1458.20 978.52 738.10 594.18
50		8.84	2925.47	+2 → +5	1480.37 992.86 749.18 603.76
51		8.89	2969.53	+2 → +5	1502.29 1007.94 760.18 611.76
52		8.91	3013.58	+2 → +5	1524.87 1022.53 771.10 620.51
53		8.96	3057.63	+2 → +5	1545.79 1038.19 781.94 629.51
54		9.01	3101.68	+3 → +5	1051.86 794.35 638.93
55		9.04	3145.74	+3 → +5	1066.28 804.19 647.35
56		9.07	3189.79	+3 → +5	1081.28 815.77 655.77
57		9.09	3233.84	+3 → +6	1095.61 826.19 664.60 557.68
58		9.12	3277.89	+3 → +6	1110.61 837.02 673.60 565.10
59		9.17	3321.95	+3 → +6	1125.19 848.19 682.18 572.35
60		9.22	3366.00	+3 → +6	1139.61 859.19 691.93 579.68

61	9.25	3410.05	+3 → +6	1154.28	870.19	700.10	586.85
62	9.32	3454.10	+3 → +6	1169.20	882.69	708.60	594.35
63	9.38	3498.15	+4 → +6	892.44	717.77	601.51	
64	9.43	3542.21	+4 → +6	903.44	726.93	607.93	
65	10.09	4467.31	+5 → +7	911.94	762.60	657.68	
66	10.12	4555.41	+5 → +7	929.94	777.69	669.35	
67	10.17	4599.46	+5 → +7	938.02	785.02	674.68	
68	10.22	4687.57	+5 → +8	956.19	800.77	687.65	604.60
69	10.24	4775.67	+5 → +8	974.19	814.52	700.60	614.76
70	10.27	4863.78	+5 → +8	991.52	828.19	713.35	626.10
71	10.32	4907.83	+5 → +8	999.86	833.85	719.77	631.85
72	10.37	4951.88	+5 → +8	1008.94	844.02	726.10	637.93
73	10.40	4995.94	+6 → +8	851.10	732.35	643.93	
74	10.42	5039.99	+6 → +8	858.52	738.35	649.10	
75	10.45	5084.04	+6 → +8	865.69	745.52	652.77	
76	10.48	5172.15	+6 → +8	880.60	757.35	665.60	
77	10.50	5216.20	+7 → +9	763.60	670.43	598.01	
78	10.53	5260.25	+7 → +9	769.94	674.85	602.18	
79	10.58	5304.30	+7 → +9	776.69	681.43	607.85	
80	10.60	5348.36	+7 → +9	782.77	687.18	611.85	
81	10.63	5392.41	+7 → +9	788.94	692.68	617.43	
82	10.65	5436.46	+7 → +9	795.52	698.27	622.35	
83	10.68	5480.51	+7 → +9	801.69	702.77	625.60	
84	10.7	5524.56	+7 → +9	807.94	708.02	631.26	
85	10.73	5568.62	+7 → +9	814.52	713.35	636.77	
86	10.76	5612.67	+7 → +9	819.81	719.58	641.63	
87	10.78	5700.77	+7 → +9	833.35	730.27	651.93	
88	10.81	5744.83	+8 → +10	736.10	657.85	597.68	
89	10.83	5788.88	+8 → +10	740.77	661.27	601.76	
90	10.88	5876.98	+8 → +10	751.27	670.52	611.01	
91	10.91	5921.04	+8 → +10	759.85	674.85	613.01	
92	10.96	5965.09	+8 → +11	762.27	680.68	619.93	559.18
93	10.98	6009.14	+8 → +11	768.69	685.27	623.76	563.76
94	11.01	6053.19	+8 → +11	774.27	690.18	628.93	567.10
95	11.06	6097.25	+8 → +11	779.60	695.02	632.60	571.43
96	11.09	6141.30	+8 → +11	785.10	700.18	638.68	575.26
97	11.11	6185.35	+8 → +11	790.52	705.35	641.52	579.43
98	11.14	6229.40	+8 → +11	796.02	709.60	645.93	584.85
99	11.16	6317.51	+8 → +11	807.19	719.35	653.68	592.93

(continued)

Table 6
(continued)

No.	PEG product	Retention time	Molecular weight	Charge state	Observed MS fragments [M + $n\text{NH}_4$] ⁿ⁺ (<i>m/z</i> charge state)
100		11.21	6405.61	+8 → +11	818.10 729.60 663.43 599.35
101		11.24	6493.72	+8 → +11	829.19 738.93 671.10 607.93
102		11.29	6581.82	+8 → +11	840.10 750.35 681.27 615.18
103		11.32	6669.93	+8 → +11	851.44 759.93 690.10 623.60
104		11.39	6802.08	+8 → +12	869.35 773.52 703.35 636.10 584.51
105		11.44	6890.19	+8 → +12	880.60 783.77 711.02 644.68 591.51
106		11.49	6934.24	+8 → +12	884.02 788.02 716.35 649.68 596.68
107		11.52	7066.40	+8 → +12	901.77 804.02 729.10 659.60 606.10
108		11.57	7198.56	+8 → +13	917.27 817.19 743.52 672.85 617.43 571.76
109		11.62	7286.66	+8 → +13	928.44 828.27 751.77 679.43 625.22 578.51
110		11.70	7374.77	+8 → +13	938.94 837.52 760.27 688.68 632.35 585.35
111		11.75	7506.92	+9 → +13	852.27 773.69 699.35 644.52 595.60
112	PEG 8000	11.84	7727.18	+8 → +13	984.11 875.85 795.60 720.02 662.18 612.93
113		11.86	7771.24	+8 → +13	989.02 881.19 799.94 723.68 666.35 615.35
114		11.91	7815.29	+8 → +14	994.02 885.94 804.60 727.68 668.77 619.68 575.76
115		11.94	7991.50	+8 → +14	1016.27 906.44 822.19 743.68 684.18 632.51 588.76
116		11.96	8079.60	+8 → +14	1026.28 915.02 830.10 751.60 692.60 640.68 595.51
117		11.99	8167.71	+8 → +14	1038.96 924.86 839.77 759.35 697.85 646.27 601.01
118		12.04	8343.92	+8 → +15	1060.11 945.11 857.27 776.19 713.85 659.85 613.85 574.85
119		12.12	8520.13	+8 → +16	1082.36 964.86 874.60 791.85 729.27 673.27 625.26 586.51 550.43
120		12.17	8652.29	+8 → +16	1098.86 980.77 888.10 803.69 740.52 683.68 635.93 595.68 558.18
121		12.19	8740.39	+9 → +16	988.52 896.86 811.35 747.60 690.27 642.10 601.35 564.01
122		12.22	8828.49	+10 → +16	905.77 820.44 752.60 696.85 649.35 607.10 570.26
123		12.24	8960.65	+10 → +16	919.02 833.52 764.77 707.18 657.68 616.01 578.10
124		12.29	9048.76	+10 → +16	927.52 839.60 771.44 714.43 664.35 621.60 583.01
125		12.34	9136.86	+10 → +15	936.61 847.60 779.69 720.02 669.52 627.76
126		12.37	9224.97	+10 → +15	945.44 856.44 786.10 727.52 676.77 633.18
127		12.40	9401.18	+10 → +16	963.02 872.02 801.52 741.68 689.68 645.43 605.18
128		12.42	9533.33	+10 → +16	976.02 884.67 812.02 751.27 698.93 653.02 613.26
129		12.45	9665.49	+11 → +16	896.61 823.44 761.60 708.60 662.93 621.85

Table 7
Observed MS fragments and charge states of PEG ions; [M + nH]ⁿ⁺ (n: charge state)

No.	PEG product	Retention time	Molecular weight	Charge state	Observed MS fragments [M + nH] ⁿ⁺ (n: charge state)	
1	PEG 300–400	2.28	238.28	+1	239.17	
2		2.41	282.33	+1	283.09	
3	PEG 300–600	2.57	326.38	+1	327.17	
4		2.78	370.43	+1	371.17	
5		3.00	414.49	+1	415.34	
6		3.21	458.54	+1	459.18	
7		3.46	502.59	+1	503.35	
8		3.66	546.64	+1	547.26	
9		3.88	590.70	+1	591.35	
10		4.13	634.75	+1	635.43	
11		4.32	678.80	+1 → +2	679.43 340.26	
12		4.53	722.85	+1 → +2	723.35 362.17	
13		4.75	766.91	+1 → +2	767.44 384.18	
14		4.94	810.96	+1 → +2	811.44 406.26	
15		5.11	855.01	+1 → +2	855.52 428.26	
16		5.30	899.06	+1 → +2	899.44 445.26	
17		PEG 2000	6.99	1471.74	+2 → +3	736.43 491.26
18			7.05	1515.80	+2 → +3	758.35 505.93
19	7.14		1559.85	+2 → +3	780.44 520.60	
20	7.19		1603.90	+2 → +3	802.44 535.26	
21	7.27		1647.95	+2 → +3	824.94 550.01	
22	7.33		1692.01	+2 → +3	846.44 564.60	
23	7.38		1736.06	+2 → +3	868.44 579.26	
24	7.43		1780.11	+2 → +3	890.44 594.01	
25	7.48		1824.16	+2 → +3	913.02 609.01	
26	7.59		1868.22	+2 → +3	935.02 623.35	
27	7.64		1912.27	+2 → +3	957.02 638.02	
28	7.69		1956.32	+2 → +4	979.02 652.77 489.84	
29	7.77		2000.37	+2 → +4	1001.02 667.02 501.01	
30	7.82		2044.43	+2 → +4	1022.94 682.68 511.85	

(continued)

Table 7
(continued)

No.	PEG product	Retention time	Molecular weight	Charge state	Observed MS fragments [M + rH] ^{r+} (r: charge state)
31		7.87	2088.48	+2 → +4	1045.03 697.02 523.01
32		7.95	2132.53	+2 → +4	1067.03 711.10 534.35
33		8.03	2176.58	+2 → +4	1089.53 726.02 545.10
34		8.08	2220.64	+2 → +4	1111.03 741.02 555.93
35		8.18	2264.69	+2 → +4	1133.53 755.35 567.01
36		8.21	2308.74	+2 → +4	1155.11 770.35 578.01
37		8.31	2352.79	+2 → +4	1177.11 785.10 589.10
38	PEG	8.39	2396.84	+2 → +4	1199.20 799.44 600.10
39	2000-4000	8.47	2440.90	+3 → +4	814.19 610.93
40	PEG 4000	8.44	2484.95	+3 → +5	829.10 621.85 497.76
41		8.50	2529.00	+3 → +5	844.52 632.93 506.76
42		8.53	2573.05	+3 → +5	858.10 645.60 515.68
43		8.61	2617.11	+3 → +5	872.52 654.93 524.76
44		8.66	2661.16	+3 → +5	887.52 665.93 533.01
45		8.68	2705.21	+4 → +5	677.18 541.85
46		8.73	2749.26	+4 → +5	688.18 550.85
47		8.76	2793.32	+4 → +5	699.10 559.76
48		8.78	2837.37	+4 → +5	710.18 568.51
49		8.81	2881.42	+4 → +5	721.10 577.26
50		8.84	2925.47	+4 → +6	732.37 586.10 488.68
51		8.89	2969.53	+4 → +6	743.18 595.10 496.09
52		8.91	3013.58	+4 → +6	754.39 603.51 502.93
53		8.94	3057.63	+4 → +6	765.10 612.60 510.68
54		8.99	3101.68	+4 → +6	776.35 621.35 517.68
55		9.04	3145.74	+4 → +6	786.94 630.10 524.93
56		9.07	3189.79	+4 → +6	798.44 639.02 532.93
57		9.09	3233.84	+4 → +6	809.10 648.18 540.18
58		9.12	3277.89	+4 → +6	820.52 656.85 546.93
59		9.14	3321.95	+4 → +6	831.19 665.60 555.68
60		9.17	3366.00	+4 → +6	841.94 674.35 562.10

Table 7
(continued)

No.	PEG product	Retention time	Molecular weight	Charge state	Observed MS fragments [M + nH] ⁿ⁺ (n: charge state)
97		11.04	6097.25	+5 → +11	1220.86 1016.94 872.69 763.02 678.27 610.76 555.26
98		11.04	6141.30	+5 → +11	1228.61 1024.11 878.10 768.69 683.27 615.10 559.51
99		11.04	6185.35	+5 → +11	1238.36 1031.53 884.44 774.35 688.43 619.43 563.26
100		11.06	6229.40	+5 → +10	1246.88 1039.23 891.02 779.60 693.35 623.85
101		11.09	6273.46	+5 → +11	1255.78 1046.61 897.11 785.10 698.10 628.43 571.35
102		11.09	6317.51	+5 → +11	1264.28 1054.03 903.27 790.35 702.93 632.60 575.26
103		11.16	6405.61	+6 → +11	1068.78 916.02 801.44 712.68 641.43 583.18
104		11.19	6449.67	+6 → +11	1075.61 922.69 807.27 717.85 646.10 587.60
105		11.21	6493.72	+6 → +11	1083.03 928.52 812.77 722.43 650.35 591.35
106		11.24	6537.77	+7 → +12	934.77 818.44 727.35 654.85 595.43 545.76
107		11.26	6581.82	+6 → +11	1098.28 943.52 823.60 732.43 659.18 599.35
108		11.29	6713.98	+6 → +12	1119.86 960.02 840.10 747.10 672.60 611.51 560.43
109		11.32	6758.03	+6 → +12	1126.94 966.69 845.69 752.02 676.68 615.18 564.18
110		11.34	6802.08	+5 → +12	1361.42 1134.68 972.52 853.10 756.77 681.01 619.43 567.76
111		11.39	6846.14	+5 → +12	1370.23 1142.02 979.44 856.69 762.68 685.43 623.10 571.35
112		11.44	6890.19	+6 → +12	1149.11 984.94 863.10 766.19 689.77 627.35 574.93
113		11.47	6978.29	+5 → +12	1396.66 1164.05 997.94 873.19 776.35 698.85 635.43 582.76
114		11.52	7154.50	+6 → +11	1192.36 1023.19 895.19 796.02 716.18 652.85
115		11.57	7286.66	+6 → +14	1215.36 1041.03 911.86 810.60 729.43 662.35 608.35 561.43 521.68
116		11.59	7330.71	+6 → +13	1221.45 1049.53 918.27 815.35 734.02 667.52 612.18 564.94
117	PEG 8000	11.65	7506.92	+7 → +13	1073.86 938.69 835.27 751.77 685.10 627.85 578.10
118		11.67	7550.98	+7 → +13	1079.11 944.61 839.94 756.85 687.60 630.18 582.18
119		11.72	7595.03	+7 → +13	1085.69 950.11 844.19 760.52 691.35 635.18 584.51
120		11.78	8079.60	+7 → +14	1154.36 1010.69 898.44 808.77 735.27 675.27 622.10 578.93
121		11.81	8167.71	+7 → +14	1168.53 1022.36 908.44 817.19 743.27 682.10 628.93 584.51
122		11.91	8255.81	+7 → +14	1179.11 1032.98 917.36 826.51 751.35 688.85 636.27 590.68
123		11.96	8299.87	+7 → +14	1186.61 1038.19 923.44 830.10 755.60 692.60 639.27 594.01
124		12.01	8387.97	+8 → +13	1049.69 932.94 839.60 763.52 700.02 646.43
125		12.04	8432.02	+9 → +14	937.61 844.35 767.44 703.60 649.60 603.60
126		12.06	8476.08	+7 → +15	1211.53 1059.94 942.61 848.60 771.52 707.34 653.27 606.51 566.10

127	12.12	8652.29	+7 → +14	1237.04	1082.36	962.19	866.27	787.52	722.02	666.43	619.01
128	12.17	8872.55	+9 → +14	986.69	888.10	807.44	740.52	683.68	635.93		
129	12.19	8960.65	+9 → +15	996.27	896.86	815.02	747.60	690.27	640.35	598.35	
130	12.22	9048.76	+9 → +14	1006.19	905.77	824.10	755.10	697.35	647.35		
131	12.24	9136.86	+11 → +14	831.60	762.77	703.93	653.52				
132	12.29	9224.97	+11 → +15	839.60	769.85	711.35	660.02	616.01			
133	12.34	9357.12	+11 → +15	851.69	779.69	720.02	669.52	623.60			
134	12.37	9445.23	+11 → +14	859.69	788.19	727.52	676.77				
135	12.42	9577.39	+11 → +14	870.52	799.19	737.85	684.52				
136	12.45	9709.54	+11 → +15	883.69	810.02	748.02	694.68	647.10			
137	12.53	9841.70	+11 → +15	895.61	820.35	758.10	703.52	657.68			

Acknowledgement

This research was supported by a grant (18162MFDS009) from the Ministry of Food and Drug Safety in 2018.

References

1. Hanton SD (2001) Mass spectrometry of polymers and polymer surfaces. *Chem Rev* 101(2): 527–569. <https://doi.org/10.1021/cr9901081>
2. CODEX Alimentarius (2019) Food additive details, polyethylene glycol (1521). Rome. <http://www.fao.org/gsfaonline/additives/details.html?id=270>. Accessed 3 Apr 2021
3. Shit SC, Shah PM (2014) Edible polymers: challenges and opportunities. *J Polymers* 2014(4):1–13. <https://doi.org/10.1155/2014/427259>
4. Stuart BH (2008) *Polymer analysis*, vol 30. Wiley, Chichester
5. McEwen CN, Peacock PM (2002) Mass spectrometry of chemical polymers. *Anal Chem* 74(12):2743–2748. <https://doi.org/10.1021/ac020214u>
6. Peacock PM, McEwen CN (2006) Mass spectrometry of synthetic polymers. *Anal Chem* 78(12):3957–3964. <https://doi.org/10.1021/ac040064i>
7. Watkins MA, Winger BE, Shea RC, Kenttmaa HI (2005) Ion-molecule reactions for the characterization of polyols and polyol mixtures by ESI/FT-ICR mass spectrometry. *Anal Chem* 77(5):1385–1392. <https://doi.org/10.1021/ac049031t>
8. Crotty S, Gerişlioğlu S, Endres KJ, Wesdemiotis C, Schubert US (2016) Polymer architectures via mass spectrometry and hyphenated techniques: a review. *Anal Chim Acta* 932:1–21. <https://doi.org/10.1016/j.aca.2016.05.024>
9. De Bruycker K, Welle A, Hirth S, Blanksby SJ, Barner-Kowollik C (2020) Mass spectrometry as a tool to advance polymer science. *Nat Rev Chem* 4(5):257–268. <https://doi.org/10.1038/s41570-020-0168-1>
10. Asakawa D, Chen LC, Hiraoka K (2009) The analysis of industrial synthetic polymers by electrospray droplet impact/secondary ion mass spectrometry. *J Mass Spectrom* 44(6): 945–951. <https://doi.org/10.1002/jms.1569>
11. Friia M, Legros V, Tortajada J, Buchmann W (2012) Desorption electrospray ionization-orbitrap mass spectrometry of synthetic polymers and copolymers. *J Mass Spectrom* 47(8): 1023–1033. <https://doi.org/10.1002/jms.3057>
12. Kim H, Park J, Suh HJ, Lee J, Lee C (2020) Simultaneous analysis of polyethylene glycol in dietary supplement tablets using high-performance liquid chromatography and verification with liquid chromatography–electrospray ionization mass spectrometry. *Food Chem* 326:126933. <https://doi.org/10.1016/j.foodchem.2020.126933>
13. Wasik A, McCourt J, Buchgraber M (2007) Simultaneous determination of nine intense sweeteners in foodstuffs by high performance liquid chromatography and evaporative light scattering detection—development and single-laboratory validation. *J Chromatogr A* 1157:187–196. <https://doi.org/10.1016/j.chroma.2007.04.068>



Application of UHPLC-HRMS/MS for the Analysis of Beta-Casomorphin 5 and 7 in Milk

Duc Doan Nguyen, Francesco Buseti, and Stuart Keith Johnson

Abstract

Ultra-high performance liquid chromatography coupled to high-resolution mass spectrometry (UHPLC-HRMS/MS) enables simultaneous identification and quantification of beta-casomorphine 5 (β -CM5) and beta-casomorphin 7 (β -CM7) at the level of ng/mL in milk. This analytical technique uses stable isotope-labeled beta-casomorphin 5 (β -CM5-d₁₀) and beta-casomorphin 7 (β -CM7-d₁₀) to achieve accurate quantitation of target peptides. In addition, solid-phase extraction (SPE) can be used for concentration and purification of milk extracts to improve the limits of detection and quantitation of the method.

Key words Beta-casomorphin 5, Beta-casomorphin 7, Milk, UHPLC-HRMS

1 Introduction

Bovine beta-casomorphins (β -CMs) are opioid peptides released from parent beta-casein variants after gastrointestinal enzymatic digestion or during milk processing [1–7]. Among the β -CMs, β -CM5 (Tyr⁶⁰-Pro⁶¹-Phe⁶²-Pro⁶³-Gly⁶⁴), and β -CM7 (Tyr⁶⁰-Pro⁶¹-Phe⁶²-Pro⁶³-Gly⁶⁴-Pro⁶⁵-Ile⁶⁶) have strong opioid activity and as such are a concern for human health. This concern has led to many recent developments in techniques for their analysis.

The β -CM7 peptide has been previously quantified in milk using the enzyme-linked immunosorbent assay (ELISA) [8]; however, this method can be inaccurate for quantitation of β -CM5/7 due to cross-reactivity within the complex milk matrix [9]. Moreover, ELISA cannot be used for the simultaneous determination of β -CM5/7. In recent years, liquid chromatography-tandem mass spectrometry (LC-MS/MS) has been used widely for the simultaneous identification and quantitation of β -CM5/7 in milk [1, 10–12]. While this technique is generally accurate, selective, and very sensitive, it can suffer from false-positive detection of β -CM5/7 [12].

In this chapter, the application of ultra-high performance liquid chromatography coupled to high-resolution mass spectrometry (UHPLC-HRMS/MS) for the simultaneous identification and quantification β -CM5/7 in milk is presented. The inclusion of stable isotope-labeled beta-casomorphin 5/7 (β -CM5/7-d₁₀) corrects for matrix effects and analyte losses encountered during SPE sample extraction and clean-up [1, 12].

2 Materials

All stock standard solutions, working standard solutions [13] and calibration solutions [1] are prepared as follows:

2.1 Stock Standard Solutions

1. Beta-casomorphin 5 solution, $c(\beta\text{-CM5}) = 1 \text{ mg/mL}$.
1. Accurately weigh out 5 mg of β -CM5 analytical standard in a 5 mL volumetric flask. Add ultra-pure water to the mark and mix thoroughly. Store the solution at $-80 \text{ }^\circ\text{C}$ (*see Note 1*).
2. Beta-casomorphin 7 solution, $c(\beta\text{-CM7}) = 1 \text{ mg/mL}$.
3. Accurately weigh out 5 mg of β -CM7 analytical standard in ultra-pure water in a 5 mL volumetric flask. Add ultra-pure water to the mark and mix thoroughly. Store the solution at $-80 \text{ }^\circ\text{C}$ (*see Note 1*).
4. Stable isotope-labeled beta-casomorphin 5 solution, $c(\beta\text{-CM5-d}_{10}) = 1 \text{ mg/mL}$.
5. Accurately weigh out 5 mg of analytical standard β -CM5-d₁₀ in a 5 mL volumetric flask. Add ultra-pure water to the mark and mix thoroughly. Store the solution at $-80 \text{ }^\circ\text{C}$ (*see Note 1*).
6. Stable isotope-labeled beta-casomorphin 7 solution, $c(\beta\text{-CM7-d}_{10}) = 1 \text{ mg/mL}$.
7. Dissolve 5 mg of analytical standard β -CM7-d₁₀ in ultra-pure water in a 5 mL volumetric flask. Add ultra-pure water to the mark and mix thoroughly. Store the solution at $-80 \text{ }^\circ\text{C}$ (*see Note 1*).

2.2 Working Standard Solutions

1. Beta-casomorphin 5 solution, $c(\beta\text{-CM5}) = 1 \text{ ng}/\mu\text{L}$
Pipette 1 μL of 1 mg/mL β -CM5 (*see Subheading 2.1, step 1*) in a 1.5 mL Eppendorf tube. Add 999 μL of ultra-pure water to the Eppendorf tube and mix thoroughly. Store the solution at $-80 \text{ }^\circ\text{C}$ (*see Note 1*).
2. Beta-casomorphin 5 solution, $c(\beta\text{-CM5}) = 10 \text{ ng}/\mu\text{L}$
Pipette 10 μL of 1 mg/mL β -CM5 (*see Subheading 2.1, step 1*) in a 1.5 mL Eppendorf tube. Add 990 μL of ultra-pure water to the Eppendorf tube and mix thoroughly. Store the solution at $-80 \text{ }^\circ\text{C}$ (*see Note 1*).

3. Beta-casomorphin 5 solution, $c(\beta\text{-CM5}) = 25 \text{ ng}/\mu\text{L}$
Pipette 25 μL of 1 mg/mL $\beta\text{-CM5}$ (see Subheading 2.1, **step 1**) in a 1.5 mL Eppendorf tube. Add 975 μL of ultra-pure water to the Eppendorf tube and mix thoroughly. Store the solution at -80°C (see **Note 1**).
4. Beta-casomorphin 7 solution, $c(\beta\text{-CM7}) = 1 \text{ ng}/\mu\text{L}$
Pipette 1 μL of 1 mg/mL $\beta\text{-CM7}$ (see Subheading 2.1, **step 2**) in a 1.5 mL Eppendorf tube. Add 999 μL of ultra-pure water to the Eppendorf tube and mix thoroughly. Store the solution at -80°C (see **Note 1**).
5. Beta-casomorphin 7 solution, $c(\beta\text{-CM7}) = 10 \text{ ng}/\mu\text{L}$
Pipette 10 μL of 1 mg/mL $\beta\text{-CM7}$ (see Subheading 2.1, **step 2**) in a 1.5 mL Eppendorf tube. Add 990 μL of ultra-pure water to the Eppendorf tube and mix thoroughly. Store the solution at -80°C (see **Note 1**).
6. Beta-casomorphin 7 solution, $c(\beta\text{-CM7}) = 25 \text{ ng}/\mu\text{L}$
Pipette 25 μL of 1 mg/mL $\beta\text{-CM7}$ (see Subheading 2.1, **step 2**) in a 1.5 mL Eppendorf tube. Add 975 μL of ultra-pure water to the Eppendorf tube and mix thoroughly. Store the solution at -80°C (see **Note 1**).
7. Stable isotope-labeled beta-casomorphin 5 solution, $c(\beta\text{-CM5-d}_{10}) = 10 \text{ ng}/\mu\text{L}$
Pipette 10 μL of 1 mg/mL $\beta\text{-CM5-d}_{10}$ (see Subheading 2.1, **step 3**) in a 1.5 mL Eppendorf tube. Add 990 μL of ultra-pure water to the Eppendorf tube and mix thoroughly. Store the solution at -80°C (see **Note 1**).
8. Stable isotope-labeled beta-casomorphin 7 ($\beta\text{-CM7-d}_{10}$) solution, $c(\beta\text{-CM7-d}_{10}) = 10 \text{ ng}/\mu\text{L}$
Pipette 10 μL of 1 mg/mL $\beta\text{-CM7-d}_{10}$ (see Subheading 2.1, **step 4**) in a 1.5 mL Eppendorf tube. Add 990 μL of ultra-pure water to the Eppendorf tube and mix thoroughly. Store the solution at -80°C (see **Note 1**).

2.3 Calibration Standard Solutions

1. Mixed standard beta-casomorphin 5/7, $c(\beta\text{-CM5}/7) = 10 \text{ ng}/\text{mL}$, and stable isotope-labeled beta-casomorphin 5/7 solution, $c(\beta\text{-CM5}/7\text{-d}_{10}) = 1000 \text{ ng}/\text{mL}$
Pipette 10 μL of 1 ng/ μL solutions of $\beta\text{-CM5}$ and $\beta\text{-CM7}$ (see Subheading 2.2, **step 1** and Subheading 2.2, **step 4**) in a HPLC vial. Add 100 μL of 10 ng/ μL solutions of $\beta\text{-CM5-d}_{10}$ and $\beta\text{-CM7-d}_{10}$ (see Subheading 2.2, **step 7** and Subheading 2.2, **step 8**). Add 780 μL of MeOH (see Subheading 2.4) to the HPLC vial and mix thoroughly (see **Notes 2** and **3**).
2. Mixed standard beta-casomorphin 5/7, $c(\beta\text{-CM5}/7) = 50 \text{ ng}/\text{mL}$, and stable isotope-labeled beta-casomorphin 5/7 solution, $c(\beta\text{-CM5}/7\text{-d}_{10}) = 1000 \text{ ng}/\text{mL}$

Pipette 5 μL of 10 $\text{ng}/\mu\text{L}$ solutions of $\beta\text{-CM5}$ and $\beta\text{-CM7}$ (*see* Subheading 2.2, **step 2** and Subheading 2.2, **step 5**) in a HPLC vial. Pipette 100 μL of 10 $\text{ng}/\mu\text{L}$ solutions of $\beta\text{-CM5-d}_{10}$ and $\beta\text{-CM7-d}_{10}$ (*see* Subheading 2.2, **step 7** and Subheading 2.2, **step 8**). Add 790 μL of MeOH (*see* Subheading 2.4) to the HPLC vial and mix thoroughly (*see* **Notes 2** and **3**).

- Mixed standard beta-casomorphin 5/7, $c(\beta\text{-CM5/7}) = 100 \text{ ng/mL}$, and stable isotope-labeled beta-casomorphin 5/7 solution, $c(\beta\text{-CM5/7-d}_{10}) = 1000 \text{ ng/mL}$

Pipette 10 μL of 10 $\text{ng}/\mu\text{L}$ solutions of $\beta\text{-CM5}$ and $\beta\text{-CM7}$ (*see* Subheading 2.2, **step 2** and Subheading 2.2, **step 5**) in a HPLC vial. Pipette 100 μL of 10 $\text{ng}/\mu\text{L}$ solutions of $\beta\text{-CM5-d}_{10}$ and $\beta\text{-CM7-d}_{10}$ (*see* Subheading 2.2, **step 7** and Subheading 2.2, **step 8**). Add 780 μL of MeOH (*see* Subheading 2.4) to the HPLC vial and mix thoroughly (*see* **Notes 2** and **3**).

- Mixed standard beta-casomorphin 5/7, $c(\beta\text{-CM5/7}) = 200 \text{ ng/mL}$, and stable isotope-labeled beta-casomorphin 5/7 solution, $c(\beta\text{-CM5/7-d}_{10}) = 1000 \text{ ng/mL}$

Pipette 20 μL of 10 $\text{ng}/\mu\text{L}$ solutions of $\beta\text{-CM5}$ and $\beta\text{-CM7}$ (*see* Subheading 2.2, **step 2** and Subheading 2.2, **step 5**) in a HPLC vial. Pipette 100 μL of 10 $\text{ng}/\mu\text{L}$ solutions of $\beta\text{-CM5-d}_{10}$ and $\beta\text{-CM7-d}_{10}$ (*see* Subheading 2.2, **step 7** and Subheading 2.2, **step 8**). Add 760 μL of MeOH (*see* Subheading 2.4) to the HPLC vial and mix thoroughly (*see* **Notes 2** and **3**).

- Mixed standard beta-casomorphin 5/7, $c(\beta\text{-CM5/7}) = 500 \text{ ng/mL}$, and stable isotope-labeled beta-casomorphin 5/7 solution, $c(\beta\text{-CM5/7-d}_{10}) = 1000 \text{ ng/mL}$

Pipette 20 μL of 25 $\text{ng}/\mu\text{L}$ solutions of $\beta\text{-CM5}$ and $\beta\text{-CM7}$ (*see* Subheading 2.2, **step 3** and Subheading 2.2, **step 6**) in a HPLC vial. Pipette 100 μL of 10 $\text{ng}/\mu\text{L}$ solutions of $\beta\text{-CM5-d}_{10}$ and $\beta\text{-CM7-d}_{10}$ (*see* Subheading 2.2, **step 7** and Subheading 2.2, **step 8**). Add 760 μL of MeOH (*see* Subheading 2.4) to the HPLC vial and mix thoroughly (*see* **Notes 2** and **3**).

- Mixed standard beta-casomorphin 5/7, $c(\beta\text{-CM5/7}) = 1000 \text{ ng/mL}$, and stable isotope-labeled beta-casomorphin 5/7 solution, $c(\beta\text{-CM5/7-d}_{10}) = 1000 \text{ ng/mL}$

Pipette 40 μL of 25 $\text{ng}/\mu\text{L}$ solutions of $\beta\text{-CM5}$ and $\beta\text{-CM7}$ (*see* Subheading 2.2, **step 3** and Subheading 2.2, **step 6**) in a HPLC vial. Pipette 100 μL of 10 $\text{ng}/\mu\text{L}$ solutions of $\beta\text{-CM5-d}_{10}$ and $\beta\text{-CM7-d}_{10}$ (*see* Subheading 2.2, **step 7** and Subheading 2.2, **step 8**). Add 720 μL of MeOH (*see*

Subheading 2.4) to the HPLC vial and mix thoroughly (*see Notes 2 and 3*).

7. Mixed standard beta-casomorphin 5/7, $c(\beta\text{-CM5/7}) = 5000 \text{ ng/mL}$, and stable isotope-labeled beta-casomorphin 5/7 solution, $c(\beta\text{-CM5/7-d}_{10}) = 1000 \text{ ng/mL}$

Pipette 200 μL of 25 $\text{ng}/\mu\text{L}$ solutions of $\beta\text{-CM5}$ and $\beta\text{-CM7}$ (*see Subheading 2.2, step 3* and Subheading 2.2, step 6) in a HPLC vial. Pipette 100 μL of 10 $\text{ng}/\mu\text{L}$ solutions of $\beta\text{-CM5-d}_{10}$ and $\beta\text{-CM7-d}_{10}$ (*see Subheading 2.2, step 7* and Subheading 2.2, step 8). Add 400 μL of MeOH (*see Subheading 2.4*) to the HPLC vial and mix thoroughly (*see Notes 2 and 3*).

8. Mixed standard beta-casomorphin 5/7, $c(\beta\text{-CM5/7}) = 10,000 \text{ ng/mL}$, and stable isotope-labeled beta-casomorphin 5/7 solution, $c(\beta\text{-CM5/7-d}_{10}) = 1000 \text{ ng/mL}$

Pipette 10 μL of 1 mg/mL solutions of $\beta\text{-CM5}$ and $\beta\text{-CM7}$ (*see Subheading 2.1, step 1* and Subheading 2.1, step 2) in a HPLC vial. Pipette 100 μL of 10 $\text{ng}/\mu\text{L}$ solutions of $\beta\text{-CM5-d}_{10}$ and $\beta\text{-CM7-d}_{10}$ (*see Subheading 2.2, step 7* and Subheading 2.2, step 8). Add 780 μL of MeOH (*see Subheading 2.4*) to the HPLC vial and mix thoroughly (*see Notes 2 and 3*).

9. Mixed standard beta-casomorphin 5/7, $c(\beta\text{-CM5/7}) = 25,000 \text{ ng/mL}$, and stable isotope-labeled beta-casomorphin 5/7 solution, $c(\beta\text{-CM5/7-d}_{10}) = 1000 \text{ ng/mL}$

Pipette 25 μL of 1 mg/mL each of $\beta\text{-CM5}$ and $\beta\text{-CM7}$ (*see Subheading 2.1, step 1* and Subheading 2.1, step 2) in a HPLC vial. Pipette 100 μL of 10 $\text{ng}/\mu\text{L}$ each of $\beta\text{-CM5-d}_{10}$ and $\beta\text{-CM7-d}_{10}$ (*see Subheading 2.2, step 7* and Subheading 2.2, step 8). Add 750 μL of MeOH (*see Subheading 2.4*) to the HPLC vial and mix thoroughly (*see Notes 2 and 3*).

2.4 Methanol (MeOH), HPLC Grade

2.5 Methanol Solution, c (MeOH) = 10% (v/v)

1. Dilute 25 mL of methanol (MeOH) (*see Subheading 2.4*) with ultra-pure water to 250 mL in a volumetric flask and mix thoroughly.

2.6 Formic Acid, Purity 99%

**2.7 Methanol
Containing 0.1%
Formic Acid (v/v)**

1. Pipette 1 mL of formic acid (*see* Subheading 2.6) into a 1000 mL volumetric flask. Add MeOH (*see* Subheading 2.4) to the mark and mix thoroughly.

**2.8 Ultra-Pure Water
Containing 0.1%
Formic Acid (v/v)**

1. Pipette 1 mL of formic acid (*see* Subheading 2.6) in a 1000 mL volumetric flask. Add ultra-pure water to the mark and mix thoroughly.

3 Methods

Preparation of samples [1] are carried out as follows:

**3.1 Extraction of
Beta-Casomorphin 5/7**

1. Mix the milk sample thoroughly, then accurately weigh out 10 g (± 0.0001 g) of the milk in a centrifuge tube. Add 20 μ L of 10 ng/ μ L solutions of β -CM5-d₁₀ and β -CM7-d₁₀ (*see* Subheading 2.2, step 7 and Subheading 2.2, step 8) and mix thoroughly.
2. Adjust the pH of the mixture to 4.6 by slowly adding 1 M HCl. Stand the mixture at room temperature for 10 min followed by centrifuging at $3200 \times g$ at 4 °C for 30 min. Decant the supernatant and filter through a Whatman filter paper (*see* Note 4) into a centrifuge tube.
3. Condition an SPE cartridge (*see* Note 5) with 4.5 mL of MeOH (*see* Subheading 2.4) followed by 4.5 mL of ultra-pure water. Dilute the sample filtrate with 50 mL of ultra-pure water and then mix thoroughly (*see* Note 6). Slowly load (i.e., 5 mL/min) the diluted filtrate to the SPE cartridge. Wash the SPE cartridge with 4.5 mL of 10% MeOH (*see* Subheading 2.5) and place the cartridge under vacuum for 10 min to dry out the stationary phase. Elute analytes with 3×2.5 mL of MeOH (*see* Subheading 2.4) into a glass test tube.
4. Evaporate the eluate to dryness at 30 °C in block heater under a gentle stream of nitrogen. Reconstitute the sample by adding 200 μ L of MeOH (*see* Subheading 2.4). Transfer the reconstituted sample into a HPLC vial.
5. For quality control samples (QCs), milk samples are spiked with 100 ng and 500 ng of β -CM5/7 as follows:
 - Accurately weigh 10 g (± 0.0001 g) of milk in a centrifuge tube. Add 10 μ L of 10 ng/ μ L solutions of β -CM5/7 and 50 μ L of 10 ng/ μ L solutions of β -CM5/7 (*see* Subheading 2.2, step 2 and Subheading 2.2, step 5). Then add 20 μ L of 10 ng/ μ L solutions of β -CM5-d₁₀ and β -CM7-d₁₀ (*see*

Subheading 2.2, step 7 and Subheading 2.2, step 8) and mix thoroughly.

- Extraction is conducted as described in Subheading 3.1, step 2 to Subheading 3.1, step 4.

3.2 Instrumental Analysis of β -CM5/7

1. Liquid chromatography system set-up

Chromatographic separation of β -CM5/7 can be achieved using an Ultimate 3000 UHPLC system consisting of a solvent degasser unit, a binary pump, and a 120 well-plate auto-sampler. The β -CMs are separated with an Hypersil Gold C18 UHPLC column (Thermo-Fisher Scientific USA, 2.1 mm \times 100 mm \times 1.9 μ m particle size) at a flow rate of 0.3 mL/min while the temperature is maintained at 40 °C throughout the chromatographic run. Ultra-pure water (eluent A) and methanol containing 0.1% formic acid (eluent B) are used as the mobile phases. The chromatographic run begins at 30% eluent B for 0.5 min, followed by a 4.5 min linear gradient to 95% B, held in isocratic conditions for 1 min. Afterwards, eluent B is increased to 100% in 0.1 min, and the mobile phase remains at 100% B for 3.9 min to wash the column. The initial conditions are then re-established within 0.1 min and the column is re-equilibrated for 4 min. The injection volume is 5 μ L.

Before starting the analysis of a batch of samples, the following operations need to be conducted:

- Open the purge valve on the UHPLC pump and purge the UHPLC lines at 6 mL/min for 5 min with 50% eluent B. Close the purge valve and start the UHPLC flow at 0.3 mL/min.
- Divert the Rheodyne valve into waste position and wash the UHPLC column for 15 min with 100% eluent B and then re-establish initial conditions and re-condition the UHPLC column at 30% eluent B for 10 min.
- Turn on column oven and stabilize the column temperature at 40 °C.
- Wash the fluidics thoroughly by priming the syringe (10 cycles), washing buffer loop (300 μ L) and washing the injection needle externally (10 μ L).
- Monitor the pressure in the UHPLC column and wait until it stabilizes.

2. Mass Spectrometry system set-up

The peptides β -CM5/7 can be detected, identified, and quantified using a high-resolution Q Exactive Focus Orbitrap™ mass spectrometer. Analyte ionization is achieved using a heated electrospray ionization source operated in

positive (+eV) mode with the following settings: source voltage 3.5 KV; capillary temperature 350 °C; heated gas temperature 350 °C; S-lense-RF 50 V. The sheath gas flow is set to 50 arbitrary units (Arb), while the auxiliary gas flow and sweep gas flow are set to 10 and 1 Arb, respectively. The Q Exactive Focus Orbitrap™ mass spectrometer is operated in ddMS2 mode where a full-scan spectra from 450–850 m/z at 70,000 (FWHM) resolving power is recorded followed by a data-dependent MS2 fragmentation of the Top3 intense peaks in the high collision dissociation cell. The MS2 spectra is measured in the Orbitrap™ mass analyzer at 17,500 (FWHM) resolving power. Fragmentation is achieved using a rolling collision energy of 10, 35, 60 eV in the HCD cell.

Before starting the analysis of the batch of samples, the following operations need to be conducted:

- Use a syringe pump to infuse the Pierce™ LTQ Velos ESI Positive Ion Calibration Solution at 3 $\mu\text{L}/\text{min}$ into the mass spectrometer.
- Set the source voltage to 3.5 KV; capillary temperature to 275 °C; heated gas temperature to 50 °C; S-lense-RF to 50 V. The sheath gas flow is set to 10 arbitrary units (Arb), while auxiliary gas flow and sweep gas flow are set to 0 and 0 Arb, respectively.
- Set the Q Exactive Focus Orbitrap™ mass spectrometer to full MS scan mode (150–2000 m/z) at 70,000 (FWHM) resolving power.
- While the Pierce™ LTQ Velos ESI Positive Ion Calibration Solution is infusing into the Q Exactive Focus Orbitrap™ mass spectrometer, tune the source conditions until a stable spray of ions is obtained (i.e., Inject Time $IT < 0.3\text{--}0.4$ ms; Total Ion Current (TIC) $> 7 \text{ E}7$; TIC relative standard deviation (RSD%) $< 5\%$).
- Perform routine calibration of mass positions and resolution for the Orbitrap™.
- Disconnect the capillary from the syringe pump and connect the UHPLC line Viper™ capillary.
- Set the source voltage to 3.5 KV; capillary temperature to 350 °C; heated gas temperature to 350 °C; S-lense-RF to 50 V; sheath gas flow to 50 arbitrary units (Arb); auxiliary gas flow to 10 and sweep gas flow to 1 Arb. Divert the Rheodyne valve in the ion source and check that a stable spray of ions is present (i.e., Inject Time $IT < 0.3\text{--}0.4$ ms; Total Ion Current (TIC) $> 7 \text{ E}7$; TIC relative standard deviation (RSD%) $< 5\%$).

3. Sequence Set-up

The following order of injection of blanks, standards, QCs, and samples is recommended when analyzing a batch of samples:

- Run 2 column blanks to wash the UHPLC column.
- Run the calibration curve from 10 up to 25,000 ng/mL.
- Run 1 injector blank (i.e., injection of 5 μ L of pure methanol) to check for any carryover.
- Run laboratory blanks.
- Run QCs samples.
- Run 1 injector blank (i.e., injection of 5 μ L of pure methanol) to check for any carryover.
- Run the batch of samples with about 10% re-injections.
- Run 1 injector blank (i.e., injection of 5 μ L of pure methanol) to check for any carryover.
- Re-run the calibration curve from 10 up to 25,000 ng/ μ L.
- Run 2 columns blanks to wash the UHPLC column at the end of the sequence.

Additional continuous calibration verification points can be added to the sequence.

4. Screening and quantitation of β -CM5/7

Screening and quantitation of β -CM5/7 is achieved using Tracefinder 4.1 software package (Thermo-Fisher Scientific). Quantification is performed by calculating the ratio of the peak area of the analytes to the peak area of the corresponding deuterated standards and using the external calibration curve.

A set of criteria are applied for confirmation of the presence of β -CM5/7 in the sample extracts (1) chromatographic retention time (i.e., <0.05 min retention time shift allowed); (2) deviation of the measured mass relative to the theoretical mass for the parent compound and fragments (i.e., <2 ppm relative error); (3) comparison of measured isotope patterns in samples with that obtained from isotopic simulation of β -CM5/7 elemental compositions; (4) comparison of measured MS2 spectra in the samples against calibration solutions and/or local/online spectra libraries. A step-by-step tutorial explaining how to set up a generic HRAM method for screening and quantitation of analytes using Thermo-Fisher Scientific Tracefinder software package can be found at www.mytracefinder.com [14].

Once a batch of samples is submitted to Tracefinder 4.1 for quantitation, the following steps are recommended when reviewing the dataset:

- Check all deuterated standards are integrated correctly, and analyte peaks integration are not missing.
- Check all calibration standards are integrated correctly, and analyte peak integrations are not missing.
- Build calibration curves and check that the linearity ranges and R^2 values are within acceptance criteria.
- Check injection blanks and laboratory blanks are free from carryover and/or contamination.
- Check QCs are within acceptance criteria.
- Verify analyte concentration of the samples is within the established calibration ranges and adjust calibration curves accordingly.
- Confirm retention times of analytes and deuterated standards are within acceptance criteria (i.e., RT shift less than 0.05 min).
- Confirm deviation of the measured mass relative to the theoretical mass for parent compound and fragments is less than <2 ppm relative error.
- Match MS1 isotopes pattern of detected analytes with isotope pattern observed in standard solutions (i.e., check relative intensities and peaks position).
- Match MS2 fragmentation spectra of detected analytes with MS2 fragmentation spectra observed in standard solutions and/or local/online spectra libraries (i.e., check relative intensities and peaks position).

4 Notes

1. Stock and working standard solutions can be stored at -80 °C for prolonged periods.
2. Calibration solutions and QCs should be freshly prepared before running a batch of samples.
3. To avoid possible degradation, store samples, blanks, QCs, and calibration solutions at -18 °C unless immediately analyzed.
4. Oasis HLB cartridges (Waters) with similar specifications (i.e., 500 mg stationary phase) can be used to extract and clean-up sample extracts.
5. It is recommended to dilute sample filtrates with ultra-pure water before processing them through SPE.

Acknowledgments

The method represented in this chapter has been published by Nguyen et al. (2021). Release of beta-casomorphins during in vitro gastrointestinal digestion of reconstituted milk after heat treatment. *LWT-Food Sci. Technol.* 136: 110312.

References

1. Nguyen DD et al (2021) Release of beta-casomorphins during in vitro gastrointestinal digestion of reconstituted milk after heat treatment. *LWT Food Sci Technol* 136:110312. <https://doi.org/10.1016/j.lwt.2020.110312>
2. Asledottir T et al (2018) Release of β -casomorphin-7 from bovine milk of different β -casein variants after ex vivo gastrointestinal digestion. *Int Dairy J* 81:8–11. <https://doi.org/10.1016/j.idairyj.2017.12.014>
3. Asledottir T et al (2017) Identification of bioactive peptides and quantification of β -casomorphin-7 from bovine β -casein A1, A2 and I after ex vivo gastrointestinal digestion. *Int Dairy J* 71:98–106. <https://doi.org/10.1016/j.idairyj.2017.03.008>
4. Ul Haq MR, Kapila R, Kapila S (2015) Release of β -casomorphin-7/5 during simulated gastrointestinal digestion of milk β -casein variants from Indian crossbred cattle (Karan Fries). *Food Chem* 168:70–79. <https://doi.org/10.1016/j.foodchem.2014.07.024>
5. Sienkiewicz-Szłapka E et al (2009) Contents of agonistic and antagonistic opioid peptides in different cheese varieties. *Int Dairy J* 19: 258–263. <https://doi.org/10.1016/j.idairyj.2008.10.011>
6. De Noni I (2008) Release of beta-casomorphins 5 and 7 during simulated gastro-intestinal digestion of bovine beta-casein variants and milk-based infant formulas. *Food Chem* 110:897–903. <https://doi.org/10.1016/j.foodchem.2008.02.077>
7. Brantl V et al (1979) Novel opioid peptides derived from casein (beta-casomorphins). I. Isolation from bovine casein peptone. *Hoppe Seylers Z Physiol Chem* 360: 1211–1216. <https://doi.org/10.1515/bchm2.1979.360.2.1211>
8. Cieślińska A et al (2012) Milk from cows of different β -casein genotypes as a source of β -casomorphin-7. *Int J Food Sci Nutr* 63: 426–430. <https://doi.org/10.3109/09637486.2011.634785>
9. Nguyen DD et al (2019) Evaluation of a commercial sandwich enzyme-linked immunosorbent assay for the quantification of beta-casomorphin 7 in yogurt using solid-phase extraction coupled to liquid chromatography-tandem mass spectrometry as the “gold standard” method. *J AOAC Int* 101:515–519. <https://doi.org/10.5740/jaoacint.17-0155>
10. De Noni I, Cattaneo S (2010) Occurrence of [beta]-casomorphins 5 and 7 in commercial dairy products and in their digests following in vitro simulated gastro-intestinal digestion. *Food Chem* 119:560–566. <https://doi.org/10.1016/j.foodchem.2009.06.058>
11. Juan-García A et al (2009) Nanoelectrospray with ion-trap mass spectrometry for the determination of beta-casomorphins in derived milk products. *Talanta* 80:294–306. <https://doi.org/10.1016/j.talanta.2009.06.062>
12. Nguyen DD et al (2015) Identification and quantification of native beta-casomorphins in Australian milk by LC-MS/MS and LC-HRMS. *J Food Compos Anal* 44: 102–110. <https://doi.org/10.1016/j.jfca.2015.08.009>
13. Nguyen DD et al (2014) Isotope dilution liquid chromatography-tandem mass spectrometry for simultaneous identification and quantification of beta-casomorphin 5 and beta-casomorphin 7 in yoghurt. *Food Chem* 146:345–352. <https://doi.org/10.1016/j.foodchem.2013.09.057>
14. www.mytracefinder.com, Accessed on 03/06/2021



Identification of Oligopeptides by Ultra-High-Pressure Liquid Chromatography Coupled with Quadrupole-Orbitrap Ultra-High-Resolution Mass Spectrometry

Mingjie Chen, Feng Zhao, and Naixing Ye

Abstract

Oligopeptides are widely present in almost all living species and show diverse activities. Though their importance, the identification of oligopeptides is technically challenging, largely due to their structural and compositional complexity. The recent advance in high mass accuracy of orbitrap technology and bioinformatics-based software lend us new tools to solve these problems. Here, we described an experimental procedure for the isolation, identification, and validation of oligopeptides from white tea matrix, the described method also can be modified for other food matrix.

Key words Oligopeptide, UPLC-Quadrupole-Orbitrap-UHRMS, Protein degradation, Peaks software, De novo sequencing

1 Introduction

Oligopeptide is an organic molecule consisting of a small number of amino-acid residues linked by amide bonds [1]. The exact size range is a matter of opinion, but oligopeptides described are typically comprised of about 2–40 amino-acid residues [2].

Peptides either are natural components of cells or protein degradation products; there are huge variations in amino-acid sequences and chain length. The natural peptides are produced by non-ribosomal peptide synthases or ribosomal pathways [3]. Proteins are essential macromolecules of living organisms, and every cellular protein has its own half-life time and is continuously degraded into their constituent amino acids. During proteolysis endogenous or exogenous proteins are processed by non-lysosomal proteases into intermediate-sized polypeptides [4], the resulting protein fragments of various sizes are either readily degraded into free amino acids, or captured by oligopeptidases which bind these peptide precursors, to trim them into active

form [5], or inactivate them [6], or protect the newly generated bioactive peptides from further degradation [7]. Thus, proteolysis also has the potential to generate large numbers of oligopeptides [8]). Oligopeptides show various activities such as acting as inhibitors of RNA polymerase, protease or kinase II, or serving as enzyme cofactors, ligands, antioxidants, or toxins [9]. Some oligopeptides function as signaling molecules or hormones, participate in the surveillance against pathogens or show neurological activities. It can be said that oligopeptides are involved in almost all essential aspects of life, from physiological homeostasis to immunological defense, to regulatory peptides displaying multiple action modes.

Oligopeptides also are widely present in various foods and beverages. Some peptides have been demonstrated to have significant contributions to food's flavor quality [10]. By now, the reported taste activities of oligopeptides include umami [11, 12], sweet [13], bitterness [13, 14], astringent [15], etc.

The breakthrough in peptidomics technology greatly facilitate the discovery of oligopeptides [16]. Recently, we applied ultra-high pressure liquid chromatography coupled with quadrupole-orbitrap ultra-high-resolution mass spectrometry (UPLC-Quadrupole-Orbitrap-UHRMS) to identify oligopeptides from white tea samples, the LC-MS/MS data were processed through de novo sequencing with the integration of database search, and near 200 oligopeptides were identified from white tea making processes [8]. The reported workflow can be modified for oligopeptide identification from other species or food matrix.

2 Materials

1. Mobile A: Aliquot 2 mL of formic acid into 1000 mL of Milli-Q water (*see Note 1*).
2. Mobile B: Aliquot 2 mL of formic acid into 1000 mL of acetonitrile (*see Note 2*).
3. Store above solution at room temperature.

3 Methods

Carry out all procedures at room temperature unless otherwise specified.

3.1 Oligopeptide Isolation from Tea Samples

1. Weigh ~1 g of tea sample into ceramic mortar, add liquid nitrogen, use pestle to ground sample into fine powder (*see Note 3*).

2. Allow nitrogen to evaporate completely. After sample return to room temperature, pass tea powder through a 40-mesh sieve (*see Note 4*).
3. Weigh 0.1 g tea powder, transfer into a 15-mL centrifuge tube (*see Note 5*).
4. Blank sample was prepared as above by omitting tea powder (*see Note 6*).
5. Add 10 mL of prewarmed Milli-Q water (70 °C) into the tube, vortex for 1 min to resuspend tea powder completely (*see Note 7*).
6. Place the tubes in 70 °C water bath for 10 min, vortex once for every 2 min.
7. Centrifuge the tubes at $10,000 \times g$ for 5 min in 4 °C.
8. Transfer the supernatant into 2-mL syringe, filtrate through 0.22 μm membrane, collect filtrate into a fresh centrifuge tube (*see Note 8*).
9. Prior to sample injection, transfer above filtrate into an ultra-filtration column with cellulose membrane and 3000 Da cutoff, centrifuge at $10,000 \times g$ for 5 min under 4 °C temperature, collect flow-through which contain oligopeptides (*see Note 9*).
10. Inject 10.0 μL sample for oligopeptide analysis (*see Note 10*).

3.2 Generate Analytical Method File

1. Open Xcalibur 2.2 SP2 software by double clicking the icon on the desktop, open “Method editor” (Fig. 1).
2. Set UHPLC parameters as Table 1 (*see Note 11*).
3. Set MS parameters as Table 2 (*see Note 12*).
4. Save the generated analytical method file in computer.

3.3 Sample Analysis

1. Generate sample sequence file by input sample information, method file, and data storage location in a batch injection mode, save sample sequence file.
2. Loading samples into autosampler according to sample sequence file.
3. Click “Start” to analyze samples, save data as “.raw” data file.

3.4 Oligopeptide Identification

Step 1: To create a new project

1. Open Peaks Studio 8.5 software (*see Note 13*).
2. Go to the top left corner, select “New project” button, this will bring to “Project Wizard” page to create a new project (Fig. 2a).

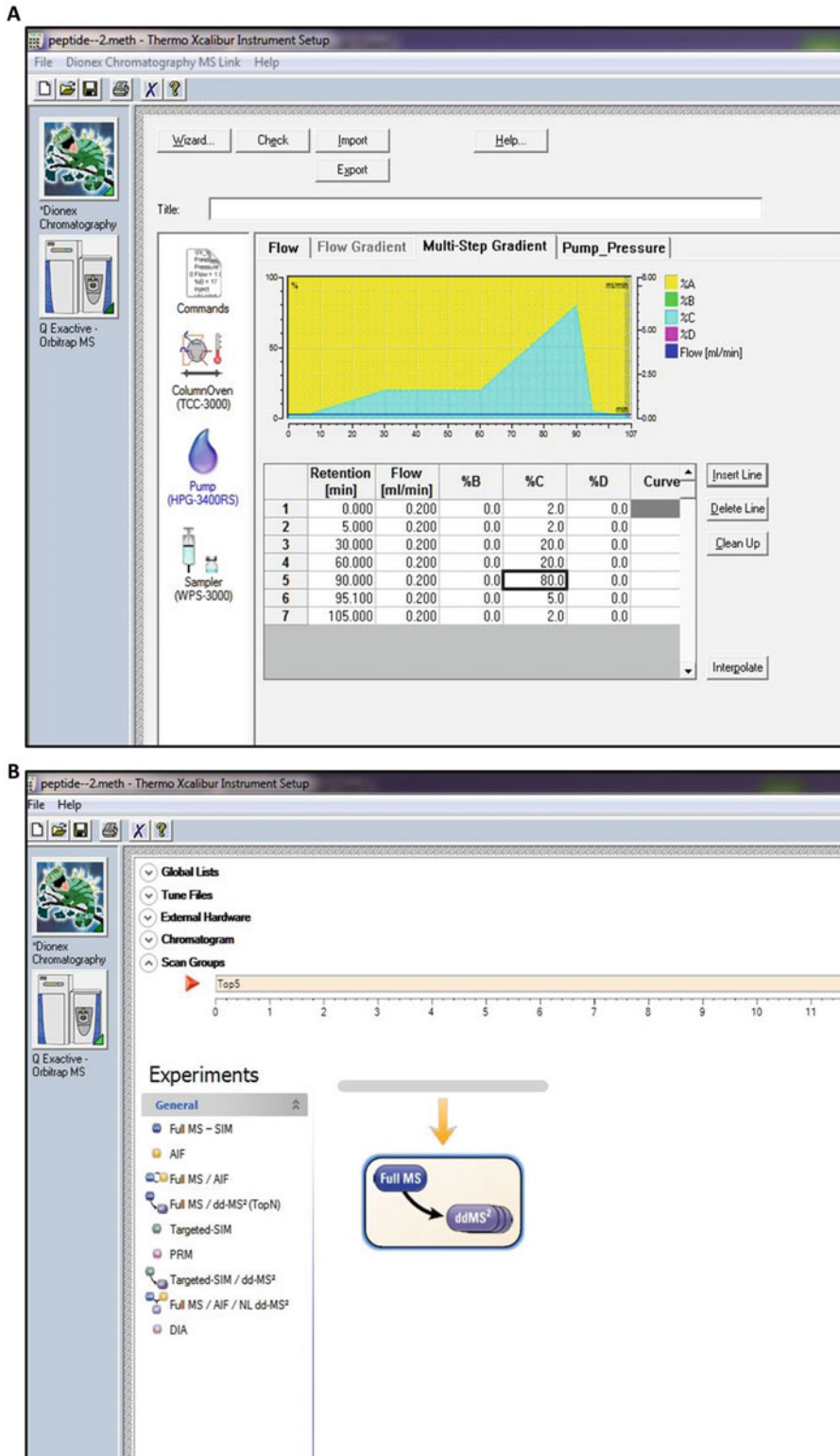


Fig. 1 Generate analytical method file in Xcalibur 2.2 SP2 software

Table 1
HPLC parameter setting

Method setting	
Instrument model	Dionex Ultimate 3000 HPLC ⁺ Focused
Column	Acquity UPLC CSH C18 (2.1 × 100 mm id, 1.7 μm particle size)
Column temperature	30 °C
Flow rate	0.2 mL min ⁻¹
Mobile phase elution gradient	0–5 min isocratic 98% A/2% B; 5–30 min linear gradient from 98% A/2% B to 80% A/20% B; 30–60 min isocratic 80% A/20% B; 60–90 min linear gradient from 80% A/20% B to 20% A/80% B; 90–95 min linear gradient from 20% A/80% B to 95% A/5% B; 95.1–105 min isocratic 95% A/5% B; 105.1–107 min 98% A/2% B for reconditioning

Table 2
Mass spectrometry parameter setting

MS setting	
Instrument model	Q-Exactive high-resolution quadrupole-Orbitrap mass spectrometry
Software	Xcalibur 2.2 SP2
Ion mode	Positive
Scan mode	Full-MS/top10 dd-ms ²
MS resolution	70,000
MS/MS resolution	17,500
Spray voltage	3.50 kV
Capillary temperature	320 °C
Aus gas heater temperature	411 °C
Aus gas flow rate	N ₂ 15 L h ⁻¹
Sheath gas flow rate	N ₂ 40 L h ⁻¹

Step 2: Data refinement

1. In the “Data Refinement” interface, select parameter as shown in Fig. 2b.

Step 3: To set identification parameter

1. Set identification parameter as shown in Table 3 and Fig. 3a. To configure tea proteome database, click “Window”, select “Config wizard”, select “tea tree protein.fas” which was built by Xia et al. (2017) [17], click “OK”. (see Notes 14 and 15).

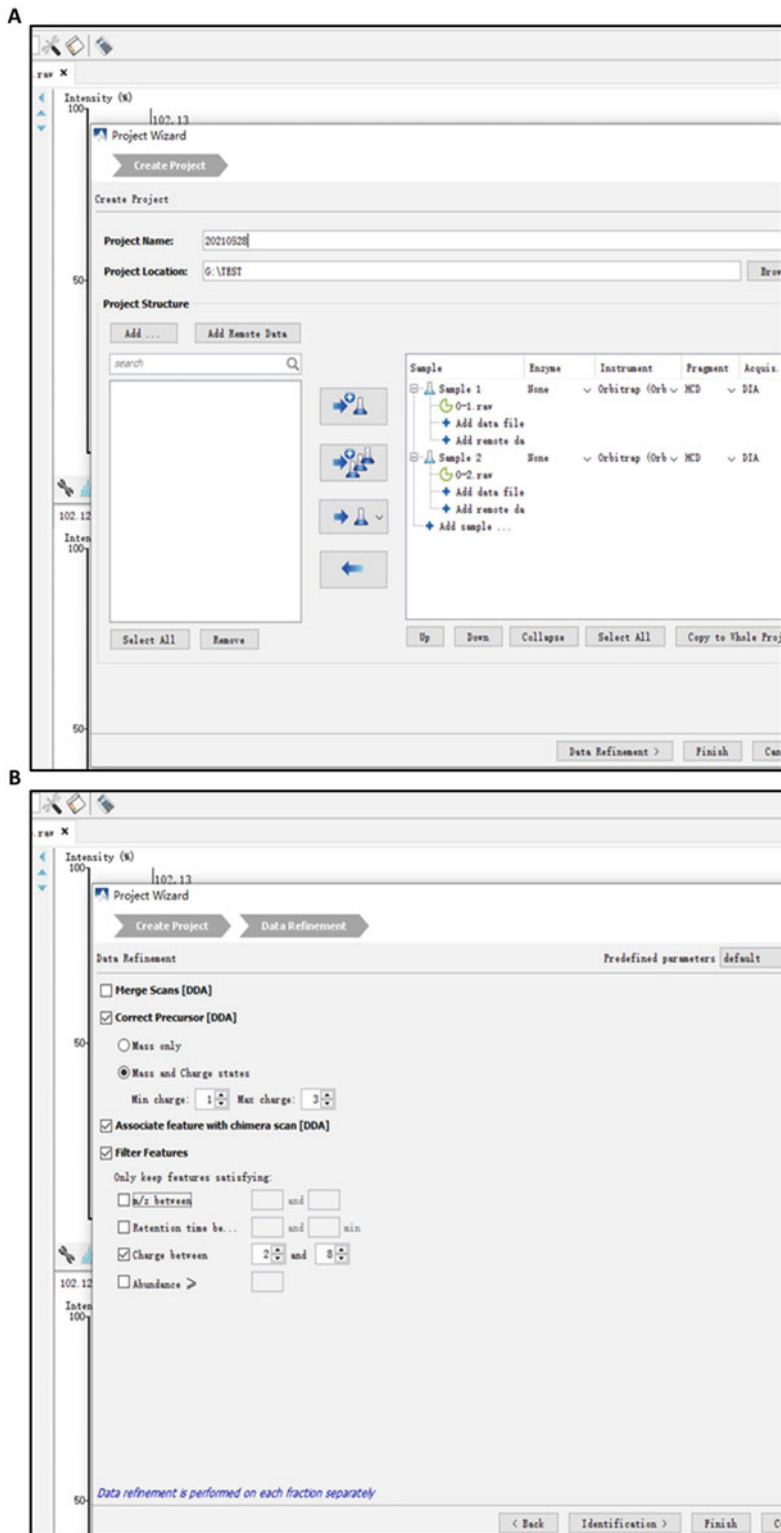


Fig. 2 Create new project and set data refinement parameters in Peaks Studio 8.5 software

Table 3
Peptide sequence indexes for Peaks software

	Search parameter setting
Protein database	tea tree protein.fas (Xia et al., 2017)
Peptide mass tolerance	15 ppm
Fragment mass error tolerance	0.02 Da
Enzyme	None
Average local confidence score (ALC)	≥ 90
$-\log p$	≥ 20 ($p \leq 0.01$)

Step 4: Set “De novo Score ≥ 90 ”, then press “Apply” button (Fig. 3b);

1. Select instrument vendor “Thermo Scientific-LTQ, orbitrap, FT instrument”, click “Next”.
2. Look at the “Summary” review. To filter the result, select “FDR”, on the toolbar navigating along curve to find desire percentage, then click “Apply filters”.
3. Once finish validate the results, export the results in the right format. To do so, click “Export”, select “DB search peptide-spectrum matches (DB search psm.csv)”, choose the location, then click “Export”.
4. Click on the “Peptide view”, you can see a list of identified peptides with the abundance from MSI (Fig. 4).

3.5 Oligopeptide Validation and Quantification by Triple-Quadrupole-Mass Spectrometry

1. To validate de novo sequencing results for selected oligopeptides, synthesize respective peptide sequence with certifications, the purity should be above 90% (see Note 16).
2. Dissolve each synthesized peptide in 20% (v/v) acetonitrile aqueous solution, make stock solution at 1.0 mg mL^{-1} , then dilute with mobile phase to make working solution at concentration of $50.0 \text{ } \mu\text{g mL}^{-1}$.
3. Open “PeakView” software, set parameter as Table 4 (see Note 17).
4. Make following oligopeptide standard gradient: 1.0, 5.0, 20.0, 30.0, and $50.0 \text{ } \mu\text{g L}^{-1}$. To make working solution, dilute stock solution with mobile phase. The oligopeptide standards were analyzed by triple-quadrupole-mass spectrometry. To reduce interference among samples, the lower gradient was analyzed first, followed by higher gradient. Each gradient was repeated three times.
5. Get the peak area, then make calibration curves in Excel.

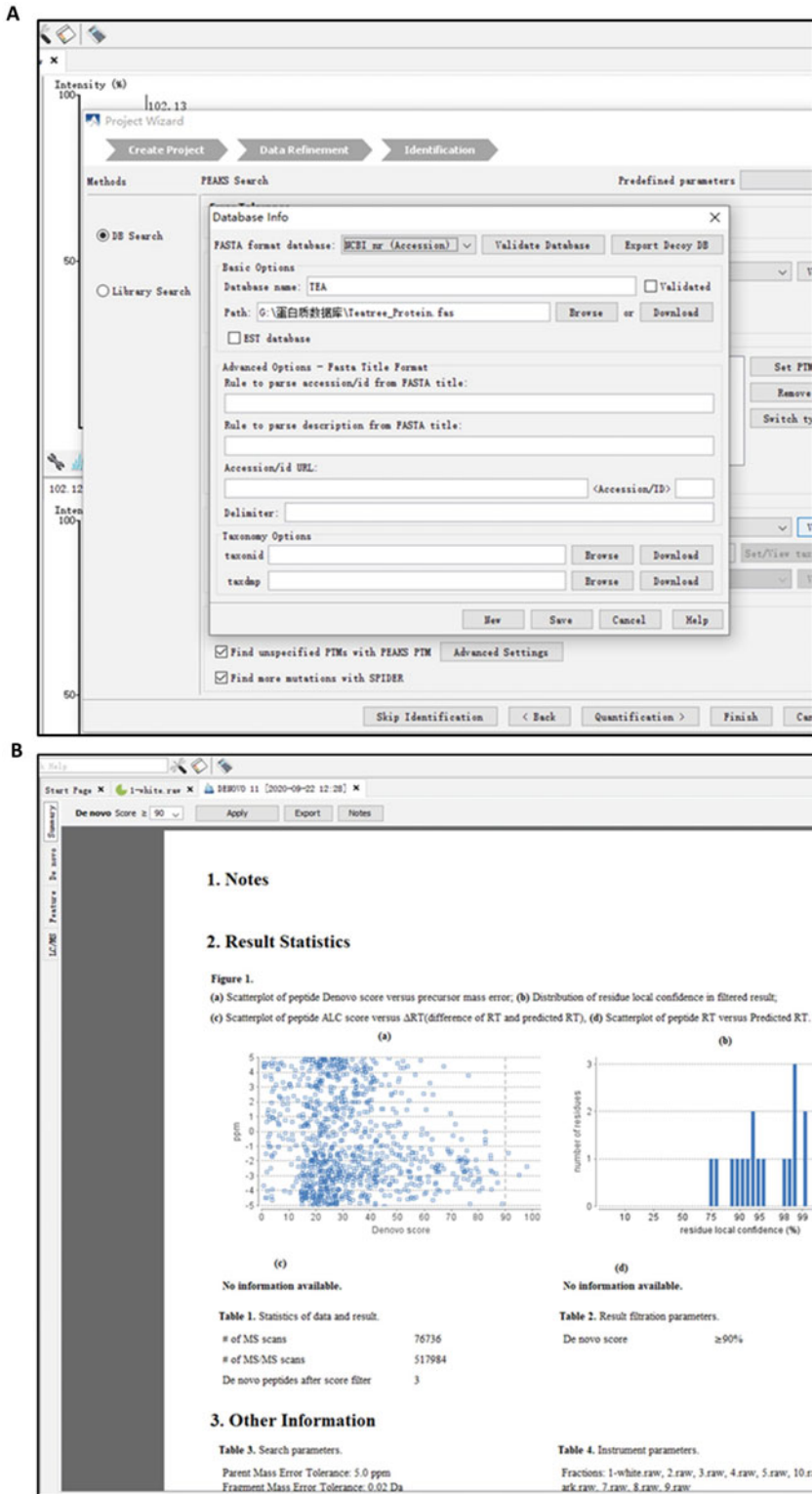


Fig. 3 Set oligopeptide identification parameters in Peaks Studio 8.5 software

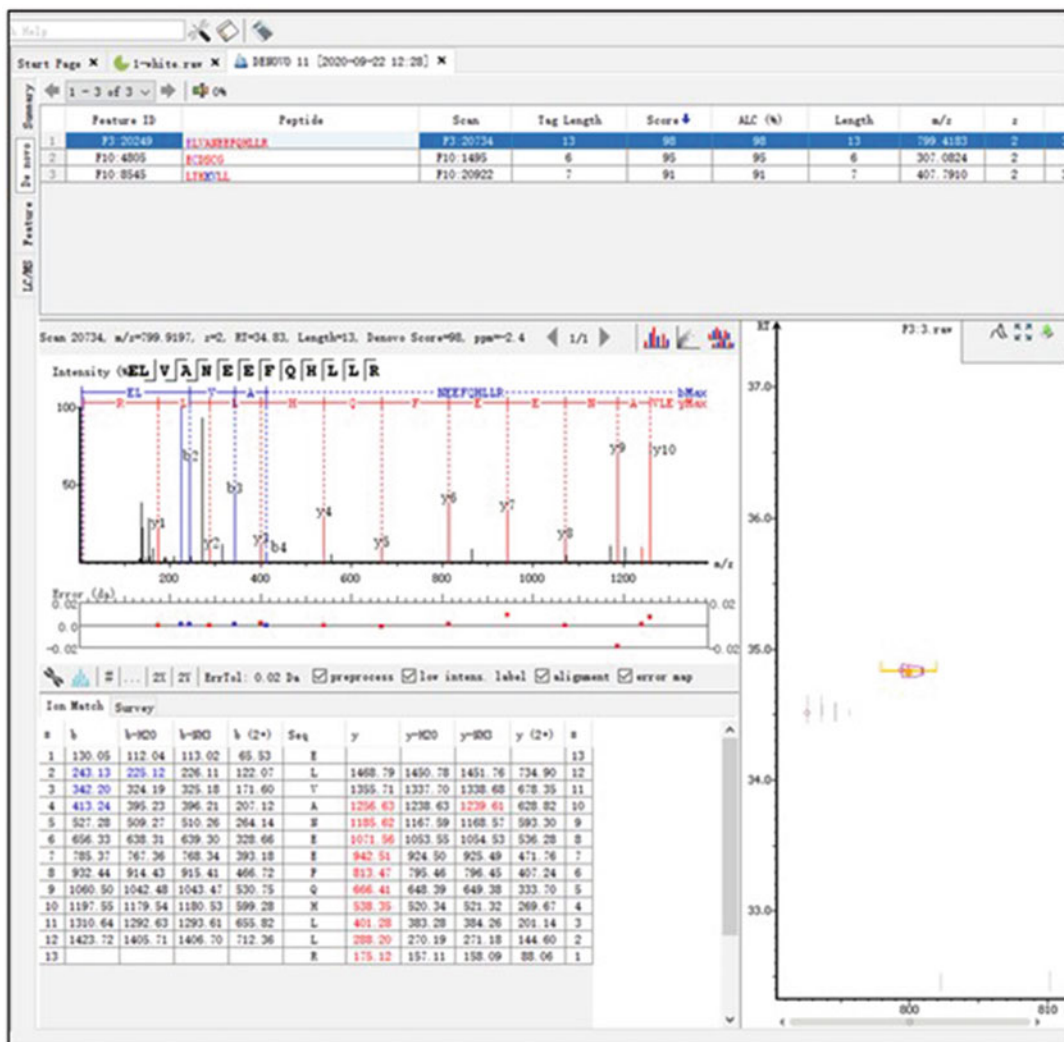


Fig. 4 Oligopeptides were identified

6. During oligopeptide standard analysis, its chromatographic retention time and three pairs of precursor/product ions are obtained and used for peptide validation.

4 Notes

1. Using ultrapure water (prepared by purifying deionized water, to attain a sensitivity of 18 MΩ-cm at 25 °C).
2. Use chromatography grade acetonitrile.

Table 4
Analysis setting of UHPLC-MS for oligopeptide validation

Method setting	
UHPLC	Shimadzu LC-20A
Column	Acquity UPLC HSS T3 (2.1 × 150 mm id, 1.7 μm particle size)
Column temperature	40 °C
Mobile phase elution gradient	0–1 min isocratic 90% C/10% D, 1–5 min linear gradient from 90% C/10% D to 30% C/70% D, 5.0–5.5 min isocratic 30% C/70% D, 5.51–8.00 min isocratic 90% C/10% D
Mobile phase flow rate	0.3 mL min ⁻¹
Sample injection volume	2.0 μL
Mass spectrometry	Sciex Triple Quad 5500
Ion mode	Positive
Quantification mode	Multiple reaction monitoring (MRM)
Ion source	Turbo spray
Curtain gas	30.0 L h ⁻¹
Collision gas	9.0 L h ⁻¹
Ion spray voltage	5.5 kV
Ion source gas 1	60.0 L h ⁻¹
Ion source gas 2	55.0 L h ⁻¹
Capillary temperature	550 °C

3. Liquid nitrogen makes the sample brittle such that facilitate grounding biological sample into powder; the low temperature also protects samples from potential protein degradation.
4. When you extract oligopeptides from fresh tissues, make sure to include proteinase inhibitor cocktail set III (Sigma-Aldrich) and appropriate oligopeptidase inhibitors to reduce protein and peptide degradation.
5. The sample amount used for oligopeptide extraction largely depend on the oligopeptide contents in your interested sample, you may need to conduct a test run to determine the optimal sample amount. If you isolate oligopeptides from fresh tissues, transfer the sample into centrifuge tube before sample melt to avoid potential protein and oligopeptide degradation.
6. Blank sample is important to identify potential systemic contaminations and exclude them from quantification.

7. If you extract oligopeptides from other tissue type, you may insert phase separation steps to separate water-soluble oligopeptides from other organic-soluble components.
8. 0.22 μm membrane can remove small particles present in the sample, thus reduce the chance to clog the column.
9. A 3000 Da cellulose ultra-filtration column allows passthrough of all desired oligopeptides while retain larger molecular weight polypeptides and proteins on the membrane.
10. Depend on oligopeptide concentration in your sample, you may need to concentrate or dilute your sample before injection into HPLC for sample analysis.
11. Octadecyl carbon chain (C18)-bonded silica is selected as stationary phase. Use slow flow rate (0.2 mL min^{-1}), isocratic and linear gradient with relatively longer running time (105 min), these procedures facilitate oligopeptide separation.
12. The de novo sequencing of oligopeptides requires high-resolution, accurate mass (HRAM). We chose a hybrid system that combines quadrupole and Orbitrap to deliver exceptional mass accuracy, spectral quality, and sensitivity.
13. Peaks studio software use LC-MS/MS data to construct peptide information through machine learning, then the resulting peptide sequences are used for database search, the integration of de novo sequencing with database search can minimize the error and extend in-depth analysis.
14. The tea tree genome has been sequenced, and we build a custom tea proteome database for this search. If the genome sequence for the species your oligopeptides derived from were not available, but the genome from its close family is available, you are suggested to use the proteome from its close family to build the database, which deliver better result compared with NCBI NPR database.
15. In this experiment, our samples were not digested by any proteases, so for the “enzyme” we select “None”. If your sample was digested by some protease for oligopeptide preparation, select the protease that you used.
16. To further validate the identified oligopeptides from your samples, synthesized peptides should be used as standards.
17. Here, we use triple-quadrupole-mass analyzer for oligopeptide validation and quantification. You also can use the original hybrid quadrupole and orbitrap mass analyzer for this purpose.

Acknowledgments

This work was supported by National Natural Science Foundation of China grant (31870803, 31270735), Startup fund from Xinyang Normal University to M.C. and Postdoctoral Science Foundation of China (2018M63075).

References

1. <https://www.biologyonline.com/dictionary/oligopeptide>. Accessed 18 Sept 2020
2. Lackie J (2010) A dictionary of biomedicine, 1st edn. Oxford University Press, London
3. Agha R, Cirés S, Wörmer L, Quesada A (2013) Limited stability of microcystins in oligopeptide compositions of microcystis aeruginosa (Cyanobacteria): implications in the definition of chemotypes. *Toxins* 5(6):1089–1104. <https://doi.org/10.3390/toxins5061089>
4. Linderstrøm-Lang K (1950) In vivo half-life of a protein is a function of its amino-terminal residue. *Cold Spring Harb Symp Quant Biol* 14:117–126. <https://doi.org/10.1101/sqb.1950.014.01.016>
5. Camargo AC, Caldo H, Reis ML (1979) Susceptibility of a peptide derived from bradykinin to hydrolysis by brain endo-oligopeptidases and pancreatic proteinases. *J Biol Chem* 254(12):5304–5307
6. Oliveira EB, Martins AR, Camargo AC (1976) Isolation of brain endopeptidases: influence of size and sequence of substrates structurally related to bradykinin. *Biochemistry* 15(9):1967–1974. <https://doi.org/10.1021/bi00654a026>
7. Silva CL, Portaro FC, Bonato VL et al (1999) Thimet oligopeptidase (EC.3.4.24.15) is a novel protein on the route of MHC class I antigen presentation. *Biochem Biophys Res Commun* 255(3):591–595. <https://doi.org/10.1006/bbrc.1999.0250>
8. Zhao F, Ye NX, Qiu XH, Qian J, Wang DH, Yue WJ, Zuo ZC, Chen MJ (2019) Identification and comparison of oligopeptides during withering process of White tea by ultra-high pressure liquid chromatography coupled with quadrupole-orbitrap ultra-high-resolution mass spectrometry. *Food Res Int* 121:825–834
9. Argos P (1990) An investigation of oligopeptides linking domains in pProtein tertiary structures and possible candidates for general gene fusion. *J Mol Biol* 211:943–958
10. Su G, Cui C, Zheng L, Yang B, Ren J, Zhao M (2012) Isolation and identification of two novel umami and umami-enhancing peptides from peanut hydrolysate by consecutive chromatography and MALDI-TOF/TOF MS. *Food Chem* 135(2):479–485. <https://doi.org/10.1016/j.foodchem.2012.04.130>
11. Zhang Y, Venkatasamy C, Pan Z, Liu W, Zhao L (2017) Novel umami ingredients: umami peptides and their taste. *J Food Sci* 82(1):16–23. <https://doi.org/10.1111/1750-3841.13576>
12. Zhang Y, Wei X, Lu Z, Pan Z, Gou X, Venkatasamy C et al (2017) Optimization of culturing conditions of recombinant *Escherichia coli* to produce umami octapeptide-containing protein. *Food Chem* 227:78–84. <https://doi.org/10.1016/j.foodchem.2017.01.096>
13. Takai S, Yasumatsu K, Inoue M, Iwata S, Yoshida R, Shigemura N et al (2015) Glucagon-like peptide-1 is specifically involved in sweet taste transmission. *FASEB J* 29(6):2268–2280
14. Pripp AH, Ardö Y (2007) Modelling relationship between angiotensin-(I)-converting enzyme inhibition and the bitter taste of peptides. *Food Chem* 102(3):880–888. <https://doi.org/10.1016/j.foodchem.2006.06.026>
15. Kaneda H, Watari J, Takashio M, Okahata Y (2002) Adsorption of tannins on lipid membrane in the presence of peptides as related to astringency. *J Food Sci* 67(9):3489–3492. <https://doi.org/10.1111/j.1365-2621.2002.tb09610.x>
16. Gelman JS, Sironi J, Castro LM et al (2011) Peptidomic analysis of human cell lines. *J Proteome Res* 10(4):1583–1592. <https://doi.org/10.1021/pr100952f>
17. Xia EH, Zhang HB, Sheng J, Li K, Zhang QJ, Kim C, Zhang Y, Liu Y, Zhu T, Li W, Huang H, Tong Y, Nan H, Shi C, Shi C, Jiang JJ, Mao SY, Jiao JY, Zhang D, Zhao Y, Zhao YJ, Zhang LP, Liu YL, Liu BY, Yu Y, Shao SF, Ni DJ, Eichler EE, Gao LZ (2017) The tea tree genome provides insights into tea flavor and independent evolution of caffeine biosynthesis. *Mol Plant* 10:866–877



Database Construction Strategies for Proteome Measurement of Novel Food Ingredients

Sophia Escobar-Correas, Utpal Bose, James A. Broadbent, Angéla Juhász, and Michelle L. Colgrave

Abstract

Proteomics is employed routinely in the food industry to characterize food components through the identification of proteins. However, the complexity and diversity of food products present challenges, including low identification rates due to inappropriate or incomplete database construction and use. In this chapter, we describe different database construction strategies to assist investigators in building custom databases that will permit optimal peptide and protein identification rates. We provide example results to demonstrate the effectiveness of different strategies using the emerging food ingredient cricket (*Acheta domesticus*).

Key words Database search, Proteogenomic, Mass spectrometry, LC-MS/MS, Novel food, Non-model organism

1 Introduction

Mass spectrometry (MS)-based proteomics is employed regularly to assess and monitor food safety, contamination, authentication, characterizing food components, and determining food adulteration [1–3]. However, the analysis of ingredients and composition of processed food can be challenging for ingredients originating from atypical and novel sources due to the absence of pre-defined protein sequence databases for protein identification. To identify and characterize proteins through mass spectrometry (MS)-based proteomics experiments, mass spectra must be searched using algorithms. Chromatographic and mass spectrometric peak profiles are built using the mass-to-charge ratio (m/z) values for the detected peptides. The mass spectra are queried against a database of theoretical spectra [3, 4]. Even with this well-established approach, identification rates of proteins from processed samples can be low because of either non-optimal sample processing or poor-quality

MS data. In addition, the use of an nonspecific or insufficient sequence databases will contribute to limited outcomes. Foods originating from non-model species that have limited genomics, transcriptomics, and proteomics sequence resources are most susceptible to lower identification rates. This chapter describes the implementation and influence of database search strategies to gain insights into the proteome. To this end, a novel food protein source, cricket (*A. domesticus*) was selected as an organism of choice for the present work.

Crickets are a good source of protein and iron and have been recently evaluated as an alternative source of food; however, proteins present in the cricket samples may cause cross-reactive allergies to a subset of people with existing allergy to shellfish [5]. Data was acquired from different protein extraction protocols used on three types of processed cricket products acquired by LC-MS using data-dependent acquisition (DDA). The resultant data files were searched against multiple custom-built databases to assess the impact of database size and complexity on proteome identification yields.

2 Materials

2.1 Bioinformatic Analysis

1. Computer: Windows 10 operating system with 32 logical processors and 32 GB RAM. Requires admin rights to download and install software.
2. LC-MS/MS data collected from your own equipment or downloaded from public repositories. In this case, we used LC-MS/MS data acquired from cricket flour extracts that is publicly available from <https://doi.org/10.25919/rb15-em18> [5].
3. Fasta files downloaded from UniProt-KB (<http://www.uniprot.org/>) and NCBI (<https://www.ncbi.nlm.nih.gov/>).
4. ProteinPilot software (SCIEX).
5. R and R studio (<https://cran.r-project.org/>, <https://www.rstudio.com/>).

3 Methods

3.1 LC-MS/MS Data Acquisition

1. LC-MS/MS raw data can be download from target publications and/or from mass spectral data repositories. Some examples of publicly available repositories are: ProteomeXchange [6]; PeptideAtlas [7]; Global Proteome Machine Database (GPMDB) [8]; Proteomics Identification Database (PRIDE) [9]; and MassIVE [10]. In this case, *A. domesticus* (cricket) raw

data was download from [5], <https://doi.org/10.25919/rb15-em18>.

2. Generally mass spectrometer vendors provide software that convert raw spectra into m/z peak lists prior to database searching. Some example of software are: Mascot (Matrix Science), SEQUEST (University of Washington), PEAKS (Bioinformatics Solutions Inc.), X!Tandem (The Global Proteome Machine Organization), MaxQuant (Max-Planck-Institute of Biochemistry), etc. In this example, we use ProteinPilot (SCIEX) (*see Note 1*).
3. The search software commences database searching using known protein sequences combined in a custom-built database. The algorithm digests the protein sequences present in the database *in silico* to then segment the database into bins based on theoretical m/z . Theoretical fragmentation spectra are then generated and are compared to the empirical MS/MS spectra for scoring based on matching criteria and probability. Choosing a suitable database will influence the identifications and accuracy of the analysis.

3.2 Database Building

1. Search for resources: Databases can be built using proteomic, genomic, and transcriptomic resources for the target organism or from sequences collected from closely related organisms. Sequences can be downloaded from the below repositories:

Uniprot (<https://www.uniprot.org/>),

NCBI (<https://www.ncbi.nlm.nih.gov/>),

Ensembl (<http://www.ensembl.org/>), for plants (<https://plants.ensembl.org/>), for bacteria (<http://bacteria.ensembl.org/>), for fungi (<http://fungi.ensembl.org/>), for protists (<http://protists.ensembl.org/>).

2. Download relevant fasta files.
3. Download the common Repository of Adventitious Proteins (cRAP) to include common protein contaminants like keratin. The database is available in fasta format from the GPM FTP site, using the URL <https://www.thegpm.org/crap/>.
4. Open fasta files in the computer using a text editor (Notepad, Notepad++, WordPad, TextEdit, Vim, etc.).
5. Clean the database to remove sequence duplicates, for example, using Seqkit (<https://bioinf.shenwei.me/seqkit/>) [11]. Instructions on how to download and run the software can be found on the website. To summarize, fasta files were copied to the seqkit directory (in Windows Explorer) and then the command prompt used to navigate to the seqkit directory:

```
> cd seqkit
```

Seqkit was then operated in the command prompt to remove redundancy from the fasta files:

```
seqkit> *.fasta | seqkit rmdup -s -o clean *.fasta
```

**3.3 UniProt
Knowledgebase
(UniProt-KB)
(<https://www.uniprot.org/>):**

1. Enter the UniProt Knowledgebase (UniProt-KB) website using the above URL (*see Note 2*).
2. Insert the name of the species or taxonomic level of interest to inspect. For a cleaner search: go to the advanced option and choose taxonomy; add the name of the species of interest. In this case, inspect the database at different taxonomy levels:
Species: *Acheta domesticus* (House cricket) [6997]
Genus: "*Acheta* [6996]"
Family: *Gryllidae* (crickets) [6995]
Order: *Orthoptera* [6993]"
3. Remove redundant proteins by clicking on option UniRef 100% on the left board (Fig. 1). This option clusters sequences that are 100% identical and retains the longest sequence only. This way only one accession will be available for each sequence.
4. Evaluate the number of accessions found for the species and when thresholding using higher taxonomic levels (Table 1).
5. Download files in *.fasta format.

UniRef

Your results in
sequence clusters
with identity of:

100%, 90% or 50%

Fig. 1 The UniRef 100% option appears on the left side of the UniProt website results

Table 1

The number of accessions found for different taxonomic levels when conducting a UniProt search and after removing redundancy with the UniRef 100% option

Taxonomic threshold	UniProt search (accessions)	UniRef100 (accessions)
<i>Acheta domesticus</i>	159	119
<i>Acheta</i>	161	121
<i>Gryllidae</i>	3,078	2,011
<i>Orthoptera</i>	20,667	16,559

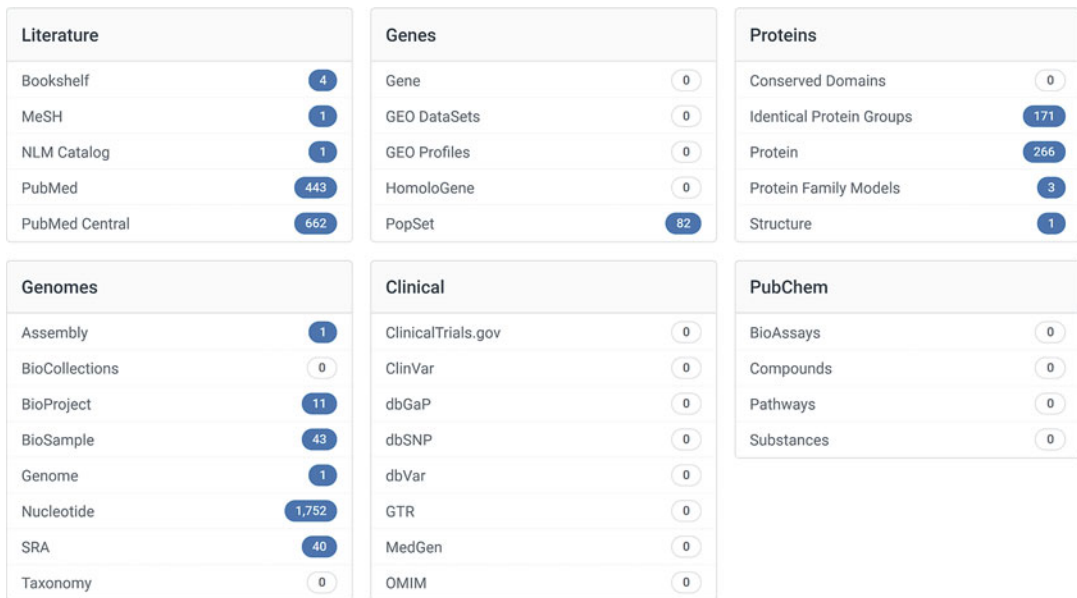


Fig. 2 Results found for *Acheta domesticus* [Organism] at NCBI

3.4 National Center for Biotechnology Information Nonredundant Database (NCBI) (<https://www.ncbi.nlm.nih.gov/>)

1. Add the name of your organism in the search bar, e.g., *Acheta domesticus* [Organism].
2. Evaluate results options. Figure 2 shows a screenshot of NCBI search.
3. For the protein option, click on the number of proteins found (236 in this case). Download the fasta file by clicking on: *Send to -> File -> Format = Fasta*
4. Nucleotide option. Click on the number of nucleotide results found (1749 in this case). Download fasta by clicking on: *Send to -> File -> Format = Fasta*

Translate nucleotide sequences to protein sequences using Seqkit (<https://bioinf.shenwei.me/seqkit/>) [11]. Instructions

Acheta domesticus (house cricket)

Acheta domesticus overview

Lineage: Eukaryota[8502]; Metazoa[4118]; Ecdysozoa[1796]; Arthropoda[1647]; Hexapoda[1517]; Insecta[1481]; Pterygota[1480]; Neoptera[1473]; Polyneoptera[32]; Orthoptera[8]; Ensifera[5]; Gryllidea[5]; Grylloidea[5]; Gryllidae[5]; Gryllinae[3]; Acheta[1]; Acheta domesticus[1]

Summary

Submitter: Naresuan University
 Assembly level: Contig
 Assembly: GCA_014858955.1 NU_Adom_1.1 scaffolds: 709,385 contigs: 709,385 N50: 1,566 L50: 177,245
 BioProjects: PRJNA612585
 Whole Genome Shotgun (WGS): INSDC: JAAVVF000000000.1
 Statistics: total length (Mb): 929.173
 GC%: 38.5

Genome Assembly Annotation

Loc	Type	Name	RefSeq	INSDC	Size (Mb)	GC%
		master WGS	-	JAAVVF000000000.1	929.17	38.5

Fig. 3 *Acheta domesticus* (PRJNA612585) genome resources found through searching NCBI

on how to download and run the software can be found on the website. To summarise, fasta files were copied to the seqkit folder (using Windows Explorer) and the command prompt was used to navigate to the seqkit directory:

```
>cd seqkit
```

Seqkit was then used to convert nucleotide sequences to protein sequences using the following commands:

```
>seqkit translate *.fasta -f 1 --clean -o *.fasta
```

The `-f` argument specifies the reading frame for translation. Changing this number to 2 or 3 and -1, -2, -3 will analyze additional reading frames.

An annotated collection of all publicly available DNA sequences can be found in GenBank (Benson et al., 2013) <https://www.ncbi.nlm.nih.gov/genbank/>.

5. Downloading and translating genome resources for proteome database preparation. Currently, one whole genome shotgun sequence assembled as contigs (*see Note 3*) is available for *A. domesticus* (PRJNA612585, Fig. 3). To download the nucleotide sequences in fasta format, click on the INSDC code. A new tab will appear. Then click at the bottom in WGS code. The new tab will have an option to download as a fasta formatted file.

Some genome projects upload the identified coding sequences and their polypeptide translations to the NCBI. However, the translated resources for *A. domesticus* used in the present work were not available in NCBI. As a result, the downloaded nucleotide contig sequences are required to translate into protein sequences prior to using them for proteomic database searches (*see Note 4*).

For translating genome data, it is necessary to have coding sequence annotations (CDS) usually provided as .gtf. This document will specify which genomic regions are expressed. If the CDS is available, download and translate this file into protein sequences.

In the case of *A. domesticus*, CDS were not available. A possible option is to download the contigs fasta files and translate into all six frame translations. This can be performed with Seqkit (<https://bioinf.shenwei.me/seqkit/>) using the command prompt as follows, from the seqkit directory:

```
>seqkit translate *.fasta -f 6 -o *.fasta
```

Other resources available within NCBI:

BioProject: A collection of biological data related to a single initiative, originating from a single organization or from a consortium. A BioProject record provides users with a single place to find links to the diverse data types generated for that project [12]. <https://www.ncbi.nlm.nih.gov/bioproject/>

BioSample: Descriptions of biological source materials used in experimental assays [13].

Transcriptome Shotgun Assembly (TSA) Database: Assembled transcript sequences from primary data such as ESTs and Next Generation Sequencing Technologies. <https://www.ncbi.nlm.nih.gov/genbank/tsa/>

Expressed Sequence Tags (EST) database: A division of GenBank that contains short sequencings from cDNA libraries, expressed mRNA sequences [14]. <https://www.ncbi.nlm.nih.gov/genbank/dbest/>

Recommendations:

1. Performing genome assembly and annotation or *de novo* transcriptome analysis will impact the proteome output. However, these processes are time consuming and require specific skill. As such, it is recommended to search for the abovementioned resources before acquiring large-scale genome or transcriptome-based data sets that require substantial processing.
2. If species-specific genomic resources are unavailable or insufficient, sequences can be used from higher taxonomic groups for a greater number of accessions to capture related sequence variance.
3. It is critical to always note the date when the search was performed and the fasta file was downloaded. Databases are constantly being updated and this might affect the accession numbers. Always report the version of the database used in the study.

4 Protein/Peptide Identification

1. Protein and peptide identification is undertaken by peptide-spectrum matching algorithms usually incorporated in the vendor software or freeware. In this case, ProteinPilot v5.0.2 software (SCIEX) which uses the Paragon algorithm [15] was employed. All data was searched together against each custom database.
2. When database searching is finished, a list of identified proteins and peptides will be reported. In some cases, it will be prudent to refine search results to remove reverse proteins, remove unusual modifications, miscleaved peptides, and threshold protein and peptide identifications at a 1% false discovery rate (FDR). Herein, an R-based script was used to carry out these tasks [16].
3. Interpretation and validation of the results. The below plots show the results when different taxonomic level resources and database platforms were used (Figs. 4, 5, and 6).

5 Notes

1. Several software packages are available. ProteinPilot is available from SCIEX as a licensed product.
2. Within UniProt-KB some protein sequences are manually annotated and reviewed (Swiss-Prot) while other are automatically annotated and are not yet reviewed (TrEMBL).
3. Genome raw reads and assembled data (regardless of the method used) are usually available.
4. For translating the genome contigs, there are different tools that can be used like seqkit (<https://bioinf.shenwei.me/seqkit/>), getorf (<https://www.bioinformatics.nl/cgi-bin/emboss/help/getorf>). However, working with a genome involves complex tasks like defining open reading frames (ORFs) and coding DNA sequences (CDS).

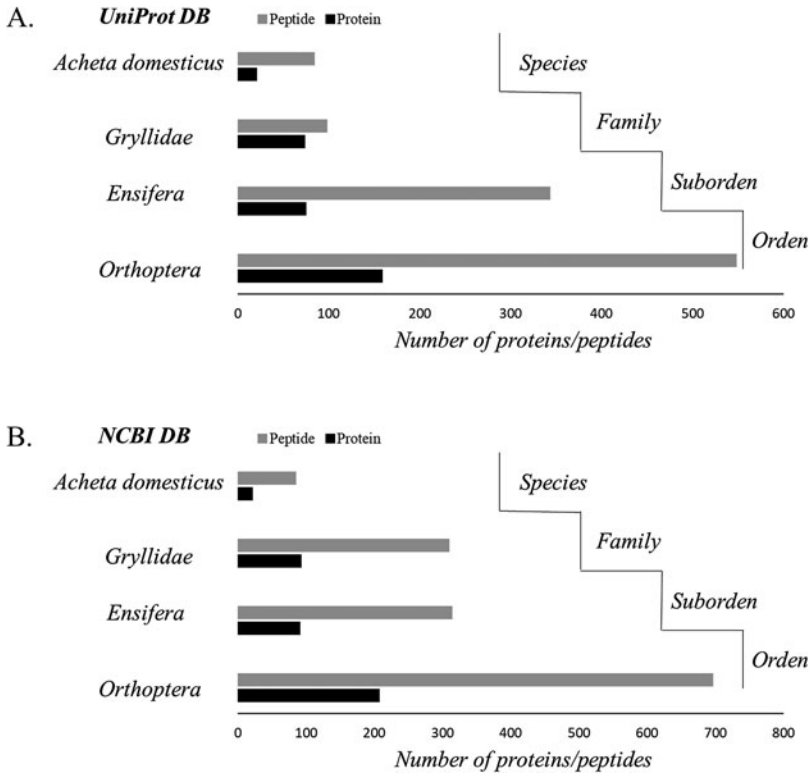


Fig. 4 Protein and peptide identification yields depend on the taxonomic level and repository selected for database construction. The number of identifications increases with a higher taxonomic level database for both database sources: (a) UniProt-KB; and (b) NCBI



Fig. 5 A Venn chart showing the comparison of peptides discovered with the Orthoptera database using NCBI and UniProt

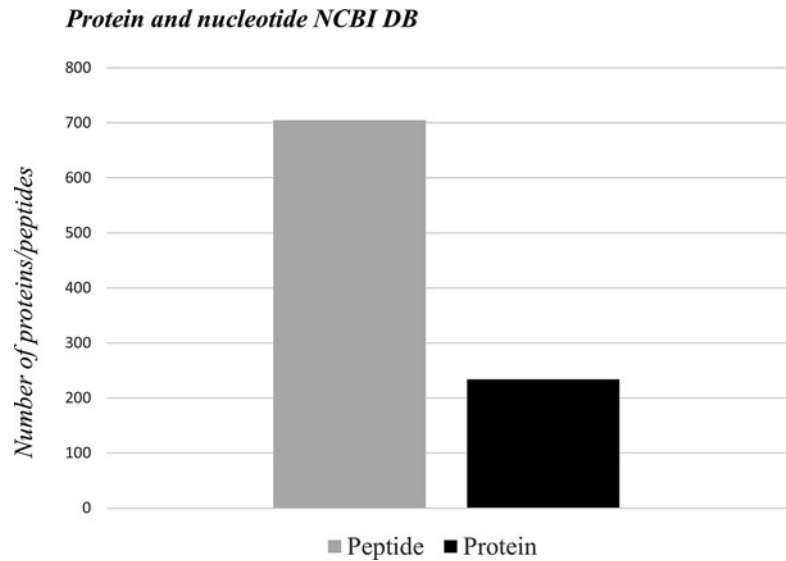


Fig. 6 Protein and peptide identification yield with a custom database constructed from both NCBI protein sequences of the order Orthoptera and translated nucleotide sequences from *Acheta domesticus*. The number of identifications increases with inclusion of protein and nucleotide databases

Acknowledgments

Sophia Escobar-Correas was supported by a Research Plus CERC Postdoctoral Fellowship from CSIRO, Australia.

References

- Domínguez I, Frenich AG, Romero-González R (2020) Mass spectrometry approaches to ensure food safety. *Anal Methods* 12: 1148–1162. <https://doi.org/10.1039/C9AY02681A>
- Kuhnert N, Dairpoosh F, Yassin G, Golon A, Jaiswal R (2013) What is under the hump? Mass spectrometry based analysis of complex mixtures in processed food—lessons from the characterisation of black tea thearubigins, coffee melanoidines and caramel. *Food Funct* 4: 1130–1147. <https://doi.org/10.1039/c3fo30385c>
- Picó Y (2015) Chapter 1. Mass spectrometry in food quality and safety: an overview of the current status. In: Picó Y (Ed.), *Comprehensive analytical chemistry, advanced mass spectrometry for food safety and quality*. Elsevier, pp 3–76. <https://doi.org/10.1016/B978-0-444-63340-8.00001-7>
- Kertesz-Farkas A, Reiz B, Myers M, Pongor S (2012) Database searching in mass spectrometry based proteomics. *Curr Bioinform* 7: 221–230. <https://doi.org/10.2174/157489312800604354>
- Bose U, Broadbent JA, Juhász A, Karnaneedi S, Johnston EB, Stockwell S, Byrne K, Limviphuvadh V, Maurer-Stroh S, Lopata AL, Colgrave ML (2021) Protein extraction protocols for optimal proteome measurement and arginine kinase quantitation from cricket *Acheta domesticus* for food safety assessment. *Food Chem* 348:129110. <https://doi.org/10.1016/j.foodchem.2021.129110>
- Vizcaíno JA, Deutsch EW, Wang R, Csordas A, Reisinger F, Ríos D, Dianas JA, Sun Z, Farrah T, Bandeira N, Binz P-A, Xenarios I, Eisenacher M, Mayer G, Gatto L, Campos A, Chalkley RJ, Kraus H-J, Albar JP, Martinez-Bartolomé S, Apweiler R, Omenn GS,

- Martens L, Jones AR, Hermjakob H (2014) ProteomeXchange provides globally coordinated proteomics data submission and dissemination. *Nat Biotechnol* 32:223–226. <https://doi.org/10.1038/nbt.2839>
7. Desiere F, Deutsch EW, King NL, Nesvizhskii AI, Mallick P, Eng J, Chen S, Eddes J, Loevenich SN, Aebersold R (2006) The PeptideAtlas project. *Nucleic Acids Res* 34:D655–D658. <https://doi.org/10.1093/nar/gkj040>
 8. Craig R, Cortens JP, Beavis RC (2004) Open source system for analyzing, validating, and storing protein identification data. *J Proteome Res* 3:1234–1242. <https://doi.org/10.1021/pr049882h>
 9. Martens L, Hermjakob H, Jones P, Adamski M, Taylor C, States D, Gevaert K, Vandekerckhove J, Apweiler R (2005) PRIDE: the proteomics identifications database. *Proteomics* 5:3537–3545. <https://doi.org/10.1002/pmic.200401303>
 10. Choi M, Carver J, Chiva C, Tzouros M, Huang T, Tsai T-H, Pullman B, Bernhardt OM, Hüttenhain R, Teo GC, Perez-Riverol Y, Muntel J, Müller M, Goetze S, Pavlou M, Verschueren E, Wollscheid B, Nesvizhskii AI, Reiter L, Dunkley T, Sabidó E, Bandeira N, Vitek O (2020) MassIVE.quant: a community resource of quantitative mass spectrometry-based proteomics datasets. *Nat Methods* 17: 981–984. <https://doi.org/10.1038/s41592-020-0955-0>
 11. Shen W, Le S, Li Y, Hu F (2016) SeqKit: a cross-platform and ultrafast toolkit for FASTA/Q file manipulation. *PLoS One* 11: e0163962. <https://doi.org/10.1371/journal.pone.0163962>
 12. Clark K, Pruitt K, Tatusova T, Mizrahi I (2013) BioProject, the ncbi handbook [internet], 2nd edn. National Center for Biotechnology Information (US), Bethesda
 13. Barrett T (2013) BioSample, the ncbi handbook [internet], 2nd edn. National Center for Biotechnology Information (US), Bethesda
 14. Boguski MS, Lowe TM, Tolstoshev CM (1993) dbEST—database for “expressed sequence tags”. *Nat Genet* 4:332–333
 15. Shilov IV, Seymour SL, Patel AA, Loboda A, Tang WH, Keating SP, Hunter CL, Nuwaysir LM, Schaeffer DA (2007) The paragon algorithm, a next generation search engine that uses sequence temperature values and feature probabilities to identify peptides from tandem mass spectra. *Mol Cell Proteom* 6:1638–1655. <https://doi.org/10.1074/mcp.T600050-MCP200>
 16. Escobar Correias S (2021) R code to filter FDR reports from discovery proteomics generated in ProteinPilot software. v2. CSIRO. Software collection. <https://doi.org/10.25919/e2aw-vd18>



Lipidomics Study of Fishes Using Hydrophilic Interaction Chromatography and Mass Spectrometry

Qing Shen, Xina Yu, Pei Luo, Pingya Wang, Qiaoling Zhao, Jie Liao, and Xiaofang Zhu

Abstract

Lipids are closely related to biological mechanisms with their critical role in membrane structures, energy storage, and signaling. Therefore, lipidomics studies have become an essential tool in a biological system applied in new drug research and the discovery of disease-related metabolic markers. Nevertheless, the physicochemical and structural diversity of lipids poses a great challenge to lipidomics research. With modern technology development, hydrophilic interaction chromatography coupled to mass spectrometry has proven to be an excellent tool to separate and identify lipids according to their fatty acyl chains and various classes. The analysis of long-chain polyunsaturated fatty acids (PUFAs) in fish oil has been a hot topic in marine biology research. Moreover, n-3 PUFA bound to phospholipids possess higher bioavailability and bioactivity as reported, which can prevent and alleviate some diseases. In this chapter, we mainly introduce the HPLC-MS method utilized in PLs research of fish samples and how to profile phospholipids from different molecular classes.

Key words Lipidomics, Fish samples, Hydrophilic interaction chromatography, Mass spectrometry, Phospholipids, Lipid profile

1 Introduction

Lipidomics, a new field of metabolomics, is focused on the studies of cellular lipids based on emerging advances and analytical chemistry principles [1]. Although lipidomics developed later than the allied field (e.g., proteomics), lipids appear unique advantages and challenges in the study of their structural and biological diversity with developing mass spectrometry (MS) [2]. With excellent accuracy and sensitivity, MS can be employed to address the difficulties in the characterization and quantification of high and low abundance lipids in complex food matrices [3].

Lipids are defined as amphiphilic molecules that are partially soluble or insoluble in water. Although lipids can be classified into

several groups in different ways, two categories have been created according to the polarity: polar lipids (glycolipids, phospholipids, sphingolipids) and nonpolar lipids (cholesterol, cholesteryl esters, triacylglycerol, etc.) [4]. Lipids are natural molecules with essential roles in cellular membrane structures, energy storage, and signaling. Meanwhile, cellular lipids are continuously switching to physiological, pathological, and environmental conditions [5]. Lipids defects are responsible for the deterioration of some devastating diseases. Therefore, the functional diversity and prevalence of lipids demonstrate their potential as special biomarkers and as necessary food nutrients [6].

Over the latest years, considerable interest has been laid on marine lipids with a high content of n-3 long-chain polyunsaturated fatty acids (PUFAs). Fish is the primary dietary source of PUFAs, especially cold-water oily fish. Among different fish, up to one-third of the eicosapentaenoic acid (EPA) and docosahexaenoic acid (DHA) may present in the form of phospholipids (PLs) [7]. Compared with n-3 PUFA bound to triacylglycerides (TAG) or ethyl esters, n-3 PUFA bound to PL possibly possesses higher bioavailability and bioactivity according to some studies of animal models [8]. It was also reported that DHA-PL and EPA-PL in fish oil could be applied in the amelioration of atherosclerosis, alleviation of rheumatoid arthritis, and prevention of cardiovascular [9–11].

The complex physicochemical properties and structural diversity of lipids pose analytical challenges in their identification and quantitation. Consequently, hydrophilic interaction chromatography and mass spectrometry (HILIC-MS) stand out with high throughput and sensitivity. This technique can reduce ion suppression and separate and analyze strong hydrophobic lipids with higher accuracy than single mass spectrometry.

Here, we will mainly describe lipidomics methods utilized in our laboratory for profiling PLs of varied fish samples. We present in detail a versatile analytical method that can be employed for different experimental needs and detect phospholipids derived from diverse sources.

2 Materials

2.1 Equipment

1. Analytical balance.
2. Centrifuge.
3. Homogenizer.
4. Vortex.
5. Nitrogen dryer.
6. Milli-Q water system.

7. HPLC solvent filtering system.
8. Model VCX-130 ultrasonic device (Sonics & Materials Inc., Newton, USA).
9. Cosmosil HILIC column (4.6 × 250 mm, 3 μm particle size).
10. Agilent series 1100 HPLC instrument (with a quaternary pump, an autosampler, and a vacuum degasser) coupled to a 4000 Q-Trap system (Applied Biosystems Sciex, Foster City, USA) with electrospray ionization (ESI) interface. Instrument control and data acquisition were executed on Analyst 1.6.3 (AB Sciex, USA).
11. Gas: high-purity N₂ (for drying extracts and ionizing under atmospheric pressure).

2.2 Reagents

1. Trichloromethane.
2. Methanol (LC-MS grade) (Merck, Darmstadt, Germany).
3. Acetonitrile (LC-MS grade) (Merck, Darmstadt, Germany).
4. Ammonium formate (Merck, Darmstadt, Germany).
5. Formic acid (Merck, Darmstadt, Germany).
6. PC (14:0/14:0) (Avanti Polar Lipids Inc., Alabaster, AL, USA).
7. PE (15:0/15:0) (Avanti Polar Lipids Inc., Alabaster, AL, USA).
8. PI (16:0/16:0) (Avanti Polar Lipids Inc., Alabaster, AL, USA).
9. PS (14:0/14:0) (Avanti Polar Lipids Inc., Alabaster, AL, USA).
10. Ultrapure water was obtained from the Milli-Q water system (Millipore, Bedford, MA, USA).

2.3 Supplies

1. 1-mL and 2-mL centrifuge tube.
2. 1-mL syringes.
3. 2-mL glass vials with Teflon cap.
4. Sealing film.
5. Organic syringe filter (0.22 μm).
6. 20-mL measuring cylinders.

3 Methods

1. The extraction process should be kept at 4 °C to lower the risk of lipid hydrolysis and oxidation. Avoid prolonged exposure of the extracts to room temperature.

Different methods of extracting phospholipids have been reported in previous literature, such as Bligh and Dyer, MTBE, and Folch

3.1 Sample Extraction

method. Chloroform-methanol extraction, also known as the B&D method, is the golden standard for lipid extraction. Here, we described a modified B & D extraction method in detail (*see Note 1*). Before extraction, fish samples should be frozen in the refrigerator at $-20\text{ }^{\circ}\text{C}$ to prevent lipase activity. The plasticizers released from common plastic centrifuge tubes will contaminate samples and MS, resulting in more noise peaks on the spectrum. Therefore, only Eppendorf tubes or glass tubes should be selected (*see Note 2*).

1. Weigh the fish tissue (0.15 g) and transfer it into Eppendorf tubes (*see Notes 3 and 4*).
2. Add 1.2 mL of chloroform and methanol (2:1, v/v) mixture solvent into homogenate and vortex for 20 s (*see Notes 5 and 6*).
3. Ultrasound-assisted extract the mixture at $4\text{ }^{\circ}\text{C}$ to fully release the lipids from the solid matrix.
4. Add 0.5 mL of ultrapure water and centrifuge the sample at $5000 \times g$ for 15 min to separate the organic and aqueous layer with a protein interface (*see Note 7*). The lower phase (organic layer) incorporates most of the lipids, while the upper aqueous phase mainly contains polar metabolites (*see Note 8*).
5. Transfer the organic layer to an individual Eppendorf tube with syringes to reduce the risk of contaminating the protein interface (*see Note 9*).
6. Re-extracted the upper phase by adding 1 mL chloroform, vibrating, and centrifuging at $5000 \times g$ for 5 min.
7. Evaporate the collected organic phase to dryness with a nitrogen gas evaporator (*see Note 10*).
8. Seal the tubes by sealing film before storing them in the $-20\text{ }^{\circ}\text{C}$ refrigerator. Analysis samples within 5 days (*see Note 11*).
9. Resolve the dried lipid extract with methanol and filtered it through an organic filter ($0.22\text{ }\mu\text{m}$) to remove impurities before injection (*see Note 12*).
10. Transfer lipid solution to a 2-mL LC glass vial and proceed to HPLC-MS analysis.

3.2 HPLC Solvents

1. Preparation: 500 mL acetonitrile, 750 mL of ultrapure water, 0.95 g ammonium formate, 3 mL formic acid, 80 mL methanol. Degas all solvents with ultrasonic for 10 min before running samples (*see Note 13*).
2. Weak wash: methanol and ultrapure water (7:3, v/v).
3. Strong wash: methanol and ultrapure water (1:9, v/v).
4. Mobile phase A: Measure out 750 mL ultrapure water and transfer it into a volumetric flask. Add 0.95 g ammonium

formate and 1.8 mL formic acid into a flask. Vacuum filter and pour it into Duran bottle before degassing.

5. Mobile phase B: Add 1.8 mL formic acid into 500 mL acetonitrile and repeat **step 4** (*see Note 14*).

3.3 HPLC-MS Data Acquisition

Lipid separation is challenging due to its various physicochemical properties. Dilute lipid standards in methanol to the expected concentration (*see Note 15*). Each lipid standard should be analyzed separately before running samples to acquire the proper chromatograms and spectra (*see Note 16*).

1. Run mobile phase A and mobile phase B (1:1, v/v) at the flow rate of 0.2 $\mu\text{L}/\text{min}$ for 30 min and two blanks (methanol) injections to obtain a smoother baseline (*see Note 17*).
2. Put sample vials into the autosampler chamber in order.
3. Set HPLC gradient profile described in Table 1 (*see Note 18*). Wash the column and adjust the ratio of mobile phase A and mobile phase B to the initial condition after the lipid separation (*see Note 19*). Flow rate: 0.6 mL/min; Injection volume: 2 μL ; Total run time was 30 min (*see Note 20*).
4. The following MS parameters were set in negative ion mode: ion spray voltage at 4.5 kV, drying gas at 24 psi, nebulizer gas at 30 psi, curtain gas 25 psi, ion spray temperature at 500 °C, collision energy (CE) at 40 V, declustering potential (DP) at 75 V. Set scan range of MS at m/z 600 to 1000 at a scan rate of 1 s per spectrum (*see Note 21*).
5. Edit a sequence that contains extraction blanks and methanol to equilibrate column and technique (*see Note 22*).
6. Equilibrate the Cosmosil HILIC column with the initial condition of mobile phase A and B at 30 °C.
7. Run every phospholipid standard individually for the identification of fish phospholipids (*see Note 23*).
8. Run fish lipid sequence using the above HPLC and MS method (*see Note 24*).
9. Wash the column with acetonitrile and water at the rate of 0.2 mL/min for 30 min, followed by a wash at 0.4 mL/min for 1 h. Unload the column from the instrument at the end of the wash.

3.4 Data Analysis and Interpretation

Examples of total ion chromatogram of phospholipids extracted from salmon tissue and analyzed on Agilent series 1100 HPLC instrument coupled to a 4000 Q-Trap system in negative ion mode is shown in Fig. 1 (*see Note 25*).

1. Identify phospholipid molecular species by referring to the retention time of phospholipid standards. Because the polar

Table 1
HPLC gradient profile for separation of lipid samples

Time (min)	Mobile phase A (%)	Mobile phase B (%)
0	5	95
10	30	70
15	50	50
20	50	50
21	5	95
30	5	95

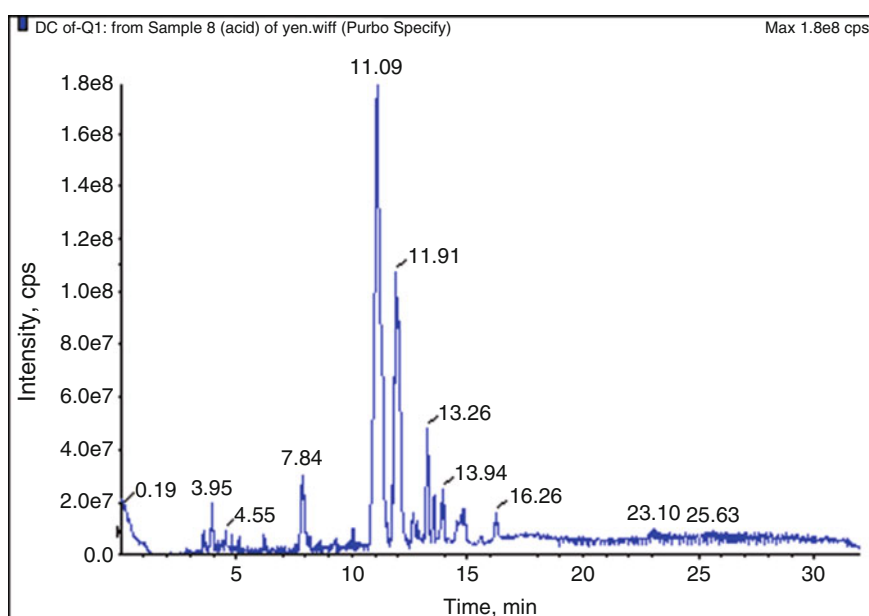


Fig. 1 Total ion chromatogram of phospholipids elution profile for extracted salmon tissue in negative ion mode using a Cosmosil HILIC column

head of phospholipids decides retention behavior, and single molecular species of the same phospholipid class possess the same retention time. PC 14:0/14:0 (11.1 min) was first eluted, followed by PE 15:0/15:0 (11.9 min), PI 16:0/16:0, and PS 14:0/14:0 (16.3 min).

2. PC molecular species are ionized as $[M + \text{HCOO}]^-$, whereas PE, PI, and PS are deprotonated as $[M - \text{H}]^-$.
3. MS spectra of PC, PE, and PS & PI of salmon tissues are shown in Fig. 2. Each peak in MS spectra corresponding to different phospholipid molecular species.

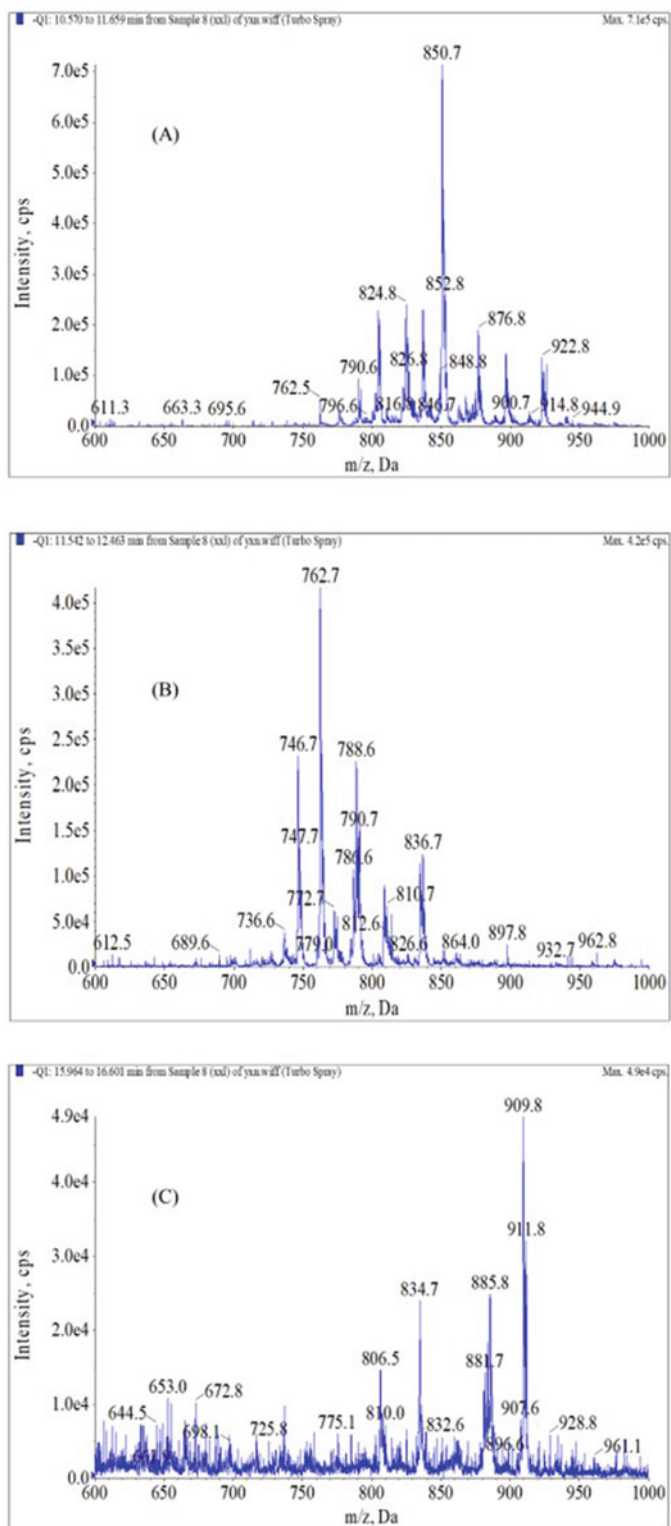


Fig. 2 MS spectra of (a) PC, (b) PE, and (c) PS & PI of salmon tissues

4. The variation of different fatty acyl chains on the glycerol backbone produces different phospholipid molecular species, which can be identified by LIPID MAPS[®] Structure Database (LMSD) and previous literature. The number of carbon atoms and double bonds could be interpreted using this software.
5. For quantification purposes, the internal standards are added into samples before the extraction procedure. Compare the peak area of every phospholipid standard and internal standards. Use the concentration of phospholipid standards as the abscissa and the peak area ratio as the ordinate to plot. Calculate the calibration curves with the least square regression method to obtain reliable quantitation data of all phospholipid molecular species.
6. The data acquired by the above steps can be transferred as a .csv file for the following data analysis.
7. Further process data with a univariate or multivariate statistical analysis, such as the FC/T test and (O) PLS-DA method (*see Note 26*).

4 Notes

1. More attention should be paid to lipid extraction reprocess with its vital role in the subsequent sample analysis.
2. Chloroform will leach plasticizers out of ordinary plastic tubes, so selecting some plastic supplies such as centrifuge tubes is essential for this experiment.
3. Only a little lipid extract can be obtained during the process of lipid extraction. Therefore, at least a few milligrams of the fish tissue sample are required to ensure an adequate instrument signal.
4. Fish tissues should be cut and weighed under freezing, as thawing at room temperature changes the lipid composition. If it is difficult to handle frozen samples, do not thaw the samples in a water bath, you can heat them with your palm, but keep the sample temperature below 0 °C.
5. Fish tissues should be fully homogenized to avoid the difference in extraction efficiency of each sample. This homogenization step is better performed after the addition of chloroform and methanol.
6. Chloroform is a potential carcinogen that quickly decomposes when exposed to light. Furthermore, chloroform mainly influences the central nervous system and may cause damage to the heart, liver, and kidneys. Therefore, the lipid extraction

experiment must be processed in a chemical fume-hood to avoid the risk of skin contact and inhalation.

7. A centrifuge that can match 2-mL tubes is in demand for the lipid extraction of fish tissues.
8. Remain the same ratio of chloroform, methanol, and water, adjust the volume of the added solution according to the amount and type of samples.
9. The last drops of the organic layer can be left in vials to avoid recovering the upper phase together.
10. To prevent inaccurate sample concentration caused by solution splashing during nitrogen blowing, adjust the pressure of the gas cylinder to make slight ripples appear on the surface of the solution. As the solvent evaporates, the flow rate needs to be adjusted periodically.
11. Configured reagents and lipid extracts should be stored at amber vials at low temperatures to avoid photolysis and oxidation.
12. Open the refrigerated reagent at room temperature to avoid condensation of water vapor in the bottle.
13. HPLC solvents should be vacuum filter and degas before lipid analysis, which helps obtain better chromatograms and mass spectrums.
14. Compared with organic solutions, aqueous solutions are prone to mold growth, so mobile phase A is replaced every 2 days, while mobile phase B can be changed once a week.
15. Phospholipid standards should be stored at low temperatures because they are unstable and are easily degraded after dissolution. Standard solutions are best used immediately after configuration. The content of phospholipid standards should be added according to the amount of endogenous lipids in weighed samples. Otherwise, standards are difficult to be identified in the spectrum.
16. Phospholipid standards can be divided into several equal parts to avoid the ineffectiveness of the standards caused by repeated freezing and thawing.
17. Run two blank (methanol) injections before running the sequence to ensure a stable baseline and retention time.
18. The HPLC method should contain wash and equilibration steps to better prepare the next sample injection in the same sequence.
19. Ensure the HILIC column is well equilibrated, the HPLC pump is purged, and the air bubbles have been removed from the pipeline before sample detection.

20. Adjust the injection volume according to the concentration and types of samples, and the highest injection volume is 10 μ L. Otherwise, the retention time will be inaccurate.
21. PC and PE can be detected in both negative and positive ion mode, while PI in fish samples only responds in negative ion mode. The signal intensity in positive ion mode will be interfered with impurities because of the protonating competition. Besides, all phospholipid classes can be simultaneously detected in a single run under negative ion mode, which increases the sample throughput and decreases the running time [12].
22. Run a solvent blank every 5–6 injections to prevent sample contamination.
23. The suitable concentration of injection sample and phospholipid standards is critical for peak intensity.
24. Do not run samples separately. Lipid extracts should be stored at -20 °C before analysis. If samples cannot be detected in time, the volume of the methanol added should be recorded because the organic solvent will volatilize even at low temperatures.
25. This experiment incorporated an Agilent series 1100 HPLC instrument coupled to a 4000 Q-Trap system (Applied Biosystems Sciex, Foster City, USA). The described HPLC-MS method combines high chromatographic separation with MS sensitive detection so that it can be applied in the detection of low concentration lipid. In contrast, the shotgun analysis injects the lipid extracts into the MS detector directly, resulting from ionization suppression and equipment contamination.
26. MetaboAnalyst 4.0. can be employed to process lipidomics data with a univariate or multivariate statistical analysis. The former includes fold change analysis, T-tests, volcano plot, one-way analysis of variance (ANOVA), correlation Heatmaps, etc. Multivariate statistical analysis used in this online software mainly includes principal component analysis (PCA) and partial least squares—discriminant analysis (PLS-DA). Cluster analysis comprises dendrogram, heatmaps, k-means, and self-organizing maps (SOM). Therefore, differential metabolites between two or more groups can be screened using the above analytical methods.

References

1. Orešič M, Hänninen VA, Vidal-Puig A (2008) Lipidomics: a new window to biomedical frontiers. *Trends Biotechnol* 26:647–652. <https://doi.org/10.1016/j.tibtech.2008.09.001>
2. Fahy E, Cotter D, Sud M, Subramaniam S (2011) Lipid classification, structures and tools. *Biochim Biophys Acta* 1811:637–647. <https://doi.org/10.1016/j.bbalip.2011.06.009>

3. Sun T, Wang X, Cong P, Xu J, Xue C (2020) Mass spectrometry-based lipidomics in food science and nutritional health: a comprehensive review. *Compr Rev Food Sci Food Saf* 19: 2530–2558. <https://doi.org/10.1111/1541-4337.12603>
4. Gugiu GB (2017) Lipid identification by untargeted tandem mass spectrometry coupled with ultra-high-pressure liquid chromatography. *Lipidomics*. 65–82. https://doi.org/10.1007/978-1-4939-6996-8_8
5. Yang K, Han X (2016) Lipidomics: techniques, applications, and outcomes related to biomedical sciences. *Trends Biochem Sci* 41:954–969. <https://doi.org/10.1016/j.tibs.2016.08.010>
6. Yu X, Chen K, Li S, Wang Y, Shen Q (2019) Lipidomics differentiation of soft-shelled turtle strains using hydrophilic interaction liquid chromatography and mass spectrometry. *J Chromatogr B* 1112:11–15. <https://doi.org/10.1016/j.jchromb.2019.02.025>
7. Burri L, Hoem N, Banni S, Berge K (2012) Marine Omega-3 phospholipids: metabolism and biological activities. *Int J Mol Sci* 13: 15401–15419. <https://doi.org/10.3390/ijms131115401>
8. Murota K, Takagi M, Watanabe Y, Tokumura A, Ohkubo T (2017) Roe-derived phospholipid administration enhances lymphatic docosahexaenoic acid-containing phospholipid absorption in unanesthetized rats. *Prostaglandins Leukot Essent Fatty Acids* 139:40–48. <https://doi.org/10.1016/j.plefa.2017.06.011>
9. Ding L, Zhang L, Wen M, Che H, Du L, Wang J, Wang Y et al (2017) Eicosapentaenoic acid-enriched phospholipids improve atherosclerosis by mediating cholesterol metabolism. *J Funct Foods* 32:90–97. <https://doi.org/10.1016/j.jff.2017.02.020>
10. Sara P, Elena P, Carrie R, Elena N (2018) The Mediterranean diet, fish oil supplements and rheumatoid arthritis outcomes: evidence from clinical trials. *Autoimmun Rev* 17:1105–1114. <https://doi.org/10.1016/j.autrev.2018.06.007>
11. Siscovick DS, Barringer TA, Fretts AM, Wu JHY, Lichtenstein AH, Costello RB, Mozaffarian D (2017) Omega-3 polyunsaturated fatty acid (fish oil) supplementation and the prevention of clinical cardiovascular disease. *Circulation* 135:e867–e884. <https://doi.org/10.1161/CIR.0000000000000482>
12. Shen Q, Dai Z, Huang YW, Cheung HY (2016) Lipidomic profiling of dried seahorses by hydrophilic interaction chromatography coupled to mass spectrometry. *Food Chem* 205:89–96. <https://doi.org/10.1016/j.foodchem.2016.02.151>



Detection of Aroma Compounds in Food by Gas Chromatography-Mass Spectrometry/Olfactometry

Nina Buck, Bianca Lok, and Philipp Denk

Abstract

The analytical detection of aroma constituents in food samples presents a challenge. Combining instrumental methods with the human sense of smell represents a state-of-the-art approach for elucidating single aroma-active compounds that contribute to the overall odor of a sample. The complementary use of human olfaction is a necessity since its sensitivity in perceiving odors is in many cases far superior to the detection limits of current instrumental systems. The characterization of odor-active compounds in a sample proceeds via an extraction and subsequent analysis. The volatile compounds, both odor-active and odorless, are typically extracted from a sample using solvent extraction followed by distillation (solvent-assisted flavor evaporation, SAFE). The resulting distillate is then analyzed by gas chromatography combined with olfactometry and mass spectrometry (GC-O and GC-MS/O). Using this tool, aroma-active compounds are detected based on their retention time (or index) and the odor impression perceived by the assessor as they individually elute from the column during chromatographic separation. Structural identification of aroma compounds at a molecular level can be elucidated via their simultaneous analysis by mass spectrometry. This protocol offers step-by-step guidelines for sample preparation and extraction, and subsequent analysis by GC-O and/or GC-MS/O.

Key words Aroma extract dilution analysis (AEDA), Gas chromatography-mass spectrometry/olfactometry, Instrumental analysis, Odor, Olfactometry, Smell, Solvent-assisted flavor evaporation (SAFE)

1 Introduction

Food aroma research and particularly the elucidation of aroma-active compounds that are responsible for the aroma of food remains a challenge, to date. Despite the existence of highly sophisticated instrumentation for the analysis and detection of volatile aroma-active compounds, the human sense of smell plays an important and largely irreplaceable role in this undertaking [1, 2]. Specifically, the detection of aroma-active compounds via olfaction, i.e., olfactometry, is combined with analytical instruments equipped

Authors Nina Buck and Bianca Lok contributed equally.

Hector Koolen (ed.), *Mass Spectrometry for Food Analysis*,
Methods and Protocols in Food Science, https://doi.org/10.1007/978-1-0716-2107-3_13,
© The Author(s), under exclusive license to Springer Science+Business Media, LLC, part of Springer Nature 2022

with highly sensitive detectors. This represents the most frequently used tool in the field of aroma research.

The challenge in aroma analytics begins with the suitable extraction of aroma-active compounds from the sample food matrix. The conventional approach is a solvent-based extraction of volatiles from the food sample, followed by distillation. The high volatility of most aroma compounds and their susceptibility to degradation impose limitations on how they can be extracted; accordingly, a specific isolation method has been developed for food chemistry applications, namely the solvent-assisted flavor evaporation (SAFE) technique [3]. A SAFE apparatus operates under high vacuum and at very low temperatures, thereby enabling the direct and gentle isolation of volatiles, including aroma-active compounds with higher boiling points than the extraction solvent used. The analysis of the obtained sample distillate usually first involves screening for aroma-active compounds using gas chromatography-olfactometry (GC-O) [4]. This technique combines conventional GC, equipped with a flame ionization detector (FID) and an odor detection port (ODP), whereby the carrier gas exiting the GC column is split into two equal parts between the two detectors, and an assessor continuously sniffs the gas at the latter, allowing aroma-active compounds to be perceived and distinguished from odorless volatiles as single aroma impressions. A comparison of the perceived odor quality (i.e., how the compound smells) and the retention time—or its calculated linear retention index (RI) [5]—with odorant databases provides a first indication of the identity of the odorant. The olfactory component not only offers additional qualitative information, but sometimes potent odorants with very low odor thresholds that are present in sample distillates at concentrations below the instrumental detection limit are nevertheless clearly perceivable by the human nose and are thereby detected at the ODP. An unequivocal identification of individual compounds requires further information, namely its retention index on at least another column of different polarity, as well as its mass spectrum after ionization, requiring a mass spectrometer detector, as is employed in gas chromatography-mass spectrometry/olfactometry (GC-MS/O) [6]. Subsequently, these parameters are compared with reference values through the complementary analysis of representative reference standards. This approach provides structural information on a molecular level, with the perceived odor quality offering additional clues to determine the identity of the individual odorant. Frequently, the co-elution of volatiles leads to overlap and prevents the generation of characteristic mass spectra; the use of comprehensive (two-dimensional) GC-MS/O can overcome this problem, but this approach is not covered further in this protocol [7].

Besides elucidating the structural identification of an odorant, determining its contribution to the overall aroma of a sample is an important parameter. Aroma extract dilution analysis (AEDA) is a

commonly applied dilution-to-threshold technique to examine the relative odor intensities of single odorous substances within a sample [8]. The method involves successively diluting the original distillate of the sample and then analyzing these dilutions by GC-O. The number of perceivable aroma compounds will diminish with each dilution, with the flavor dilution (FD) factor providing a measure of the maximum dilution at which a compound can still be perceived [8]. Accordingly, the FD factors highlight the importance of single aroma-active substances for the overall smell of a sample by indicating their relative odor potency. Exact quantification requires further steps (not discussed in this protocol) and is typically performed via stable isotope dilution assays (SIDA) [9]. With the concentration of the aroma compounds and their respective odor threshold in the specific matrix, odor activity values (OAVs) can be calculated to verify the importance of the individual odorants [10].

2 Materials

It is a prerequisite that all materials used, as well as the systems themselves, are free of odor (e.g., by baking them out).

2.1 Basic Laboratory Equipment, Consumables, and Chemicals

1. Laboratory equipment: scales, spatula, Erlenmeyer flasks with plastic plugs, measuring cylinder, magnetic stirrer with PTFE-coated magnetic stir-bar, glass funnel, SAFE apparatus (Fig. 1) with high vacuum turbo molecular pump (TMP) and membrane roughing pump, and water bath [3], Dewar vessels, glass funnel, round-bottom flasks, Vigreux column (e.g., 50 cm × 1 cm i.d.), and micro-Vigreux column with micro-flasks [11], micro-syringes (100 µL, 10 µL), two lab jacks, a tripod and clamps.
2. Chemicals and consumables: freshly distilled solvent for extraction (*see Note 1*), freshly distilled ethanol, acetone, liquid N₂, anhydrous sodium sulfate, filter paper, baked-out cotton wool, GC vials with inserts and caps, Pasteur pipettes, cork rings, Teflon sealing rings.

2.2 Instruments for Gas Chromatography-Olfactometry (GC-O) and Gas Chromatography-Mass Spectrometry/Olfactometry (GC-MS/O)

1. Instruments:

GC-O: gas chromatograph with a flame ionization detector (FID), an odor detection port (ODP) and an on-column injector (Fig. 2). Capillary setting (coating details of capillary columns: *see Note 2*): 5 m uncoated pre-column (i.d. depending on the type of injector) starting in the on-column injector connected to 30 m main capillary column (0.32 mm i.d.), followed by 1 m uncoated capillary (0.32 mm i.d.) connected to a Y-type splitter leading to two uncoated capillaries of 1 m each (0.2 mm i.d.) ending in the FID and ODP detector,

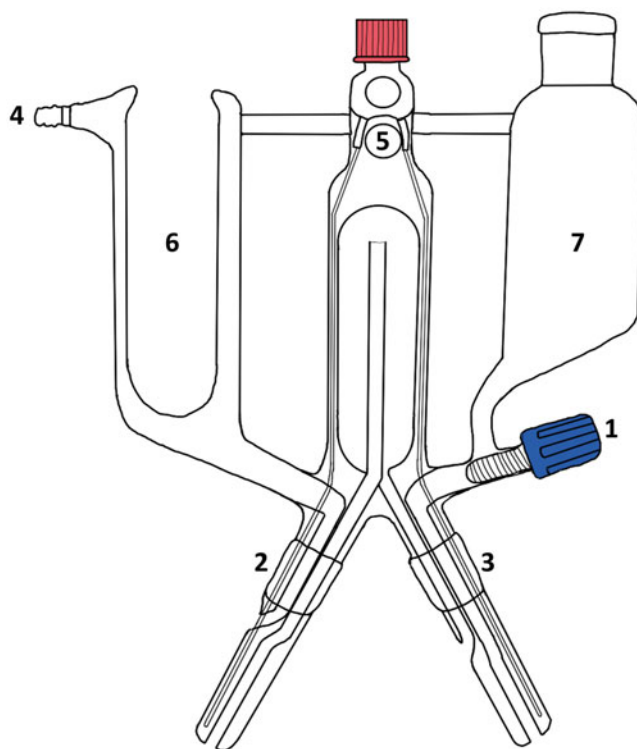


Fig. 1 Schematic drawing of the glass apparatus specifically designed for performing the solvent-assisted flavor evaporation (SAFE) as adopted by Engel et al. [3]. Explanation of the numbers is given in the text (see Subheading 3.1.2)

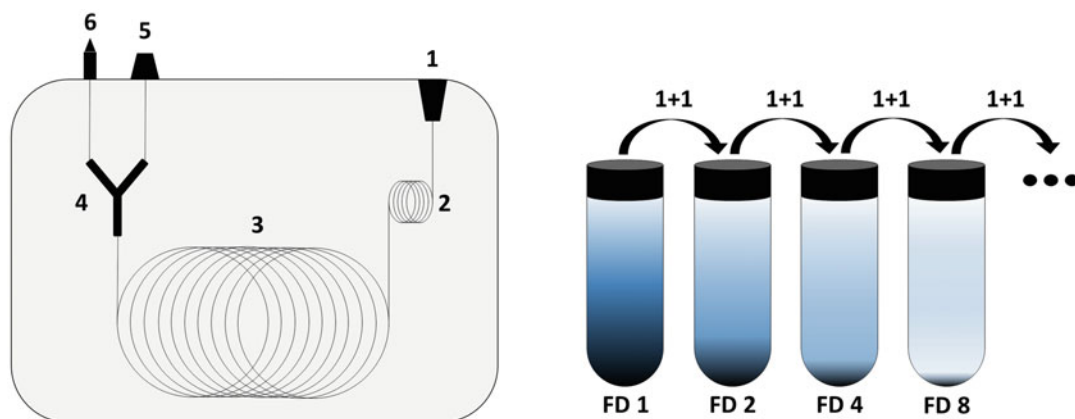


Fig. 2 *Left side*: schematic illustration of a GC-O system including (1) on-column injector, (2) pre-column, (3) main capillary column, (4) Y-type splitter, (5) FID detector, (6) ODP detector, and *right side*: schematic principle of AEDA with an exemplary stepwise dilution of 1 + 1 (v/v) (see Note 19)

respectively (see Note 2). Capillary columns are connected with inert (press-fit glass) connectors. Additionally, a data recording program or a simple chart recorder printer is needed.

GC-MS/O: gas chromatograph with an on-column injector (*see Note 3*) coupled to a mass spectrometer (MS) and an ODP. Capillary settings are the same as described for GC-O with the sole exception of the capillaries ending in the MS and ODP detector (*see Note 2*).

2. Consumables and chemicals:

Capillary columns: e.g., DB-FFAP and DB-5 (e.g., both 30 m × 0.32 mm or 0.25 mm i.d., film thickness 0.25 μm, *see Note 4*); uncoated deactivated fused silica capillaries (0.2 mm, 0.32 mm, and 0.53 mm i.d.), inert Y-splitter, mixture of alkanes (C₆–C₂₆) in pentane (0.005%, *see Note 5*), helium as carrier gas, hydrogen for the FID.

3 Methods

3.1 Sample Preparation

3.1.1 Solvent Extraction

In a first step, the sample material is subject to a solvent-based extraction, e.g., using dichloromethane or diethyl ether. Optional sample pre-treatment (*see Note 6*) and details of the extraction such as time or type of solvent strongly depend on the food matrix to be analyzed (*see Note 7*).

1. Use the laboratory scale to weigh the sample into an Erlenmeyer flask (*see Note 8*), add a magnetic stir-bar and the measured amount of solvent (*see Note 7*).
2. Close the Erlenmeyer flask with a plastic plug and place it on the magnetic stirrer. The extraction is conducted by stirring vigorously (200–500 rpm) for a specified time, e.g., 30 min at room temperature (*see Note 9*). To ensure complete extraction, repeat the step several times until the residual sample is almost odorless.
3. After extraction, filter the sample using a glass funnel with rinsed filter paper and collect the solvent extracts in a clean flask (*see Note 10*).

3.1.2 Solvent-Assisted Flavor Evaporation

The isolation of volatiles, including aroma compounds, from the solvent extract (*see Subheading 3.1.1*) is achieved through SAFE distillation—the most commonly used method for the gentle and direct extraction of odorants from food matrices [3]. For samples with a high fat content, the following procedure can also be applied more than once [12].

1. Heat the water bath to a temperature just above the boiling point of the solvent (e.g., 50 °C for DCM) and start the magnetic stirrer (situated on top of a lab jack).
2. For preparing the SAFE apparatus, first insert and tighten the Teflon tap (1, Fig. 1). Then, mount the Teflon sealing rings on the joint of both branches of the glass apparatus (2 and 3),

making sure that the rings are not twisted. On the left side (2), attach a 250 mL round-bottom flask with a bracket and a 500 mL round-bottom flask on the right branch (3) (*see Note 11*), equipped with a small magnetic stir-bar.

3. Affix the SAFE apparatus to a tripod using clamps, ensuring a firm fit. Connect the vacuum tube of the high vacuum TMP to the SAFE apparatus (4). Next, connect the tubes of the circulation thermostat to both water connections (5) of the SAFE apparatus (*see Note 12*) and switch on the circulating thermostat, setting the water temperature to 55 °C (for DCM) (*see Note 13*).
4. Switch on the TMP and roughing pump system and wait until a pressure of less than 10^{-3} mbar is achieved (*see Note 14*).
5. Carefully fill the cold trap (6) of the SAFE apparatus with liquid N₂. Refill during the distillation procedure if necessary.
6. Position the right-hand side round-bottom flask in the preheated water bath by extending the lab jack upwards—the water level should be slightly lower than the joint. Make sure that the small magnetic stir-bar inside the round-bottom flask is rotating.
7. Use a second lab jack to place the Dewar filled with liquid N₂ under the left round-bottom flask. Keep the level of liquid N₂ at about 1 cm below the joint throughout the whole distillation procedure.
8. Fill the sample extract into the reservoir (7) using a glass funnel and leave the glass funnel in this position until the end of the distillation to reduce loss by solvent evaporation.
9. Start the SAFE distillation procedure by slowly opening the Teflon tap very gently. Use caution during this step and feed the extract drop by drop into the apparatus to prevent venting the high vacuum system. Add the sample extract in this manner until only about 0.5 cm of the neck of the reservoir is filled with extract.
10. Switch off the vacuum pump and wait for the TMP to come to a complete halt.
11. Open the Teflon tap slightly and slowly feed the remaining extract into the system. Then, open the Teflon tap completely to vent the apparatus. Remove the water bath, the tube to the vacuum pump and the Dewar. Next, remove both round-bottom flasks.
12. Switch off the circulation thermostat and remove the lower tube of the circulation thermostat from the SAFE apparatus. Wait for the water to pass through the upper tube before removing the SAFE apparatus from the tripod.
13. Clean the SAFE apparatus thoroughly before reuse (*see Note 15*).

3.1.3 Distillation and Micro-Distillation

1. If the sample extract obtained by SAFE distillation was placed in frozen storage immediately after extraction, wait for it to defrost before drying over anhydrous sodium sulfate.
2. Meanwhile, turn on the water bath of the Vigreux distillation apparatus (50 °C for DCM), as well as the cooling water. Rinse the whole distillation setting thoroughly with the same solvent used for the sample extraction to eliminate any contamination of the system with aroma-active substances.
3. Filter the dried extract with a rinsed filter paper (*see Note 16*) into a 250 mL round-bottom flask and add 2–3 boiling stones.
4. Connect the flask containing the distillate to the Vigreux distillation apparatus, place the flask in the preheated water bath, and distill the sample until only the boiling stones are covered with the extract (about 3 mL).
5. Another commonly applied step (e.g., for samples with high acid concentration, such as chocolate [12]) is the separation of the organic phase into a neutral-basic and an acidic phase, which is not further described at this point.
6. Transfer the concentrated sample distillate to a micro-flask using a Pasteur pipette and rinse with the chosen solvent to ensure complete transfer of the distillate. Add two small boiling stones (*see Note 17*), attach the micro-flask to the micro-Vigreux column and start the micro-distillation [11].
7. Observe the micro-distillation carefully and stop the distillation as soon as only about three-quarter of the tip of the micro-flask is filled with distillate (e.g., 150 µL).
8. Transfer the obtained concentrated distillate (about 150 µL in total) into a GC vial with a 200 µL insert (*see Note 18*) and use for subsequent analyses.
9. If AEDA is performed (*see Subheading 3.2*), the original distillate (corresponding to FD 1) is diluted stepwise with the solvent used for extraction (Fig. 2). For this, place the chosen amount of solvent (e.g., 20 µL, *see Note 19*) in a GC vial with insert using a micro-syringe, add the corresponding aliquot of the original distillate (e.g., an additional 20 µL) and mix thoroughly by extending and retracting the syringe several times in succession. Repeat the procedure using the latest pipetted dilution until reaching the dilution corresponding to the final FD.
10. For quality control (*see Note 20*), a blank sample should be analyzed analog to above described procedure by using the same amount of solvent and chemicals, but without any sample material. By this manner, possible contamination of the system or the solvent itself with aroma-active compounds can be detected and considered during the evaluation of the actual

sample. Furthermore, the extraction and the following instrumental analyses should be performed in duplicate to ensure the validity of the results.

3.2 Gas Chromatography-Olfactometry (GC-O) and Aroma Extract Dilution Analysis (AEDA)

Gas chromatography-olfactometry (GC-O; *see* Subheading 2.2 for details of the instrumental settings) enables the elucidation of single aroma-active regions in a sample distillate. Performing aroma extract dilution analysis (AEDA, [8]) gives additional insights into relative odor intensities of individual aroma-active regions (*see* Note 21).

1. Before commencing the analysis, visually inspect the pre-column for impurities that might be present from previous analyses and cut and remove the contaminated section of the pre-column, if necessary (*see* Note 22).
2. Program the GC by setting the initial oven temperature at 40 °C (2 min), then raise the temperature at 8 °C/min to 235 °C (for a DB-FFAP capillary column; 250 °C for a DB-5) and hold the final temperature for 5 min. Note that the temperatures and temperature ramps can be adjusted to suit the nature of the column, the sample matrix, and the targeted compounds (*see* Note 23).
3. Set the helium carrier gas to the optimum flow rate for the system, which is calculated by the van Deemter equation [13]. Set the temperatures of both the ODP and the FID detector according to the manufacturer's specification (e.g., 250 °C). Finally, ignite the FID detector and prepare the data acquisition program (or the chart recorder printer).
4. Check the whole system for leaks using a carrier gas-sensitive leak detector (*see* Note 24).
5. Start a GC analysis of 1 µL of the *n*-alkanes mixture (*see* Subheading 2.2; alternatively apply a quality assurance test solution prior to that, to verify proper functioning of the GC system) with a 10 µL micro-syringe directly into the on-column injector (*see* Note 25). Simultaneously, start the GC program and data acquisition.
6. When it comes to analyzing the sample, inject 2–5 µL (depending on the length of the pre-column) of the undiluted sample distillate into the column via the on-column injector (analog to the alkane mixture); sniffing at the ODP detector should commence only after the solvent has eluted completely. Note the perceived odor qualities together with the corresponding retention time of the GC run or simply note the perceived odors onto the chart recorder printer (*see* Notes 26 and 27).
7. Proceed with analyzing each dilution step of the sample distillate (AEDA) until none or only a few aroma-active compounds

are perceivable at the ODP during the GC run. Analyze the blank sample in the same way.

3.3 Gas Chromatography-Mass Spectrometry/Olfactometry (GC-MS/O)

1. Apply the same procedure for GC-MS/O analyses as described for GC-O (*see* Subheading 3.2); the main difference is the use of an MS detector instead of the FID at the end of the capillary column (*see* Subheading 2.2 for details of the instrumental setting). Perform GC-MS/O analyses of a sample distillate suitable for a good separation performance and mass spectra acquisition, as these analyses are primarily intended to obtain a mass spectrum for the unequivocal identification of aroma-active compounds. Generate mass spectra in the electron ionization (EI) mode (70 eV) over a typical m/z range of 35–400.

3.4 Evaluation

1. A tentative identification of single aroma-active substances is made using the calculated linear retention indices (RIs) of the substances on two capillary columns of different polarity (e.g., DB-FFAP and DB-5) in combination with the odor quality on each column perceived at the ODP. Calculate the RI of each perceived aroma-active substance with the help of a homologous series of *n*-alkanes (C₆–C₂₆ for DB-FFAP) that was analyzed prior to the sample [5]. Compare the calculated RIs with the perceived odor quality with in-house or public odorant databases for a first structural suggestion.
2. The acquisition of a mass spectrum of an odorant of interest enables further unequivocal structural elucidation at a molecular level (*see* Note 28). Here, it is important to ensure a simultaneous mass spectral acquisition and odor quality detection at the ODP, further making sure that this matches with the odorant previously detected in the initial GC-O analyses.
3. A comparison of the RI, mass spectrum, and odor quality to those of a reference compound mark the final step in reliably identifying the odorant.
4. Further assignment of the flavor dilution step in which an odorant was last perceived during AEDA indicate additional information about the importance/odor potency of detected single odorants for the overall smell.

4 Notes

1. The use of freshly distilled solvent is important to ensure higher purity and avoid contamination of the solvent itself with aroma-active substances. Dichloromethane is most often used for the extraction of odorants from food matrices, but can be replaced by other solvents (*see* Note 7).

2. For GC-O, the uncoated capillaries leading from the Y-type splitter to the FID and ODP detector must have the same length to ensure a 1:1 split ratio and therefore a simultaneous detection of FID signal and odor impression at the ODP. In the GC-MS/O system, the MS operates under high vacuum while the ODP is set at atmospheric pressure, which influences the split ratio of the GC effluent. Therefore, the length and inner diameter of these two capillary columns must be adjusted accordingly to achieve an optimal split ratio and thereby obtain an appropriate and simultaneous signal at both detectors.
3. The type of injector system commonly used for the analyses of odorants is the on-column injector, which prevents additional thermal load or any losses of highly volatile and/or easily degradable odorants [14]. Other types of injection methods used in the field of aroma analyses are, amongst other, dynamic or static headspace, or thermal desorption techniques, which are primarily applied to sampling highly volatile aroma-active compounds. These techniques are not discussed in this protocol.
4. The DB-FFAP and DB-5 capillary columns are two of the most commonly used capillary columns in the field of instrumental aroma analyses. Other capillary columns, such as DB-1701, DB-Heavy Wax, or chiral columns, are used for special application areas, depending on the polarity of the analytes of interest [15].
5. An easier assignment of the *n*-alkanes and their corresponding peaks can be achieved by varying the concentration of a single alkane within the mixture (e.g., C₁₇).
6. Optional sample pre-treatment: grinding, crushing, or similar steps to reduce the size of the sample material may be necessary to achieve sufficient homogenization and extraction of the matrix. Use caution especially during intense, high temperature or excessive shear force steps since odorants are often very sensitive to thermal or enzymatic degradation or even the formation of new odorants may occur. This is a general precaution, which must be applied during all sample preparation and extraction steps and may be considered as one of the most critical sources of errors in sample preparation for aroma analyses. Cooling the sample material during crushing is often needed. For example, in case of some types of fruit or vegetables, freezing with liquid N₂ or addition of CaCl₂ may be necessary for easier sample comminution or to deactivate enzymes, respectively [16, 17].
7. Details of the extraction of the sample strongly depend on the properties of the sample material. Since there is a multitude of food matrices, it is recommended that details described in

appropriate literature on the type of samples to be analyzed are adhered to. Nevertheless, some general notes are summarized in the following:

The common solvent used for sample extraction is dichloromethane because of its beneficial polarity (other solvents include diethyl ether, pentane, methanol, or mixtures of those solvents [18]). The ratio of sample material to solvent usually ranges from 2+1 to 1+10 (v+v) [19, 20]. Rule of thumb: use as much solvent as needed to cover the sample material completely, but as little as possible to avoid emulsification, especially for sample materials with a high fat content. In the case of liquid samples, a simple liquid-liquid extraction followed by phase separation via a separating funnel may be adequate.

8. The required amount of sample material depends on the odor intensity of the sample. Common amounts typically used for extraction range between 1 g (for high odor intensity samples, [21, 22]) and 300 g (for low odor intensity samples, [19, 23]).
9. The time for appropriate extraction is an important factor that strongly depends on the food matrix. Extraction times of up to 30 min are commonly applied [19, 23, 24]. To ensure an exhaustive extraction, also higher extraction times can be applied [20].
10. For sample material with high fat content or for emulsions, adding baked-out cotton wool on top of the filter paper can be helpful to shorten the time of filtration since (fat) particles adhere to the cotton wool first instead of clogging the filter paper. In extreme cases, filtration can be carried out with cotton wool only or by using a Büchner funnel.
11. The volume of the flask on the distillate side should be at least twice as large as the extract volume to be distilled.
12. For connecting the tubes of the circulation thermostat, do not use clamps—danger of breakage—and connect the tube feeding the water from the thermostat in the upper position, with the outlet tube being positioned lower. Wrap the tubes tightly around the Teflon tap feeding the extract into the SAFE apparatus to make sure that the extract does not freeze.
13. The water temperature of the circulating thermostat should be 5 °C higher than the temperature of the water bath on the distillation side.
14. If a high vacuum of less than 10^{-3} mbar cannot be achieved, try to gently twist the two round-bottom flasks. If this is unsuccessful, replace the Teflon sealing rings with new ones, as these rings tend to get thin after multiple use and thereby no longer

provide an effective seal. Further, a tiny glass breakage at any part of the apparatus or flasks can result in a poor vacuum.

15. Thorough cleaning of all parts of the SAFE apparatus is essential to avoid cross contamination of different sample extracts with aroma-active compounds. Start with cleaning all tiny openings with tube cleaners dipped into a detergent solution. Then, fix two round-bottom flasks to the branches—also filled with detergent solution—and rinse the SAFE apparatus with hot water via the connection for the vacuum tube for 15–30 min until no detergent foam is left. Remove the flasks, clean the SAFE apparatus with dichloromethane and/or acetone and purge the system with dry air or N₂ to dry it. Check sufficient cleaning by smelling at both branches to make sure that there is no odor left. Remove the cap at the dome and dry the SAFE apparatus in the drying oven (105 °C) for several hours.
16. Rinsing the filter paper with solvent ensures the removal of odorous contaminants likely to be present in the filter paper itself.
17. Micro-distillation is often hindered by inefficient use of the boiling stones in the micro-flask. To prevent this, reduce the size of the boiling stones by crushing them in a mortar, add two small boiling stones to the micro-flask, attach it to the micro-Vigreux column and immediately (!) start the micro-distillation.
18. The concentrated distillate of the sample is best stored in a capped GC vial additionally sealed with Parafilm and stored at –20 °C. By this means, the distillate can be stored for subsequent analyses. To ensure the quality of the sample and to notice possible degradation processes, regular inspection of the odor of the distillate is recommended.
19. The dilution of the original distillate is carried out in a stepwise procedure with the solvent used for the extraction. The dilution steps depend on the odor intensity of the sample and the favored accuracy of the analysis; usually 1+1 (v/v) or 1+2 (v/v) are performed [7]).
20. Before starting instrumental analyses, it is important to verify a successful and complete extraction and distillation. This can be checked easily by dripping a tiny drop of the distillate onto a filter paper and comparing the odor of the distillate with the odor of the input sample material.
21. Aroma extract dilution analysis (AEDA) is a useful and efficient approach for indicating the importance of single aroma-active substances in a sample distillate. Variations in FD factors using a comparative approach of two different sample materials can indicate quantitative differences of single odorants.

22. The optimum length of the GC pre-column depends on its inner diameter, the injection volume and the expansion volume of the solvent (e.g., 3–5 m for the settings described in this protocol).
23. Switch to a lower temperature increased rate (6 °C/min) in the case of many co-eluting odorants or acidic/alkaline separation, if proper detection at the ODP becomes difficult if the rate is too high. Besides, the hold time of the final temperature can be extended (e.g., to 10 min) if (matrix) volatiles are still eluting at the end of the GC run.
24. The capillary column connections (glass press-fit connectors, Y-type splitter) are especially prone to leaking. As such, check those connections thoroughly before starting a GC run. Heating a glass press-fit connection with a naked flame (e.g., of a cigarette lighter) may tighten the connector and eliminate the leak.
25. Application of sample aliquots into the on-column injector with a micro-syringe should be done as fast as possible to avoid problems such as peak tailing or double peaks at the FID and ODP.
26. GC-O analyses of the original sample distillate should be made by at least three trained panelists to ensure that no relevant odorants have been missed, for example, because of partial anosmia or lower odor sensitivities of an individual panelist to a specific substance. Likewise, samples can be analyzed repeatedly on different days to take into account daily variations in olfactory acuity of individual panelists. Further, panelists performing GC-O should be trained on a repeated basis to be able to detect and describe all aroma-active compounds fast and with defined odor descriptors.
27. A problem during GC-O analyses may be peak tailings (noticeable by the perception of aroma-active regions over several seconds up to minutes) or the complete absence of less volatile (and therefore later eluting) substances. Common sources of error of these phenomena can be a capillary column fracture inside the ODP or a cold spot at the very end of the capillary column, leading to the condensation of volatiles. Furthermore, peak tailings are common for the separation of highly polar substances on nonpolar columns (e.g., acids on a DB-5 capillary column). For further GC troubleshooting, consider the manufacturer's website or additional literature [25].
28. A mass spectrum of potent odorants is not often easily obtainable, either because the substance is present at a concentration below the limit of detection (but still perceivable for the human nose), or because other odorless matrix compounds overlap and therefore overlay the mass spectrum of the odorant of

interest. In these cases, programs such as the automated mass spectral deconvolution and identification system software (AMDIS) can help obtaining a mass spectrum anyway [26]. Sometimes, a co-elution can only be circumvented by previous separation by other chromatographic separation techniques or performing multi-dimensional GC-MS/O.

Acknowledgments

We greatly appreciate Eva Ortner and Jonathan Beauchamp for their constructive comments and input on this protocol. Moreover, we thank Andrea Buettner for her support and mentorship.

References

1. Wardencki W, Chmiel T, Dymerski T (2013) Gas chromatography-olfactometry (GC-O), electronic noses (e-noses) and electronic tongues (e-tongues) for in vivo food flavour measurement. In: Instrumental assessment of food sensory quality, p 195–229. <https://doi.org/10.1533/9780857098856.2.195>
2. Deisingh AK, Stone DC, Thompson M (2004) Applications of electronic noses and tongues in food analysis. *Int J Food Sci Technol* 39(6): 587–604. <https://doi.org/10.1111/j.1365-2621.2004.00821.x>
3. Engel W, Bahr W, Schieberle P (1999) Solvent assisted flavour evaporation: a new and versatile technique for the careful and direct isolation of aroma compounds from complex food matrices. *Eur Food Res Technol* 209:237–241. <https://doi.org/10.1007/s002170050486>
4. Fuller GH, Steltenkamp R, Tisserand G (1964) The gas chromatograph with human sensor: perfumer model. *Ann N Y Acad Sci* 116(2): 711–724. <https://doi.org/10.1111/j.1749-6632.1964.tb45106.x>
5. van den Dool H, Kratz PD (1963) A generalization of the retention index system including linear temperature programmed gas-liquid partition chromatography. *J Chromatogr* 11: 463–471. [https://doi.org/10.1016/S0021-9673\(01\)80947-X](https://doi.org/10.1016/S0021-9673(01)80947-X)
6. Molyneux RJ, Schieberle P (2007) Compound identification: a journal of agricultural and food chemistry perspective. *J Agric Food Chem* 55(12):4625–4629. <https://doi.org/10.1021/jf070242j>
7. Delahunty CM, Eyres G, Dufour JP (2006) Gas chromatography-olfactometry. *J Sep Sci* 29(14):2107–2125. <https://doi.org/10.1002/jssc.200500509>
8. Grosch W (1993) Detection of potent odourants in foods by aroma extract dilution analysis. *Trends Food Sci Technol* 4(3):68–73. [https://doi.org/10.1016/0924-2244\(93\)90187-F](https://doi.org/10.1016/0924-2244(93)90187-F)
9. Grosch W (2001) Evaluation of the key odourants of foods by dilution experiments, aroma models and omission. *Chem Senses* 26(5): 533–545. <https://doi.org/10.1093/chemse/26.5.533>
10. Grosch W (1994) Determination of potent odourants in foods by aroma extract dilution analysis (AEDA) and calculation of odour activity values (OAVs). *Flavour Fragr J* 9(4): 147–158. <https://doi.org/10.1093/chemse/26.5.533>
11. Bemelmans JMH (1978) Review of isolation and concentration techniques. In: Land DG, Nursten HE (eds) *Progress in flavour research*. Applied Science Publishers Ltd., London, pp 79–98
12. Seyfried C, Granvogl M (2019) Characterization of the key aroma compounds in two commercial dark chocolates with high cocoa contents by means of the sensomics approach. *J Agric Food Chem* 67(20):5827–5837. <https://doi.org/10.1021/acs.jafc.8b06183>
13. Van Deemter J, Zuiderweg F, Klinkenberg AV (1995) Longitudinal diffusion and resistance to mass transfer as causes of nonideality in chromatography. *Chem Eng Sci* 50(24): 3869–3882. [https://doi.org/10.1016/0009-2509\(96\)81813-6](https://doi.org/10.1016/0009-2509(96)81813-6)
14. Grob K, Grob K (1978) On-column injection on to glass capillary columns. *J Chromatogr A* 151(3):311–320. [https://doi.org/10.1016/S0021-9673\(00\)88346-6](https://doi.org/10.1016/S0021-9673(00)88346-6)
15. Engewald W, Dettmer-Wilde K, Rotzsche H (2014) Columns and stationary phases. In:

- Practical gas chromatography. Springer, p 59–116. https://doi.org/10.1007/978-3-642-54640-2_3
16. Buttery RG, Teranishi R, Ling LC (1987) Fresh tomato aroma volatiles: a quantitative study. *J Agric Food Chem* 35(4):540–544. <https://doi.org/10.1021/jf00076a025>
 17. Schuh C, Schieberle P (2006) Characterization of the key aroma compounds in the beverage prepared from Darjeeling black tea: quantitative differences between tea leaves and infusion. *J Agric Food Chem* 54(3):916–924. <https://doi.org/10.1021/jf052495n>
 18. Semmelroch P, Grosch W (1996) Studies on character impact odorants of coffee brews. *J Agric Food Chem* 44(2):537–543. <https://doi.org/10.1021/jf9505988>
 19. Greger V, Schieberle P (2007) Characterization of the key aroma compounds in apricots (*Prunus armeniaca*) by application of the molecular sensory science concept. *J Agric Food Chem* 55(13):5221–5228. <https://doi.org/10.1021/jf0705015>
 20. Czerny M, Buettner A (2009) Odor-active compounds in cardboard. *J Agric Food Chem* 57(21):9979–9984. <https://doi.org/10.1021/jf901435n>
 21. Jagella T, Grosch W (1999) Flavour and off-flavour compounds of black and white pepper (*Piper nigrum* L.) II. Odour activity values of desirable and undesirable odorants of black pepper. *Eur Food Res Technol* 209(1):22–26. <https://doi.org/10.1007/s002170050450>
 22. Tairu A, Hofmann T, Schieberle P (1999) Identification of the key aroma compounds in dried fruit of *Xylopia aethiopica*. In: Janick J (ed) *Perspectives on new crops and new uses*. ASHS Press, Alexandria, pp 474–478. <https://doi.org/10.1021/jf990228>
 23. Martín DA, Osorio C (2019) Identification of aroma-active volatile compounds in *Pouteria sapota* fruit by aroma extraction dilution analyses (AEDA). *Química Nova* 42:607–610. <https://doi.org/10.21577/0100-4042.20170369>
 24. Blank I, Grosch W (1991) Evaluation of potent odorants in dill seed and dill herb (*Anethum graveolens* L.) by aroma extract dilution analysis. *J Food Sci* 56(1):63–67. <https://doi.org/10.1111/j.1365-2621.1991.tb07976.x>
 25. Dettmer-Wilde K, Engewald W Appendix B: troubleshooting tips. In: *Practical gas chromatography*, p 859
 26. Meyer MR, Peters FT, Maurer HH (2010) Automated mass spectral deconvolution and identification system for GC-MS screening for drugs, poisons, and metabolites in urine. *Clin Chem* 56(4):575–584. <https://doi.org/10.1373/clinchem.2009.135517>



Solid-Phase Microextraction and Comprehensive Two-Dimensional Gas Chromatography for Food Analysis

Andre Cunha Paiva, Juliana Crucello, Victor Hugo Cavalcanti Ferreira, and Leandro Wang Hantao

Abstract

In this research protocol, we present helpful guidelines that could be adopted during food analysis, specifically during the development of headspace solid-phase microextraction (HS-SPME) methods. HS-SPME is a useful technique to volatile and semi-volatile profiling of food matrices, but its experimental parameters should be carefully optimized by means of multivariate approaches, such as design of experiments (DoE), for a successful analysis. In addition, guidelines for comprehensive two-dimensional gas chromatography (GC×GC) method development are also provided, especially when the technique is hyphenated with mass spectrometry (GC×GC-MS). To illustrate these good practices, commercial coffee capsules and brewing hops are presented as the model food samples.

Key words Beer, Comprehensive two-dimensional gas chromatography, Design of experiments, Espresso coffee, Foodomics, Solid-phase microextraction

1 Introduction

First introduced by Pawliszyn and co-workers [1], fiber-based solid-phase microextraction (SPME) has gained increased attention in analytical sciences with new methods being reported in many fields for targeted and untargeted analysis, including food, environmental, forensics, and bioanalytical applications [2]. As a solvent-free technique with a reusable and immobilized extraction phase, SPME-based methods represent a concrete step towards green chemistry, especially when performed in the headspace (HS) mode. Another advantage of HS extraction is a larger sorbent lifespan in comparison with direct immersion (DI) mode since it prevents the irreversible sorption of non-volatile contaminants, such as macromolecules (e.g., proteins) and humic materials. Such unwanted compounds may jeopardize method's precision and accuracy. However, a significant drawback in HS-based

techniques is the limited extraction of low volatility analytes compared to highly volatile ones. The interested reader is referred elsewhere to a review on strategies to overcome such shortcomings [2].

The experiments performed in this protocol employ fiber-based SPME, which is commercially available as a rod-shaped flexible or rigid fused silica core coated with a thin layer (typically less than 100 μm) of sorbent material. Typical fiber length is up to 2 cm, and it is housed inside a protecting needle in a syringe like device [2]. Headspace SPME (HS-SPME) is generally performed in three consecutive steps (Fig. 1):

1. Pre-equilibrium step, which aims to promote analyte transfer from the sample matrix to the HS—typically an endothermic process. In this step, the sample is normally conditioned at the extraction temperature for a preset period of time. It should be stated that such procedure is not always mandatory.

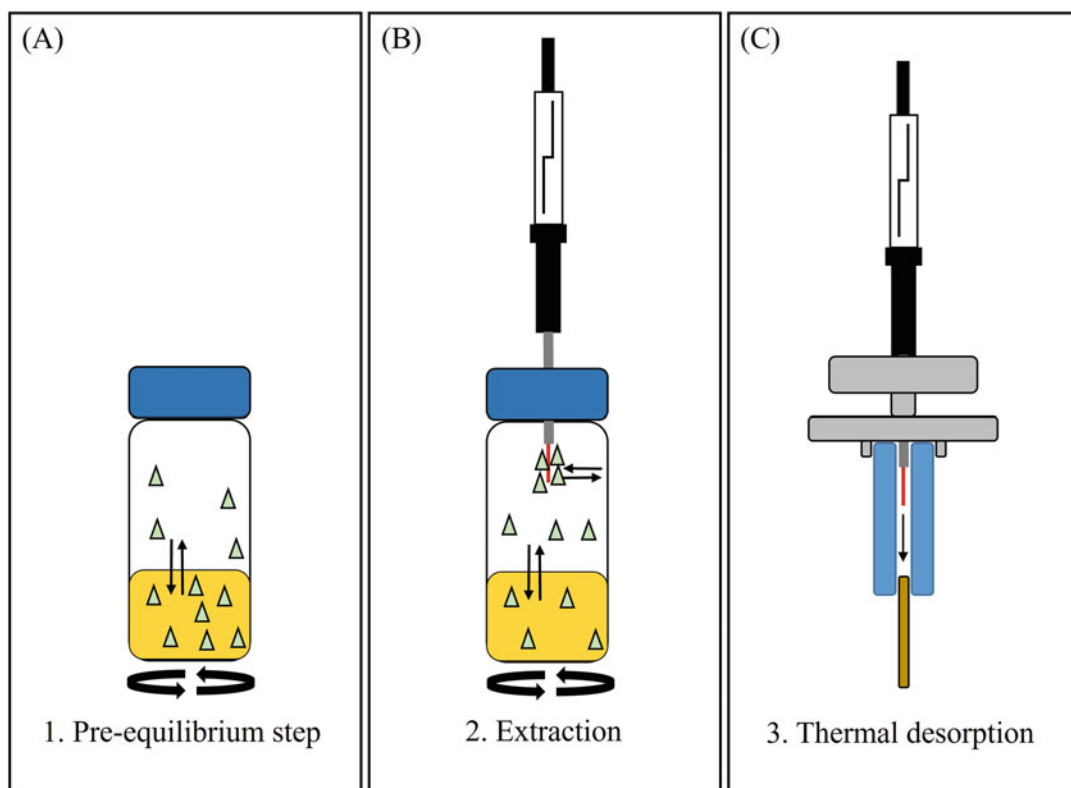


Fig. 1 Three consecutive steps involved in headspace solid-phase microextraction (HS-SPME). (a) Pre-equilibrium step promoting analyte transfer from sample matrix to headspace. (b) Analyte extraction from headspace by the sorbent phase (e.g., fiber). (c) analytes are thermally desorbed into the heated GC injection port [12]

2. The sorbent phase is exposed to sample's HS for a time interval set by the user (the extraction time).
3. The sorbent phase is withdrawn from the headspace and exposed into the heated GC injection port, where the analytes are thermally desorbed and separated in the analytical column.

During HS-SPME method development, it is important to evaluate and optimize the main experimental factors that affect the kinetics and thermodynamics of the experiment. Such factors include HS and sample volumes, extraction time, extraction temperature, and agitation speed. It is worth-mentioning that the extraction time plays a central role during HS-SPME method development. For aqueous matrices, the ionic strength (or salting out effect) and pH of the medium may also play a major role, the latter being especially important for analytes with acidic or basic sites [3].

In this scenario, a univariate SPME optimization will likely fail to evaluate the synergistic and antagonistic interactions between the extraction factors. Therefore, a multivariate approach with a design of experiments (DoE) should be explored to select the most important parameters, and to estimate their optimum values for the method. The use of DoE benefits HS-SPME methods due to its ability to evaluate each variable individually and the interactions between them. Several methods are available for DoE and the central composite design (CCD) is the most popular so far [2]. Thus, CCD was selected as an example for this protocol.

HS-SPME is an ideal companion for gas chromatography-based (GC) methods, especially when dealing with the analysis of volatile and semi-volatile organic compounds from food matrices. However, complex samples that exhibit hundreds to thousands of compounds may overcome the average peak capacity of conventional GC (1D-GC) methods, resulting in overlapped peaks [4]. In this scenario, comprehensive two-dimensional gas chromatography (GC×GC) explores the use of complementary separation stages, which is embodied by two columns and an interface. The combination of columns with different solvation properties enables the user to explore complementary separation mechanisms to harness the peak capacities of the individual dimensions, resulting in increased resolving power [5].

The GC×GC instrument relies on the modulator, an interface that preserves the chemical information of each individual dimension by means of multiplexing [6–8]. To preserve the separation attained in each dimension, the secondary separation is optimized to be typically a few seconds to avoid the mixing of the bands already separated in the primary column. The ¹D separation is designed to exhibit roughly the same duration as in conventional 1D-GC. The separation window of the ²D is defined by the modulation period (MP). Its optimization is a fundamental step in

GC \times GC experiments. For instance, if a peak exhibits a retention time in the secondary column that is longer than MP, this peak will be out of phase and may coelute with the compounds introduced in the subsequent modulation cycle. Peaks that exhibit this behavior are unwanted and it can benefit from longer MP values or chromatographic conditions that reduce the retention factor in the 2D [9]. Many principles are available for modulation such as thermal gradients or direct mechanic actuation, but indirect flow-based interfaces are interesting alternatives for GC \times GC [10]. Thus, GC \times GC is an interesting solution for food analysis, especially when hyphenated with mass spectrometry (GC \times GC-MS) to provide a detailed characterization of constitutional isomers and diastereomers.

The development of a successful HS-SPME-GC \times GC-MS method relies on the fine tuning of the extraction and separation parameters, and a clear understanding about the analytical scope. In this protocol, we highlight and exemplify helpful guides for method development in food analysis, which can be easily adapted according to different matrices and analytical necessities (e.g., sensitivity and/or selectivity). Coffee and brewing hops were carefully selected as representative food samples to illustrate good practices that could be adopted by HS-SPME and GC \times GC-MS methods.

2 Materials

1. Commercial coffee capsules and brewing hops were used as samples. Coffee samples were kept in the capsule and stored at ambient temperature until analysis. The brewing hops were kept under refrigeration at 4 °C until analysis.
2. 10 mL of ultrapure water and 10 mL of aqueous NaCl (30% w/w) were used in the solution and salting out experiments, respectively. An aliquot of 8 μ L of a C₈-C₂₀ *n*-alkanes standard was used to determine the linear temperature programming retention index (LTPRI) of the peaks. Such standard was kept under refrigeration until analysis.
3. SPME fibers including the 50/30 μ m divinylbenzene/carboxen/polydimethylsiloxane (DVB/CAR/PDMS), 85 μ m polyacrylate (PA), and 65 μ m DVB/PDMS were evaluated for the extraction of volatile organic compounds (VOCs). All fibers were pre-conditioned at the temperature and time conditions specified by the manufacturer before usage.
4. The GC \times GC-QMS analysis were performed on a TRACE1310 gas chromatograph coupled to an ISQ LT mass spectrometer (Thermo Scientific—Waltham, MA, USA) and equipped with a TriPlus RSH Autosampler (Thermo Scientific—Waltham, MA, USA). An SPME-GC \times GC-QMS analysis

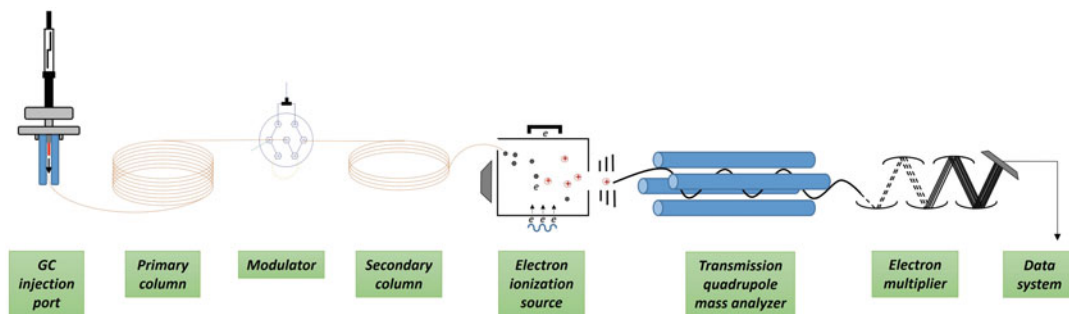


Fig. 2 Schematic diagram of an SPME-GC \times GC-QMS analysis. Analytes are thermally desorbed from the SPME fiber into the heated **GC injection port**, then carrier gas sweeps them to the **primary column**. After ^1D separation, a differential flow **modulator** continuously collects all the effluent from ^1D and periodically transfers it to the **secondary column** as sharp bands for additional separation. ^2D effluent is then transferred to the hyphenated QMS equipment where a collimated beam of electrons interacts with analyte molecules to produce ions into the **ionization source**. Produced ions are repelled from the ionization chamber towards the **transmission quadrupole mass analyzer**, which mass filter the ions. The ions with stable trajectories are transmitted through the quadrupole filter to the detector, an **electron multiplier**, which amplifies the signal through a “cascading effect” until **data system** collects it

is shown diagrammatically in Fig. 2. A splitless liner with internal diameter of $0.75\ \mu\text{m}$ was used in the GC injector port. An INSIGHT flow modulator (SepSolve Analytical—Waterloo, CA) performed the differential flow modulation in reverse fill/flush configuration. Helium was used as carrier and auxiliary gas. A $20\ \text{m} \times 0.18\ \text{mm-i.d.}$ ($d_f\ 0.25\ \mu\text{m}$) poly(dimethylsiloxane) column was used as ^1D , and a $5\ \text{m} \times 0.25\ \text{mm-i.d.}$ ($d_f\ 0.25\ \mu\text{m}$) poly(dimethyl-diphenylsiloxane) with 50% diphenylsiloxane monomer incorporation column was used as ^2D . Both columns were pre-conditioned according to the manufacturer’s instructions before analysis. A $2.5\ \text{m} \times 0.10\ \text{mm-i.d.}$ deactivated fused silica capillary tubing was used as restrictor for the modulator. Electron ionization ($70\ \text{eV}$) was used as the ionization method in all experiments.

- GC Image software (Zoex Corporation, Houston, TX, USA) was used for peak integration. NIST14 library was used for the putative identification of compounds.

3 Methods

3.1 HS-SPME Procedure for Coffee Analysis

- Open the coffee capsule and immediately weigh 1.5 g of it in a 20 mL vial. Close sample vial with a proper magnetic cap containing a septum, which will be pierced by the SPME needle. Avoid overtightening the cap to prevent damaging the SPME needle and fiber during septum piercing. **Notes 1**

and 2 should be consulted for general considerations about sample amount, vial size, and closure.

2. If using an automatic sampler such as Triplus RSH, place the sample vials at the corresponding positions in sampler trail according to GC sequence and start the sequence. If manually performing the HS-SPME procedure, perform the next steps.
3. Place sample vial in a heated block held at 60 °C under agitation at 250 rpm for 5 min to perform pre-equilibration.
4. Pierce through the septum with the SPME needle.
5. Fasten the SPME holder in a proper support, placing the SPME needle as close possible to the top of the vial. The benefits of correct positioning of fiber in vial may be found in **Note 3**.
6. Expose the DVB/CAR/PDMS fiber to the sample's HS for 40 min. Note that sample vial must be kept at the same conditions of pre-equilibration, i.e., 60 °C and 250 rpm. Some general considerations about coating, agitation speed, time, and temperature selection are present in **Notes 4–6**. Additionally, **Notes 7–9** present matrix-related orientations for method development.
7. Retract the fiber to the needle, remove the SPME device from the vial, and immediately introduce it into the GC port.
8. Expose the fiber inside the GC inlet and start the GC method.
9. Leave the fiber exposed in the injector during 5 min for sampling and conditioning, then retrieve it to its needle. Remove the SPME device. **Note 10** exposes some considerations about fiber conditioning between runs.

3.2 HS-SPME Procedure for Hop Analysis

1. Grind hop samples, some considerations are found in **Notes 7 and 8**.
2. Weigh 300 mg of hop in a 20 mL vial. Close sample vial with a proper cap containing a septum, which the SPME needle will pierce.
3. Place sample vial in a heated block held at 51 °C under agitation at 250 rpm for 5 min to perform pre-equilibration. Extraction temperature was optimized through design of experiment (DoE).
4. Pierce through the cap septum with the SPME needle.
5. Fasten the SPME holder in a proper support, placing the SPME needle as close as possible to the top of the vial. The benefits of correct positioning of fiber in vial may be found in **Note 3**.
6. Expose the DVB/CAR/PDMS fiber in sample's HS for 31 min. Note that sample vial must be kept at the same

conditions of pre-equilibration, i.e., 51 °C and 250 rpm. Extraction time was optimized through DoE.

7. Retract the fiber to the needle, remove the SPME device, and immediately introduce it into the GC port.
8. Expose the fiber inside the GC inlet and start the GC method.
9. Leave the fiber exposed in the injector during 5 min for sampling and conditioning, then retrieve it to its needle. Remove SPME device. **Note 6** exposes some considerations about fiber conditioning between runs.

3.3 GC × GC-QMS Method

1. Install a 20 m × 0.18 mm-i.d. (d_f 0.18 μm) poly(dimethylsiloxane) column as ^1D column, and a 5 m × 0.25 mm-i.d. (d_f 0.25 μm) poly(dimethyl-diphenylsiloxane) with 50% diphenyl monomer incorporation column as the ^2D column. Make sure both columns were conditioned and check for gas leaks (injector, modulator, transfer line nut) before analysis.
2. It must be noted that in these studies, an automatic sampler was used (Table 1). Since the automatic sampler has a proper module for fiber conditioning, *see Note 10* for adjustment of carrier gas conditions, if such step will be performed at GC injection port. Set the FM-GC×GC-QMS parameters according to Table 2. Considerations for GC×GC-QMS method optimization may be found in **Notes 11–18**.
3. Set the sequence table at the GC software according to the order of sample analysis.
4. After assuring all sample vials are in the correct order in the sampler tray, start the FM-GC×GC-QMS sequence.

3.4 Data Processing

1. Perform automatic peak integration at the GC Image software in the chromatograms setting the detection parameters according to Table 3. *See Note 19* for peak integration considerations.
2. Generate a peak table with all relevant information of each peak, such as retention times and indices, as well as peak volume.
3. Identify the analytes of interest based on mass spectra similarity match with database libraries such as NIST and similarity indices. The Wiley library is very interesting for food analysis. Figure 3 showcases a GC×GC chromatogram obtained from hop analysis with 25 analytes chosen to be identified. Table 4 presents the putative identification of such analytes. **Note 20** lists some considerations on analyte identification.

3.5 DoE: Central Composite Design

1. Consider the factors that need to be optimized, e.g., extraction temperature and time for hop analysis.

Table 1
HS-SPME conditions performed by Triplus RSH Autosampler

Pre-equilibration	Time/min	5
	Temperature/°C	60 (C); 51 (H)
Equilibration	Time/min	40 (C); 31 (H)
	Temperature/°C	60 (C); 51 (H)
Agitation	Mode	ON (10s)/OFF (10s)
	Speed/rpm	250
Sampling/desorption	Time/min	3
	Temperature/°C	240 (GC inlet)
Fiber conditioning	Time/min	3
	Temperature/°C	200

(C) must be used for coffee analysis

(H) must be used for hop analysis

Table 2
GC×GC-QMS parameters optimized for coffee and hop samples

GC×GC parameters	Injector	Mode	Splitless
		Temperature/°C	240
	Carrier gas	Type	Helium 5.0
		Flow/mL min ⁻¹	0.4 (constant flow)
	Auxiliary gas	Type	Helium 5.0
		Flow programming	9.2 mL min ⁻¹ (1 min) then increase to 11.5 mL min ⁻¹ at 10 mL min ²
	Modulation period	Total/s	6
		Flush/ms	400
	Oven	Temperature programming	35 °C (3 min) then increase to 208 (C)/228 (H) °C at 4 °C min ²
QMS parameters	Transfer line	Temperature/°C	240
	Ion source	Type	EI
		Ionization energy/eV	70
		Temperature/°C	220
	Quadrupole	Mode	Full MS
		Mass range/ <i>m/z</i>	50–322
Acquisition rate/Hz		40	

(C) must be used for coffee analysis

(H) must be used for hop analysis

- Set the range of each factor. For instance, extraction temperature ranging from 35 to 60 °C and extraction time from 15 to 45 min. Remarks are found in **Notes 21** and **22**.
- Prepare at least 11 samples to test combinations of extraction temperature and time. Table 5 presents the conditions in which

Table 3
Peak integration parameters used in the GC Image software

Smoothing	First column	0.2
	Second column	2.5
Peak filter	Minimum area	100
	Minimum value	100
	Minimum peak	100
	Minimum peak reference	Relative

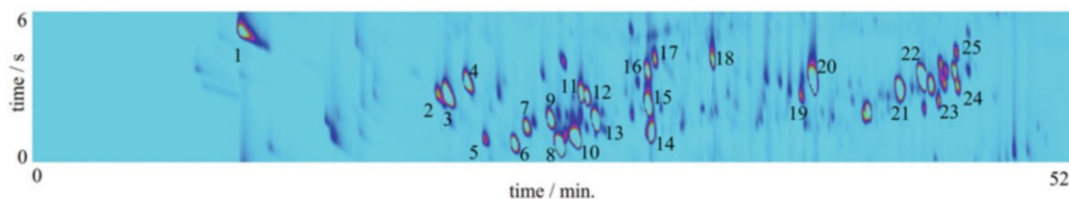


Fig. 3 GC×GC obtained from the extraction of hop volatiles in optimized conditions. 25 peaks along different parts of the chromatogram were selected to be putatively identified

each of the 11 hop samples were analyzed. It is statistical good practice to randomize the experiments, as shown in Table 5.

4. Generate a peak table for each sample and determine the total number of peaks and the sum of all peak volumes for each sample. These properties will be used as responses to the design of experiment and to calculate a desirability function. **Note 23** further explains the reason for using these parameters.
5. Use a proper fitting to model the response surface, such as the quadratic fitting used for hop analysis shown in Fig. 4. Ascertain that the model is statistically consistent using ANOVA.
6. Determine the maximum region in the surface to obtain the optimized conditions for the experiments. If the maximum region is not clear, it might be necessary to augment the model. An explanation on how to augment a CCD model is found in **Note 24**.

4 Notes

1. Vial size will influence the HS volume, which affects method robustness and reproducibility. Make sure to select an adequate vial size to perform your HS-SPME procedure. It must have enough space between the SPME fiber and the sample, avoiding problems such as splashing liquids (or solids) onto the fiber. A general recommendation is to leave one third of the vial

Table 4
Putative identification of 25 peaks in the optimized HS-SPME-GC×GC-QMS method

#	Analyte identity	M.F.	Similarity	LTPRI exp.	LTPRI lit.	CAS
1	3-methyl-1-butene-3-ol	C ₅ H ₁₀ O	908	639	614	115-18-4
2	Ethylbenzene	C ₈ H ₁₀	940	851	855	100-41-4
3	p-xylene	C ₈ H ₁₀	939	864	865	106-42-3
4	o-xylene	C ₈ H ₁₀	954	882	887	95-47-6
5	2-methylpropyl isobutyrate	C ₈ H ₁₆ O ₂	894	902	910	97-85-8
6	(R)- α -pinene	C ₁₀ H ₁₆	939	937	929	7785-70-8
7	Camphene	C ₁₀ H ₁₆	944	951	952	79-92-5
8	β -Myrcene	C ₁₀ H ₁₆	955	993	991	123-35-3
9	β -Pinene	C ₁₀ H ₁₆	915	979	979	127-91-3
10	2-methylbutyl isobutyrate	C ₉ H ₁₈ O ₂	928	1010	1016	2445-69-4
11	Methyl 4-methylenehexanoate	C ₈ H ₁₄ O ₂	797	1015	–	73,805-48-8
12	p-cymene	C ₁₀ H ₁₄	951	1022	–	99-87-6
13	Limonene	C ₁₀ H ₁₆	951	1032	1030	138-86-3
14	Pentyl 3-methylbutyrate	C ₁₀ H ₂₀ O ₂	924	1100	1110	25,415-62-7
15	Cyclohexane, 2-ethenyl-1,1-dimethyl-3-methylene	C ₁₁ H ₁₈	783	1095	–	95,452-08-7
16	4H-cyclopenta[c]furan, hexahydro-1,1-dimethyl-4-methylene	C ₁₀ H ₁₆ O	879	1095	–	344,294-72-0
17	(3S,4R,5R,6R)-4,5-bis(hydroxymethyl)-3,6-dimethylcyclohexene	C ₁₀ H ₁₈ O ₂	784	1105	–	–
18	Cis-3,7-dimethyl-2,6-octadienal	C ₁₀ H ₁₆ O	814	1180	1194	–
19	Methyl 4-decenoate	C ₁₁ H ₂₀ O ₂	919	1292	1289	1191-02-2
20	Methyl geranoate	C ₁₁ H ₁₈ O ₂	949	1312	1324	1189-09-9
21	Caryophyllene	C ₁₅ H ₂₄	950	1438	1419	87-44-5
22	Humulene	C ₁₅ H ₂₄	931	1472	1454	6753-98-6
23	(1S)-(-)- β -pinene	C ₁₀ H ₁₆	896	1497	–	18,172-67-3
24	Cadinene	C ₁₅ H ₂₄	936	1525	1524	16,729-01-4
25	(1S)-cis-calamenene	C ₁₅ H ₂₂	914	1528	1531	483-77-2

Table 5
Experimental conditions and their coded values for CCD in a randomized order of experiments

Experiment	Extraction time	Extraction temperature	Coded time	Coded temperature
1	9	48	$-\sqrt{2}$	0
2	51	48	$+\sqrt{2}$	0
3	45	60	+1	+1
4	30	48	0	0
5	15	35	-1	-1
6	30	65	0	$+\sqrt{2}$
7	30	48	0	0
8	45	35	+1	-1
9	30	48	0	0
10	30	30	0	$-\sqrt{2}$
11	15	60	-1	+1

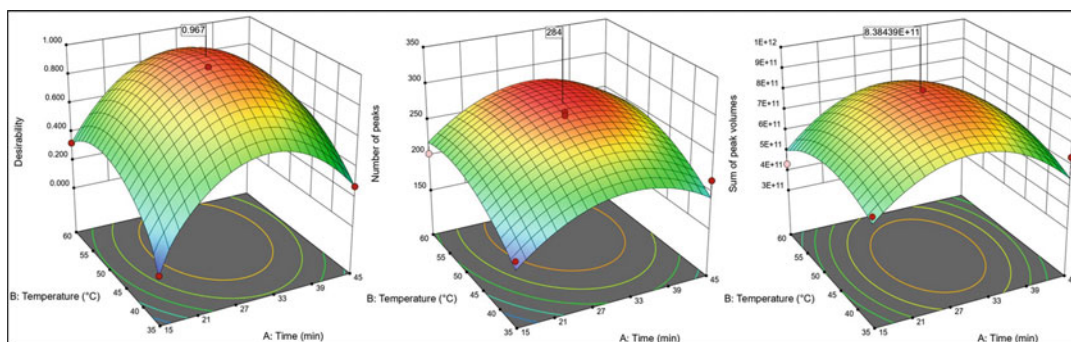


Fig. 4 Quadratic surface areas obtained from CCD model for desirability function, total number of peaks, and sum of peak volumes. Red circles represent experimental data above surface and pink circles the experimental data below the surface. Optimized conditions are flagged with the optimized value shown for each of the surfaces

volume for the HS. Use high-quality glass vials to prevent unwanted analyte adsorption to the inner surfaces.

- Sample volume or weight must be optimized since it directly affects method's sensitivity. Avoid using large amounts of sample to leave enough space between sample and SPME fiber. Lower sample volume may also be beneficial to prevent column overloading leading to the occurrence of broad and unsymmetrical peaks. For instance, using more than 300 mg of hop resulted in broad peaks in the chromatograms, hindering good GC \times GC resolution.

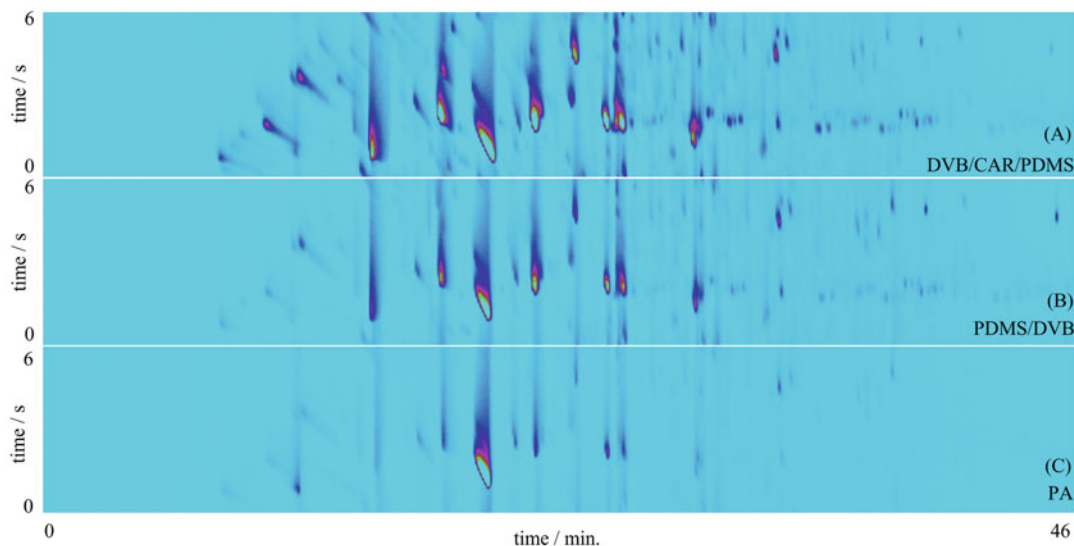


Fig. 5 Comparison of VOCs extraction profile obtained with DVB/CAR/PDMS fiber (a), DVB/PDMS fiber (b), and PA fiber (c). Note that the chromatogram obtained by the DVB/CAR/PDMS fiber has more detected peaks than the others

3. Making sure the fiber is close to the top of the vial ensures its exposition in a colder region. Such procedure avoids the decrease in the distribution constant of the analytes between the HS and the fiber, which affects the extraction capacity.
4. Fiber selection is one of the most important parameters affecting extraction, thus coating evaluation must be performed. For instance, for untargeted methods, mixed-phases such as the DVB/CAR/PDMS are indicated because of the wide range of compounds that may be extracted. Indeed, Fig. 5 shows the chromatograms obtained for the extraction of VOCs from coffee with different SPME fibers. The DVB/CAR/PDMS phase allowed the detection of a higher number of compounds when compared with PDMS/DVB and PA.
5. Sample agitation ensures a higher mass transfer of the analytes to the headspace; thus, it must be assured that agitation is kept constant during all experiments to achieve adequate repeatability. Avoid using fast velocities to prevent sample splashing in the vial walls and in the SPME fiber. Additionally, the agitation performed by vortexing the entire vial is preferred in comparison to magnetic stirring since it allows a simultaneous motion of both the liquid and HS phases within the vial, leading to a superior performance.
6. Time and temperature have important roles in HS experiments, and both must be optimized. Higher temperatures ensure higher extraction kinetics of most analytes. However, it must

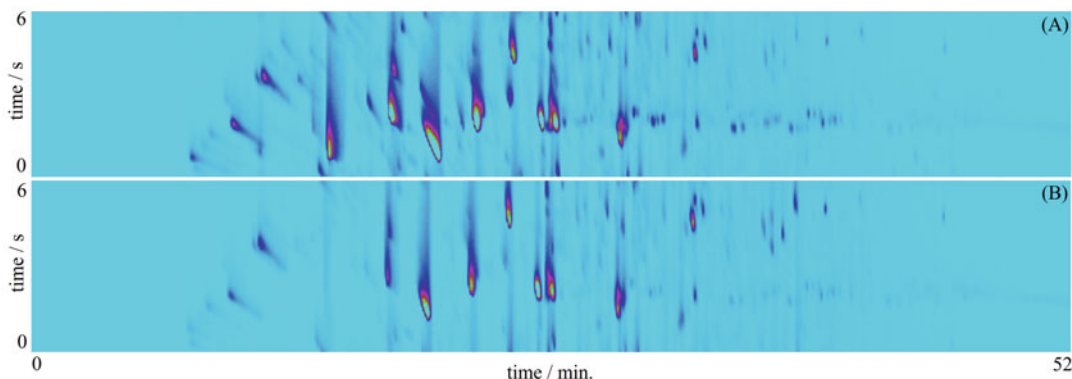


Fig. 6 Comparison of VOCs extraction profile obtained by the analysis of 1.5 g of pure coffee sample (a), and a solution containing 1.5 g of coffee sample in 10 mL of salinized water (NaCl, 30% w/w) (b)

be noted that elevated temperatures also decrease fiber's extraction capacity. Using mild temperatures may help to avoid such problem. Lower temperatures may require longer extraction times to reach adequate method sensitivity.

7. For solid samples such as hops, fruits, cheese, and others, a homogenization procedure such as grinding may be performed previously to extraction. It increases the superficial area of the sample, assisting with the overall mass transfer.
8. Sample matrix also has to be considered during method development. For instance, solid samples may be directly analyzed by HS-SPME or they can also be previously homogenized with water. If a homogenization step is desired and performed in sample vial, make sure to carefully increase the agitation speed to avoid splashing sample in the vessel walls and cap septum. Such procedure avoids fiber contamination during septum piercing. However, it must be noted that water homogenization step is not always beneficial for analysis. For instance, the VOCs profile obtained with pure coffee (Fig. 6a) has a higher number of compounds than the sample homogenized with salinized water (Fig. 6b).
9. To increase ionic strength, salt may be added to an aqueous sample as a solution or as a solid. The salt added must be fully solubilized and well homogenized for better efficiency. Salt addition improves method's sensitivity in most applications. For instance, we can see an enhancement in the VOCs extraction profile for a coffee sample when 10 mL of aqueous NaCl (30% w/w) is added to the sample (Fig. 7), in comparison to the addition of 10 mL of distilled water. Also, the peak volume of ten selected VOCs is shown in Fig. 8 for a coffee aqueous solution with and without salt addition. The peak volume achieved for most compounds were higher with salt addition.

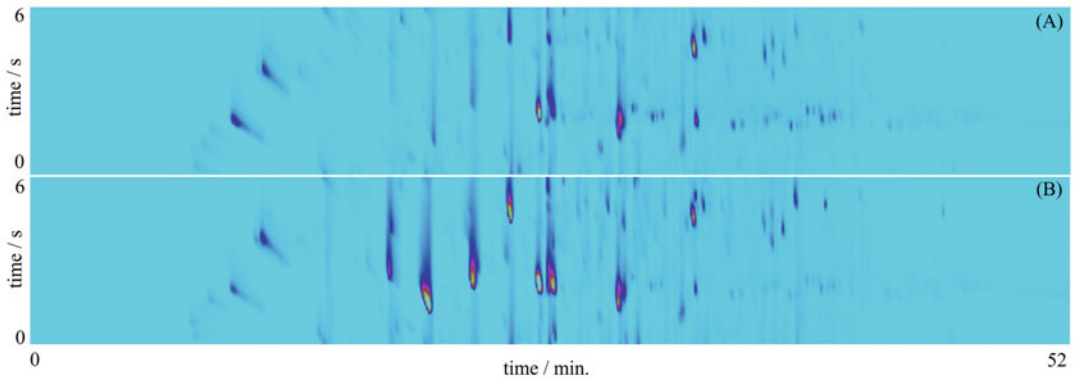


Fig. 7 The salting out effect may be seen on the VOCs profile obtained when comparing a coffee (1.5 g) + 10 mL water solution (a), and a coffee (1.5 g) + 10 mL of aqueous NaCl (30% w/w) solution (b). Observe the gain in peak intensity for almost all detected peaks

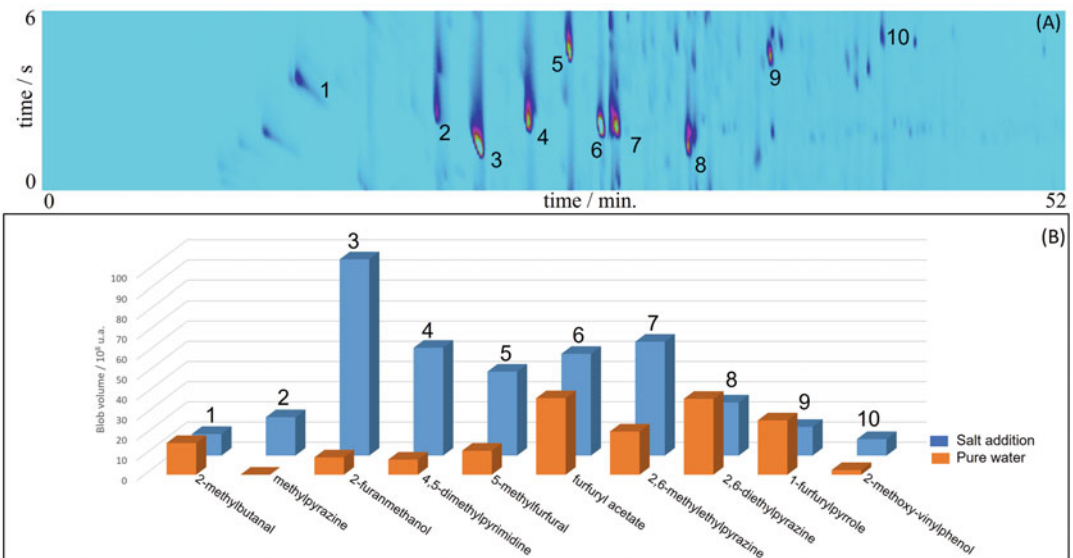


Fig. 8 Selected analytes used for comparison of salting out effect (a) and resulting peak volumes obtained for an aqueous solution of coffee with and without salt addition (b)

However, this step must be carefully evaluated and optimized during method development. For instance, even with salt addition, the analysis of pure coffee exhibits higher extraction efficiency for most compounds than the coffee solution analysis as seen in Fig. 6.

10. Fiber conditioning between analytical runs is a good practice to avoid carry-over effects. In many automatic samplers, such as

Triplus, a conditioning module is integrated to the system to perform such step. Table 1 exhibits such conditions for the automatic sampler. Alternatively, if there is no available module, the GC injection port may be used for fiber conditioning after adjusting carrier gas flow and mode. For such, set GC's splitless time for the sampling period (2 min) and set a split ratio of 100:1. Leave the fiber at the injection port for 3 min after sampling period.

11. It is also important to optimize the GC×GC separation in order to achieve the best chromatographic resolution. For instance, the temperatures used in the method were determined after a few initial test runs. Initially, the GC oven program would start at 40 °C for 3 min and heated to 280 °C at 6 °C min⁻¹. The lower initial temperature allowed for peak focusing. It was also noticed that there were no peaks detected after 208 and 228 °C for coffee and hops samples, respectively. So, the final oven temperatures were lowered accordingly to reduce analysis time. Finally, the heating rate was changed from 6 to 4 °C min⁻¹ to increase peak resolution in ¹D column.
12. Constant flow rates in the auxiliary gas are in general successful to obtain good GC×GC chromatograms, but they can be improved with minor changes. For instance, flow programming used here guarantees a constant flow throughout most of the chromatographic run. Only the first few seconds have a higher primary flow rate. Even though it is brief, this short ramp allowed for a more efficient analyte desorption from the fiber. With a lower flow rate in the auxiliary gas in the beginning of the chromatographic run, the ¹D carrier gas flows at a higher linear velocity and efficiently sweeps the desorbed analytes from injection port to the column. For this tip, the final auxiliary gas flow rate should not be increased by more than 40% of its initial flow rate, or else there could be a loss in the efficiency of ¹D separation.
13. Modulation period (MP) also need to be optimized beforehand. For both coffee and hop samples, it was found that MPs of 6 s were preferred over 4 s. With two or three tests runs it should be possible to notice which MP conditions will be better suited for sample analysis. If there is noticeable wrapping around, MPs should be increased. However, if there are large areas in the upper side of the chromatograms devoid of peaks, the MP may probably be decreased.
14. Column combination may also be optimized to achieve better resolution. Different column selectivity can be explored, but always assure to employ columns with distinct separation

mechanisms in ^1D and ^2D . The classic column combination used in GC \times GC analysis employs a non-polar \times semipolar set. Recommended column geometries for the primary and secondary columns are 20 m \times 0.18 mm-id and 5 m \times 0.25 mm-id, respectively. A minimum phase ratio (β) of 250 is recommended for general purposes.

15. Transfer line to MS must be held at temperatures equal to the final GC oven temperature to avoid band broadening in the MS transfer line. Higher temperatures are unnecessary and may lead to high baseline due to column bleed.
16. The ionization energy of 70 eV is conventionally used in qualitative analysis, which enables the use of mass spectral databases, such as NIST, FFNSC, and Wiley.
17. Acquisition rate is an important parameter that must assure that a sufficient number of points are acquired for each chromatographic peak. An average of 15–20 points per peak is recommended, thus the average peak width must be considered to adjust the proper acquisition rate. The average peak width for 1D-GC is 6 s, thus acquisition rates of 5 Hz are enough. For GC \times GC, modulated peaks have average width of 400 ms, thus high acquisition rates (e.g., ≥ 25 Hz) are necessary.
18. Make sure to select a proper mass range based on analytes present in sample. An adequate mass range should include an interval that assures the detection of all VOCs extracted. When using the QMS, do not use excessively large mass intervals to avoid jeopardizing method's sensitivity.
19. Peak integration parameters must be optimized tentatively according to the chromatograms obtained, assuring that all peaks were integrated and that no undesired regions such as baseline or column bleed were considered as responses. Alternatively, such step may be manually performed, but make sure to try to use the same integration parameters in all chromatograms.
20. To improve analyte identification in GC-MS and GC \times GC-MS analysis, the use of linear temperature-programmed retention index (LTPRI, Eq. 1) is highly recommended whenever possible. For an SPME method, this could be obtained adding 8 μL of C₈-C₂₀ n-alkane standard solution in a 20 mL vial and performing an SPME extraction with the same procedure used for the samples. The LTPRI considers the retention time of the analyte, as well as the retention times of the closest *n*-alkane that comes after and also before the analyte. So far, the LTPRI value is calculated only for the retention in the ^1D . In

FM-GC×GC, LTPRI filtering has a higher tolerance window than 1D-GC.

$$\text{LTPRI} = 100n + 100 \left(\frac{t_{R,a} - t_{R,n}}{t_{R,n+1} - t_{R,n}} \right) \quad (1)$$

where n is the number of carbons in the closest alkane standard before the analyte, $t_{R,a}$ the retention time of the analyte, $t_{R,n}$ the retention time of the closest n -alkane before the analyte, and $t_{R,n+1}$ the retention time of the closest n -alkane after the analyte.

21. The range used for a factor in a DoE should be carefully thought out. The lower and higher values should not be too close to exhibit a real difference, but it should not be too far apart from each other. For instance, in terms of temperature, it may not be useful to test a lower value of 50 °C and a higher value of 55 °C, as both would probably have chromatograms that are too similar to each other. Also, chemical reactions (e.g., Maillard reactions) might occur at temperatures higher than 60 °C and, as such, the identified analytes may be a by-product of these reactions, rather than actually being an analyte found in the sample [11]. Regarding the extraction time, one should consider the equilibrium between the SPME fiber and the headspace just as well as the total time needed for the analysis. Considering that the chromatograms are usually the slowest process in an analysis, the extraction time should try to be faster than that, so it does not become the bottleneck of the method.
22. Design of experiments' factors are coded in a useful pattern to standardize them. In a 2 factor central composite design (CCD), the low value is coded as -1 and the high value as $+1$, midrange (center) value is coded as 0 . For hop analysis, an extraction temperature of 35 °C was coded as low and 60 °C was coded as high. In relation to extraction time, 15 min was coded as low and 45 min as high. Four experiments use all the coded different combinations. The error is estimated by the central point at 48 °C and 30 min, in which three replicates are performed. The last four experiments are performed applying the central condition in one factor and an axial value in the other factor. High axial value is coded as $\sqrt{2}$, while low axial value is $-\sqrt{2}$. Table 5 exhibits all the levels investigated.
23. For an untargeted approach, the total number of peaks in a chromatogram can attest to a wider range of compounds attained in an extraction though many of them might be at trace levels with signal-to-noise ratio that makes it difficult to

identify them. At the same time, increasing the sum of all peak volumes in a chromatogram is an interesting way to favor broader peaks, which are easier to identify later on. However, this approach may favor the extraction of major constituents instead, decreasing the overall number of peaks detected by the HS-SPME method. The best approach is to combine both concepts using a desirability function, which creates a 0 to 1 scale in which the highest value relates to a higher number of peaks and a higher sum of peak volumes at the same time.

24. As the aim of CCD is to find the maximum region for a given response, sometimes higher response value may not be found in the central point. However, there is no guarantee that a non-central region with a higher response is in fact the maximum region, it might just be nearer to it than the rest of the experiments performed. In such cases, it is recommended to augment the CCD and perform a set of new experiments in which the previous best response would be the center to a new CCD. The experiments already performed is carried over to the new model, which decreases the number of new experiments needed. Upon doing the new experiments, a new surface is modeled to find out if the conditions tested are already in the optimal region or if there is a need to further augment the DoE. Usually, the need for augmenting the CCD is related to the initial factors' values used. Thus, working with familiar matrices can help in choosing better initial values, whereas it is common to need to augment the model with unfamiliar samples.

References

1. Arthur CL, Pawliszyn J (1990) Solid phase microextraction with thermal desorption using fused silica optical fibers. *Anal Chem* 62:2145–2148. <https://doi.org/10.1021/ac00218a019>
2. Paiva AC, Crucello J, de Aguiar Porto N, Hantao LW (2021) Fundamentals of and recent advances in sorbent-based headspace extractions. *TrAC Trends Anal Chem* 139:116252. <https://doi.org/10.1016/j.trac.2021.116252>
3. Verzera A, Conduro C (2012) Sampling techniques for the determination of the volatile fraction of honey. In: Pawliszyn J (ed) *Comprehensive sampling and sample preparation*. Elsevier Inc., Amsterdam, pp 92–97
4. McNair HM, Miller JM (2009) *Basic gas chromatography*. Wiley, New York
5. Seeley JV, Seeley SK (2013) Multidimensional gas chromatography: fundamental advances and new applications. *Anal Chem* 85: 557–578. <https://doi.org/10.1021/ac303195u>
6. Dimandja J-MD (2020) Introduction and historical background: the “inside” story of comprehensive two-dimensional gas chromatography. In: *Separation science and technology*. Elsevier, New York, pp 1–40
7. Edwards M, Mostafa A, Górecki T (2011) Modulation in comprehensive two-dimensional gas chromatography: 20 years of innovation. *Anal Bioanal Chem*

- 401:2335–2349. <https://doi.org/10.1007/s00216-011-5100-6>
8. Tranchida PQ, Purcaro G, Dugo P et al (2011) Modulators for comprehensive two-dimensional gas chromatography. *TrAC Trends Anal Chem* 30:1437–1461. <https://doi.org/10.1016/j.trac.2011.06.010>
 9. Chow H-YJ, Górecki T (2017) Temperature programming of the second dimension in comprehensive two-dimensional gas chromatography. *Anal Chem* 89:8207–8211. <https://doi.org/10.1021/acs.analchem.7b02134>
 10. Seeley JV, Micyus NJ, McCurry JD, Seeley SK (2006) Comprehensive two-dimensional gas chromatography with a simple fluid modulator. *Am Lab* 38:24–26
 11. Rivellino SR, Hantao LW, Risticovic S et al (2013) Detection of extraction artifacts in the analysis of honey volatiles using comprehensive two-dimensional gas chromatography. *Food Chem* 141:1828–1833. <https://doi.org/10.1016/j.foodchem.2013.05.003>
 12. Paiva AC (2020) Caracterização de cervejas utilizando a GC×GC-MS e análise multivariada de dados. Master's thesis. University of Campinas



Identification of Lactic Acid Bacteria in Food Matrices by High-Resolution Nano-LC-ESI MS/MS

Mariangela Valletta, Angela Chambery, and Rosita Russo

Abstract

Over the past decades, a dietary supplement with probiotic foods represents a growing trend among consumers for their benefits on human health. Fermented dairy products have been extensively studied as functional foods given their enrichment with probiotic bacteria. Among these, lactic acid bacteria (LAB) significantly contribute to the flavor, texture, nutritional value, and microbial safety of fermented foods and are widely employed in the food industry. Efficient identification methods are needed for monitoring and controlling lactic acid bacteria in food production. Recently, due to the high sensitivity and specificity, MS-based approaches proved to be an attractive alternative to traditional techniques for bacteria detection/identification. This chapter describes a straightforward protocol based on high-resolution (HR) nano-LC-ESI MS/MS for the reliable, sensitive, and selective identification of LAB species in food matrices. Crucial issues related to bacteria culture conditions, sample preparation, and mass spectrometry analysis are discussed. Furthermore, an overview of computational tools for data analysis is also presented.

Key words High-resolution mass spectrometry, Lactic acid bacteria, Peptide marker, Ribosomal proteins, Food

1 Introduction

In recent years, international organizations such as Food and Agriculture Organization (FAO) and World Health Organization (WHO) are increasingly promoting functional foods containing probiotic microorganisms for their health and nutritional benefits such as improved nutritional value and contribution to the overall flavor and texture of foods [1]. Lactic acid bacteria (LAB) are among the most important probiotic microorganisms endowed with strain-dependent probiotic features on the immune system and gastrointestinal tract such as the control of intestinal infections and the improved digestion of lactose [2]. Probiotic LAB are usually employed in the food industry and as starter cultures in the production of fermented dairy products such as cheese and yogurts [3, 4]. Despite the knowledge of LAB composition is of

high relevance for several industrial and biotechnological applications, the comprehensive identification of LAB species in food matrices can be technically challenging. DNA-based molecular methodologies targeting the 16S ribosomal RNA (rRNA) are complementary to those relying on classical morphological and phenotypic characterization of bacterial species. Indeed, 16S rRNA genes have become the gold standard for bacteria phylogenetic typing or identification since they contain both conserved and variable sequence regions that can be used as molecular signatures of species [5, 6]. Several PCR-based DNA fingerprinting methods have been extensively applied for the identification of LAB isolated from different food matrices [7].

More recently, the availability of more sensitive and specific MS technologies allowed the development of protein-based approaches for bacteria detection/identification with potential application in diverse research fields [8–10]. A large body of literature reports the application of gas chromatography-mass spectrometry (GC-MS) to the characterization of the bioactive compounds and the volatile profiles of fermented foods containing probiotic LAB [11–20]. Matrix-assisted laser desorption/ionization time-of-flight mass spectrometry (MALDI-TOF MS) has also emerged as a reliable technology to analyze complex mixtures of proteins isolated from microorganisms or even intact bacteria cells. Moreover, MALDI-TOF-based strategies provide advantages related to sample preparation, rapid acquisition times, accuracy, and reproducibility. Thus, this technology has been widely used for bacteria protein profiling, allowing the detection of microorganisms and their classification at the genus, species and, sometimes, at the subspecies level. Many MALDI-TOF MS-based approaches have been developed for the rapid classification and identification of lactic acid bacteria within complex food matrices (Table 1). Moreover, the unparalleled sensitivity and resolving power of high-resolution mass spectrometers also allowed the development of tandem MS methodologies for the characterization of microorganisms [21–26], including applications for the identification of LAB proteins and peptides within fermented food matrices (Table 1). Although LC-ESI MS/MS bacterial profiling has been mainly proposed for clinical applications finalized to identify common pathogenic bacteria [27, 28], a tandem MS methodology for the characterization and the molecular profiling of LAB species has also been reported [29].

This chapter describes an experimental workflow for LAB identification by high-resolution tandem MS analysis of tryptic peptides from the enriched ribosomal proteins fraction. Critical issues related to bacteria culture conditions, ribosomal protein extraction, and nano-LC-MS-based analysis are discussed. Finally, an overview of the bioinformatics tools for data analysis is also presented.

Table 1
Studies published in the last 10 years reporting applications of MALDI-TOF and LC-ESI-based mass spectrometry to lactic acid bacteria identification within food matrices

MS technique	Food matrix	Aim of the analysis	Target of the analysis	Software/DB	LAB genus	Reference
MALDI-TOF	Cheese	LAB identification	Extracted proteins	BioNumerics	Lactobacillus, Lactococcus, Leuconostoc, Pediococcus, Enterococcus	[30]
MALDI-TOF	Fermented seafood	LAB identification	Isolated colonies	Flexcontrol, MALDI Biotyper	Enterococcus, Tetragenococcus, Pediococcus, Lactobacillus, Staphylococcus, Leuconostoc	[31]
MALDI-TOF	Fermentation starter	LAB identification	Isolated colonies	Flexcontrol, MALDI Biotyper	Lactobacillus, Pediococcus	[32]
MALDI-TOF	Milk	LAB identification	Isolated colonies	MALDI Biotyper	Lactobacillus, Pediococcus	[33]
MALDI-TOF	Cheese	LAB identification	Isolated colonies	MALDI Biotyper	Lactobacillus, Enterococcus, Leuconostoc	[34]
MALDI-TOF	Fermented foods	LAB identification	Isolated colonies	MALDI Biotyper	Pediococcus	[35]
MALDI-TOF	Fermented foods	Weisella identification	Isolated colonies	MALDI Biotyper, in house database	Weisella	[36]
MALDI-TOF	Yogurt	LAB identification	Isolated colonies	MALDI Biotyper	Enterococcus, Lactobacillus	[37]
MALDI-TOF	Dairy foods	LAB identification	Isolated colonies	MALDI Biotyper, in house database	Lactobacillus, Enterococcus, Lactococcus, Leuconostoc, Streptococcus	[38]
MALDI-TOF	Fruit pulp	LAB identification	Extracted proteins	MALDI Biotyper	Lactobacillus	[39]
MALDI-TOF	Fermented foods	LAB identification	Ribosomal proteins	BioNumerics	Lactobacillus.	[40]
LC-MS/MS	Dairy products	Identification of antibacterial proteins	Extracted proteins	Mascot	Lactobacillus, Pediococcus	[41]

(continued)

Table 1
(continued)

MS technique	Food matrix	Aim of the analysis	Target of the analysis	Software/DB	LAB genus	Reference
LC-MS	Sour cream	Identification of antifungal peptides	Extracted proteins	Compass Data Analysis, MatLab	Lactobacillus	[42]
LC-MS/ MS	Wine	Identification of bacteriocins	Extracted proteins	Proteome Discoverer	Enterococcus	[43]
LC-MS/ MS	Probiotic preparations	Quantitative analysis of bacteriocins	Extracted proteins	Proteome Discoverer	Lactobacillus	[44]
LC-MS/ MS	Fermented foods	Proteomic characterization	Extracted proteins	Mascot	Lactobacillus	[45]
LC-MS/ MS	Cheese	Quantitative analysis of bacterial enzymes	Secreted proteins	Mascot	Streptococcus, Lactobacillus	[46]

2 Materials

Prepare all solutions by using ultrapure water and analytical grade reagents. Fresh liquid media or autoclaved liquid media can be stored at room temperature until use (several weeks).

2.1 Bacterial Cell Cultures

1. De Man, Rogosa, and Sharpe (MRS) medium suitable for microbiology (Condalab, Cat. #1555).
2. ESTY medium suitable for microbiology (Condalab, Cat. #1043).
3. Incubator maintained at 30 °C or 37 °C.
4. Sterile culture flasks.

2.2 Protein Extraction, Precipitation, and Quantification

1. Formic acid (FA) for LC-MS.
2. 70% FA in water.
3. Acetonitrile (CH₃CN) for LC-MS.
4. Ethanol (−20 °C).
5. 50 mM NH₄HCO₃ pH 7.8 (394 mg of NH₄HCO₃ in 100 mL of H₂O).
6. Bio-Rad Protein Assay Dye Reagent (Cat. #5000006) or Pierce™ BCA Protein Assay Kit (Cat. #23225).

7. 250 mL polypropylene centrifuge tubes.
8. Vortex.
9. SpeedVac concentrator.

2.3 Reduction, Alkylation, and Tryptic Digestion

1. 100 mM 1,4-Dithio-DL-threitol (DTT, 15.4 mg of DTT in 1 mL of H₂O).
2. Water bath incubator maintained at 55 °C or 37 °C.
3. 300 mM Iodoacetamide (IAM, 55.5 mg of IAM in 1 mL of H₂O; light sensitive).
4. Trypsin TPCK-treated from bovine pancreas (Sigma-Aldrich, Cat. #T1426).

2.4 LC-MS/MS Analysis

1. Thermo Fisher Scientific Q-Exactive Orbitrap mass spectrometer.
2. Thermo Fisher Scientific Dionex UltiMate 3000RSLC nanosystem.
3. Thermo Fisher Scientific PepMap™ 100 µCartridge column C18 (300 µm × 0.5 cm, 5 µm, 100 Å).
4. Thermo Fisher Scientific EASY-Spray analytical column (15 cm × 75 µm ID PepMap RSLC C18, 3 µm, 100 Å).
5. Solvent A: 0.1% formic acid, 99.9% water.
6. Solvent B: 0.1% formic acid, 99.9% CH₃CN.
7. Trifluoroacetic Acid (TFA), sequencing grade.
8. 2% TFA in water.
9. Thermo Fisher Scientific Xcalibur software v 3.1.

2.5 Data Analysis

1. Thermo Fisher Scientific Proteome Discoverer software v 2.4.
2. SEQUEST database search engine.

3 Methods

A pipeline of the workflow for the high-resolution nano-LC-ESI MS/MS analysis of lactic acid bacteria is reported in Fig. 1.

3.1 Bacterial Cell Culture

For proteins extraction, bacterial pellets can be obtained from direct centrifugation of food matrices or from bacteria cell cultures on suitable media (*see Note 1*). These preliminary steps are of utmost importance for a reliable analysis of lactic acid bacteria, whose growth is strongly influenced by culture media (*see Note 2*). The following procedure has been tested on exemplary strains of common genera of probiotic bacteria (i.e., *Streptococcus*

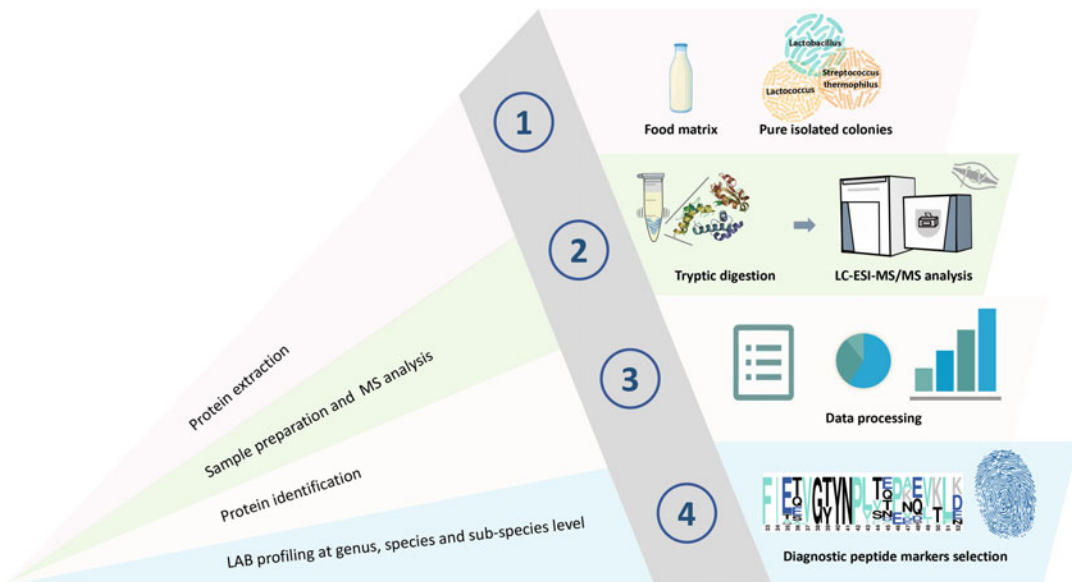


Fig. 1 Experimental workflow for the identification of lactic acid bacteria by high-resolution nano-LC-MS/MS. The procedure starts with the extraction of a protein fraction, highly enriched of ribosomal proteins, from bacterial pellets that can be obtained from direct centrifugation of food matrices or from pure colonies previously isolated from foods. Following sample preparation (i.e., reduction, alkylation, and tryptic digestion) and LC-MS analysis, a reliable profiling of LAB proteins is obtained by data processing. Finally, a further characterization of LAB at the genus, species, and subspecies levels can be performed by selecting and monitoring the presence of species-specific peptide markers of ribosomal proteins highly diagnostic for LAB species of interest

thermophilus, *Lactococcus lactis* subsp. *lactis*, *Lactococcus lactis* subsp. *cremoris*, and *Lactobacillus helveticus* and *Lactobacillus plantarum*).

1. From the agar plate, pick up one colony (in triplicate) of *L. plantarum* and *L. helveticus* and inoculate in 40 mL of MRS medium (see **Note 3**) at 30 °C and 37 °C, respectively, without shaking. Incubate for 12–24 h, until the stationary phase is reached.
2. From the agar plate, pick up one colony (in triplicate) of *L. lactis* subsp. and *S. thermophilus* and inoculate, without shaking, in ESTY medium (see **Note 4**) containing 1% lactose at 30 °C and 37 °C, respectively. Incubate for 12–24 h, until the stationary phase is reached.
3. Collect bacterial cells by centrifugation at $3500 \times g$ at 4 °C for 10 min.
4. Wash twice with 40 mL of Milli-Q water and store at –20 °C until protein extraction.

3.2 Extraction of Proteins from Bacterial Cells

1. Resuspend bacterial pellets in 200 μL of 70% formic acid (in water) by vortex-mixing.
2. Add 200 μL of pure acetonitrile and mix carefully by vortexing.
3. Centrifuge the samples at $10,000 \times g$ for 2 min and collect the supernatants in new Eppendorf tubes (*see Note 5*).
4. Pool the supernatants from the three replicates and dry under vacuum in a Savant SpeedVac concentrator.
5. Wash the protein pellet three times with 200 μL of Milli-Q water (*see Note 6*).
6. Reconstitute the protein pellet in 50 μL of Milli-Q water by vortex-mixing.
7. Precipitate the proteins with cold ethanol (1:9, v/v) for 30 min at -20°C .
8. Centrifuge samples at $10,000 \times g$ for 5 min and discard the supernatant.
9. Wash the protein pellet with 200 μL of cold ethanol.
10. Centrifuge samples at $10,000 \times g$ for 5 min and discard the supernatant.
11. Air-dry the protein pellets (*see Note 7*).
12. Reconstitute the protein pellet in 50 μL of 50 mM NH_4HCO_3 pH 7.8 (*see Note 8*).
13. Measure the protein concentration of each sample by Bradford or bicinchoninic acid (BCA) assays (*see Note 9*).

3.3 Disulfide Reduction/Alkylation and Tryptic Digestion

1. For disulfide bridges reduction, add DTT 10 mM (final concentration in 50 mM NH_4HCO_3 pH 7.8) to aliquots (50 μg) of extracted proteins (*see Note 10*).
2. Vortex samples and incubate the mixture for 1 h at 55°C .
3. For thiol alkylation (*see Note 11*), add 7.5 mM IAM (final concentration).
4. Vortex samples and incubate for 30 min at room temperature in the dark.
5. For trypsin digestion (*see Note 12*), add TPCK-treated trypsin to a final enzyme:substrate ratio of 1:50 (w/w) and incubate samples at 37°C overnight (*see Note 13*).
6. Following the incubation, centrifuge the samples at $15,000 \times g$ for 15 min and transfer the supernatants containing the tryptic peptides into new tubes (*see Note 14*).
7. For LC-MS/MS analysis, properly dilute samples in Solvent A or 2% TFA (*see Note 15*). Typically, 2 μg of the tryptic digest is a suitable amount that can be analyzed on a Q-Exactive instrument.

Table 2
Settings for the Ultimate 3000 UHPLC nanosystem (A) and the Q-Exactive Orbitrap mass spectrometer (B) for LC tandem mass spectrometry analysis of tryptic peptides derived from the LAB-enriched ribosomal protein fraction

A: LC conditions	
Flow rate (Trap column)	10 μ L/min
Column temperature	35 $^{\circ}$ C
Flow rate (Analytical column)	300 nL/min
Mobile phase	A = 0.1% formic acid in water B = 0.1% formic acid in acetonitrile
Gradient	Time, mins %B
	0.0 4
	53.0 22
	63.0 35
	68.0 90
	73.0 90
	88.0 4
Stop time	90.0 min
B: MS parameters	
Polarity	positive
Nano-spray source	
Spray voltage	1.9 kV
Capillary temperature	280 $^{\circ}$ C
Full MS	
Resolution	70,000
AGC target	3×10^6
Scan range	375–500 m/z
Maximum IT	100 ms
Top N	5
Spectrum data type	Profile

(continued)

Table 2
(continued)

B: MS parameters	
MS2	
Resolution	17,500
AGC target	1 * 10 ⁵
Maximum injection time	50 ms
Scan range	200–2000 <i>m/z</i>
Fragmentation method	HCD
Isolation width	2 <i>m/z</i>
Normalized collisional energy (NCE)	27
Spectrum data type	Centroid
Dynamic exclusion	15s

3.4 High-Resolution Nano-LC-Tandem Mass Spectrometry Analysis

Any tandem mass spectrometry platform may be used for the analysis of tryptic peptides obtained by the above procedures. Below, a data-dependent scheme for peptide identification optimized for the LC-MS/MS analysis on a Q-Exactive Orbitrap instrument equipped with an Ultimate 3000 UHPLC nanosystem from Thermo is described (*see Note 16*). A detailed description of the LC and MS parameters is reported in Table 2a and b, respectively (*see Note 17*).

3.5 Data Processing

Several software packages are available to process MS data for protein identification. Here, we describe in detail a workflow using Proteome Discoverer 2.4 software.

1. Open Proteome Discoverer 2.4 application and select “New Study/Analysis” on the start page.
2. Choose a name for the study and a root directory. Click “OK”.
3. Click “Add Files” and select the mass spectrometry raw files. Proteome Discoverer accepts .raw, .mgf, .mzData, .mzXML, and .mzML file formats as input files.
4. Open “New Analysis”, select and drag the input file from the “Input file” page to the “Analysis” window.
5. Select the “Workflows” tab to create workflows to use for the “Processing” and “Consensus” steps.
6. Create a Processing Workflow by dragging and connecting the following nodes into the tree window: “Spectrum Files”, “Sequest HT”, “Fixed Value PSM Validator” or “Target Decoy PSM Validator” nodes (Fig. 2a).

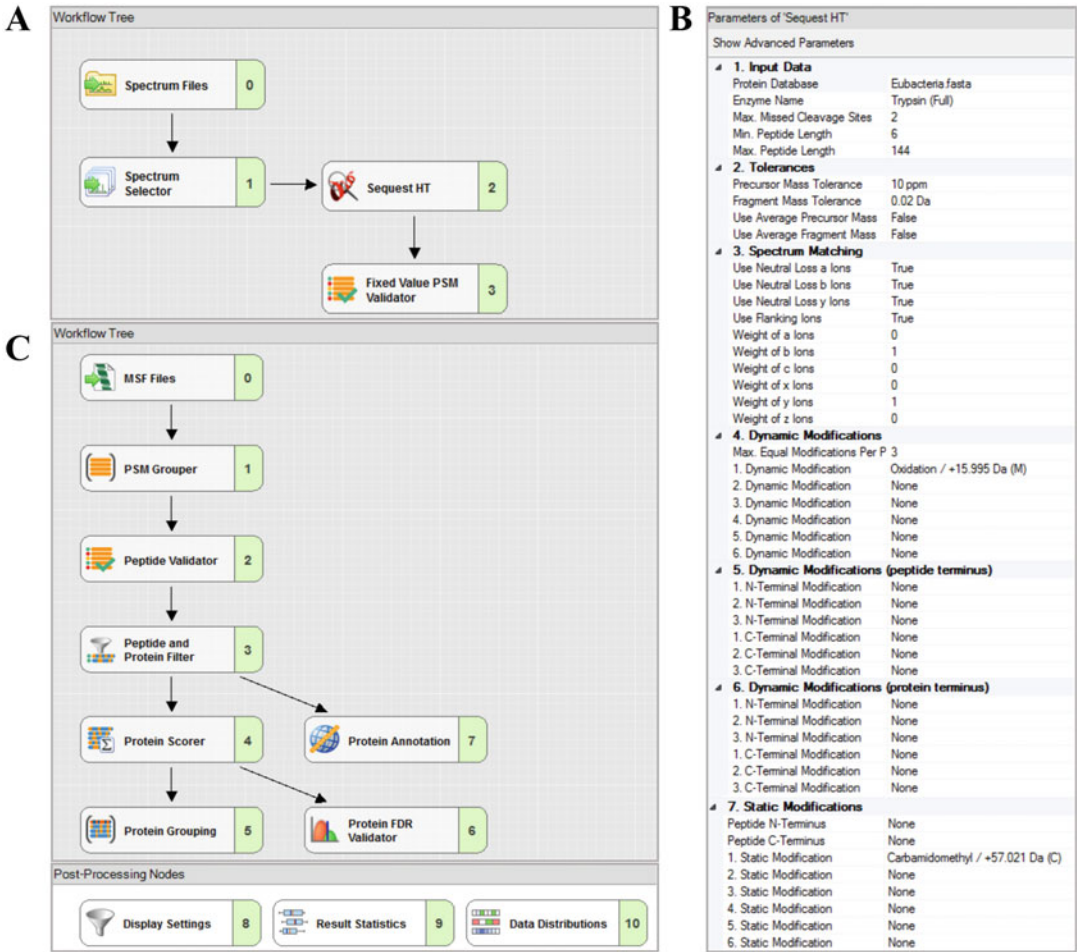


Fig. 2 Proteome Discoverer 2.4 settings. (a) Processing Workflow nodes. (b) Sequest HT parameters. (c) Consensus Workflow nodes

- Set the parameters for the “Sequest HT” node (Fig. 2b).
- Upload the appropriate database by choosing the “Maintain Fasta file” option from the “Administration” menu on the software start page. Click “Add” and select the appropriate location for indexing the file and adding it to the list of the available databases. For the analysis of the ribosomal protein-enriched fraction, both the UniprotKB_SwissProt Bacteria database or the whole UniprotKB_SwissProt database can be used.
- Select trypsin as digestion enzyme with a maximum of two missed cleavages and a minimum peptide length of six residues.
- Set precursor mass tolerance to ± 10 ppm and fragment mass tolerance to ± 0.02 Da.

11. Set up carbamidomethylation (+57.021 Da) of cysteine residues and oxidation of methionines (+15.995 Da) as static and dynamic modifications, respectively.
12. Create a Consensus Workflow Tree (default settings): “MSF (Magellan Storage File) Files”, “PSM (Peptide Spectrum Match) Grouper”, “Peptide Validator”, “Peptide and Protein filter”, “Protein Scorer”, “Protein Grouping”, “Protein annotation”, “Protein FDR Validator”. Include post-processing nodes (Fig. 2c).
13. Calculate and filter false discovery rates (FDRs) for peptide spectral matches (PSMs) using the Target Decoy PSM Validator Node with the following settings: maximum Delta Cn: 0.05; strict target FDR: 0.01; relaxed target FDR: 0.05.
14. Validate protein identifications based on q -values. Identified proteins with a q -value < 0.01 are classified as high-confidence identifications; proteins with $0.01 < q$ -value < 0.05 are classified as medium confidence identifications. Low confidence identifications (q -value > 0.05), displayed within the protein list highlighted in red, should be filtered out and not further considered.
15. Typically, the output protein list may be further filtered by considering only proteins identified with more than one peptide and in at least two out of three replicate injections. Also, the optional removal of common contaminant proteins from the protein list (e.g., keratin and tryptic peptides) is usually performed.

3.6 Proteotypic Markers Selection for LAB Characterization in Food Matrices

Most of the bacterial proteins identified by the protocol shown here are of ribosomal origin. Despite the high similarity of their primary structures, minor sequence variations exist within bacteria subspecies and strains. Due to their diverse phylogenetic evolution rates, several fingerprinting methods, at both DNA and protein levels, rely on ribosomal sequences for phylogenetic detection and classification of bacteria. Besides LAB identification, the LC-ESI MS/MS bacterial profiling described above may also allow further characterization of LAB at the genus, species, and subspecies levels by selecting sequence regions of ribosomal proteins (e.g., S16 ribosomal protein) highly diagnostic for LAB species of interest (Fig. 3). To identify suitable proteotypic peptide markers of ribosomal proteins the following general procedure can be applied:

1. Perform an in silico multiple sequence alignment of ribosomal proteins identified by LC-ESI MS/MS (see Subheadings 3.4 and 3.5) or selected within the UniprotKB_SwissProt database by using the Clustal Omega algorithm freely available at <https://www.ebi.ac.uk/Tools/msa/clustalo/> (see Note 18).

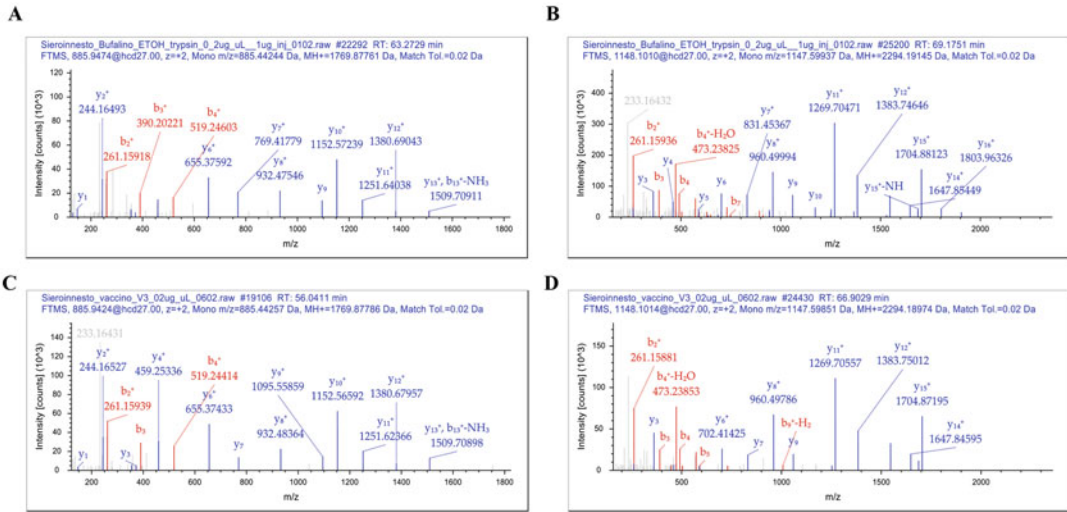


Fig. 3 Representative MS/MS fragmentation spectra of ions corresponding to the preteotypic peptides from the S16 ribosomal protein of *L. delbrueckii bulgaricus* (a and c) and *S. thermophilus* (b and d), detected in buffalo (a and b) and bovine (c and d) whey starter cultures. (a) MS/MS fragmentation spectrum of the ion at m/z 885.947, corresponding to the doubly charged ion of the region 33–47 of the S16 ribosomal protein from *L. delbrueckii bulgaricus* (AC: Q049R6, 33-FIEEVGYNPVSPQK-47, theoretical monoisotopic $[M+H]^+$ mass 1769.878 Da, $\Delta = 1.77$ ppm) detected in buffalo whey starter culture. (b) MS/MS fragmentation spectrum of the ion at m/z 1148.101, corresponding to the doubly charged ion of the region 33–52 of the S16 ribosomal protein from *S. thermophilus* (AC: Q5LYM4, 33-FIETVGTYNPLVEENQVTLK-52, theoretical monoisotopic $[M+H]^+$ mass 2294.191 Da, $\Delta = 0.00$ ppm). (c) MS/MS fragmentation spectrum of the ion at m/z 885.942, corresponding to the doubly charged ion of the region 33–47 of the S16 ribosomal protein from *L. delbrueckii bulgaricus* (AC: Q049R6, 33-FIEEVGYNPVSPQK-47, theoretical monoisotopic $[M+H]^+$ mass 1769.878 Da, $\Delta = 1.91$ ppm) detected in bovine whey starter culture. (d) MS/MS fragmentation spectrum of the ion at m/z 1148.101, corresponding to the doubly charged ion of the region 33–52 of the S16 ribosomal protein from *S. thermophilus* (AC: Q5LYM4, 33-FIETVGTYNPLVEENQVTLK-52, theoretical monoisotopic $[M+H]^+$ mass 2294.190 Da, $\Delta = 0.74$ ppm)

- Analyze the amino acid sequence identity/similarity at the taxonomic level and select theoretical tryptic peptides containing amino acid differences within bacteria genus, species, and subspecies.
- Validate the presence of candidate species-specific peptide markers by evaluating their ionization efficiency within LC-MS base peak chromatograms of samples and verifying their specificity for the discrimination of LAB species within food matrices of interest (see Note 19).

4 Notes

- The extraction of a basic protein fraction, highly enriched of ribosomal proteins, has been adapted from the protocol

reported by Freiwald and Sauer for MALDI-TOF MS detection of *Enterobacteriaceae* [47]. The procedure can be applied on both selected food matrices or pure colonies previously isolated from foods. Bacterial strains used for this protocol were previously isolated from fermented dairy products. Bacterial pellets may also be obtained from direct centrifugation of food matrices that are rich in probiotic lactic acid bacteria. For example, centrifugation for 15 min at $10,000 \times g$ of aliquots (200 mL) of bovine and buffalo natural whey starter cultures provide an adequate amount of proteins for subsequent analyses [29]. In this instance, following centrifugation, supernatants were discarded and the pellets are processed as described for isolated colonies.

2. The growth of lactic acid bacteria cultures significantly depends on the complexity of the food matrix and cultivation media [48]. In this workflow, cultivation media that are suitable and commonly used for Lactobacillales growth have been reported. In particular, MRS is a widely used selective medium for lactic acid bacteria cultivation. However, MRS is considered to be an expensive medium due to its nitrogen source (meat and yeast extract) and does not support the growth of all LAB [48]. Therefore, ESTY medium (M17) is also commonly used for culturing LAB such as lactic streptococci or yogurt bacteria [49]. Since no universal selective medium exists for the cultivation of all lactic acid bacteria, LAB media may be appropriately modified by changing the supplement composition, the pH, incubation times, and culture temperature. Cultivation media for LAB used in dairy products are extensively reviewed in [48].
3. Prepare De Man, Rogosa, and Sharpe (MRS) medium: weigh 52 g of the MRS medium powder, put 1 L of water and mix thoroughly. Autoclave at 121 °C for 15 min prior to use.
4. Prepare ESTY medium: weigh 48.25 g of the ESTY medium powder, put 900 mL of water, mix thoroughly, and heat it to completely dissolve the powder. Autoclave at 121 °C for 15 min, cool to 50 °C, and add 100 mL of sterile 10% lactose solution.
5. Following the centrifugation step, supernatants should be collected without contaminations. Tubes must be slowly removed from the centrifuge to carefully aspirate supernatants with the pipette by avoiding mixing with cell debris.
6. A yellow pellet is typically clearly visible at the bottom of the Eppendorf tube. A careful pellet washing is necessary for removing trace amounts of residual formic acid. During washes, place tubes inside the centrifuge so that the hinges face outward to consistently position the pellet.

7. Protein pellets should not be overdried as this will make them more difficult to resuspend. Do not use the SpeedVac at this step.
8. Typically, a 50 μL volume of buffer results in a good capacity for dissolving the protein pellet. If there is too much protein in the pellet, the volume of the buffer may be increased up to 100 μL . Larger volumes may cause an excessive sample dilution. The pH of the ammonium bicarbonate solution increases up to 8.5 upon storage for a few weeks. Use freshly prepared solutions and check the pH before use (pH \sim 7.8).
9. The enrichment of ribosomal proteins can be evaluated by analyzing aliquots (15 μg) of resuspended pellets by SDS-PAGE. A pattern of low molecular weight bands is expected mainly in the range of 10–20 kDa.
10. DTT is susceptible to oxidation and should be freshly prepared.
11. IAM is sensitive to light and should be freshly prepared and kept in the dark.
12. Dissolve lyophilized trypsin in 50 mM NH_4HCO_3 , pH 7.8. The addition of freshly prepared trypsin to protein pellet in three subsequent steps with enzyme to substrate ratios (w/w) of 1:200 for 4 h, 1:100 for 3 h, and 1:50 for 16 h is suggested to increase the efficiency of the enzymatic hydrolysis.
13. If needed, the protocol can be stopped after digestion and samples stored at -20°C .
14. To prevent plugging of the nano-LC system, an additional centrifugation step at $15,000 \times g$ for 15 min can be performed
15. To monitor potential memory effects (carry-over), it is suggested to perform blank injections between LC runs of samples.
16. Before LC runs of samples, it is strongly suggested to perform a preliminary analysis of 100 fmol of a BSA Protein Digest Standard (Thermo Fisher Scientific, Cat. #88341) to test the chromatographic system and MS performance.
17. Prepare all solutions for sample preparation for LC-MS analysis by using LC-MS-grade reagents. Avoid contamination by external protein sources (e.g., keratin originating from dust, hairs, and finger skin). It is recommended to work in a clean and dust-free space and to wear a lab coat, gloves, and possibly a hair net.
18. The Clustal Omega default settings usually fulfill the needs of most users. Several options are available to optimize the alignment (e.g., gaps removal, iteration parameters) and to change the output format for generated multiple sequence alignment.

19. Fermented dairy products are a convenient source for applying the proposed workflow. As we have shown recently [29], using the preparation and mass spectrometry protocol described herein, we detected signature species-specific peptide markers corresponding to regions 33–52 and 72–82 of the S16 ribosomal that proved to be useful for the accurate classification and identification of about 30 LAB at the genus, species, and subspecies level in complex matrices such as whey starter cultures used for the production of cheese and fermented foods. Depending on the food matrix properties, the limitation of the protocol may consist of the need for LAB cell culturing to harvest sufficient amounts of bacterial cells suitable for the analysis. The strength of the protocol is the reliability of identifications given the high mass accuracy (1–5 ppm) and resolution (~150,000) of the Orbitrap mass analyzer.

References

- Morelli L, Capurso L (2012) FAO/WHO guidelines on probiotics: 10 years later. *J Clin Gastroenterol* 46:S1–S2. <https://doi.org/10.1097/MCG.0b013e318269fdd5>
- Ayivi RD, Gyawali R, Krastanov A, Aljaloud SO, Worku M, Tahergorabi R, Silva RCD, Ibrahim SA (2020) Lactic acid bacteria: food safety and human health applications. *Dairy* 1(3):202–232. <https://doi.org/10.3390/dairy1030015>
- Fenster K, Freeburg B, Hollard C, Wong C, Rønhave Laursen R, Ouwehand AC (2019) The production and delivery of probiotics: a review of a practical approach. *Microorganisms* 7(3):83. <https://doi.org/10.3390/microorganisms7030083>
- Evivie SE, Huo GC, Igene JO, Bian X (2017) Some current applications, limitations and future perspectives of lactic acid bacteria as probiotics. *Food Nutr Res* 61(1):1318034. <https://doi.org/10.1080/16546628.2017.1318034>
- Wilson KH, Blitchington RB, Greene RC (1990) Amplification of bacterial 16S ribosomal DNA with polymerase chain reaction. *J Clin Microbiol* 28(9):1942–1946. <https://doi.org/10.1128/jcm.28.9.1942-1946.1990>
- Yarza P, Yilmaz P, Pruesse E, Glockner FO, Ludwig W, Schleifer KH, Whitman WB, Euzéby J, Amann R, Rossello-Mora R (2014) Uniting the classification of cultured and uncultured bacteria and archaea using 16S rRNA gene sequences. *Nat Rev Microbiol* 12(9):635–645. <https://doi.org/10.1038/nrmicro3330>
- Sharma A, Lee S, Park YS (2020) Molecular typing tools for identifying and characterizing lactic acid bacteria: a review. *Food Sci Biotechnol* 29(10):1301–1318. <https://doi.org/10.1007/s10068-020-00802-x>
- Sauer S, Kliem M (2010) Mass spectrometry tools for the classification and identification of bacteria. *Nat Rev Microbiol* 8(1):74–82. <https://doi.org/10.1038/nrmicro2243>
- Van Oudenhove L, Devreese B (2013) A review on recent developments in mass spectrometry instrumentation and quantitative tools advancing bacterial proteomics. *Appl Microbiol Biotechnol* 97(11):4749–4762. <https://doi.org/10.1007/s00253-013-4897-7>
- Krásný L, Hynek R, Hochel I (2013) Identification of bacteria using mass spectrometry techniques. *Int J Mass Spectrom* 353(1):67–79. <https://doi.org/10.1016/j.ijms.2013.04.016>
- Adebo O, Oyeyinka S, Adebisi J, Feng X, Wilkin J, Kewuyemi Y, Abrahams A, Tugizimana F (2020) Application of gas chromatography-mass spectrometry (GC-MS)-based metabolomics for the study of fermented cereal and legume foods: a review. *Int J Food Sci Tech* 56(4):1514–1534. <https://doi.org/10.1111/ijfs.14794>
- Adebo OA, Kayitesi E, Tugizimana F, Njobeh PB (2019) Differential metabolic signatures in naturally and lactic acid bacteria (LAB) fermenting (a Southern African food) with different tannin content, as revealed by gas chromatography mass spectrometry (GC-MS)-based metabolomics. *Food Res Int*

- 121:326–335. <https://doi.org/10.1016/j.foodres.2019.03.050>
13. Carpena M, Fraga-Corral M, Otero P, Nogueira RA, Garcia-Oliveira P, Prieto MA, Simal-Gandara J (2021) Secondary aroma: influence of wine microorganisms in their aroma profile. *Foods* 10(1):51. <https://doi.org/10.3390/foods10010051>
 14. Chen C, Lu Y, Yu H, Chen Z, Tian H (2018) Influence of 4 lactic acid bacteria on the flavor profile of fermented apple juice. *Food Biosci* 27(1):30–36. <https://doi.org/10.1016/j.fbio.2018.11.006>
 15. Guarrasi V, Sannino C, Moschetti M, Bonanno A, Di Grigoli A, Settanni L (2017) The individual contribution of starter and non-starter lactic acid bacteria to the volatile organic compound composition of Caciocavallo Palermitano cheese. *Int J Food Microbiol* 259:35–42. <https://doi.org/10.1016/j.ijfoodmicro.2017.07.022>
 16. Harada R, Yuzuki M, Ito K, Shiga K, Bamba T, Fukusaki E (2017) Influence of yeast and lactic acid bacterium on the constituent profile of soy sauce during fermentation. *J Biosci Bioeng* 123(2):203–208. <https://doi.org/10.1016/j.jbiosc.2016.08.010>
 17. Lee SM, Hwang YR, Kim MS, Chung MS, Kim YS (2019) Comparison of volatile and nonvolatile compounds in rice fermented by different lactic acid bacteria. *Molecules* 24(6):1183. <https://doi.org/10.3390/molecules24061183>
 18. Nsongning Dongmo S, Sacher B, Kollmannsberger H, Becker T (2017) Key volatile aroma compounds of lactic acid fermented malt based beverages—impact of lactic acid bacteria strains. *Food Chem* 229:565–573. <https://doi.org/10.1016/j.foodchem.2017.02.091>
 19. Reale A, Renzo T, Boscaino F, Nazzaro F, Fratianni F, Aponte M (2019) Lactic acid bacteria biota and aroma profile of italian traditional sourdoughs from the Irpinian area in Italy. *Front Microbiol* 10:1621. <https://doi.org/10.3389/fmicb.2019.01621>
 20. Tian H, Shi Y, Zhang Y, Yu H, Mu H, Chen C (2019) Screening of aroma-producing lactic acid bacteria and their application in improving the aromatic profile of yogurt. *J Food Biochem* 43(10):e12837. <https://doi.org/10.1111/jfbc.12837>
 21. Lo AAL, Hu A, Ho YP (2006) Identification of microbial mixtures by LC-selective proteotypic-peptide analysis (SPA). *J Mass Spectrom* 41(8):1049–1060. <https://doi.org/10.1002/jms.1064>
 22. Hu A, Chen CT, Tsai PJ, Ho YP (2006) Using capillary electrophoresis–selective tandem mass spectrometry to identify pathogens in clinical samples. *Anal Chem* 78(14):5124–5133. <https://doi.org/10.1021/ac060513+>
 23. Dworzanski JP, Snyder AP, Chen R, Zhang H, Wishart D, Li L (2004) Identification of bacteria using tandem mass spectrometry combined with a proteome database and statistical scoring. *Anal Chem* 76(8):2355–2366. <https://doi.org/10.1021/ac0349781>
 24. Obolensky OI, Wu WW, Shen RF, Yu YK (2012) Using dissociation energies to predict observability of b- and y-peaks in mass spectra of short peptides. *Rapid Commun Mass Spectrom* 26(8):915–920. <https://doi.org/10.1002/rcm.6180>
 25. Dworzanski JP, Deshpande SV, Chen R, Jabbour RE, Snyder AP, Wick CH, Li L (2006) Mass spectrometry-based proteomics combined with bioinformatic tools for bacterial classification. *J Proteome Res* 5(1):76–87. <https://doi.org/10.1021/pr050294t>
 26. Alves G, Wang G, Ogurtsov AY, Drake SK, Gucek M, Suffredini AF, Sacks DB, Yu YK (2016) Identification of microorganisms by high resolution tandem mass spectrometry with accurate statistical significance. *J Am Soc Mass Spectrom* 27(2):194–210. <https://doi.org/10.1007/s13361-015-1271-2>
 27. Cheng K, Chui H, Domish L, Hernandez D, Wang G (2016) Recent development of mass spectrometry and proteomics applications in identification and typing of bacteria. *Proteomics Clin Appl* 10(4):346–357. <https://doi.org/10.1002/prca.201500086>
 28. Lasch P, Schneider A, Blumenschein C, Doellinger J (2020) Identification of microorganisms by liquid chromatography-mass spectrometry (LC-MS1) and in silico peptide mass libraries. *Mol Cell Proteomics* 19(12):2125–2139. <https://doi.org/10.1074/mcp.TIR120.002061>
 29. Russo R, Valletta M, Rega C, Marasco R, Muscariello L, Pedone PV, Sacco M, Chambery A (2019) Reliable identification of lactic acid bacteria by targeted and untargeted high-resolution tandem mass spectrometry. *Food Chem* 285:111–118. <https://doi.org/10.1016/j.foodchem.2019.01.127>
 30. Gantzias C, Lappa IK, Aerts M, Georgalaki M, Manolopoulou E, Papadimitriou K, De Brandt E, Tsakalidou E, Vandamme P (2020) MALDI-TOF MS profiling of non-starter lactic acid bacteria from artisanal cheeses of the Greek island of Naxos. *Int J Food Microbiol*

- 323:108586. <https://doi.org/10.1016/j.ijfoodmicro.2020.108586>
31. Lee Y, Cho Y, Kim E, Kim HJ, Kim HY (2018) Identification of lactic acid bacteria in galchi-and myeolchi-jeotgal by 16S rRNA sequencing, MALDI TOF mass spectrometry, and PCR-DGGE. *J Microbiol Biotechnol* 28(7): 1112–1121. <https://doi.org/10.4014/jmb.1803.03034>
 32. Ahmadsah LSF, Kim E, Jung YS, Kim HY (2018) Identification of LAB and fungi in laru, a fermentation starter, by PCR-DGGE, SDS-PAGE, and MALDI-TOF MS. *J Microbiol Biotechnol* 28(1):32–39. <https://doi.org/10.4014/jmb.1705.05044>
 33. Makete G, Aiyegoro O, Thantsha M (2017) Isolation, identification and screening of potential probiotic bacteria in milk from South African Saanen goats. *Probiotics Antimicrob Proteins* 9(3):246–254. <https://doi.org/10.1007/s12602-016-9247-5>
 34. Nacef M, Chevalier M, Chollet S, Drider D, Flahaut C (2017) MALDI-TOF mass spectrometry for the identification of lactic acid bacteria isolated from a French cheese: the maroilles. *Int J Food Microbiol* 247:2–8. <https://doi.org/10.1016/j.ijfoodmicro.2016.07.005>
 35. Cho Y, Kim E, Lee Y, Han SK, Kim CG, Choo DW, Kim YR, Kim HY (2016) Rapid and accurate identification of *Pediococcus* species isolated from Korean fermented foods by MALDI-TOF MS with local database extension. *Int J Syst Evol Microbiol* 67(3): 744–752. <https://doi.org/10.1099/ijsem.0.001626>
 36. Kim E, Cho Y, Lee Y, Han S-K, Kim C-G, Choo D-W, Kim Y-R, Kim H-Y (2017) A proteomic approach for rapid identification of *Weissella* species isolated from Korean fermented foods on MALDI-TOF MS supplemented with an in-house database. *Int J Food Microbiol* 243:9–15. <https://doi.org/10.1016/j.ijfoodmicro.2016.11.027>
 37. Karaduman A, Ozaslan MO, Kilic IH, Bayil-Oguzkan S, Kurt BS, Erdogan N (2017) Identification by using MALDI-TOF mass spectrometry of lactic acid bacteria isolated from non-commercial yogurts in southern Anatolia, Turkey. *Int Microbiol* 20(1):25–30. <https://doi.org/10.2436/20.1501.01.282>
 38. Mahajan B, Sohuche Y, Hayes J, Marotta F, Yadav H, Singh V (2017) MALDI-TOF MS spectrophotometric and 16S rRNS gene sequencing identification of probiotic lactic acid bacteria isolated from dairy food products. *Int J Probiotics Prebiotics* 12(4):199–210
 39. Garcia EF, Luciano WA, Xavier DE, da Costa WCA, de Sousa OK, Franco OL, de Morais Júnior MA, Lucena BTL, Picão RC, Magnani M, Saarela M, de Souza EL (2016) Identification of lactic acid bacteria in fruit pulp processing byproducts and potential probiotic properties of selected *Lactobacillus* strains. *Front Microbiol* 7:1371. <https://doi.org/10.3389/fmicb.2016.01371>
 40. Doan NTL, Van Hoorde K, Cnockaert M, Brandt E, Aerts M, Binh L, Vandamme P (2012) Validation of MALDI-TOF MS for rapid classification and identification of lactic acid bacteria, with a focus on isolates from traditional fermented foods in northern Vietnam. *Lett Appl Microbiol* 55(4):265–273. <https://doi.org/10.1016/j.ijfoodmicro.2012.01.008>
 41. Garcia-Cano I, Rocha-Mendoza D, Ortega-Anaya J, Wang K, Kosmerl E, Jiménez-Flores R (2019) Lactic acid bacteria isolated from dairy products as potential producers of lipolytic, proteolytic and antibacterial proteins. *Appl Microbiol Biotechnol* 103(13): 5243–5257. <https://doi.org/10.1007/s00253-019-09844-6>
 42. McNair L, Siedler S, Vinther J, Hansen A, Neves A, Garrigues C, Jäger A, Franzky H, Staerk D (2018) Identification and characterization of a new antifungal peptide in fermented milk product containing bioprotective *Lactobacillus* cultures. *FEMS Yeast Res* 18(8): foy094. <https://doi.org/10.1093/femsyr/foy094>
 43. Ndlovu B, Schoeman H, Franz C, Du Toit M (2015) Screening, identification and characterization of bacteriocins produced by wine-isolated LAB strains. *J Appl Microbiol* 118(4): 1007–1022. <https://doi.org/10.1111/jam.12752>
 44. Nandakumar R, Talapatra K (2014) Quantitative profiling of bacteriocins present in dairy-free probiotic preparations of *Lactobacillus acidophilus* by nanoliquid chromatography-tandem mass spectrometry. *J Dairy Sci* 97(4): 1999–2008. <https://doi.org/10.3168/jds.2013-7470>
 45. Cárdenas C, Barkla B, Wachter C, Delgado-Olivares L, Rodríguez-Sanoja R (2014) Protein extraction method for the proteomic study of a Mexican traditional fermented starchy food. *J Proteomics* 111:139–147. <https://doi.org/10.1016/j.jprot.2014.06.028>
 46. Jardin J, Mollé D, Piot M, Lortal S, Gagnaire V (2012) Quantitative proteomic analysis of bacterial enzymes released in cheese during ripening. *Int J Food Microbiol* 155(1-2):19–28. <https://doi.org/10.1016/j.ijfoodmicro.2012.01.008>

47. Freiwald A, Sauer S (2009) Phylogenetic classification and identification of bacteria by mass spectrometry. *Nat Protoc* 4(5):732–742. <https://doi.org/10.1038/nprot.2009.37>
48. Hayek SA, Gyawali R, Aljaloud SO, Krastanov A, Ibrahim SA (2019) Cultivation media for lactic acid bacteria used in dairy products. *J Dairy Res* 86(4):490–502. <https://doi.org/10.1017/S002202991900075X>
49. Reuter G (1985) Elective and selective media for lactic acid bacteria. *Int J Food Microbiol* 2(1):55–68. [https://doi.org/10.1016/0168-1605\(85\)90057-1](https://doi.org/10.1016/0168-1605(85)90057-1)

Part II

Emerging MS-Based Techniques



Acetylcholinesterase (ACHE) and α -Glucosidase Inhibitory Assay by Effect-Directed Analysis on High Performance Thin-Layer Chromatography Coupled to Mass Spectrometry

Mario Aranda, Jonathan Carrasco, and Karem Henríquez

Abstract

The traditional study of natural sources bioactivity is based on the evaluation of diverse biological activities like antioxidant or enzymes inhibition. For that, conventional methods involve the preparation of different polarities extracts, which are submitted to a various chemical and biological assays. If any extract shows some bioactivity, a large and time-consuming process begins. First, the extract composition is defined applying different types of chromatographic systems such as high-performance liquid chromatography (HPLC), high performance thin-layer chromatography (HPTLC), and gas chromatography (GC). Then, fractioning and purification processes are required to isolate as many compounds as possible employing special techniques like semi-preparative chromatography. All isolated groups or compounds are individually reevaluated in order to find which compound or family possess the biological activity. To shorten this process, some hyphenation methods that coupled analytical separation and bioassays have been developed, for example, HPTLC-bioassay coupled to mass spectrometry (MS).

Key words α -Glucosidase, Thin-layer chromatography, Online assays, Phenolic compounds

1 Introduction

Acetylcholinesterase (AChE, EC 3.1.1.7) is a relevant enzyme at central nervous system; its inhibition could be helpful to treat several diseases such as Alzheimer [1], Parkinson's disease dementia [2], schizophrenia [3], and autism [4]. Therefore, the discovery of new inhibitors is highly relevant for human health. α -glucosidase (EC 3.2.1.20) inhibitors delay the enzyme activity avoiding the poly- and oligosaccharides hydrolysis. Its inhibition is clearly beneficial for patients with altered glucose metabolism like type 2 diabetes mellitus because retard carbohydrates absorption in the small intestine, which produces a lowering effect on postprandial blood glucose and insulin levels [5]. The screening of this kind of molecules in nature resulted in the discovery of acarbose and

1-deoxynojirimycin, which lead to the synthesis of miglitol; both drugs are currently used as therapeutics [6].

Effect-directed analysis (EDA) is a study strategy that combines chemical analysis with biological effects. EDA has increasingly attracted attention in the field of food science to evaluate functional foods, food safety, foodborne diseases, and health care [7, 8]. EDA consists of two principal steps; first, the separation of molecules from food matrix is necessary, and then the obtained fractions are evaluated for biological activity (effect)[7, 9]. HPTLC is an excellent tool to carry out EDA, after molecules separation from food matrix (chromatography), the effect (biological assay) is directly determined on the plate (in situ) without any incompatibility with mobile phase because all solvents are fully evaporated before carrying out the bioassay. The hyphenation of HPTLC and EDA is well known in both domains, autography coupled with chemical analysis (e.g., DPPH) and bioautography (bioassay) coupled with biological system or biological evaluation (e.g., enzymatic inhibition)[10, 11].

Thus, applying reliable EDA-HPTLC-MS method it is possible to discover new acetylcholinesterase and α -glucosidase inhibitors as first step for nutraceutical and/or active pharmaceutical ingredients development.

2 Materials

Prepare all solutions using ultra-pure water (18.2 M Ω cm) and analytical grade reagents. Store all solutions at 4 °C and enzyme at -24 °C.

1. HPTLC or HPTLC-MS plates: 10 cm \times 10 cm coated with 200 μ m layer of silica gel 60 F₂₅₄.
2. Semi- or automatic TLC sampler.
3. TLC chambers: flat bottom or twin trough.
4. TLC plate heater.
5. TLC sprayer.
6. Photo-documentation system.
7. TLC-MS interface.
8. Mass spectrometer.
9. Acarbose or caffeic acid (positive control for α -glucosidase enzyme assay): 300 mg/L in methanol.
10. Donepezil (positive control for the AChE enzyme assay): 300 mg/L in methanol.

11. Phosphate buffer 100 mM, pH 7.4: dissolve 0.91 g KH_2PO_4 and 0.57 g K_2HPO_4 in 95 mL of water. Adjust pH with NaOH 2 M and filled up to 100 mL with water. Store at 4 °C.
12. 2-naphthyl-D-glucopyranoside (substrate for the α -glucosidase enzyme assay): 1 mg/mL in methanol.
13. 1-naphthyl acetate (substrate for the AChE enzyme assay): 1.5 mg/mL in methanol.
14. α -glucosidase enzyme from *Saccharomyces cerevisiae* (E.C. number 3.2.1.20): 1.25 U/mL in 100 mM phosphate buffer, pH 7.4. Divide into 100 μL aliquots and store at -24 °C.
15. AChE enzyme from *Electrophorus electricus* (electric eel) (E.C. number 3.1.1.7): 0.75 U/mL in 50 mM Tris-HCl buffer at pH 7.8. Divide into 100 μL aliquots and store at -24 °C.
16. Fast Blue B salt solution: 1.5 mg/mL in water.

3 Method

Carry out all procedures at room temperature unless otherwise specified. Each enzyme assay must be separately performed.

1. Wash the plates with proper solvent mixture (e.g., methanol: acetonitrile 1:1 v/v) and dry on plate heater for 20 min at 120 °C.
2. Apply an adequate amount of sample (1–20 μL) and positive control (2–3 μL) on the HPTLC plate by means of semi- or automatic TLC sampler. It is suggested the following settings: band length 6–8 mm, track distance 10.0 mm, dosage velocity 120 nL/s, and first application x -axis and y -axis at 10.0 mm.
3. Apply the samples in triplicate on each HPTLC plate and then divide, using plate cutter, into three sections: the first section is used for bioassay, the second section for chemical derivatization (optional) and the third for MS analysis.
4. Carry out the chromatographic separation in 10 cm \times 10 cm twin trough chamber up to a migration distance of 50–70 mm using a proper mobile phase.
5. Dry the HPTLC plate on the plate heater for 30 min at 60–100 °C to remove the mobile phase. If compounds under study are thermolabile, it is recommended to dry at temperatures not higher than 60 °C. Otherwise, dry at 85 °C.
6. Detect α -glucosidase inhibitors spraying 3 mL of 2-naphthyl-D-glucopyranoside solution on the HPTLC plate, and for AChE inhibitors, 3 mL of 1-naphthyl acetate solution.

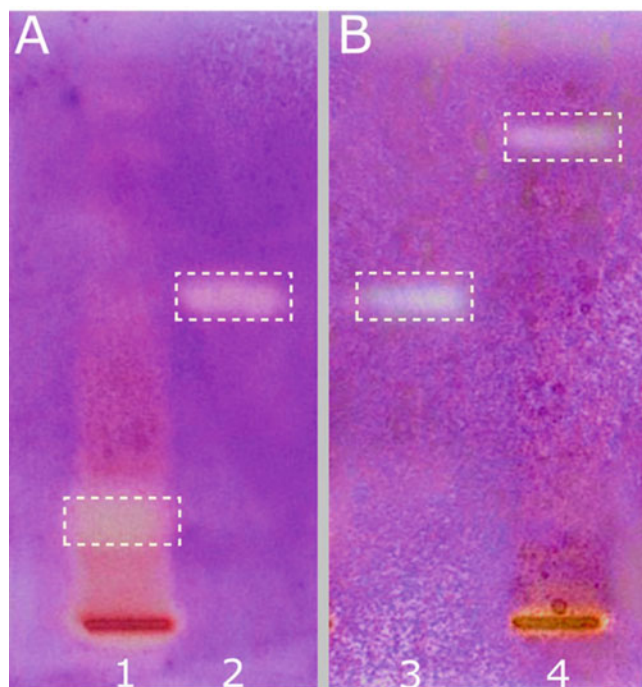


Fig. 1 α -glucosidase inhibitory assay (a). AChE inhibitory assay (b). Plant extracts showing inhibitory bands/compounds (1, 4) and the corresponding positive controls (2, 3)

7. For both assays, dry the plate at 60 °C for 10 min on the TLC plate heater, cool down to room temperature and spray 3 mL of the respective enzyme solution.
8. Place the HPTLC plate in a pre-warmed humidified plastic container at 37 °C for 10 min, avoiding direct contact between the water and the plate.
9. After the incubation process, spray the HPTLC plate with 3 mL of freshly prepared Fast Blue B salt solution. After 2–4 min, the presence of inhibitory compounds is observed under visible light as colorless bands on purple background (Fig. 1).
10. Using a soft pencil mark the inhibitory bands on the third section of HPTLC plate based on migration distance (hRF) visualized under plate cabinet (254 and 366 nm). Identify the inhibitors applying two complementary steps using for both the TLC-MS interface (Fig. 2): (i) elute the bands of interest to MS (Fig. 3); and (ii) extract the inhibitory bands from HPTLC plate to 1.5 mL micro-vial to be analyzed by HPLC-DAD-MS/MS. It is recommended to assemble the TLC-MS interface with oval elution head (4.0 × 2.0 mm); elute the bands with proper solvent at a flow rate of 0.2 mL/min for 2 min.

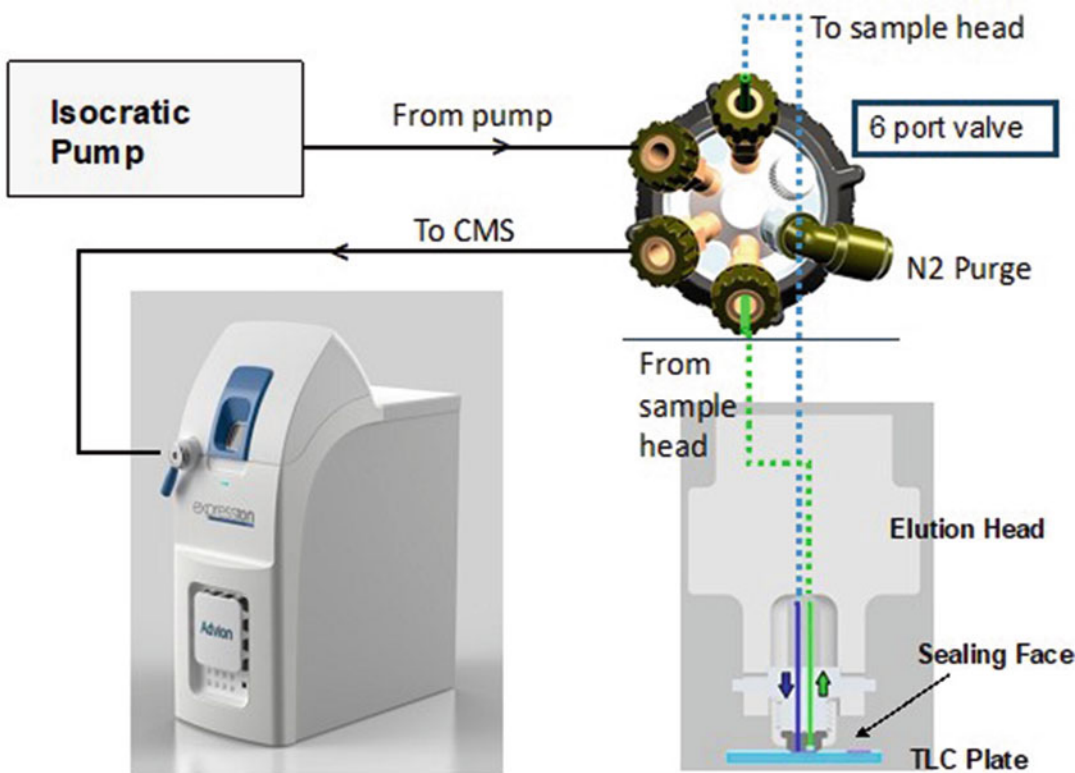


Fig. 2 Schematic diagram of HPTLC-MS coupling using Advion Plate Express TLC-MS interface (Reproduced with permission from Advion-Interchim)

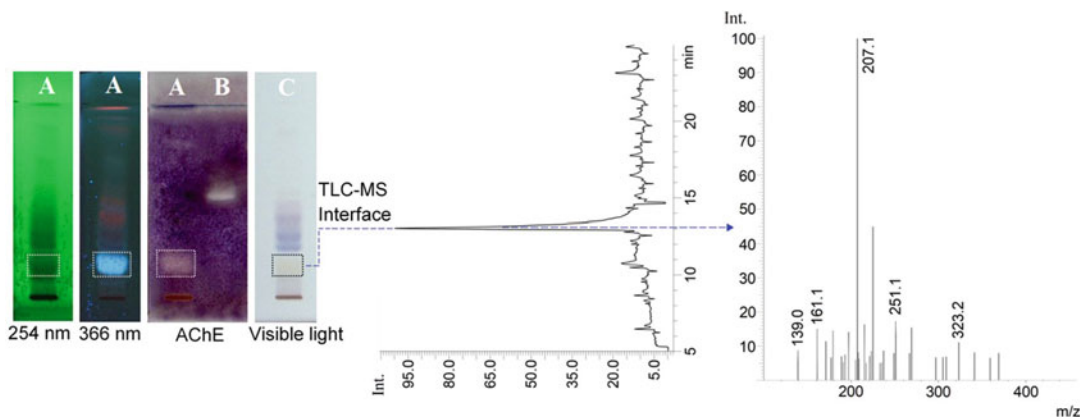


Fig. 3 Example of HPTLC-bioassay-ESIMS assay to detect AChE inhibitors present in plant extracts. HPTLC plates are observed under UV (254, 366 nm) and Vis light (C). Plant extracts (A) and positive control (B)

Extract at least two plate blanks to obtain the MS background spectrum. MS analysis is performed in mass spectrometer with electrospray ionization (ESI) or atmospheric pressure chemical

ionization (APCI) sources operated in standard or appropriate conditions according to the analytes, e.g., capillary voltage 4.0 kV, nebulizing gas (N₂) 3 L/min, drying gas (N₂) 15 L/min, desolvation line temperature 250 °C, and block temperature 400 °C. To acquire the MS spectra in full scan mode between *m/z* values of 50 and 2000. Plate background signals should be subtracted for each analysis. HPLC-DAD-MS/MS is performed as a complementary method to obtain comparative data for compound identification such as retention time, UV-Vis spectrum, MS and MS/MS spectra.

References

1. Kumar A, Singh A, Ekavali (2015) A review on Alzheimer's disease pathophysiology and its management: an update. *Pharmacol Rep* 67: 195–203. <https://doi.org/10.1016/j.pharep.2014.09.004>
2. Rolinski M, Fox C, Maidment I, McShane R (2012) Cholinesterase inhibitors for dementia with Lewy bodies, Parkinson's disease dementia and cognitive impairment in Parkinson's disease. *Cochrane Database Syst Rev* 3: CD006504. <https://doi.org/10.1002/14651858.CD006504.pub2>
3. Ribeiz SR et al (2010) Cholinesterase Inhibitors as Adjunctive Therapy in Patients with Schizophrenia and Schizoaffective Disorder. *CNS Drugs* 24: 303–317. <https://doi.org/10.2165/11530260-000000000-00000>
4. Rossignol DA, Frye RE (2014) The use of medications approved for Alzheimer's disease in autism spectrum disorder: a systematic review. *Front Pediatr* 2:87. <https://doi.org/10.3389/fped.2014.00087>
5. van de Laar FA et al (2005) α -Glucosidase inhibitors for patients with type 2 diabetes: results from a cochrane systematic review and meta-analysis. *Diabetes Care* 28:154–163. <https://doi.org/10.2337/diacare.28.1.154>
6. Grabley S, Thiericke R (1999) *Drug Discovery from Nature*. Springer, pp 3–37. ISBN 3-540-64844-5
7. Oresanya IO et al (2020) Isolation of flavonoids from *Musa acuminata* Colla (Simili radjah, ABB) and the in vitro inhibitory effects of its leaf and fruit fractions on free radicals, acetylcholinesterase, 15-lipoxygenase, and carbohydrate hydrolyzing enzymes. *J Food Biochem* 44. <https://doi.org/10.1111/jfbc.13137>
8. Klingelhofer I, Morlock GE (2015) Bioprofiling of surface/wastewater and bioquantitation of discovered endocrine-active compounds by streamlined direct bioautography. *Anal Chem* 87:11,098–11,104. <https://doi.org/10.1021/acs.analchem.5b03233>
9. Moricz AM et al (2020) Distinction and valorization of 30 root extracts of five goldenrod (*Solidago*) species. *J Chromatogr A*. <https://doi.org/10.1016/j.chroma.2019.460602>
10. Agatonovic-Kustrin S, Morton DW (2020) Hyphenated TLC as a tool in the effect-directed discovery of bioactive natural products. *Appl Sci* 10:1123. <https://doi.org/10.3390/app10031123>
11. Hosu A, Cimpoiu C (2020) Evaluation of various biological activities of natural compounds by TLC/HPTLC. *J Liquid Chromatogr Rel Technol* 43:305–318. <https://doi.org/10.1080/10826076.2020.1725548>



Application of Paper Spray Ionization for Preliminary Amazonian Berry Fruits Components Identification

Luiz Paulo Morais de Oliveira, Débora de Sena Raposo, Luciana dos Santos Ipiranga Rodrigues, Silvio Oliveira Assunção Junior, Francinaldo Araujo da Silva-Filho, Bruna Ribeiro de Lima, Emmanoel Vilaça Costa, Afonso Duarte Leão de Souza, Hector Henrique Ferreira Koolen, and Felipe Moura Araujo da Silva

Abstract

Berry fruits, especially non-conventional berries, represent a significant source of bioactive compounds, including natural antioxidants with health promotion potential. However, their phytochemical content is almost unexplored in the Amazon region, mainly due the time-consuming, laborious, and expensive procedures. Thus, in this chapter, we describe how to access the preliminary chemical data, such as polyphenols, organic acids, and sugars, from Amazonian berries through the paper spray (PS) ionization, a simple and low-cost ambient ionization technique.

Key words Ambient ionization, Mass spectrometry, Non-conventional berries, Polyphenols, Organic acids

1 Introduction

The Amazon fruits, including berry fruits, represent a very important economic resource and a significant source of bioactive compounds [1, 2]. Regarding berry fruits, such as açai and non-conventional berries, several studies have pointed out these matrices as rich sources of natural antioxidants, thus supporting that their consumption results in health benefits, reduces the risk of various chronic diseases, including cardiovascular diseases, diabetes mellitus, cancer, and other diseases [3–5].

Although berries are rich sources of natural antioxidants such as flavonoids, tannins, and phenolic acids, other natural compounds such as organic acids and sugars are also recurrent in these matrices [3, 4, 6]. On the other hand, although several berries, especially

non-conventional berries, can be of special interest to the agroindustry due to their supposed nutritional value, their phytochemical content are almost unexplored, especially in the Amazon region [2, 7]. An example is the bluish or black-colored berries from *Clidemia* genus (Melastomataceae), known in Brazil as “buchuchu,” “buxuxu,” or “buxixu” whose few published studies highlight these species as good source for dietary fibers, minerals, polyphenols, organic acids, and sugars [7, 8].

Mass spectrometry-based approaches, including hyphenated (e.g., LC-MS) and non-hyphenated (e.g., direct infusion) approaches, have proved to be useful in the detection, quantification, and characterization of polyphenols, organic acids, and other compounds from berries extracts [9–11]. More recently, ambient ionization techniques, such as paper spray, also have been proved to be useful to the qualitative and quantitative chemical analysis of berries extracts [12]. This approach is characterized as a rapid and low-cost sampling method for preliminary analysis of complex mixtures, minimizing or eliminating sample preparation procedures [13, 14].

Here, we will describe a simple and low-cost method based on the paper spray ionization in negative and positive ion mode for preliminary chemical components identification of Amazonian berries samples, including polyphenols, organic acids, and sugars.

2 Materials

2.1 Equipment

1. Triple quadrupole mass spectrometer, model TSQ Quantum Access (Thermo Scientific, San Jose, CA, USA) equipped with a paper spray (PS) ionization source (*see Note 1*). Instrument control and data acquisition were executed on Xcalibur 2.07 (Thermo Scientific, San Jose, CA, USA).
2. Gas: high-purity argon (for collision-induced dissociation).
3. Milli-Q system (Millipore, Bedford, MA, USA).

2.2 Reagents

1. Methanol (HPLC grade) (Merck, Darmstadt, Germany).
2. Ultrapure water was obtained from the Milli-Q system.

2.3 Supplies

1. Mortar and pestle.
2. Syringes or pipettes with proper tips for handling solvents.
3. Filter paper (Whatman International Ltd., Maidstone, England). (chromatography paper can be used).

3 Methods

After collection or purchase, the berry fruits should be washed with distilled water and kept at $-5\text{ }^{\circ}\text{C}$ shielded from ambient light until analysis to avoid oxidation and other degradative processes.

3.1 Sample Preparation

1. Transfer a portion (approximately 200 mg) of the berries to a mortar.
2. Use the pestle to crush the berries until a paste is formed.

3.2 Paper Spray (PS) Analysis

1. Cut the paper filter into a triangular shape, 10 mm long and 5 mm wide at the base.
2. Put the triangular filter paper in contact with the berries paste until the paper is completely drenched.
3. Place the drenched triangular filter paper into the metal clip.
4. Position the triangular filter paper approximately 10 mm from the MS inlet (Fig. 1).
5. Turn on the mass analyzer and enable the continuous acquisition mode (positive or negative ion mode) (don't apply high voltage yet).
6. Transfer, with a syringe or pipette, 20–30 μL of a methanol/water solution (1:1, v:v) to the triangular filter paper.
7. Apply high voltage (3.5–5 kV) and adjust the position and distance between the sample and MS inlet until the signal stabilizes (*see* Notes 2 and 3).
8. Acquire at least 20 spectra from both, negative and positive ion modes (*see* Note 4).
9. Perform the fragmentation (MS/MS analysis) of the ions of interest (*see* Notes 5 and 6).

3.3 Data Processing and Interpretation

An example of paper spray mass spectra of Amazonian berries (*Clidemia* sp) in negative and positive ion mode is shown in Fig. 2. Also, the MS/MS spectra of some polyphenols and organic acids present in this species is shown in Fig. 3.

1. Open the raw file with Xcalibur software: Qual Browser > File > Open (*see* Note 7).
2. With the TIC window enabled, right-click > ranges > scan filter > select the desired filter (a region in TIC will be highlighted).
3. Enable the mass spectrum window and process at least 10 spectra from the TIC for full scan (negative and positive ion modes) and MS/MS data (*see* Note 8).
4. Compare the MS/MS spectra with previously published data (*see* Note 9).

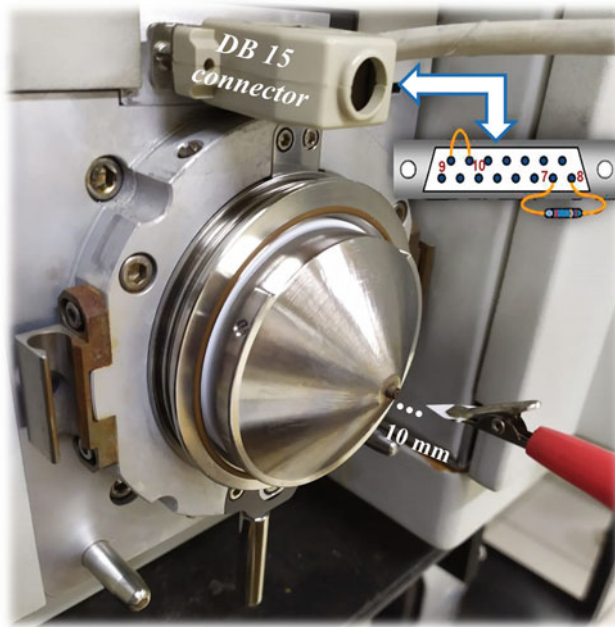


Fig. 1 Home-built paper spray interface with a DB15 connector prepared to promote ESI source recognition

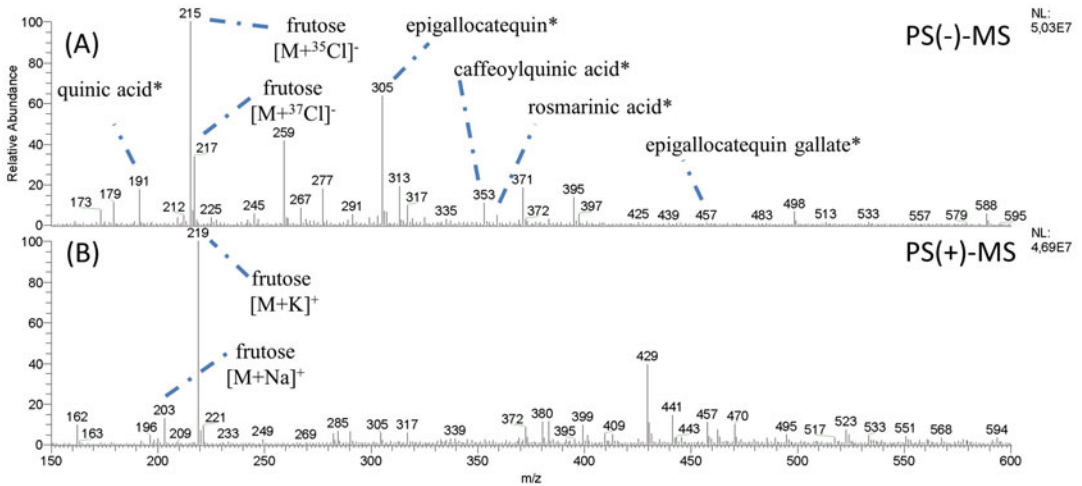


Fig. 2 Paper spray mass spectra of *Clidemia* sp. in negative (a) and positive (b) ion modes with * denoting the compounds tentatively identified by manual interpretation of MS/MS spectra and comparison with literature data

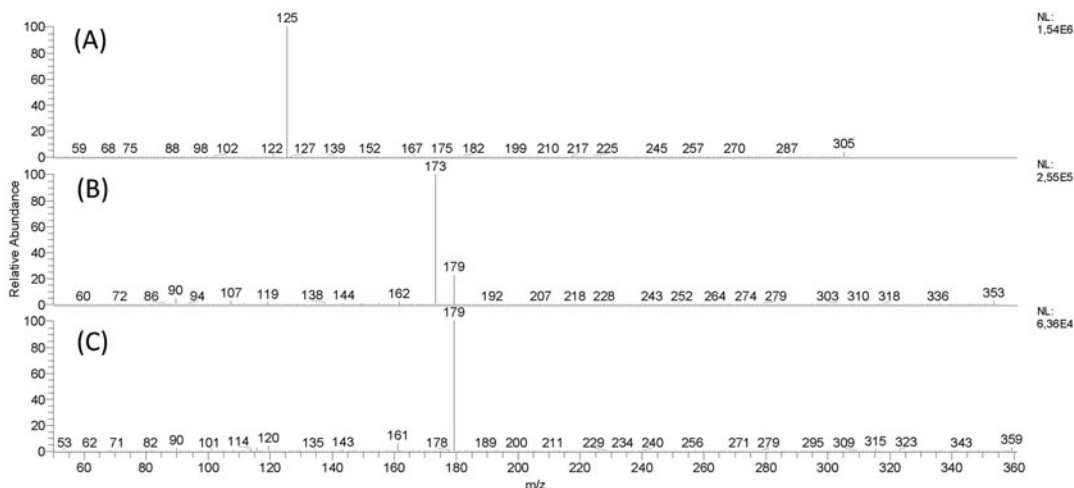


Fig. 3 MS/MS spectra of the ions at m/z 305 (a), 353 (b), and 359 (c)

4 Notes

1. For Thermo Scientific mass spectrometers such as the models TSQ Quantum Access and the LCQ Fleet, the substitution of the housing for a DB15 male connector promote the LS-MS interface. For this, a jumper must be created between sockets 9 and 10, and a 2k Ohm resistor must be attached directly between sockets 7 and 8 (Fig. 1).
2. Take care, high voltage applied combined with a distance between the sample and the MS inlet less than 5 mm can promote an electric arc and collapse the instrument.
3. If the triangular filter paper dries and signal loss occurs, more of the methanol/water solution (1:1, v:v) should be added.
4. The cone needs to be cleaned after 10 samples to avoid ion suppression.
5. It is recommended to fragment the ions with the relative abundance above 20%. On the other hand, a brief survey of the literature of related species can assist in the selection of minority ions.
6. In triple quadrupole mass spectrometers, the fragmentation of adduct ions, such as $[M+Na]^+$, $[M+K]^+$, $[M-Cl]^-$ cannot occur, or occurs with great difficulty.
7. This protocol can be used with Xcalibur version 2.07 or higher.
8. Due to their acidic character, the ionization of polyphenols and organic acids had occurred mainly in the negative mode. On the other hand, for *in natura* samples, sugars are mainly

observed as adduct ions (e.g., $[M+Na]^+$, $[M+K]^+$, $[M-Cl]^-$) (Fig. 2).

9. The MS/MS data for a large amount of organic acids and polyphenol compounds, previously reported in berry fruits, can be found in food journals and related, mainly in LC-MS/MS-based works.

References

1. Bataglion GA, da Silva FM, Eberlin MN, Koolen HH (2015) Determination of the phenolic composition from Brazilian tropical fruits by UHPLC-MS/MS. *Food Chem* 180: 280–287. <https://doi.org/10.1016/j.foodchem.2015.02.059>
2. Gordon A, Jungfer E, da Silva BA, Maia JGS, Marx F (2011) Phenolic constituents and antioxidant capacity of four underutilized fruits from the Amazon region. *J Agric Food Chem* 59:7688–7699. <https://doi.org/10.1021/jf201039r>
3. Schreckinger ME, Lotton J, Lila MA, de Mejia EG (2010) Berries from South America: a comprehensive review on chemistry, health potential, and commercialization. *J Med Food* 13:233–246. <https://doi.org/10.1089/jmf.2009.0233>
4. Szajdek A, Borowska EJ (2008) Bioactive compounds and health-promoting properties of berry fruits: a review. *Plant Foods Hum Nutr* 63:147–156. <https://doi.org/10.1007/s11130-008-0097-5>
5. Paredes-López O, Cervantes-Ceja ML, Vignapérez M, Hernández-Pérez T (2010) Berries: improving human health and healthy aging, and promoting quality life—a review. *Plant Foods Hum Nutr* 65:299–308. <https://doi.org/10.1007/s11130-010-0177-1>
6. Mikulic-Petkovsek M, Schmitzer V, Slatnar A, Stampar F, Veberic R (2012) Composition of sugars, organic acids, and total phenolics in 25 wild or cultivated berry species. *J Food Sci* 77:C1064–C1070. <https://doi.org/10.1111/j.1750-3841.2012.02896.x>
7. Gordon A, Schadow B, Quijano CE, Marx F (2011) Chemical characterization and antioxidant capacity of berries from *Clidemia rubra* (Aubl.) Mart. (Melastomataceae). *Food Res Int* 44:2120–2127. <https://doi.org/10.1016/j.foodres.2011.01.015>
8. Serna DMO, Martínez JHI (2015) Phenolics and polyphenolics from Melastomataceae species. *Molecules* 20:17818–17847. <https://doi.org/10.3390/molecules201017818>
9. Tian Y, Liimatainen J, Alanne AL, Lindstedt A, Liu P, Sinkkonen J, Kallio H, Yang B (2017) Phenolic compounds extracted by acidic aqueous ethanol from berries and leaves of different berry plants. *Food Chem* 220:266–281. <https://doi.org/10.1016/j.foodchem.2016.09.145>
10. Pietrzak W, Nowak R, Gawlik-Dziki U, Lemieszek MK, Rzeski W (2017) LC-ESI-MS/MS identification of biologically active phenolic compounds in mistletoe berry extracts from different host trees. *Molecules* 22:624. <https://doi.org/10.3390/molecules22040624>
11. McDougall G, Martinussen I, Stewart D (2008) Towards fruitful metabolomics: high throughput analyses of polyphenol composition in berries using direct infusion mass spectrometry. *J Chromatogr B* 871:362–369. <https://doi.org/10.1016/j.jchromb.2008.06.032>
12. Cody RB, Tamura J, Downard KM (2018) Quantitation of anthocyanins in elderberry fruit extracts and nutraceutical formulations with paper spray ionization mass spectrometry. *J Mass Spectrom* 53:58–64. <https://doi.org/10.1002/jms.4033>
13. Liu J, Wang H, Manicke NE, Lin JM, Cooks RG, Ouyang Z (2010) Development, characterization, and application of paper spray ionization. *Anal Chem* 82:2463–2471. <https://doi.org/10.1021/ac902854g>
14. Wang H, Manicke NE, Yang Q, Zheng L, Shi R, Cooks RG, Ouyang Z (2011) Direct analysis of biological tissue by paper spray mass spectrometry. *Anal Chem* 83: 1197–1201. <https://doi.org/10.1021/ac103150a>



Analysis of Food Components by MALDI Imaging Mass Spectrometry: Sample Preparation for Identification of Peptides in Dry-Cured Ham

Dina Rešetar Maslov

Abstract

Matrix-assisted laser desorption/ionization (MALDI) imaging mass spectrometry (IMS) is a modern analytical tool that in parallel enables identification of analytes and visualization of their spatial distribution through sample (cryo-)section. Although primarily *ex vivo* tissue samples in biological and clinical research are analyzed by MALDI IMS, this analytical method is slowly introduced also into food analysis and foodomics. Here, we present and discuss important sample preparation steps and good practice in sample handling prior to MALDI IMS identification of peptides on/in dry-cured ham cryo-sections. Optimized sample preparation analytical workflow is composed of the following procedures: (1) embedding and cryostat cutting of dry-cured ham sample, (2) mounting of cryo-section on a glass slide, (3) washing of mounted cryo-section, and (4) MALDI matrix sublimation and recrystallization. Systematic sample preparation enabled preservation of sample morphology and thoroughly removed high salt and lipid content present in samples due to dry-curing production.

Key words MALDI imaging MS, Mass spectrometry, Food, Dry-cured ham, Peptides

1 Introduction

Mass spectrometry (MS) in combination with chemometrics has matured into a vital analytical technique with an array of modern applications in food research and, especially, foodomics [1]. The systematic sample preparation and optimization/validation of analytical method along with the development of advanced analytical instrumental platforms composed of hyphenated separation techniques contributed to the latter. Such instrumental platforms are, for example, liquid/gas chromatography (LC or GC) or capillary electrophoresis (CE) coupled with high-resolution mass spectrometry (HRMS) instruments [2–4]. In general, the improved and/or novel analytical approaches facilitate and accelerate food analysis and enable deep characterization of in food present analyte

molecules, both food compounds and contaminants [5]. The analytical workflows composed of MS-based hyphenated methods frequently ask for food homogenization, followed by extraction or isolation of analyte(s) prior to their separation, detection, and identification/quantification [6, 7]. The latter analytical workflow makes it difficult to study the physical position or spatial distribution of analyte(s) molecules in the analyzed sample.

On the contrary, the matrix-assisted laser desorption/ionization (MALDI) imaging mass spectrometry (IMS) is a “soft” ionization technique predominately used for screening of analyte molecules on *ex vivo* tissue (histology) biological samples [8]. Since recently, the MALDI IMS has been more frequently applied in food research and foodomics, both in analysis of food of animal and plant origin [9–13]. Based on acquired m/z values, the MALDI IMS enables precise structural characterization and label-free identification of multiple analytes, such as lipids, proteins, peptides, or small molecules. When compared to previously mentioned MS-hyphenated methods, the MALDI IMS is advanced as allows for generation of spatially resolved analytical information. In other words, the MALDI IMS enables visualization of spatial arrangement of detected and, subsequently, identified analyte molecules that are present on thin sample (cryo-)section, frequently fixed on classic microscopic glass slide (Fig. 1). In contrast to traditional microscopy-based histological techniques, the MALDI IMS provides simultaneous identification of multiple molecules without prior application of labels or antibodies, that is, in a label-free approach. Accordingly, the dedicated image-processing algorithms for MALDI IMS data usually enable (1) visualization of spatial distribution for detected analytes, (2) investigation of molecular heterogeneity of samples, (3) region-specific mapping and regionally specific classification based on molecular differences, and (4) statistical analysis of hundreds to thousands of molecular ions detected in a single MS experiment.

The quality of MALDI IMS data highly depends, next to sample preparation treatments, on configuration of applied mass spectrometer, particularly the characteristics of MALDI laser and mass analyzer. To achieve high mass accuracy and resolving power, the usage of HRMS mass spectrometers is highly recommended, for example, mass spectrometers with quadrupole time-of-flight (QTOF), Fourier transform ion cyclotron resonance (FTICR), and orbitrap mass analyzers. Furthermore, instruments with smaller MALDI laser beam diameter (30–50 μm for non-imaging dedicated MALDI MS instruments, let us say regular MALDI MS instrument) and smaller raster steps (for instance, below $20 \times 20 \mu\text{m}$ for non-imaging dedicated MALDI MS instruments) contribute to higher lateral resolution. More recently, dedicated (scanning) MALDI IMS instruments were introduced by different instrument vendors. Such scanning MALDI MS instruments are

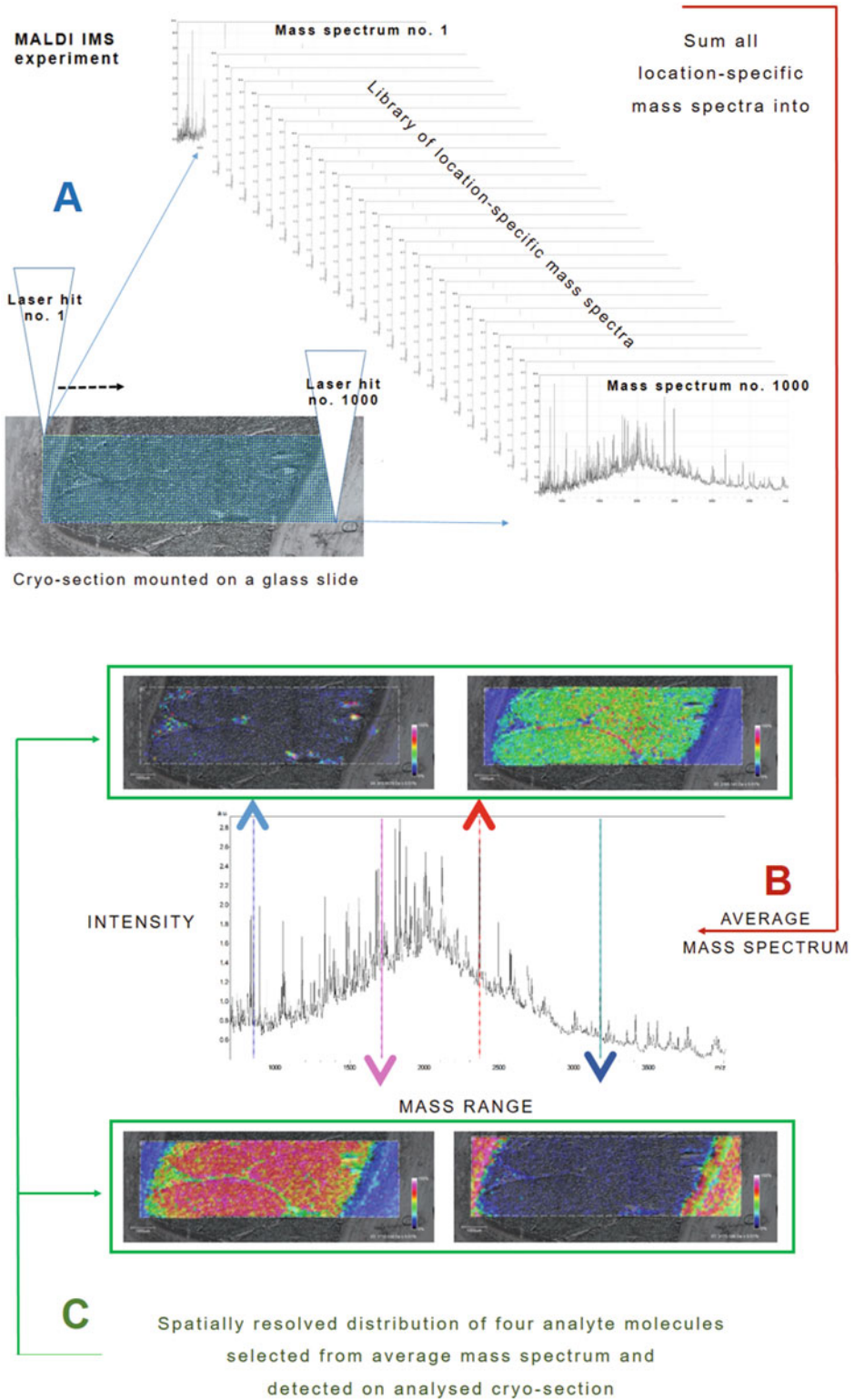


Fig. 1 MALDI IMS data acquisition, processing, and image reconstruction

equipped with specific optical set-up for focusing the laser beam, and mechanical systems that accelerate scanning of the sample area.

As shown in Fig. 1a, in the MALDI IMS method the laser scans step-by-step through tissue cryo-section mounted on a glass slide such as clinical tissue or food (cryo-)section. After exposure to MALDI laser beam, the analyte molecules present on sample (cryo-)section, firstly desorb/ionize and enter the mass spectrometer, secondly, are separated by their mass-to-charge ratio (m/z value) in mass analyzer and finally, are detected on mass detector. In described process, the analyte molecules that are present either on or near the surface of analyzed tissue sections and within the laser focus, ionize and transfer into the gas phase. After separation by their m/z value, analyte molecules will be represented within MALDI IMS mass spectrum as singly charged ions. During the MALDI IMS experiment, for every scanning position in raster (marked with blue dots that form rectangle in Fig. 1a) one mass spectrum is created. In other words, a library of location-specific mass spectra is generated during one MALDI IMS experiment, with pre-defined lateral resolution (set prior MALDI IMS experiment start with selection of instrumental settings) and lateral assignment for each mass spectrum. Therefore, during one MALDI IMS experiment hundreds to thousands of location-specific mass spectra can be acquired. The total number of mass spectra depends on the scanning (raster) size. The intensity of mass signals that represent detected analyte molecules in a spectrum is transferred into a greyscale value (or rainbow color code) and prescribed to a matching position in a raster (pixel) map.

In addition, per every analyzed tissue sample a MALDI IMS average mass spectrum is generated (Fig. 1b), which represents the profile of all detected molecular ions for scanned sample, in pre-defined instrumental detection settings, such as mass detection range. When an ion is selected from MALDI IMS average spectrum, an image-processing algorithm creates the spatial and intensity distribution map, with as many pixels as the number of acquired single mass spectra (Fig. 1c). Distribution maps can be created for all molecular ions or just few selected ions present in an average mass spectrum. The latter depends on the experimental question and set research goals.

Many image-processing algorithms enable image overlap of sample (cryo-)section image obtained by light microscope and MALDI IMS data (Fig. 1c). The latter visualization facilitates interpretation of MALDI IMS data. Furthermore, to increase the identification rate of detected molecular ions, the MALDI tandem mass spectrometry (MS/MS), fragmentation mode of measurement, may be optimized and applied. In such a way, generated fragmentation mass spectra facilitate identification of detected analyte molecules even on/in complex food samples. For example, peptides generated during production of dry-cured hams may be

identified after selective and optimized removal of lipid fraction and salts, that is, during sample treatment prior to MALDI IMS experiment.

Here, we demonstrate that MALDI IMS with comprehensively optimized sample preparation is excellent analytical tool for visualization of spatial distribution of peptides generated during dry-cured ham production. With application of optimized analytical workflow and instrumental settings, we were able to detect and identify peptides present on/in dry-cured ham sections with intramuscular fat content ranging from 3.6 to 4.7 (%) and salt (NaCl) content from 5 to 6.5 %.

1.1 Sample Preparation Analytical Workflow Prior to MALDI IMS Experiment

The set of sample preparation steps applied prior to MALDI IMS experiment is highly dependent on the complexity and characteristics of sample tissue and the physical-chemical properties of target analyte(s). Therefore, a specific and optimized sample preparation protocol is an essential requirement for MALDI IMS detection of exact molecular profiles [14, 15], for example, peptides in dry-cured ham. Comprehensive sample preparation optimization is frequently employed for every sample type and application and may include optimization of several equally important steps one after another or in parallel (Fig. 2). The latter contributes to (1) preservation of sample morphology, (2) removal of interfering compounds, that is, reduction of ion interference and/or ion suppression, and detection of exact molecular profiles, (3) improvement of signal quality, intensity, and increased lateral image resolution. All handling of sample must be conducted without causing loss of sample morphology and without significant lateral transfer of target analyte molecules. If available, the automation of all or majority of sample preparation steps is highly wanted as this may increase data reproducibility and method robustness and reduce human errors and processing time per sample.

In general, the optimized sample preparation workflow and instrumental settings allow for MALDI IMS to be used either for (1) fingerprinting of molecules with similar chemical characteristics in pre-defined m/z (mass-to-charge) detection range or in (2) targeted approaches for profiling of great variety of biomolecules. During development and optimization of new MALDI IMS applications, the assessment of protocol, method robustness and MALDI IMS data reproducibility is essential. Therefore, the comparison of MALDI IMS data obtained for technical replicates is important part of sample preparation, both during optimization and during real experiments. Finally, sample preparation workflows and data acquisition settings must be regularly updated with development of new or improved sample preparation methods, protocols, and devices as well as with introduction of novel MALDI IMS instruments.

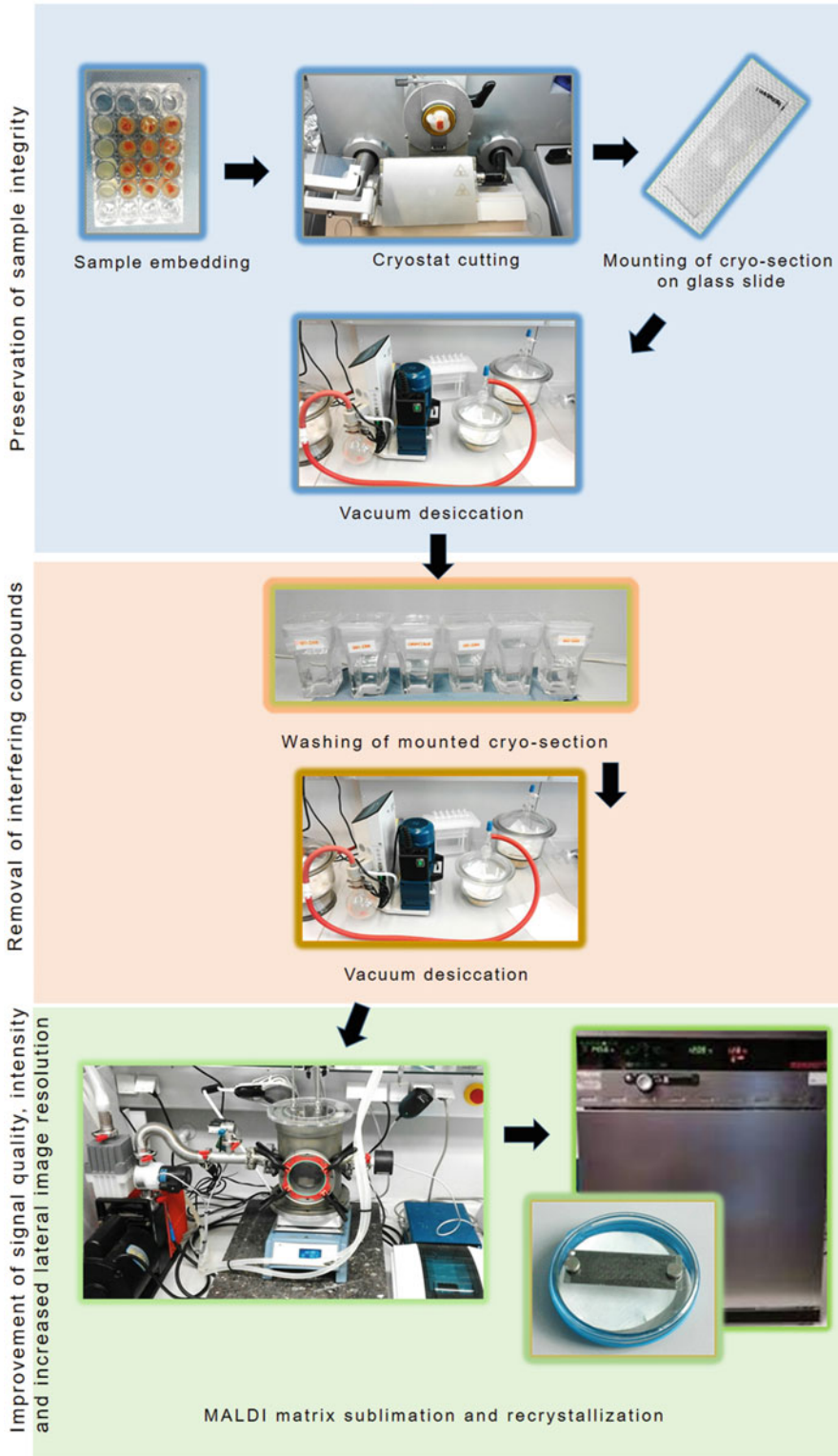


Fig. 2 Sample preparation prior to MALDI IMS analysis of peptides on/in dry-cured ham cryo-sections

*1.1.1 Preservation of
Tissue Morphology: Tissue
Embedding and Cutting
Steps Followed by
Mounting of Cryo-Section
on Glass Slide*

To preserve morphological features of sample, the whole or a piece of sample may be embedded into non-polymer soft materials, such as (1) gelatine and agarose for embedding of soft tissues or (2) carboxymethyl cellulose (CMC) for embedding of larger and stiffer specimens [16–18]. Embedding media mixtures, with different adhering properties to sample tissue surface are also taken into consideration. The role of embedding material is to provide firm support during sample (cryo-)sectioning, which contributes to preservation of sample integrity, that is, tissue section morphology. The embedding material must be stable at cutting and storage ($-80\text{ }^{\circ}\text{C}$) temperatures and through washing procedures. No cross-contamination, that is, transfer of embedding medium molecules on tissue surface should occur at any time of sample preparation or MALDI IMS analysis.

The evaluation of sample morphology by light microscopy is highly recommended during sample sectioning and other steps during sample preparation. The sample handling during (cryo-)sectioning may similarly contribute to loss of sample morphology if this is poorly performed. Therefore, comprehensive optimization is crucial to achieve high quality (cryo-)sections. Several cutting parameters should be taken into considerations, namely, (1) the optimal cutting temperature, (2) the section thickness, (3) the temperature of sectioning, (4) the orientation of the cryostat blade relative to sample, and (5) the glass slide mounting conditions.

If analyte molecules and/or sample are temperature sensitive, the cryo-slicing is a better option than cutting at a room temperature. For example, when working with animal tissues, the reported thickness of cryo-sections is in the range from eight to $20\text{ }\mu\text{m}$, while the mostly used temperature range of cryo-sectioning chamber is from $-40\text{ }^{\circ}\text{C}$ to $-20\text{ }^{\circ}\text{C}$. Thicker sections may also be cut, but one should bear in mind that thicker sections need longer to dry, and the inspection of section morphology with light microscopy is less feasible. Additionally, when thicker sections are fixed on conductive glass slide, such as optically transparent indium-tin oxide (ITO)-coated glass slides, the insufficient effect between section and glass slide may result in poor MALDI IMS data. Therefore, cutting sample into the lowest possible cutting thickness proves to be optimal for majority of sample types for MALDI IMS. The selection of optimal sectioning temperature depends on sample characteristics, such as fat content and density. For instance, the low sectioning temperatures are recommended for samples with high fat content, while many suggest sectioning at warmer temperatures for denser tissues [14]. However, the best practice is to conduct comprehensive sample preparation optimization for every sample type and application.

The cryo-sections may be mounted on a microscopic glass: (1) slide adapted to cryostat chamber temperature using the

thaw-mounting method, or (2) kept at a room temperature, while section transfer is conducted by gently pressing the glass slide against section on a cryostat. Moreover, any tissue section transferring method is acceptable if this results with a well-fixed section, with even surface and without or with minimal tears and bumps that do not affect subsequent MALDI IMS analysis. However, the transfer of molecules between different regions of cryo-section or from other surfaces on the cryo-section through direct or indirect contact should be avoided or minimized if washing of slides is not performed subsequently. Immediately after mounting of cryo-section, the on glass-mounted cryo-section should be dried using a vacuum desiccator to mitigate sample instability before further sample preparation or storage.

1.1.2 Removal of Interfering Compounds: Washing of Mounted Tissue Cryo-Section

The next equally delicate MALDI IMS sample preparation step is washing. Specific washing procedures are optimized based on the analytical characteristics of target analyte and sample type [14, 15]. Washing protocols are composed of several consecutive steps of submerging the glass-mounted cryo-section into containers with washing (organic/inorganic) solvents for a defined time. Sometimes, also gentle swirling is performed, however, this should be done with caution as swirling may increase transfer of molecules from different section regions and/or facilitate detachment of cryo-section from glass slide. In general, the washing workflow should enable selective removal of molecules present on mounted tissue cryo-sections. More specifically, washing procedures contribute to complete or partial removal of interfering compounds present in food matrix. As liquids are used during washing step, the substantial lateral delocalization of analyte over the sample (cryo-) section or analyte degradation may be the result of poor solvent or washing program selection. The latter, may have a negative effect on analytical resolution. Preferably, the target compound should not be affected at all by washing.

For instance, the lipids that easily desorb/ionize, suppress other molecular ions present in lower abundance or those that desorb/ionize less easily. Consequently, lipids are the dominant ion fraction in most MALDI IMS spectra if not removed during washing procedures with organic solvents of different polarity (Table 1). If present in higher abundance, lipids might reduce ionization of target analyte(s), such as peptides. Next to lipids, salts are also present in high amount in dry-cured ham. If not removed by washing with water-based solvent, the presence of salt on/in tissue samples can negatively affect MALDI ionization and/or increase formation of salt adducts with proteins and peptides, consequently hampering the identification of molecular ions. Finally, the presence of interfering compounds on cryo-sections may negatively affect the sample preparation procedures that follow

Table 1
Organic solvents commonly used in washing procedures prior to MALDI IMS experiments

Solvent name	Formula	Relative polarity ^a
Cyclohexane	C ₆ H ₁₂	0.006
Pentane	C ₅ H ₁₂	0.009
Hexane	C ₆ H ₁₄	0.009
Heptane	C ₇ H ₁₆	0.012
Toluene	C ₇ H ₈	0.099
Benzene	C ₆ H ₆	0.111
Ether	C ₄ H ₁₀ O	0.117
Methyl t-butyl ether	C ₅ H ₁₂ O	0.124
Chlorobenzene	C ₆ H ₅ Cl	0.188
Acetone	C ₃ H ₆ O	0.355
Acetonitrile	C ₂ H ₃ N	0.460
2-propanol	C ₃ H ₈ O	0.546
Acetic acid	C ₂ H ₄ O ₂	0.648
Ethanol	C ₂ H ₆ O	0.654
Methanol	CH ₄ O	0.762
Water	H ₂ O	1

^aRelative polarity value were extracted from "Solvents and Solvent Effects in Organic Chemistry," Christian Reichardt, <https://onlinelibrary.wiley.com/doi/book/10.1002/9783527632220>

later on, for example, the MALDI matrix application. In more detail, if present on cryo-sections in higher abundance, the interfering compounds such as lipids may cause MALDI matrix crystallization problems or induce the formation of heterogeneous MALDI matrix coverage, the so-called sweet spots of MALDI matrix [15]. The latter are localized higher concentrations of MALDI matrix crystals that result in poor MALDI IMS results. Although the washing procedures may increase the signal quality and intensity in the MALDI IMS spectrum, washing must be conducted with extreme care and patience. The inadequate sample handling and selection of solvents can dramatically change the quantity and spatial distribution of target analyte within a sample.

1.1.3 Application of MALDI Matrix

In MALDI IMS, the application of MALDI matrix is equally important step as washing. The MALDI matrices are chemically synthesized or natural compounds that easily evaporate and have strong optical absorption in either the ultraviolet or the infrared range. Moreover, the MALDI matrix crystallizes fast when

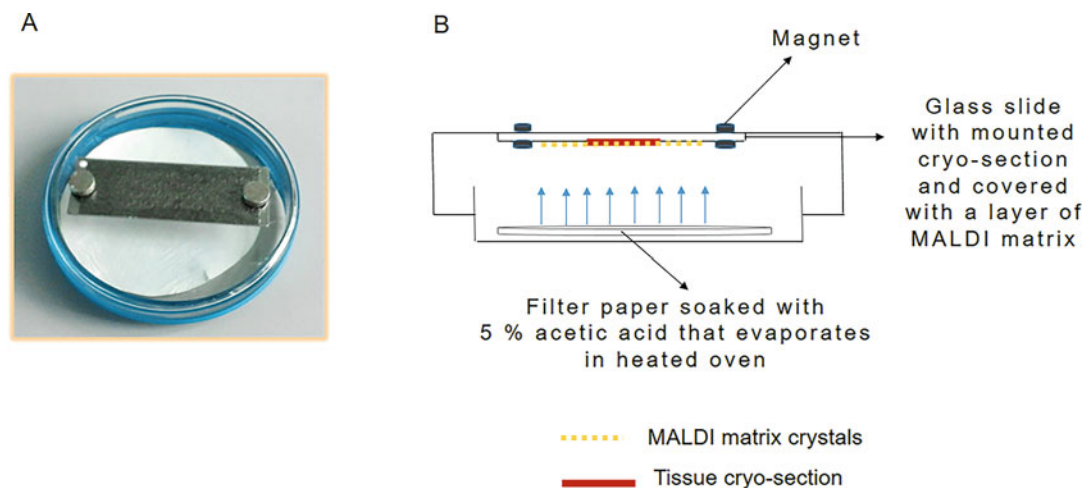


Fig. 3 MALDI matrix recrystallization in Petri dish, real experiment (a) and scheme (b)

deposited along with sample solution on MALDI target plate. Analyte molecules should co-crystallize with MALDI matrix; therefore, the homogeneous application and formation of small MALDI matrix crystals is crucial when aiming at high lateral resolution in MALDI IMS. In MALDI MS, the matrix acts as a buffer between analyte molecules on/in sample surface and MALDI laser and protects bio(-molecules) from direct exposure to a powerful MALDI laser. Moreover, the MALDI matrix provides proton donor or acceptor needed for ionization of molecules (Fig. 3).

There are different MALDI matrices available as a first choice for different class of analytes and analytical questions, and only a small selection is shown in Table 2. For instance, the α -cyano-4-hydroxycinnamic acid (HCCA) is used in majority of proteomics MALDI MS experiments, such as peptide-mass-fingerprints and fragmentation (MS/MS) experiments. The size and shape of MALDI matrix crystals is particularly important in MALDI IMS experiments. In addition, the selection of right MALDI matrix and dissolution solvents should be optimized for each application and for MALDI instrument available because the MALDI laser type also influences on quality of MALDI IMS results. A mixture of MALDI matrices or dissolution solvents in different ratios may also be under investigation with the aim of fine-tuning protocols.

When peptides are targeted by MALDI MS, the two types of MALDI matrices are more frequently used than others, these are namely, α -cyano-4-hydroxycinnamic acid (HCCA) and 2,5-dihydroxybenzoic acid (DHB). These MALDI matrices have low molecular weight and, in positive ionization mode, they mostly produce ions below m/z 500, which is useful in MALDI MS analysis of analyte molecules with $MW \geq 500$. Furthermore, they both easily evaporate, which makes them suitable in analysis of

Table 2
Commonly used MALDI matrices and their applications. The two MALDI matrices marked in bold are frequently used in MALDI MS analysis of peptides

MALDI matrix	Frequently used abbreviation	Application
1,5-diaminonaphthalene	1,5-DAN	MALDI IMS of lipids, detection possible in positive and negative ionization modes
3,5-dimethoxy-4-hydroxycinnamic acid (Sinapinic acid)	SA	MALDI IMS and MS of high-weight molecules, such as proteins ($MW \geq 5000$ Da), mostly in positive ionization mode
α-cyano-4-hydroxycinnamic acid	HCCA	MALDI IMS, MS, and MS/MS of middle-weight molecules, such as proteins and peptides ($MW \leq 20000$ Da), mostly in positive ionization mode
2,5-dihydroxybenzoic acid	2,5-DHB	MALDI IMS and MS of lower-weight molecules, such as peptides, oligosaccharides, nucleotides, and synthetic polymers, mostly in positive ionization mode
9-aminoacridine	AA	MALDI IMS and MS of lower-weight molecules such as lipids and metabolites, mostly in negative ionization mode

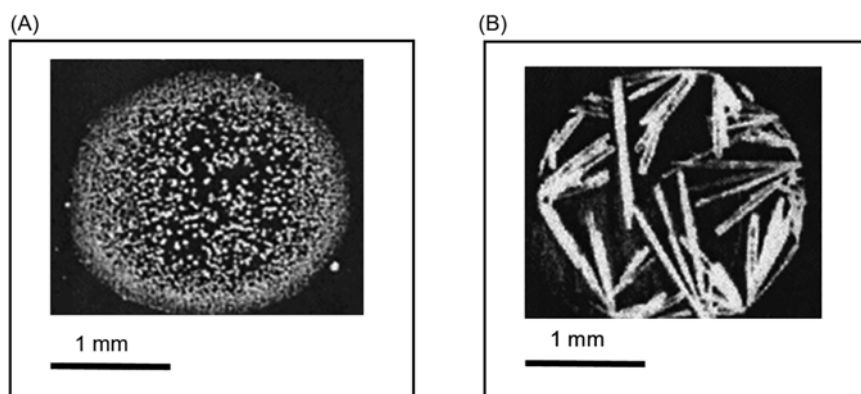


Fig. 4 Comparison of crystals size and shape for two MALDI matrices, namely (a) α -cyano-4-hydroxycinnamic acid (HCCA) and (b) 2,5-dihydroxybenzoic acid (DHB)

lower- and middle-weight molecules. However, due to crystal's micro-size and shape (Fig. 4), the HCCA is better suited for MALDI IMS applications in which higher spatial resolution is targeted.

In MALDI IMS approach, the sublimation of MALDI matrix under vacuum is favored compared to other MALDI matrix deposition techniques, such as spraying and spotting of MALDI matrix solution on (cryo-)sections. During vacuum sublimation, the MALDI matrix is deposited on top of sample (cryo-)section as a homogeneous, thin layer of smaller and equally shaped MALDI matrix crystals. The latter advantage is particularly important if analytical sensitivity and spatial resolution of target molecules should be conserved. For molecular classes that ionize less easily, such as peptides, the interaction between MALDI matrix and analyte molecules must be further induced in order to achieve optimal ion formation [19]. Therefore, resolubilization or recrystallization step is performed to induce axial diffusion either of analyte molecules into the MALDI matrix layer or vice versa. The recrystallization of MALDI matrix and its deeper penetration in sample tissue is induced by solvent evaporation, such as acetic acid, which is at the same time good proton donor and facilitates analyte ionization. The recrystallization step should be performed with care, without causing any (or with minimal) lateral analyte migration.

2 Materials

In preparation, use solvents of analytical or mass spectrometry grade and ultrapure water ($\Omega_m < 18 \text{ S/cm}$ at $22 \text{ }^\circ\text{C}$) prepared by purifying deionized water. If possible, use only laboratory glassware and other containers made of glass.

2.1 Embedding of Dry-Cured Ham

1. Embedding media: 20% (w/v) gelatin plus 7% (w/v) carboxymethyl cellulose. Weigh 20 g of gelatine and 7 g of CMC. Transfer both into a glass beaker and gradually add ultrapure water until total of 100 mL is reached. Mix all with a glass rod and gradually warm up to $50 \text{ }^\circ\text{C}$ in a water bath. Constantly mix solution during heating until you have homogenous viscous solution (*see Note 1*).
2. One 24-well sterile culture plate with flat bottom comprised of clear nontreated polystyrene (*see Note 2*).
3. At least one sample cube (1 cm^3) dry-cured ham (*see Note 3*).
4. Refrigerator ($-20 \text{ }^\circ\text{C}$).

2.2 Cryostat Sectioning and ITO Glass Slide Mounting

1. Cryostat and cryostat blades (*see Note 4*).
2. Optically transparent indium-tin oxide (ITO)-coated glass slides and glass slide rack (*see Note 5*).
3. Embedded dry-cured ham (sample).
4. Prepare 5 mL of ultrapure water for freeze mount of embedded sample on the cryostat.

5. Refrigerator ($-80\text{ }^{\circ}\text{C}$).
6. Vacuum desiccator.

2.3 Washing of Mounted Cryo-Sections

1. Nine glass containers for solvents (*see Note 6*).
2. Prepare 50 mL of each washing solvent per sample: 100% isopropanol (in three containers), 70% isopropanol (in three containers), Carnoy's solution, modified Carnoy's solution, and ultrapure water (for the last three solvents one container for each). For Carnoy's solution, mix 60% (v/v) ethanol, 30% (v/v) chloroform, and 10% (v/v) glacial acetic acid. For modified Carnoy's solution, mix 60% (v/v) ethanol, 30% (v/v) methyl-tert-butyl ether, 10% (v/v) glacial acetic acid (*see Note 7*).
3. Vacuum desiccator.

2.4 MALDI Matrix Application and Recrystallization

1. MALDI matrix solution: weigh 25 mg of α -cyano-4-hydroxycinnamic acid (HCCA) and dissolve it in 3 mL of acetone/ acetonitrile solution (7/3, v/v) (*see Note 8*).
2. Prepare MALDI matrix sublimation apparatus according to vendor provided protocol. Here, we used an in-house method and apparatus.
3. For recrystallization step prepare (needed material per one glass slide):
 - (a) Prepare 3 mL of 5 % (v/v) acetic acid solution. For dilution of acetic acid, use ultrapure water.
 - (b) Prepare one Petri dish made of glass, four magnets (0.5–1 cm in diameter), five layers of filter paper (should be at least the same size as glass slide, not smaller).
 - (c) Laboratory oven ($85\text{ }^{\circ}\text{C}$).

2.5 MALDI IMS Measurement

1. Prepare MALDI MS instrument, MALDI glass slide holder and software for MALDI IMS data processing and visualization. In the preparation of the latter, please follow the instrument vendor provided guidelines. Here, we used the MALDI-TOF/RTOF MS (UltrafleXtreme, Bruker Daltonics) equipped with smartbeam-II laser (10 μm laser beam size) and vendor provided software (FlexControl and FlexImaging, Bruker Daltonics)
2. Prepare standard mixture (calibrant) for external five-point calibration of MALDI MS instrument. Perform calibration of MS instrument before each MALDI IMS experiment. For this step, peptide standard mixture was used composed of the following peptides: bradykinin fragment 1–5 ($[\text{M}+\text{H}]^+$ m/z 573.3150), angiotensin II human ($[\text{M}+\text{H}]^+$ m/z 1046.5424), neurotensin ($[\text{M}+\text{H}]^+$ m/z 1672.9176), ACTH clip 18–39 ($[\text{M}+\text{H}]^+$ m/z 1465.1989), and insulin bovine β -chain oxidized ($[\text{M}+\text{H}]^+$ m/z 3494.6514) (*see Note 9*).

3 Methods

All protocols were conducted at room temperature and atmospheric pressure unless otherwise specified.

3.1 Embedding of Dry-Cured Ham

1. Place dry-cured ham cube in the center of a well of 24-well plate.
2. Slowly pour the embedding solution around and on top of dry-cured ham cube (*see Note 10*).
3. To provide good polymerization conditions, hold a 24-well plate with embedded dry-cured ham sample at $-20\text{ }^{\circ}\text{C}$ for at least 5 h before cryo-sectioning step.

3.2 Cryostat Sectioning and ITO Glass Slide Mounting

1. Adjust the cryostat chamber and cutting temperature to $-40\text{ }^{\circ}\text{C}$. Mount the cryostat blade. Remove embedded dry-cured ham from the well and put it in the cryostat chamber (*see Note 11*).
2. Use approximately 1 mL of ultrapure water to freeze mount embedded sample on a chuck in the cryostat. Let it freeze at least 30 min before cutting.
3. Start cutting embedded sample using bigger cutting steps (e.g., $100\text{ }\mu\text{m}$), until you reach sample tissue and nice even sample surface is formed. Then, adjust sectioning thickness to $12\text{ }\mu\text{m}$ and start cutting sample cryo-sections (*see Note 12*).
4. Mount a cryo-section on ITO glass slide that was kept at room temperature by gently pressing the slide against the tissue section and cryostat. You can also collect the cryo-section from the anti-roll plate of the cryostat (*see Note 13*).
5. Vacuum dry ($<8\text{ mbar}$) mounted cryo-section at least 1 h at room temperature (*see Note 14*).

3.3 Washing of Mounted Cryo-Sections

1. Submerge the mounted cryo-section into series of solvents for defined period, following the protocol in Table 3. Do not swirl or mix solution in the containers, while glass slide with mounted sample is inside (*see Note 15*).
2. Vacuum dry ($<8\text{ mbar}$) mounted cryo-section at least 1 h at room temperature before the next step (*see Note 16*).

3.4 MALDI Matrix Application and Recrystallization

1. Pour the CHCA solution in the sublimation chamber and perform the vacuum sublimation procedure at $185\text{ }^{\circ}\text{C}$ and 35 mTorr or by following the vendor provided guidelines (*see Note 17*).

Table 3
Washing procedure protocol

Solvent name	Volume (mL)	Washing duration (min)
100% isopropanol	50	1
70% isopropanol		1
Carnoy's solution ^a		2
70% isopropanol		1
Modified Carnoy's solution ^b		2
100% isopropanol		1
Ultrapure water		4
70% isopropanol		1
100% isopropanol		1

^aCarnoy's solution (C.s.) = 60% (v/v) ethanol, 30% (v/v) chloroform, 10% (v/v) glacial acetic acid

^bModified C.s. = 60% (v/v) ethanol, 30% (v/v) methyl-tert-butyl ether, 10% (v/v) glacial acetic acid

2. After vacuum sublimation, perform recrystallization step. For this step, slide on the inner side of Petri dish cover using magnets. Place Petri dish in pre-heated oven at 85 °C for 2 min.
3. Take Petri dish out of oven, quickly place filter paper soaked in 3 mL of 5% acetic acid in Petri dish below glass slide that was fixed in previous step. Close Petri dish and place it in pre-heated oven (85 °C) for 4 min (*see Note 18*).
4. After 4 min take the Petri dish out of oven and open it.
5. The tissue cryo-section is ready for MALDI IMS experiment (*see Note 19*).

3.5 MALDI IMS Measurement

1. Adjust the MALDI instrumental parameters following the instructions in Table 4. These parameters are optimal for the MALDI-TOF/RTOF MS (UltrafleXtreme,
2. Bruker Daltonics).
3. Calibrate the MALDI MS instrument according to vendor guidelines.
4. Perform MALDI IMS experiment (*see Note 20*).

4 Notes

1. Prepare embedding material fresh prior to the embedding of sample. To remove air bubbles from embedding solution (prior embedding your sample), use sonication option in water bath until all bubbles come out of solution.
2. Instead of well plate, you can use silicone mold for making pralines. Once the polymerization of embedding media is finished, you will be able to remove embedded samples more easily from silicone mold.

Table 4
MALDI IMS instrumental settings

Data acquisition mode	Linear positive ion mode on MALDI-TOF/ RTOF MS
Detection mass range	Between m/z 700 and 4000
The number of laser shots accumulated at one raster position	500
The raster step size	100 μm
Laser attenuator offset	60% (constant laser power)
Laser frequency	2 kHz
Pulsed ion extraction	120 ns
Sampling rate	2.00 GS/s

3. Wash scalpel between cuts with fresh ethanol. Dry scalpel before further cutting.
4. Clean cryostat blade between samples with ethanol. Dry cleaned blade before mounting on cryostat. New cryostat knife may also be used for each sample to speed up the sectioning step.
5. Always wash glass slides prior the usage. Even when glass slides are new, a certain amount of dust and other contamination particles are present on them. Clean glass slide will increase quality of sample mounting and effect between sample and glass for ITO slides. For washing glass slides: place the slides on a rack and submerge all in a series of freshly prepared solvents in beakers following the line: (1) acetone, (2) methanol, (3) ultrapure water, and (4) methanol. Wash glass slides in first three solvents for 10 min each and just rinse with methanol as the fourth solvent. Placing the beakers with solvents into ultrasonic bath will improve the washing procedure.
6. Use glass containers rather than plastic. Plastic containers might release polymers that can deposit on your sample cryo-section and result in irreversible contamination of your sample. The newly purchased glass-staining jars with lids, as used in microscopy, are suitable.
7. Change washing solvents with fresh batch after each glass slide.
8. Use ultrasonic bath to speedup dissolution until all MALDI matrix crystals are dissolved completely.
9. The selected peptide mixture was chosen based on the preferred measurement mass range. For this experiment, peptides

were measured between m/z 700 and 4000. For example, if peptides with m/z value above 3494.6514 are targeted, additional peptide standard with higher mass must be added into standard mixture and calibrant list.

10. For slowly pouring the embedding medium around your sample, use pipette with a sterile 5 mL tip or a syringe. Avoid formation of air bubbles. If these do form, you can sonicate your well plate for a few seconds until bubbles come out.
11. Close cryostat chamber and leave all at least half an hour before the next step. In this way, all parts of the cryostat chamber and embedded sample will adjust to cutting temperature; they will equilibrate well before cutting.
12. The perpendicular cryostat blade orientation is favorable during cryo-sectioning of muscle sample, that is, tissue made of fibers, as fibers tend to curl when parallel orientation of blade is used.
13. While mounting the cryo-section on a glass slide, make sure that sample morphology is preserved and that a flat surface is achieved. To observe the latter, you can inspect the quality of cryo-sections mounted on glass slide by visual inspection and with more detail by light microscopy. Mounting of several sections on one glass slide is definitely a plus for increased method robustness, but repeated mounting may lead to the structure collapse of previously mounted sections.
14. After vacuum drying, you can proceed with the following sample preparation step (washing) or mounted cryo-section can be stored at $-80\text{ }^{\circ}\text{C}$ in airtight container (e.g., 50 mL plastic tube) for at least couple of month. However, cryo-sections are hygroscopic and one should prevent accumulation of humidity in storage container, which can happen while opening the refrigerator door and container cap.
15. If the cryo-section was held at $-80\text{ }^{\circ}\text{C}$ before washing step, perform vacuum drying ($<8\text{ mbar}$) at least 1 h at room temperature before starting the washing procedure. A “no wash” control, cryo-section that was not subjected to washing, can be used in the evaluation of effectiveness of applied washing procedure and signal intensities may be used as quality indicators. Precisely, peptide-ion signals are observed above m/z 1000 and lipid ion signals below m/z 1000. Reduction or complete removal of lipid ion signals is considered as an improvement.
16. Washed cryo-section can be held in the vacuum drying chamber over night to prevent accumulation of humidity until the next sample preparation procedure.
17. As additional quality control step, the weight of the ITO glass slide with mounted cryo-section before and after sublimation

can be measured. Subsequently, the average amount of matrix per cm^2 can be calculated as the ration of MALDI matrix on glass slide (mg) and total area of glass slide (cm^2).

18. The filter paper soaked in 5% acetic acid must be directly below glass slide. Do not change their positions as the 5% acetic acid solution should evaporate and cause MALDI matrix recrystallization. Therefore, it is important that glass slide is fixed on Petri dish cover. The maneuverer during which soaked filter paper is put in Petri dish must be completed in a fast (15 s) and precise manner. Therefore, practicing in advance is strongly suggested.
19. After MALDI matrix vacuum sublimation and recrystallization do not store the cryo-section for later. The MALDI IMS experiment should be performed within one day. Until MALDI IMS analysis, to prevent accumulation of humidity and possible analyte molecule relocation, keep glass slide in vacuum desiccator.
20. After MALDI IMS experiment, tissue sections mounted on glass slide may be used in the following tissue staining protocols, such as hematoxylin and eosin (H & E) staining.

Acknowledgment

This work was supported by the bilateral Science and Technology Cooperation project “The application of mass spectrometry-based ‘omics’ technologies to characterize products relevant for biotechnology and agriculture” funded by OeAD and the Croatian Ministry of Science and Education. Dina Rešetar Maslov acknowledges: (1) support from a TU Wien-Shimadzu Mass Spectrometry CEE fellowship, (2) guidance and help during MALDI IMS sample preparation given by Full Prof. Martina Marchetti Deschmann, PhD and her research group (Anastasiya Svirikova, Melike Dinc, and Matthias Holzlechner), and (3) access to equipment provided by TU Wien and Full Prof Günter Allmaier.

References

1. Ibáñez C, Simó C, García-Cañas V, Acunha T, Cifuentes A (2015) The role of direct high-resolution mass spectrometry in foodomics. *Anal Bioanal Chem* 407(21):6275–6287. <https://doi.org/10.1007/s00216-015-8812-1>
2. Acunha T, Ibáñez C, García-Cañas V, Cifuentes A, Simó C (2016) CE-MS in food analysis and foodomics. In: de Jong G (ed) *Capillary electrophoresis-mass spectrometry (CE-MS): principles and applications*. Wiley-VCH Verlag GmbH & Co. KGaA, pp 193–215
3. Gilbert-López B, Valdés A, Acunha T, García-Cañas V, Simó C, Cifuentes A (2017) Foodomics: LC and LC-MS-based omics strategies in food science and nutrition. In: Fanali S, Haddad PR, Poole C, Riekkola M-L (eds) *Liquid chromatography: applications*, 2nd edn. Elsevier, pp 267–299

4. Majchrzak T, Kalinowska K, Lubinska-Szczygeł M, Różańska A, Dymerski T, Wardencki W et al (2021) Recent applications of 1D GC-MS and 2D GC-MS in foodomics studies. In: *Comprehensive foodomics*. Elsevier, pp 19–38
5. Rešetar D, Pavelić SK (2018) Application of foodomics for food toxins. In: *Reference module in food science*. Elsevier
6. Moreda-Piñeiro J, Moreda-Piñeiro A (2021) Sample preparation in foodomics. Combination of assisted-extraction techniques to the comprehensive foodomics. In: *Comprehensive foodomics*. Elsevier. p. 581–608
7. Martinović T, Šrajter Gajdošik M, Josić D (2018) Sample preparation in foodomic analyses. Vol. 39, *Electrophoresis*. Wiley-VCH Verlag, pp 1527–1542. <https://doi.org/10.1002/elps.201800029>
8. Norris JL, Caprioli RM. Analysis of tissue specimens by matrix-assisted laser desorption/ionization imaging mass spectrometry in biological and clinical research. Vol. 113, *chemical reviews*. American Chemical Society; 2013. p. 2309–2342. doi: <https://doi.org/10.1021/cr3004295>
9. Canela N, Rodríguez MÁ, Baiges I, Nadal P, Arola L (2016) Foodomics imaging by mass spectrometry and magnetic resonance. *Electrophoresis*. 37(13):1748–1767. <https://doi.org/10.1002/elps.201500494>
10. Li B, Dunham SJB, Dong Y, Yoon S, Zeng M, Sweedler JV (2016) Analytical capabilities of mass spectrometry imaging and its potential applications in food science. *Trends Food Sci Technol* 47:50–63. <https://doi.org/10.1016/j.tifs.2015.10.018>
11. Yoshimura Y, Goto-Inoue N, Moriyama T, Zaima N (2016) Significant advancement of mass spectrometry imaging for food chemistry. *Food Chem* 210:200–211. <https://doi.org/10.1016/j.foodchem.2016.04.096>
12. Yoshimura Y, Zaima N (2020) Application of mass spectrometry imaging for visualizing food components. *Foods* 9(5):575. <https://doi.org/10.3390/foods9050575>
13. Morisasa M, Sato T, Kimura K, Mori T, Goto-Inoue N (2019) Application of matrix-assisted laser desorption/ionization mass spectrometry imaging for food analysis. *Foods* 8(12):633. <https://doi.org/10.3390/foods8120633>
14. Goodwin RJA (2012) Sample preparation for mass spectrometry imaging: Small mistakes can lead to big consequences. *J Proteomics* 75(16): 4893–4911. <https://doi.org/10.1016/j.jprot.2012.04.012>
15. Kaletaş BK, van der Wiel IM, Stauber J, Dekker LJ, Güzel C, Kros JM et al (2009) Sample preparation issues for tissue imaging by imaging MS. *Proteomics* 9(10):2622–2633. <https://doi.org/10.1002/pmic.200800364>
16. Altelaar AFM, van Minnen J, Jiménez CR, Heeren RMA, Piersma SR (2005) Direct molecular imaging of *lymnaea stagnalis* nervous tissue at subcellular spatial resolution by mass spectrometry. *Anal Chem*. 77(3): 735–741. <https://doi.org/10.1021/ac048329g>
17. Cillero-Pastor B, Heeren RMA (2014) Matrix-assisted laser desorption ionization mass spectrometry imaging for peptide and protein analyses: a critical review of on-tissue digestion. *J Proteome Res* 13(2):325–335. <https://doi.org/10.1021/pr400743a>
18. Vandenbosch M, Nauta SP, Svirikova A, Poeze M, Heeren RMA, Siegel TP et al (2021) Sample preparation of bone tissue for MALDI-MSI for forensic and (pre)clinical applications. *Anal Bioanal Chem* 413(10): 2683–2694. <https://doi.org/10.1007/s00216-020-02920-1>
19. Yang J, Caprioli RM (2011) Matrix sublimation/recrystallization for imaging proteins by mass spectrometry at high spatial resolution. *Anal Chem* 83(14):5728–5734. <https://doi.org/10.1021/ac200998a>



Modern Tools in Food Chemical Characterization Using Mass Spectrometry Data and Molecular Networking: Revisiting the Study Case of Solanaceae Family

Celio Fernando Figueiredo Angolini and Ana Paula Aparecida Pereira

Abstract

Untargeted chemical characterization approaches can be performed via many different mass spectrometry (MS) experiments and frequently generate hundreds of data. Interpreting such type of information can be tricky, once many molecules can be detected on both MS modes and lot of isomers can be found. Herein, we will show some bioinformatic tools using GNPS online platform and their applicability in food analysis, using as examples chemical characterization of two Solanum fruits: fruta-do-lobo (*Solanum lycocarpum* St. Hill) and the juá-açu (*Solanum oocarpum* Sendtn). Using molecular networking, we were able to detect 15 spermidine derivatives (kukoamine analogs) and 8 steroidal glycosides (saponins), which could be further improved to 19 spermidine derivatives and 31 steroidal glycosides using feature-based molecular networking.

Key words Molecular network, Dereplication, Fragmentation patterns, Global Natural Products Social Molecular Networking

1 Introduction

When working with unknown or poorly characterized samples, the first approach to follow is using the most comprehensive characterization as possible (untargeted methodologies), especially with crude samples, when an overview of sample constituents can bring better insights about the study. Mass spectrometry (MS) is a great analytical technique for such tasks; however, dozens of different experiments can be made and also hundreds of data can be generated and its interpretation can become overwhelmed. To start with, if no idea of the constituents of samples are known, we strongly suggest to perform positive and negative MS analysis, and if possible, using some chromatographic separations (LC, CE, or even GC depends on the studied molecules). Further, together with the biological studied phenomenon, more detailed and

targeted analysis can be made. Also, interpret such type of data can be tricky, once many molecules can be detected on both MS modes and lot of isomers can be found.

A great tool in chemical characterizations which can help avoid most of those concerns is Global Natural Products Social Molecular Networking (GNPS). GNPS aimed to be a web-based mass spectrometry open-access tool for wide organization and sharing of raw, processed, or identified tandem mass spectrometry data (MS/MS). Different approaches can be used with GNPS for resolving different issues in food chemical characterization, such as classical Molecular Networking (MN), Merge Network, Feature-Based Molecular Network (FBMN), MolNetEnhancer, and others [1]. Herein, we will show some GNPS applicability in food analysis, using as examples chemical characterization of two *Solanum* fruits.

The Solanaceae family has approximately 98 genera being around 1500 species belong only to the genus *Solanum*. Only in Brazil about 500 native species are found and many of them are recognized due to their effects as antioxidant, antiproliferative, anti-leishmania, and growth promoters of probiotic bacteria [2–6]. Considering the potential of this fruit, many studies have been conducted to identify the main compounds present in these plants. Alkaloids and phenolic compounds are the most abundant, and they can be found in fruta-do-lobo (*Solanum lycocarpum* St. Hill) and the juá-açu (*Solanum oocarpum* Sendtn) [7]; in this protocol, we will show how the dereplication of crude fraction of both fruits can be easily achieved.

2 Materials

All solutions need to be prepared with ultrapure water and at least LC grade solvents. For LC solvent additives, use ultrapure reagents preferably >98% of purity. Despite your chosen chemical characterization approach, the sample preparation step is one of the most important. The first concern is about solvents and additives choices for sample extraction, they need to be compatible with the further used analytical techniques. The solvent should have the correct polarity to extract your compounds of interest, and additives (acids, bases, salts) must be compatible with MS. Give preference for organic and volatile additives such as formic or acetic acid and ammonium salts. Some of them are compatible but tend to enhance adduct formation during MS ionization, such as TFA, so use them only if necessary. Also, the sample preparation needs to be designed according to the objective of the experiment. In our example, we are studying two different fruits from same family, which are known in folk medicine for their antidiabetic properties. In our scenario, we decided to explore the crude sample characterization before any biological experiment, once the fruits were poorly studied and fewer information were known about their compositions.

2.1 Sample

Preparation: Crude Extracts

1. Workbench freeze-dryer Liotop L101, Liobras (Brazil).
2. Blender Colombo AR 2L (Brazil).
3. Ultra-Turrax T-25 Digital Homogenizer (Germany).
4. Shaking water bath C76 New Brunswick Scientific Classic Series (EUA).
5. Benchtop Centrifuge Rotanta 460R, Hettich Zentrifugen, (Germany).
6. Rotavapor[®] Essencial coupled to Regulated Vacuum Pump and to Recirculating Chiller, Buchi (Switzerland).
7. PVDF/L filters 0.22 μm .

2.2 Acquiring Mass

Spectra, File Preparation, and Analysis

1. A Q-ToF iFunnel 6550 mass spectrometer (Agilent Technologies) was used with an electrospray ionization (ESI) source.
2. A Poroshell 120 SB-Aq 2.7 μm column (2.1 \times 100 mm, Agilent).
3. MassHunter Qualitative Analysis software (Agilent). [8]
4. Open-source software: Proteowizard (msconvert) [9], GNPS online platform (<https://gnps.ucsd.edu/>) [10], Mzmine 2 [11], and Cytoscape [12].

3 Methods

3.1 Sample

Preparation: Crude Extracts

1. Select the fruits according to the desired ripening stage. The fruits must be standardized as to ripening stage, size/weight, and to presenting structural integrity (absence of injuries).
2. Wash the fruits under running water to remove dirt.
3. Carefully separate the pulp and skin with a sharp knife. And separate the pulp from the seeds (*see Note 1*).
4. Lyophilize the fractions separately for 48 h or until complete removal of moisture (*see Notes 2 and 3*).
5. To improve the extraction process, grind the samples in a processor or blender.
6. Homogenize each lyophilized fraction with ethanolic solution (ethanol: water; 70: 30 /v: v) in a homogenizer (Ultra-Turrax) for 2 min at a concentration of 100 mg/mL (*see Note 4*).
7. Then, homogenize the solution with constant stirring for 2 h in a shaking water bath (200 rpm) at room temperature.
8. Centrifuge the extract (5 °C, 15 min, 10,000 rpm) and remove the supernatant.
9. Concentrate the extract under vacuum until complete drying.
10. Resuspend the extract in deionized water to the initial concentration (100 mg/mL).
11. Filter the extract through PVDF/L filters to avoid column clogging.

3.2 Acquiring Mass Spectra and MS Data File Preparation

Before any mass spectrometric data collections, you need to determine which methodology will be used to data treatment. Once it could have great impact on the format the data need to be collected. Here, we used the GNPS platform, specifically, MN and FBMN, both followed with MolNetEnhancer. Both approaches give different results and also need different types of data (*see Note 5*). To perform an MN analysis, it is necessary to acquire MS/MS data, and it would be better if it is in an untargeted way to achieve a comprehensive chemical characterization, with minimal or none bias inf featured selection. Therefore, the most suitable MS experiment is the data-dependent mass spectrometry analysis (DDA) with Top N feature selection.

1. Program a suitable HPLC and mass spectrometry untargeted method using the mass spectrometer control software, *see Note 6*. We use: Mobile phase A: milli-Q water with 0.1% of formic acid (FA); and mobile phase B: ACN with 0.1% of FA. The linear gradient: 0–1 min, 5% B; 1–10 min, 5% B to 18% B; 10–13 min 18% B to 70% B; 13–15 min, 70% B to 100% B (clean up) and 3 min of post time at 5% B, at a flow rate of 0.45 mL/min. The mass spectrometer voltages and temperatures were set as: VCap 3000 V; fragmentor voltage at 150 V; OCT IRF Vpp at 750 V; Gas Temperature at 290 °C; Sheath Gas Temperature at 350 °C; Drying Gas at 12 L/min and the fragmentations were performed using normalized collision energy (NCE) of 30. Mass spectra were acquired in profile and positive or negative ion mode and the acquisition range was 100–1200 m/z using DDA with top 4 peak selection and high resolution for MS and MS/MS spectra were used, resulting in a cycle time 1.2 s and approximately 6 points per chromatographic peak.
2. Dilute sample for a 1 mg/mL solution and run samples analysis. More dilutions could be needed for less complex extracts.
3. Convert mass spectra files to *.mzXML format, most vendor format conversion could be performed using MSConvert from Proteowizard. For better details and conversion parameters, see GNPS documentations (<https://ccms-ucsd.github.io/GNPSDocumentation/fileconversion/>).
4. After creating an account at GNPS platform, upload the converted LC-MS/MS files into GNPS database. Two options are available, using a File Transfer Protocol or direct at Browser through the online platform. For more details, see <https://ccms-ucsd.github.io/GNPSDocumentation/fileupload/>.

3.3 Classical Molecular Networking (MN)

For classical MN, no retention time information were used/needed, so it is possible to perform even direct infusion MS analysis (without chromatography). Nonetheless, we also intend to perform FBMN, so to save MS time we choose to perform LC-MS/MS analysis and use it for both approaches. This was necessary because FBMN takes into consideration compound retention time, once it enables the method to detect and identify different isobars, even with similar fragmentation spectra, but with different elution time. Those similar compounds are clustering together in classical MN and therefore analyzed as one feature (*see Note 7*).

1. Login in GNPS and select the option “Create Molecular Network”. Add a job title.
2. Basic options. Select the mzXML files to perform the molecular network. They can be organized in up to six groups. Also select the libraries for the dereplication routine (*see Note 8*).
3. Select the precursor ion mass tolerance and fragment ion mass tolerance, 0.05 and 0.5 Da, respectively (*see Note 9*).
4. **Advanced Network Options.** For beginners, leave those parameters as default values. If you want to change advanced parameters, read the GNPS documentation first (<https://ccms-ucsd.github.io/GNPSDocumentation/>).
5. Choose an e-mail for receiving an alert when the work is done and submit the job (Fig. 1). The complete job can be accessed here (<https://gnps.ucsd.edu/ProteoSAFe/status.jsp?task=9057807e4ed940d8bf036c1cbd45be56>).

4 FBMN Analysis

For FBMN, a more curate data pre-treatment was needed. Several options are possible and the steps will depend on your MS spectrometer, we will report here the steps for Agilent (*.D) data files, but for other mass spectrometer see <https://ccms-ucsd.github.io/GNPSDocumentation/featurebasedmolecularnetworking/>.

1. Open LC-MS files on MassHunter Qualitative analysis. Export all files in *.mzdata extension.
2. Open Mzmine2 and upload the mzdata files and follow the instructions from GNPS tutorial (<https://www.youtube.com/watch?v=5jjMllbwD-U&t=171s>). Some modifications were done as shown above.
3. Perform both levels of mass detections. (MS1 noise level—5E02, MS2 noise level—1E01).
4. Use “ADAP chromatogram builder” instead of “chromatogram builder”. (Min group size—4, Group int. 5E01, Min High. 1E02, *m/z* tolerance—10 ppm) (*see Note 10*). This

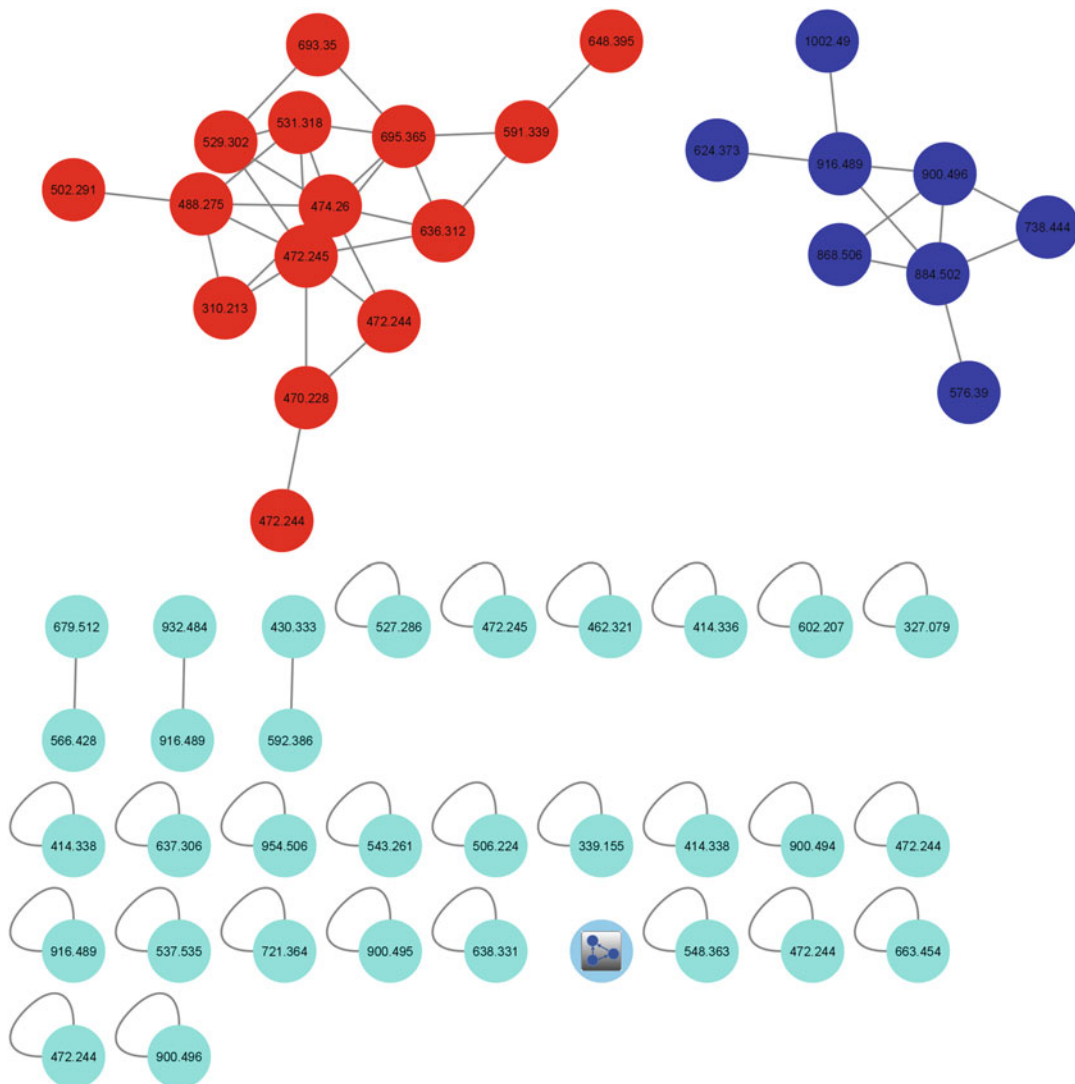


Fig. 1 A molecular network was created from both fruit analysis, red nodes were classified as phenols, but belong to the class of kukoamines, dark blue nodes were classified as steroidal glycosides (*solasonine* and *solamargine* analogs), light blue has no automated classification via MolNetEnhancer. The data was filtered by removing all MS/MS fragment ions within ± 17 Da of the precursor m/z . MS/MS spectra were window filtered by choosing only the top 6 fragment ions in the ± 50 Da window throughout the spectrum. The precursor ion mass tolerance was set to 0.05 Da and an MS/MS fragment ion tolerance of 0.5 Da. A network was then created where edges were filtered to have a cosine score above 0.65 and more than 5 matched peaks. Further, edges between two nodes were kept in the network if and only if each of the nodes appeared *in each other's* respective top 10 most similar nodes. Finally, the maximum size of a molecular family was set to 100, and the lowest scoring edges were removed from molecular families until the molecular family size was below this threshold. The spectra in the network were then searched against GNPS spectral libraries. The library spectra were filtered in the same manner as the input data. All matches kept between network spectra and library spectra were required to have a score above 0.7 and at least 6 matched peaks. To enhance chemical structural information within the molecular network, information from *in silico* structure annotations from GNPS Library Search were incorporated into the network using the GNPS MolNetEnhancer workflow (<https://ccms-ucsd.github.io/GNPSDocumentation/molnetenhancer>). Chemical class annotations were performed using the ClassyFire chemical ontology

task will create an extract ion chromatogram (XIC) for each feature detected.

5. Now for separate isobars as different features, perform the “chromatogram deconvolution”. Different algorithms are available to use Wavelets (ADAP) (m/z range—0.02, RT range 0.4). Also perform deisotope peak grouper to avoid feature redundancy.
6. Align and filter your samples (Join aligner and Filter list rows, min peak = 3, min peak isotope = 3) *see* **Note 11**.
7. Gap filling could improve your sample coverage, but should be performed with care. In our data, we observed some isobars, with very close RT, being clustering together, so we did not use it.
8. Export the *.csv file containing table list information and *.mgf files containing MS2 information.
9. Go to GNPS platform and perform the FBMN, upload *.mgf and *.csv files. The complete result can be accessed here: <https://gnps.ucsd.edu/ProteoSAFe/status.jsp?task=c8756dd7daf34c07977098373504bd10>
10. After finishing the job, download the FBMN cytoscape data and open it on Cytoscape for change color and visualizations attributes (Fig. 2).

5 MolNetEnhancer Analysis

In order to pre-classify features according to their class family, it is possible to perform the MolNetEnhancer analysis, which can combine several other identification tools find in GNPS platform to provide a more comprehensive chemical overview of metabolites. It not only excludes manual data curation, but also helps on that task.

1. After performing MN or FBMN, go to “Experimental tools box”. Analyze and choose MolNetEnhancer.
2. Insert a job title and insert ID number of your MN or FBMN analysis. Submit the job.
3. Before finishing, open the web browser view or download the file and open it on Cytoscape[®], for visualization adjustments.
4. After MolNetEnhancer analysis, we detect 15 spermidine derivatives (kukoamine analogs) and 8 steroidal glycosides (saponins) using MN and could improve it to 19 spermidine derivatives and 31 steroidal glycosides using FBMN. Some of them were automatic dereplicated (tentatively identified) by their MS/MS pattern. And now a manual data curation is needed to identify the other possible new isomers.

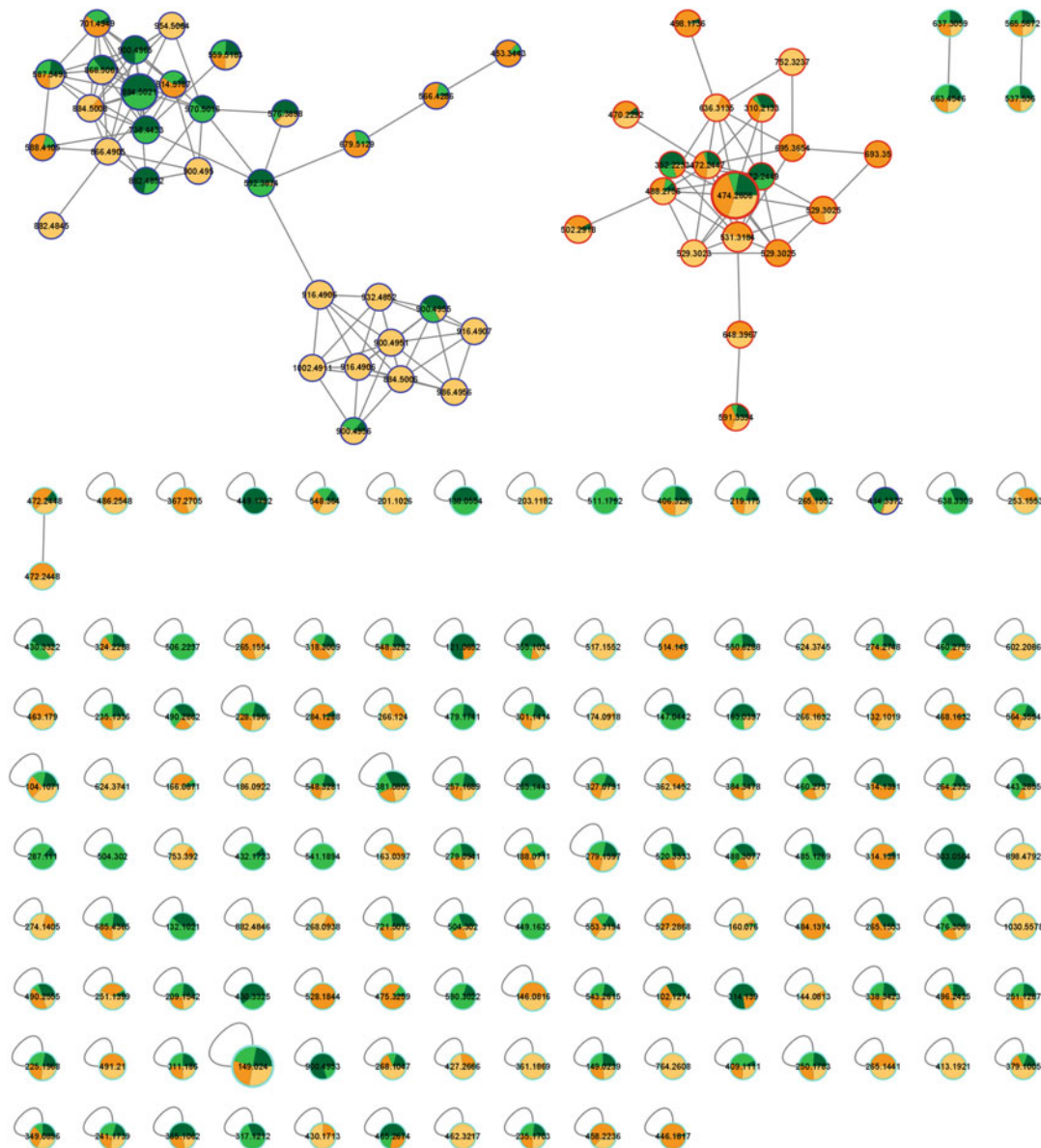


Fig. 2 A molecular network was created with the Feature-Based Molecular Networking (FBMN) workflow on GNPS. Red border nodes were classified as phenols, but belong to the class of kukoamines, dark blue border nodes were classified as steroidal glycosides (solasonine and solamargine analogs), light blue has no automated classification. Pie chart are related to the feature abundance of chromatogram analysis being dark orange and light orange Juá-açu peel and pulp, respectively, dark green and light green fruta-do-lobo peel and pulp, respectively. The mass spectrometry data were first processed with MZMINE2 and the results were exported to GNPS for FBMN analysis. The data was filtered by removing all MS/MS fragment ions within ± 17 Da of the precursor m/z . MS/MS spectra were window filtered by choosing only the top 6 fragment ions in the ± 50 Da window throughout the spectrum. The precursor ion mass tolerance was set to 0.05 Da and the MS/MS fragment ion tolerance to 0.05 Da. A molecular network was then created where edges were filtered to have a cosine score above 0.6 and more than 5 matched peaks. Further, edges between two nodes were kept in the network if and only if each of the nodes appeared in each other's respective top 10 most similar nodes. Finally, the maximum size of a molecular family was set to 100, and the lowest scoring edges

6 GNPS Clusters Annotations

1. For cluster annotation, start with clusters that contain library hits (*see* **Note 12**).
2. Elucidate the fragmentation mechanism route, it will help to tentatively identify the other compounds from the cluster (Fig. 3).
3. Initiate tentatively identification for the closest nodes and expand to all nodes in the cluster. In this cluster, only one node has a library hit, but 13 compounds could be tentatively identified after manual annotation (*see* **Note 13**, Fig. 4).

7 Notes

1. If the fruits are fully ripe, the seeds can be removed, together with the jelly portion, with the aid of a spoon. If the fruits are totally unripe, the seeds must be separated with the sharp knife.
2. To facilitate the process of removing moisture, cut each fraction into small pieces.
3. Lyophilized samples can be stored for later use, if they are packaged in suitable conditions. It is recommended that they be vacuum packed in low density polyethylene bags and frozen at -18°C until grinding.
4. This solution was selected due to the polarity of the compounds of interest (glycoalkaloids).
5. See more in GNPS documentations <https://ccms-ucsd.github.io/GNPSDocumentation/fileconversion/>
6. Both high- and low-resolution mass spectrometer are possible to be used, but it is mandatory to have MS/MS experiments with scanning fragmentation spectra (SRM, MRM, and other similar fragmentation experiments won't work). Make sure your MS acquisition method give the most quantity possible of MS/MS spectra with good quality for achieved a comprehensible MN. Generally for good MS/MS spectra not more than 4–6 precursor ion selections in each scan were needed in DDA. However, it will depend on your MS analyzer and their scan time. Generally, lower MS cycle time is needed in order to

Fig. 2 (continued) were removed from molecular families until the molecular family size was below this threshold. The spectra in the network were then searched against GNPS spectral libraries The library spectra were filtered in the same manner as the input data. All matches kept between network spectra and library spectra were required to have a score above 0.7 and at least 6 matched peaks. The molecular networks were visualized using Cytoscape software

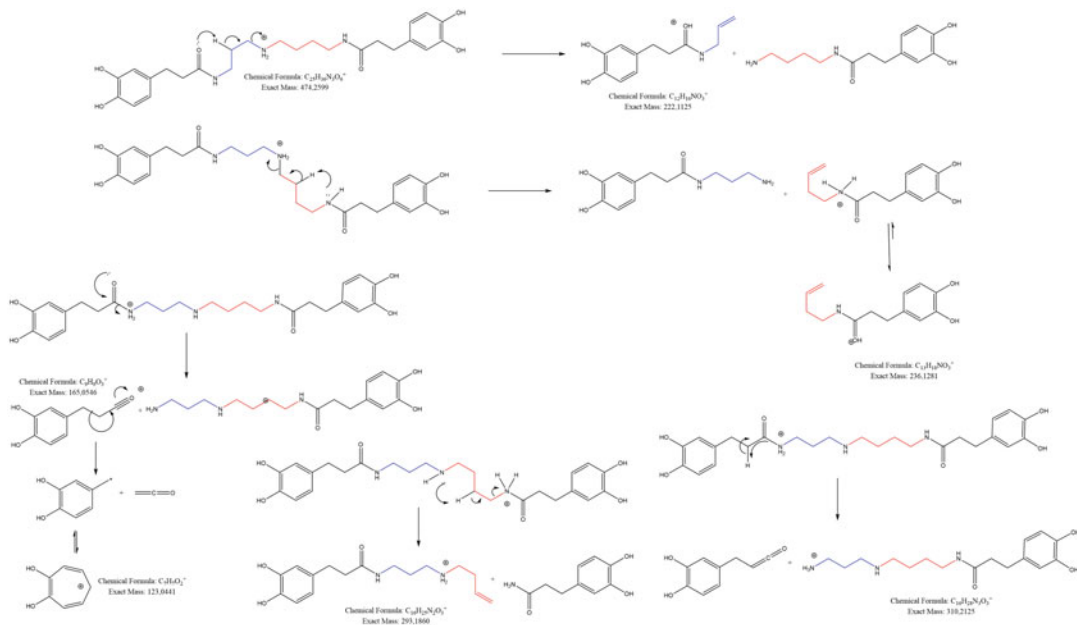


Fig. 3 Proposed MS/MS fragmentation mechanism for *N*¹,*N*¹⁰-bis(dihydrocaffeoyl)spermidine

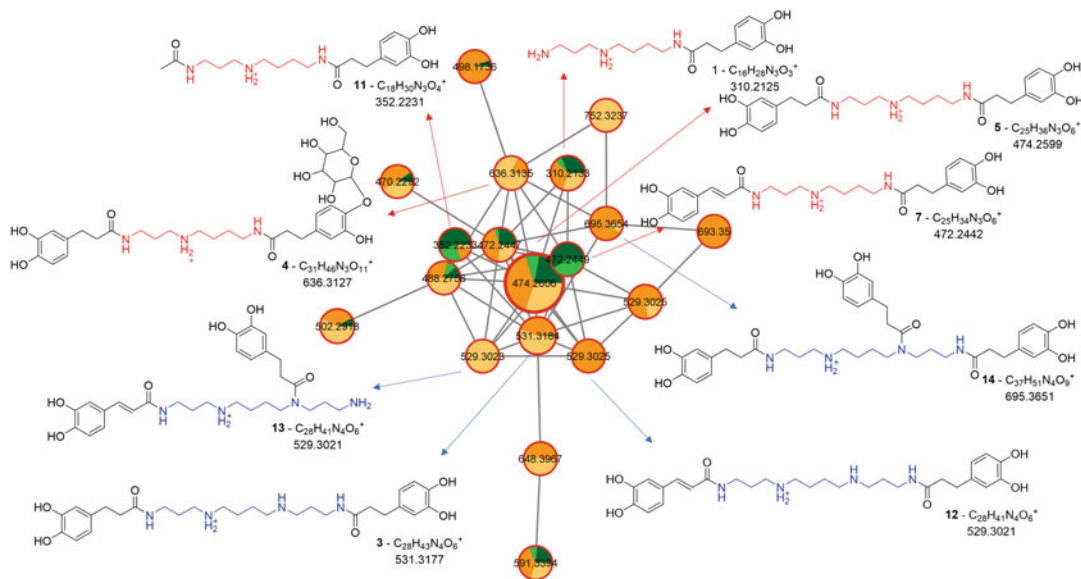


Fig. 4 FBMN Kukoamine cluster annotations from Fig. 2

fulfill MS experiments between 15 and 20 full cycles during a chromatographic peak elution (FHMW/Cycle time = 15–20) if you also perform a quantification and need good peak shape. If possible, you can lower the resolution in MS/MS spectra for

achieving such velocity, once the higher resolution is more important in full scan (MS spectra). For characterization and/or relative quantification, lower points could be used (FHMW/Cycle time = 5–10), it will generate better MS/MS spectra, but at the expense of peak shape.

7. MN use MSCluster [13], which merges the similar MS/MS spectra into a single consensus MS/MS spectrum, and once elution time is not taken into consideration this process can merge very similar isobars, detecting less features/compounds. To avoid such bias, FBMN should be used.
8. Choosing libraries is possible also to perform sample dereplication [1, 14], besides networking constructions. This step could help avoid time-consuming data analysis of already known compounds. Also, the groups did not interfere in molecular network construction; this information will be used only in the graphical representation.
9. The selected mass tolerances depend on the resolution and accuracy of the used mass spectrometer.
10. These parameters will depend on your chromatogram properties, maybe adjustments will be needed.
11. The number of features in a row will depend on how many replicates do you have of each sample, here we perform three biological replicates.
12. Even with a library hit, a manual MS/MS spectra curation were needed, compare the data with literature or standards if possible.
13. Linked node has higher cosine, which means they have similar structure. In our case, we observe different levels of instauration on hydroxycinnamic acids portions and spermine or spermidine backbone structure. These information, together with mechanism fragmentation elucidation, become easy for the identification of other analogs based on MS/MS spectra annotations. Advanced users can try some automated in silico tools at GNPS (Table 1).

Acknowledgments

This work was supported by São Paulo Research Foundation (FAPESP, grant number #2019/08853-9) and by National Council for the Improvement of Higher Education (CAPES)—Finance Code 001.

Table 1
Mass spectral data and tentative identification of compounds in extract of Juá-açu (*Solanum oocarpum* Sendtn) from kukoamine cluster

Extract	Tentatively identification	<i>m/z</i>	RT	MS/MS
Juá-açu 1	<i>N</i> -caffeoylspermidine	310.2133	0.7	222/165/123
2	<i>N</i> -caffeoylputrescine	251.1400	1.8	163/145/135/117/108
3	<i>N</i> ¹ , <i>N</i> ¹⁴ -bis(dihydrocaffeoyl)spermine (kukoamine A)	531.3191	2.4	293/222/123
4	Glu- <i>N</i> ¹ , <i>N</i> ¹⁰ -bis(dihydrocaffeoyl)spermidine (Lycibarbarspermidines)	636.3144	4.5	474/384/222/165
5	<i>N</i> ¹ , <i>N</i> ¹⁰ -bis(dihydrocaffeoyl)spermidine	474.2605	4.7	293/236/222/165/123
6	<i>N</i> ¹ , <i>N</i> ¹⁰ -bis(dihydrocaffeoyl)spermidine (isomer)	474.2608	4.8	310/236/222/165/123
7	<i>N</i> ¹ -caffeoyl, <i>N</i> ¹⁰ -dihydrocaffeoyl spermidine	472.2441	6.6	455/383/222/165
8	Unknown	502.2932	8.4	307/236/179/137
9	Solasonine	884.5002	11.8	414/396/253/147/129
10	Robeneoside B	868.5070	11.9	725/379/253/212/129
11	<i>N</i> ¹ -acetyl, <i>N</i> ¹⁰ -dihydrocaffeoyl spermidine	352.2233	1.77	222/165/123
12	<i>N</i> ¹ -caffeoyl, <i>N</i> ¹⁴ -(dihydrocaffeoyl)spermine	529.3025	6.38	367/293/222/163/129
13	<i>N</i> ¹ -caffeoyl, <i>N</i> ¹⁰ -(dihydrocaffeoyl)spermine	529.3023	2.38	458/293/222/165/129
14	<i>N</i> ¹ , <i>N</i> ¹⁰ , <i>N</i> ¹⁴ -tris(dihydrocaffeoyl)spermine	695.3654	9.2	531/293/222/165/123

References

- Wang M, Carver JJ, Phelan VV, Sanchez LM, Garg N, Peng Y et al (2016) Sharing and community curation of mass spectrometry data with Global Natural Products Social Molecular Networking. *Nat Publ Gr*. <https://doi.org/10.1038/nbt.3597>
- Carvalho IPS, Miranda MA, Silva LB, Chrysostomo-Massaró TN, Paschoal JAR, Bastos JK et al (2019) In vitro anticancer activity and physicochemical properties of SOLANUM LYCOCARPUM alkaloidic extract loaded in natural lipid-based nanoparticles. *Colloids Interface Sci Commun* 28:5–14. <https://doi.org/10.1016/j.colcom.2018.11.001>
- Da Costa CL, Arenas Velásquez AM, Passalacqua G, De Almeida L, Graminha MAS, Martins GZ et al (2018) In vitro activities of glycoalkaloids from the *Solanum lycocarpum* against *Leishmania infantum*. *Rev Bras Farmacogn* 28:673–677. <https://doi.org/10.1016/j.bjp.2018.07.008>
- Munari CC, Francielli De Oliveira P, Costa J, Campos L, De S, Lima Martins P et al Anti-proliferative activity of *Solanum lycocarpum* alkaloidic extract and their constituents, solamargine and solasonine. *Tumor Cell Lines*. <https://doi.org/10.1007/s11418-013-0757-0>
- Pereira APA, Lauretti LBC, Alvarenga VO, Paulino BN, Angolini CFF, Neri-Numa IA et al (2020) Evaluation of fruta-do-lobo (*Solanum lycocarpum* St. Hill) starch on the growth of probiotic strains. *Food Res Int* 133:109187. <https://doi.org/10.1016/j.foodres.2020.109187>
- Tioosi RFJ, Da Costa JC, Miranda MA, Praça FSG, McChesney JD, Bentley MVLB et al (2014) In vitro and in vivo evaluation of the delivery of topical formulations containing

- glycoalkaloids of *Solanum lycocarpum* fruits. *Eur J Pharm Biopharm* 88:28–33. <https://doi.org/10.1016/j.ejpb.2014.01.010>
- Pereira APA, Angolini CFF, Paulino BN, Lauratti LBC, Orlando EA, Silva JGS et al (2019) A comprehensive characterization of *Solanum lycocarpum* St. Hill and *Solanum oocarpum* Sendtn: chemical composition and antioxidant properties. *Food Res Int* 124:61–69. <https://doi.org/10.1016/j.foodres.2018.09.054>
 - Software AM (2015) Agilent MassHunter Software-your faster route to insight. BrochureAgilent
 - Kessner D, Chambers M, Burke R, Agus D, Mallick P (2008) ProteoWizard: open source software for rapid proteomics tools development. *Bioinformatics* 24:2534–2536. <https://doi.org/10.1093/bioinformatics/btn323>
 - Wang M, Carver JJ, Phelan VV, Sanchez LM, Garg N, Peng Y et al (2017) Sharing and community curation of mass spectrometry data with GNPS. *Nat Biotechnol* 34:828–837. <https://doi.org/10.1038/nbt.3597.Sharing>
 - Pluskal T, Castillo S, Villar-Briones A, Orešič M (2010) MZmine 2: modular framework for processing, visualizing, and analyzing mass spectrometry-based molecular profile data. *BMC Bioinformatics* 11. <https://doi.org/10.1186/1471-2105-11-395>
 - Shannon P, Markiel A, Ozier O, Baliga NS, Wang JT, Ramage D, Amin N, Schwikowski B, Ideker T et al (1971) Cytoscape: a software environment for integrated models. *Genome Res* 13:426. <https://doi.org/10.1101/gr.1239303.metabolite>
 - Frank AM, Monroe ME, Shah AR, Carver JJ, Bandeira N, Moore RJ et al (2011) Spectral archives: extending spectral libraries to analyze both identified and unidentified spectra. *Nat Methods* 8:587–594. <https://doi.org/10.1038/nmeth.1609>
 - Horai H, Arita M, Kanaya S, Nihei Y, Ikeda T, Suwa K et al (2010) MassBank: a public repository for sharing mass spectral data for life sciences. *J Mass Spectrom* 45:703–714. <https://doi.org/10.1002/jms.1777>



Traveling Wave Ion Mobility-Mass Spectrometry to Address Chemical Food Safety Issues

Maykel Hernández-Mesa, Gaud Dervilly, and Bruno Le Bizec

Abstract

There is growing interest in ion mobility spectrometry in the field of food analysis as a consequence of its hyphenation with mass spectrometry and increased commercialization of ion mobility-mass spectrometry instruments. In this regard, ion mobility spectrometry brings several advantages to traditional liquid chromatography-mass spectrometry workflows, including information on the collision cross section of the detected ions. This parameter provides more confidence for the identification and confirmation of compounds, which is of great value for analytical methods applied in chemical food safety as it carries legal consequences. This protocol describes the steps to follow for the implementation of traveling wave ion mobility-mass spectrometry in food safety applications, and for which the analysis of steroid metabolites has been selected as an illustrative example.

Key words Ion mobility-mass spectrometry, LC-IM-MS methods, Collision cross section, Food safety, Steroids

1 Introduction

The successful integration of ion mobility spectrometry (IMS) into traditional liquid chromatography (LC)-mass spectrometry (MS) workflows is currently attracting the attention of researchers in many fields [1]. Furthermore, interest in this separation technique has increased exponentially in recent years due to the commercialization of hyphenated ion mobility-mass spectrometry (IM-MS) instruments, which is contributing to the development of IMS-based applications in numerous fields such as food analysis [2, 3].

IMS is an electrophoretic technique in which ionized molecules are separated based on their mobility (K) in a cell filled with a neutral gas, usually N_2 , He, or CO_2 , and under an electric field. The mobility of the ions depends on their charge, size, and shape

and refers to the time required for the ions (t_d) to pass through the entire length of the mobility cell (l), as indicated in Eq. 1:

$$K = \frac{v_d}{E} = \frac{l}{t_d E} \quad (1)$$

where v_d refers to the velocity of the ions in the mobility cell and E to the applied electric field. Furthermore, the mobility of the ions is also affected by temperature and pressure as well as the physico-chemical properties of the buffer gas in the mobility cell [4].

IMS can be integrated as an additional separation dimension between chromatographic separation (seconds up to minutes range) and MS analysis (microseconds range) due to its fast separation speed on the milliseconds time scale. In this context, IMS brings several advantages to traditional LC-MS methods: (1) isobaric molecules and isomers, which can co-elute in the LC dimension and cannot be distinguished in the MS dimension, can potentially separate in the IMS dimension when showing different geometric conformation in gas phase; (2) the analytes of interest are separated from the chemical background improving the detection sensitivity, as well as cleaner mass spectra are obtained; (3) IMS provides additional information to retention indexes (e.g., retention time) and mass spectra, the so-called collision cross section (CCS), increasing confidence in molecular identification or confirmation [5].

Nowadays, there are different IMS technologies hyphenated to MS that are commercially available. Each of these technologies comes with its advantages and disadvantages over the others [6], so the choice of IMS technology to use depends on the analytical question raised. In the field of chemical food safety, there are currently high expectations about the potential of CCS to be implemented as an identification parameter in the analysis of chemical residues and contaminants in food [3]. The implementation of analytical methods for the determination of chemical residues and contaminants in food products may have legal consequences; therefore, the CCS parameter provides additional evidence to confirm the identity of a compound and increases confidence in the results of analyzes. In this sense, it should be noted that not all IMS technologies allow CCS measurements, with drift-tube ion mobility (DTIM)-MS and traveling wave ion mobility (TWIM)-MS being the most frequently applied technologies for this purpose [2]. The more recent commercialization of trapped ion mobility (TIM)-MS instruments has expanded the options available in the market to implement IM-MS technology in routine analysis and generalize CCS measurements [7].

The CCS represents the averaged momentum transfer impact area of the ion and depends on analyte–buffer gas interactions. It is not strictly an intrinsic molecular property of each compound because it depends on the experimental conditions (i.e., gas nature,

temperature, electric field), but it is a characteristic that provides specific information about the compounds analyzed [8]. This is the reason why the development of CCS databases has recently been encouraged to generate information for using this parameter for identification purposes. Within this framework, a wide range of CCS databases have been published for use in the analysis of pesticides [9], mycotoxins [10], veterinary drugs [11], among others [12]. High reproducibility of CCS measurements performed on different IM-MS instruments working under the same or similar experimental conditions has been observed [13, 14]. Thus, CCS databases can be relied upon for more confident confirmation of the presence or absence of chemical residues and contaminants in food products analyzed by LC-IM-MS. In this sense, it is important to be careful when reporting and using CCS databases since the acquisition conditions must be clearly indicated to be able to compare CCS values [4, 8]. In addition, it is necessary to take into account that the comparison of CCS values obtained by different IMS technologies is not possible or straightforward based on the first studies carried out in this regard [15].

The drift time (previously referred as t_d) is the parameter related to the ion mobility dimension generally measured by IM-MS instruments. However, for example, drift time (or ion mobility) can be directly related to CCS according to Mason-Schamp equation (Eq. 2) in DTIM systems operating under low electric field conditions. The reader is advised to consult specialized literature for more details on the fundamentals of IMS [16].

$$CCS = \frac{3}{16} \left(\frac{2\pi}{\mu k_B T} \right)^{1/2} \frac{ze}{NK} \quad (2)$$

where z and e represent the absolute charge of the ion and the elementary charge, respectively; μ indicates the reduced mass of the ion-neutral drift gas pair (i.e., $\mu = mM/(m + M)$; m and M are the ion and gas-particle masses, respectively); and k_B is the Boltzmann constant. K represents the mobility of the ions (as indicated in Eq. 1) while N refers to the gas number density.

In general, primary methods using mainly DTIM-MS systems allow direct CCS measurements under specific working conditions [13]. However, not all DTIM-MS methods are primary methods, so CCS values must be obtained through an instrumental calibration function. For example, data acquisition by primary methods involves long acquisition times and is not compatible with chromatographic separation methods, so CCS values are generally obtained from CCS calibration curves when using LC-DTIM-MS methods [3]. Calibration curves are built from data of calibrant ions with known CCS values and provide a faster manner to perform CCS measurements. In general, the application of CCS calibration curves is also the normal operating mode of TWIM-MS and

TIM-MS instruments for CCS measurements [4]. Since CCS measurements are typically carried out by secondary methods that require CCS calibration, CCS calibration has become an important step in any laboratory protocol intended to use IMS technology for CCS measurements.

This protocol describes the analytical workflow, including (1) sample preparation, (2) data acquisition, and (3) data analysis, implemented in our research group for the analysis of phase II steroid metabolites in urine samples in a public health context related to chemical food safety. Steroid analysis represents just one of multiple challenges facing chemical food safety and has been chosen as an example to illustrate the implementation of TWIM-MS technology, including CCS measurements, in this field. The administration of steroids to animals intended for human consumption and, more specifically, the application of substances with hormonal actions as growth promoters (e.g., anabolic steroids) has been prohibited in the countries of the European Union (EU) since 1988 [17]. The control of steroid levels in biological matrices of food-producing animals, including metabolites, therefore makes it possible to detect any alteration in the steroid profiles associated with the abuse of hormones to promote growth [18]. In this context, LC-TWIM-MS has recently been applied to the analysis of steroid metabolites in urine samples [19], and large CCS databases for steroids are currently available in the literature [14, 20].

Execution of this protocol involves the specific use of TWIM-MS technology, and more specifically, a Synapt G2-S HDMS instrument from Waters Corporation. In addition, it focuses on the experimental workflow to be followed for CCS measurements, highlighting important technical aspects such as CCS calibration. Data analysis (i.e., generation of CCS values) following this protocol implies the use of Driftscope software, which is also commercially available from Waters Corporation. We suggest consulting the recent book edited by Paglia and Astarita [21] that contains other protocols involving the application of IM-MS systems and alternative software to those used in the protocol described here. Finally, this protocol can be applied to numerous applications in the field of food safety if the same TWIM-MS instrumentation is used. For obvious reasons, sample preparation must be tailored to the food matrix (or related matrix), analytes of interest and associated concentration levels.

2 Materials

2.1 Reagents

1. Acetonitrile (LC-MS Chromasolv[®] grade, Sigma Aldrich).
2. Propan-2-ol (LC-MS Chromasolv[®] grade, Sigma Aldrich).

3. Ethanol (for HPLC, Promochem[®], LGC Standards).
4. Sodium formate (0.5 mM in 90/10 (% v/v) propan-2-ol/water) prepared from sodium hydroxide (1 M; Fisher Chemical[™], Fisher Scientific) and formic acid (Promochem[®], LGC Standards).
5. Formic acid (eluent additive for LC-MS, LGC Standards GmbH).
6. Sodium hydroxide (Puriss. grade, 98–100.5%, pellets, Sigma Aldrich).
7. Major Mix IMS/Calibration Kit (cat. no. 186008113, Waters Corporation).
8. Leucine-enkephalin (cat. no. 186006013, Waters Corporation).
9. Estriol 3-sulfate (cat. no. E2734-000, Steraloids), etiocholanolone glucuronide (cat. no. A3625-000, Steraloids), estradiol diglucuronide (cat. no. E1010-000, Steraloids), estrone 3-sulfate (cat. no. E2335-000, Steraloids), and testosterone glucuronide (cat. no. A6913-000, Steraloids) standard solutions in ethanol (1 mg/mL) were stored in dark at -20°C .
10. Standard Quality Control (QC) mix containing the following compounds: estriol 3-sulfate, etiocholanolone glucuronide, estradiol diglucuronide, estrone 3-sulfate, and testosterone glucuronide. Prepare an intermediate standard solution in ethanol (100 $\mu\text{g}/\text{mL}$) containing all five steroids from the stock standard solution of each steroid (1 mg/mL). The intermediate standard solution should be stored in dark at -20°C . Take an aliquot of the intermediate standard solution, transfer it to an HPLC vial and dry it with a stream of nitrogen. Reconstitute with 95/5 (v/v) water/acetonitrile containing 0.1% (v/v) formic acid to obtain a Standard QC mix with a concentration of $1\ \mu\text{g}\ \text{mL}^{-1}$ for each steroid. The Standard QC mix should be prepared each day before running sample analysis.

2.2 Samples

Bovine urine samples kept at LABERCA biobank were used for preparing this protocol. These samples were collected with the authorization for the use of animals for scientific purposes n°02323.01, in accordance with the provisions of article R. 214-124 and R. 214-125 of the French Rural Code.

2.3 Labware

1. 1.5-mL HPLC vials, including caps with polytetrafluoroethylene (PTFE) liner.
2. HPLC vials with inserts (200 μL).
3. VWR[®] centrifugal tubes (polyethersulfone (PES) membrane, 10 kDa, 500 μL ; cat. no. 82031-350).

4. 4-mL and 40-mL amber vials (for storage of standard solutions).
5. Eppendorf pipettes tips.
6. 20-mL volumetric flasks.
7. Volumetric pipettes (1 ± 0.008 mL; 0.5 ± 0.005 mL).

2.4 Equipment

1. TWIM-MS system: Synapt G2-S HDMS equipped with an ESI source (Waters Corporation).
2. LC system: Acquity UPLC[®] System (Waters Corporation).
3. LC column: Acquity UPLC[®] BEH C18, 2.1×100 mm, $1.7 \mu\text{m}$ (Waters Corporation).
4. Corning[®] LSE[™] vortex mixer.
5. Thermo Scientific[™] Sorvall[™] Legend[™] MicroCL 17R microcentrifuge.
6. Eppendorf Research plus single channel pipettes (2–20 μL ; 10–100 μL ; 20–200 μL ; 100–1000 μL).

2.5 Data Generation and Processing

1. MassLynx (version 4.2, Waters[®]) software, used for data acquisition.
2. Driftscope (version 2.8, Waters[®]) software, used for data processing and interpretation (i.e., CCS values).

3 Methods

This protocol addresses the UPLC-TWIM-MS workflow applied to the analysis of phase II steroid metabolites in urine samples. This approach is intended to detect the illegal use of steroids in food-producing animals. A similar strategy to that proposed in this protocol can be applied to the targeted or semi-targeted analysis of chemical residues and contaminants in food products and related matrices. In this sense, sample preparation must be adapted to both the matrix to be analyzed and the physicochemical properties and concentration levels of the analytes to be characterized, while data acquisition settings must be optimized for the compounds of interest. On the contrary, general settings must be established in the case of non-targeted analysis, so in this case, for example, LC-TWIM-MS protocols used in metabolomics studies can be applied [22].

3.1 Sample Preparation

1. Store urine samples at -20 °C and thaw at room temperature before sample preparation (*see Note 1*).
2. Filter the urine samples by centrifugation at $10,000 \times g$ and 15 °C for 10 min using centrifugal filters with a molecular weight cut-off of 10 kDa.

3. Recover the filtered urine sample and transfer 10 μL to a chromatographic vial with insert (*see Note 2*).
4. Dilute the sample 10 times with 0.1% (v/v) aqueous formic acid containing internal standards (if necessary for quality assurance (QA) purposes) (*see Note 3*).
5. Homogenize the sample by vortex agitation for a few seconds (~ 10 s) (*see Note 4*).
6. Submit the samples for UPLC-TWIM-MS analysis.

3.2 TWIM-MS Parameters: Tuning and Calibration

1. Prepare the sodium formate calibration solution (0.5 mM in 90/10 (% v/v) propan-2-ol/water) (*see Note 5*). To do this, first prepare a 5 mM sodium formate solution in 90/10 (v/v) propan-2-ol/water from a 0.1 mM sodium hydroxide solution in water and formic acid. Then, add 2 mL of 5 mM sodium formate solution to a 20-mL volumetric flask using a 1-mL pipette. Make up to 20 mL with 90/10 (v/v) propan-2-ol/water. Finally, sonicate the solution for 5 min for homogenization.
2. Prepare the leucine-enkephalin “lock mass” solution (2 $\mu\text{g}/\text{mL}$ in 50/50 (% v/v) water/acetonitrile solution with 0.1% (v/v) formic acid). To do this, first prepare 400 $\mu\text{g}/\text{mL}$ of leucine-enkephalin in water. Then, transfer 100 μL of the 400 $\mu\text{g}/\text{mL}$ leucine-enkephalin solution to a 20-mL volumetric flask using a 200- μL Eppendorf pipette. Make up to 20 mL with 50/50 (v/v) acetonitrile/water containing 0.1% formic acid. Finally, sonicate the solution for 5 min to homogenize it.
3. Startup the instrument according to the supplier’s instructions and set the “TOF” and “High Resolution” modes (*see Note 6*).
4. Set the ionization source conditions as indicated in Table 1 and keep “default conditions” for other instrument parameters.
5. Infuse the sodium formate calibration solution and the leucine-enkephalin “lock mass” solution directly into the TWIM-MS system at 10 $\mu\text{L}/\text{min}$ using the sample and “lock mass” capillaries, respectively.
6. As part of the QA protocol, acquire the leucine-enkephalin mass spectrum twice for 2 min each with a scan time of 0.5 min (*see Note 7*). Reference values (i.e., mass-to-charge ratio (m/z) and CCS) for the use of the leucine-enkephalin as “lock mass”: m/z 556.2771 and 229.8 \AA^2 (ESI+ conditions); m/z 554.2615 and 225.3 \AA^2 (ESI-conditions).
7. As part of the QA protocol, verify that the mass spectrum of the sodium formate calibration solution corresponds to the mass spectra commonly observed when performing mass calibration

Table 1
Electrospray ionization (ESI) conditions

Parameter	Set at . . .
Capillary voltage (sample capillary)	+3.0 kV for ESI+, –2.5 kV for ESI–
Capillary voltage ('lock mass' capillary)	+2.5 kV for ESI+, –2.5 kV for ESI–
Sampling cone	40 V
Source offset	50 V
Source temperature	150 °C
Desolvation temperature	450 °C
Desolvation gas flow	650 L/h
Cone gas flow	50 L/h
Nebulizer gas flow	6 bar

(i.e., m/z of detected ions, signal intensity, signal ratio between ions), as well as ensure the stability of the ion beam.

8. Perform the mass calibration in both ionization modes within the m/z range of 50–1200, applying the automated calibration mode and with the instrument conditions indicated in the point 4 (Table 1) as tuning setup (*see Note 8*). Signal attenuation for calibration and root-mean-square (RMS) residual mass are the parameters to be checked as part of the mass calibration quality control. A threshold of 1.0 ppm for RMS residual mass is set to accept the mass calibration carried out. Also, the entire set of ions included in mass calibration reference file must be found when performing mass calibration to accept it.
9. Switch the instrument from the “TOF” mode to the “Mobility-TOF” mode (also referred to as HDMS mode) and replace the sodium formate calibration solution with the CCS Major Mix (*see Note 9*). The ion mobility-mass spectrometry system must remain in “Operate” mode for at least 1 h prior to CCS calibration (or CCS measurements) to ensure system stability.
10. Configure the TWIM-MS settings as indicated in Table 2 for CCS calibration (*see Notes 10–12*). The “default” values are kept for other instrument parameters, such as those related to “Step Wave” conditions.
11. As part of the QA protocol, verify that the mass spectrum of the CCS Major Mix solution corresponds to the mass spectra typically observed when performing the CCS calibration (i.e., m/z of detected ions, signal intensity, signal ratio between ions) under the established TWIM-MS settings, as well as ensure the stability of the ion beam. Table 3 indicates the

Table 2
TWIM-MS setup for steroid analysis when including LC separation

			ESI+	ESI-
Conditions of the ionization source	Capillary voltage (sample capillary)		+3.0 kV	-2.5 kV
	Capillary voltage ('lock mass' capillary)		+2.5 kV	-2.5 kV
	Sampling cone		31 V	
	Source offset		40 V	
	Source temperature		150 °C	
	Desolvation temperature		350 °C	
	Desolvation gas flow		1000 L/h	
	Cone gas flow		50 L/h	
	Nebulizer gas flow		6 bar	
Gas flow rates	Helium gas		180 mL/min	
	IMS gas		90 mL/min	100 mL/min
	Trap gas		2.0 mL/min	0.4 mL/min
Triwave DC	Trap DC	Entrance	3.0	
		Bias	47.0	
		Trap DC	0.0	
	IMS DC	Exit	0.0	
		Entrance	20.0	
		Helium cell DC	50.0	
		Helium exit	-20.0	
		Bias	3	2
		Exit	0.0	
	Transfer DC	Entrance	5.0	
		Exit	3.0	
Triwave	Trap	Wave velocity	311 m/s	
		Wave height	4.0 V	
	IMS	Wave velocity	1000 m/s	550 m/s
		Wave height	40.0 V	
	Transfer	Wave velocity	219 m/s	
		Wave height	4.0 V	

composition of CCS Major Mix; therefore, the ions to monitor. Mass spectra of CCS Major Mix recorded under ESI+ and ESI- conditions are included in Fig. 1.

- Perform the CCS calibration within the m/z range of 50–1200 applying the automated calibration mode and selecting the instrument conditions indicated in the point 10 (Table 2) (*see Note 13*). CCS calibration can be performed for both ionization modes. Signal attenuation should be noted and monitored as part of the CCS calibration quality control.
- CCS calibration must be accepted by the user (Fig. 2). Since TWIM-MS settings are generally optimized for the analytes to be further analyzed and not for the CCS calibration mix (*see Note 14*), it is important to verify that the proposed calibration curve includes enough calibration points (*see Note 15*).

Table 3
Composition of CCS Major Mix, as well as m/z and CCS of protonated and deprotonated ions observed within the m/z range between 50 and 1200

Composition of CCS Major Mix	[M+H] ⁺ (ESI+ conditions)		[M-H] ⁻ (ESI- conditions)	
	m/z	CCS (Å ²)	m/z	CCS (Å ²)
Acetaminophen	152.0712	130.4	150.0555	131.5
Caffeine	195.0882	138.2		
Sulfaguanidine	215.0603	146.8	213.0446	145.2
Sulfadimethoxine	311.0814	168.4	309.0658	170.1
L-Valyl-L-tyrosyl-L-valine	380.2185	191.7	378.2029	192.5
Verapamil	455.2910	208.8		
Terfenadine	472.3216	228.7		
Polyalanine (oligomer; number of repeating units (n) = 7)	516.2782	211.0	514.2631	209.0
Leucine-enkephalin	556.2771	229.8	554.2615	225.3
Polyalanine (n = 8)	587.3153	228.0	585.3002	223.0
Reserpine	609.2812	252.3	607.2656	265.2
Polyalanine (n = 9)	658.3524	243.0	656.3368	242.1
Polyalanine (n = 10)	729.3895	256.0	727.3739	255.9
Polyalanine (n = 11)	800.4266	271.0	798.4110	268.5
Polyalanine (n = 12)	871.4637	282.0	869.4481	280.2
Polyalanine (n = 13)	942.5008	294.0	940.4852	294.6
Polyalanine (n = 14)	1013.5379	306.0	1011.5223	308.8

14. The TWIM-MS instrument is now ready for data acquisition. It is important to verify that both the loaded mass and CCS calibration profiles correspond to the calibrations performed previously (Fig. 3). As part of the QA protocol, it is necessary to note the mass and CCS calibration profiles that are used in data acquisition.

3.3 LC System Setup

1. Prepare mobile phases A and B as follows: add 1 mL of formic acid into a bottle containing 999 mL of water (phase A: 0.1% (v/v) aqueous formic acid) and add 1 mL of formic acid into a bottle containing 999 mL of acetonitrile (phase B: acetonitrile containing 0.1% (v/v) formic acid) (*see* **Note 16**).

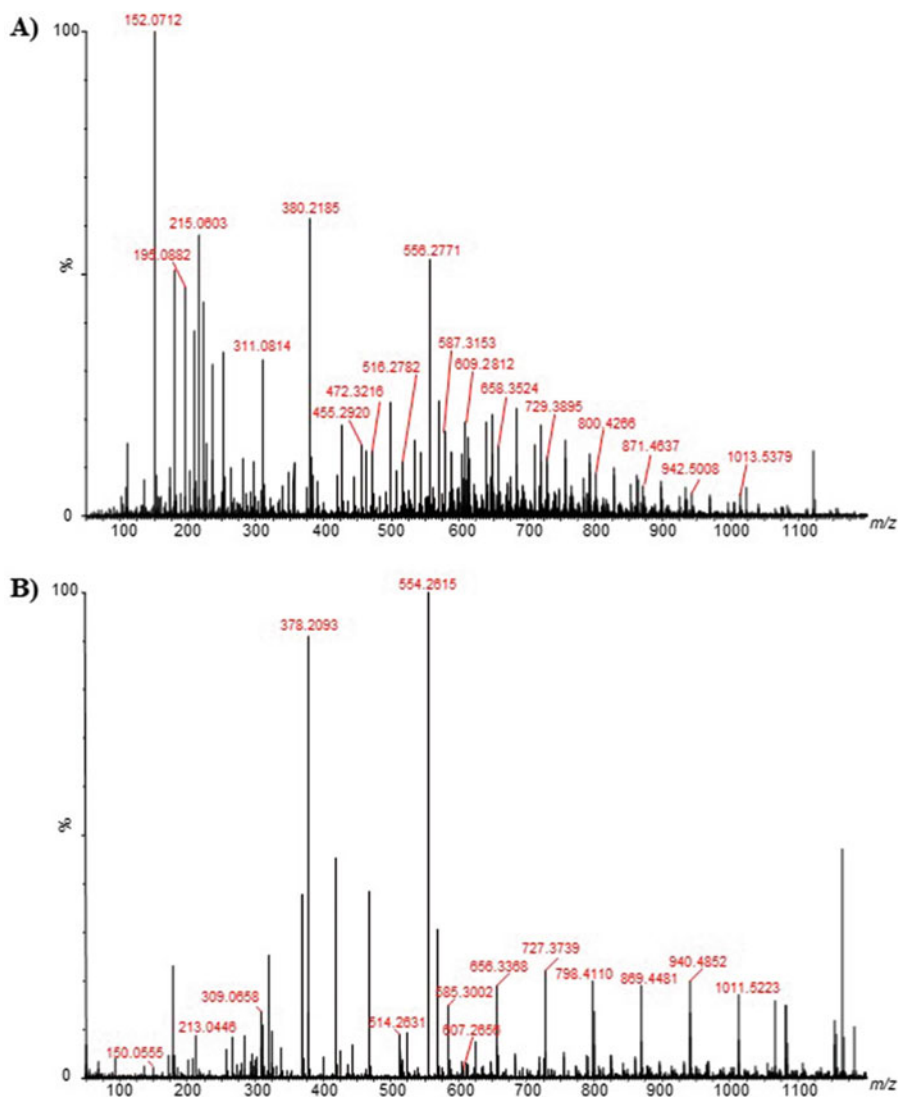


Fig. 1 Mass spectra of CCS Major Mix acquired under ESI+ (a) and ESI- (b) conditions

2. Cap and shake the mobile phase bottles vigorously to homogenize the mobile phase solutions.
3. Install the mobile phase bottles in the LC system and purge mobile phase tubes to remove air bubbles from the system.
4. Insert the column into the column compartment. An Acquity UPLC[®] BEH C18 column (2.1 × 100 mm, particle size 1.7 μm) is proposed for the analysis of phase II steroid metabolites.
5. Adjust the column temperature to 50 °C and gradually increase the flow rate of the mobile phase to 0.6 mL/min.

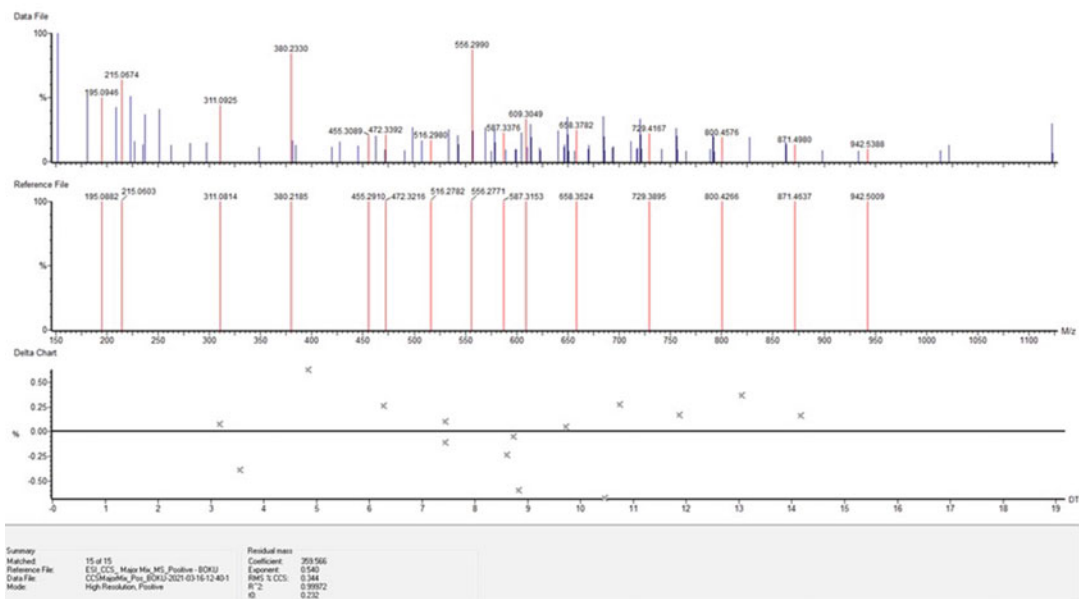


Fig. 2 Screenshot of the report generated after CCS calibration under ESI+ conditions, and which must be accepted by the user before continuing to work with the instrument. This provides information on the detected peaks compared to a set of reference ions, as well as information on the calibration curve created (corrected drift time (t_d') vs normalized cross section (Ω^2); the calibration curve is a power trend line [23], $y = Ax^b$). A 1% threshold has been set for RMS, as well as a determination coefficient (R^2) > 0.99, to accept the calibration curve

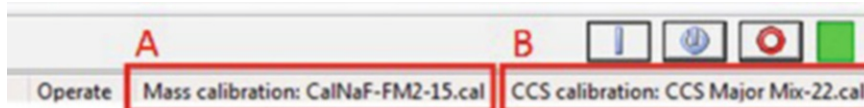


Fig. 3 Partial screenshot of the tuning instrument page showing the mass (a) and CCS (b) calibration profiles loaded into the system after performing both calibrations and before performing sample acquisition

- Set the injection volume to 5 μL and the autosampler temperature to 10 $^{\circ}\text{C}$.
- Set the elution gradient program as indicated in Table 4.

3.4 Data Acquisition

- Set ESI-conditions, as negative ionization mode is recommended for analysis of phase II steroid metabolites [24].
- Prepare the HDMS method (i.e., the acquisition method for TWIM-MS analysis). Set the m/z acquisition range to 50–1200 and the scan time to 0.5 s. Make sure the “add drift time function” and “maintain mobility separation” options are checked in the “Mobility” window. In the “Options” window, indicate that the “lock mass” solution must be refilled at the beginning of each run, and set the “lock mass” acquisition to an average of 3 scans (scan time, 0.2 s) every 15 s. Do not select

Table 4
Proposed elution gradient program for analysis of phase II steroid metabolites by LC-TWIM-MS

Time (min)	Mobile phase (%B)
0	5
0.3	5
9.6	43
10.5	100
12.5	100
13	5
16.5	5

“automatic application of ‘lock mass’ correction” as it will be applied during post-acquisition data processing.

3. Set data acquisition to “continuous” or “profile” mode and not to “centroid” mode.
4. Create the acquisition sequence indicating TWIM-MS settings and the LC and HDMS methods to be used in data acquisition, as indicated in Table 2, Subheading 3.3, and step 2 of this section, respectively. Important: TWIM-MS settings must be the same as those set for CCS calibration (Table 2) to ensure that CCS measurements are carried out correctly (*see Note 17*).
5. It is recommended to include two blank samples at the beginning of the acquisition sequence to ensure that the LC-TWIM-MS system is equilibrated when the sample analysis is performed. Also, run the analysis of the standard QC mix first to evaluate the performance of the LC-TWIM-MS workflow.
6. Run the samples. It is recommended to analyze the samples in triplicate when performing CCS measurements to check the repeatability of the measurement.

3.5 Data Processing

1. Import the CCS calibration data file into the Driftscope software (*see Note 18*).
2. Perform peak detection by selecting “non-chromatographic mode.” The “Minimum Intensity Threshold” parameter must be adjusted to detect ions related to the calibration solution and avoid detection of peaks associated with the background noise.
3. In the “peak detection” window, select “calibrate peaks” and “new calibration.”

4. Open the reference file that contains the information for the ions in the calibration solution (i.e., m/z and CCS).
5. In the “peaks” window, select the “auto select...” option to compare “reference” and “measured” peaks (m/z tolerance, 0.1 Da; intensity threshold, 5%).
6. Save the calibration profile if the determination coefficient (R^2) > 0.99 in accordance with the results observed in Sub-heading 3.2, step 13. If not, check that the peak selection has been carried out correctly since unsatisfactory calibration curves are often the result of incorrect peak selection.
7. Import the LC-TWIM-MS data into the Driftscope software.
8. Perform peak detection by selecting “chromatographic mode” and applying “Lock Mass” correction (m/z 556.2771 for ESI+ conditions, and m/z 554.2615 for ESI- conditions) (see Note 19).
9. Visualize the detected peaks on the 2D plot (m/z vs drift time) provided by the Driftscope software (Fig. 4).
10. In the “peak detection” window, select “apply calibration” to apply the previously created CCS calibration curve (point 6 of this section) (see Note 20).
11. ‘Export peak list’ to an Excel file.
12. Search the detected peaks in the published CCS databases for steroids [14, 20].

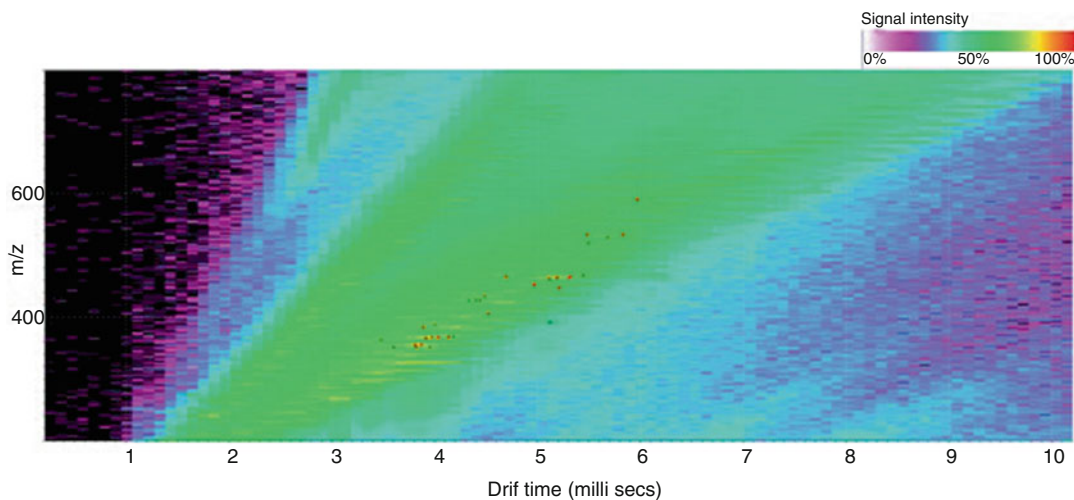


Fig. 4 Representation of m/z vs drift time for a bovine urine sample analyzed according to the proposed protocol. The red dots indicate the peaks detected in a retention time range between 3.0 and 9.0 min and a m/z range between 350 and 625. The peak detection ranges have been established according to previous knowledge of LC-MS for phase II steroid metabolites [19]

13. In addition, select a region of interest from the mobility spectra (drift time range) on the 2D plot to verify the presence and separation of isomers and isobaric compounds.
14. Export the data to the MassLynx software for better visualization (Fig. 5) (*see Note 21*). Separation in the ion mobility dimension indicates differences in the CCS of the related ions (*see Note 22*). In TWIM-MS instruments, more compact ions (with smaller CCS) reach the exit of the mobility cell earlier than elongated ions (with greater CCS).
15. Plan fragmentation experiments using LC-TWIM-MS workflows to generate additional information on the analytes of interest and gain more confidence in the identification or confirmation of compounds (*see Note 23*). As a starting point, perform HDMS^E experiments by setting 5 eV in the trap cell. Set the transfer cell to 5 eV for low energy fragmentations and a ramp between 20 and 40 eV for high energy fragmentations.

4 Notes

1. Samples must be stored under adequate conditions ($-20\text{ }^{\circ}\text{C}$) to ensure their biological stability over time.
2. It is recommended to use vials with inserts to reduce the sample volume required for analysis. This is especially relevant for those matrices with limited quantities.
3. It is recommended to add isotope-labeled internal standards to samples as a part of the QA protocol, especially for quantification purposes. For phase II steroid metabolites, at least two internal standards representing both steroid sulfates and glucuronides can be added (e.g., epitestosterone glucuronide-d3 and epitestosterone sulfate-d3 at $0.5\text{ }\mu\text{g}/\text{mL}$ each one).
4. It is important to check that there are no air bubbles at the bottom of the insert after homogenizing the sample. Air bubbles can prevent proper sample injection into the UPLC-TWIM-MS system.
5. Avoid any contact of the sodium formate calibration solution with the cap of the vial or other non-glass material as it has been observed to increase background noise and decrease signal sensitivity of sodium formate clusters (Fig. 6). Sodium formate solutions expire in 1 week.
6. The “High Resolution” mode is the most appropriate to be used in order to obtain more accurate measurements of the m/z . However, the signal sensitivity that can be reached using this mode can be limited and may compromise the detection of residues and contaminants present at low concentration levels in food matrices. In targeted analysis, where the analytical

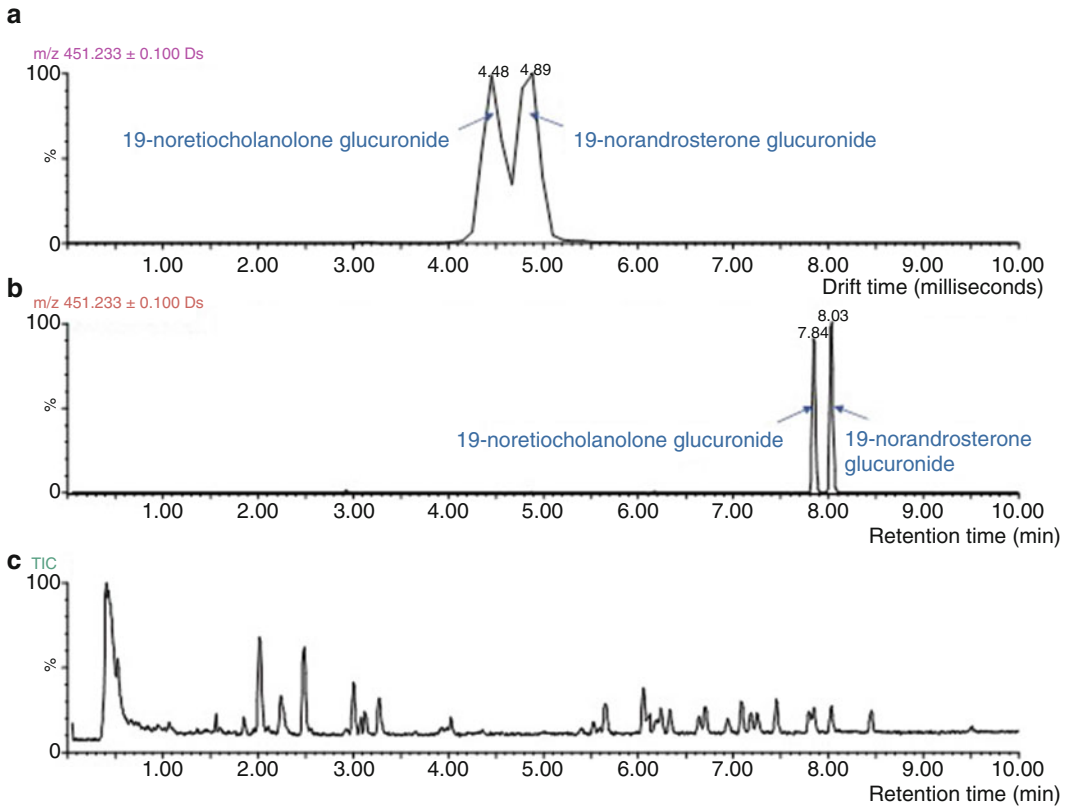


Fig. 5 Separation of two steroid isomers ($m/z\ 451.2326$) in the ion mobility dimension (a) and in the LC dimension (b) resulted from the analysis of a spiked (2 $\mu\text{g/mL}$) bovine urine sample by LC-TWIM-MS. Total ion chromatogram (TIC) observed for the analyzed sample (c)

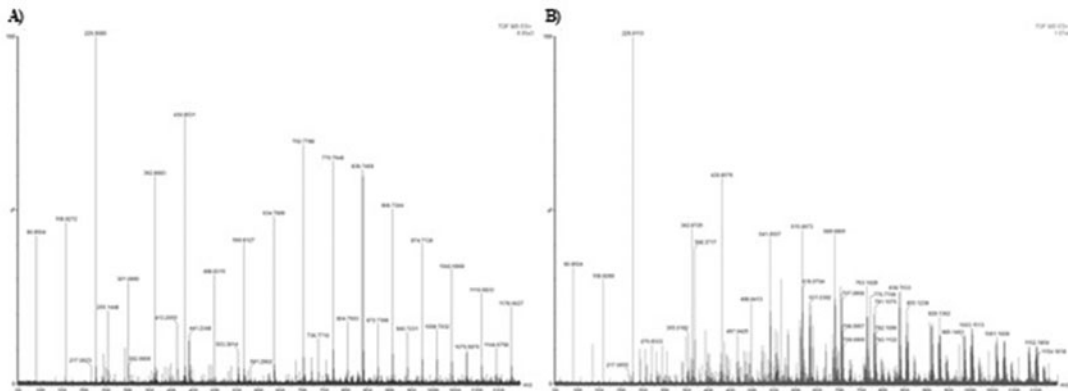


Fig. 6 Mass spectra of the sodium formate calibration solution observed under optimal acquisition conditions (a) and negatively affected by improper handling of the calibration solution (b)

information on potentially detectable compounds is known, it is recommended to evaluate the performance of the “Sensitivity” working mode to improve sensitivity of the signal to the detriment of mass accuracy.

7. It is recommended to monitor the leucine-enkephalin signal before and after mass and CCS calibration, as well as before running a sample sequence, as part of the QA protocol for IM-MS measurements. This allows the performance of the instrument to be evaluated and recorded over time in terms of signal sensitivity, mass accuracy, and CCS precision.
8. As indicated by the Vendor, the same value for “Transfer DC Exit voltage” must be set for MS and HDMS modes; otherwise, a separate mass calibration is required.
9. The sample capillary should be rinsed with acetonitrile/water (50/50;%, v/v) solution before and after injecting any calibration solution (or other solution or sample) into the instrument using the direct infusion set in order to avoid cross-contamination and obtain correct mass spectra of the infused solution.
10. TWIM-MS settings must be the same for CCS calibration and CCS measurements on samples. These parameters must be optimized for the analytes of interest or generic parameters can be set in the case of non-targeted analysis [22]. The TWIM-MS settings must allow all ions within the m/z acquisition range fit into the TWIM separation window (Fig. 7b). For example, too low wave velocities in the TWIM cell lead to poor mobility separation (Fig. 7a), whereas too high wave velocities cause a “wrapping effect” whereby the slow ions stay for too long in the TWIM cell (more than a 200 bins experiment) and are observed at the beginning of the subsequent mobility separation (Fig. 7c). For a suitable TWIM-MS method (e.g., to avoid “wrapping effects”), it is recommended to ensure that the arrival time distributions of analyte ions are observed within a drift time interval of 20 and 180 bins.
11. TWIM-MS settings can be optimized by direct infusion of a mixture of the analytes of interest (e.g., at 1 $\mu\text{g}/\text{mL}$) in both positive and negative ionization modes [25]. As indicated by the Vendor, it is recommended to set the IMS wave height at 40 V. In the event of unwanted fragmentation of the target analytes, “Trap DC bias” should be adjusted.
12. Parameters such as source temperature, desolvation temperature, and desolvation gas flow rate depend on the flow rate of the mobile phase or infused solution. Check the Vendor’s recommendations to establish satisfactory values for these parameters.

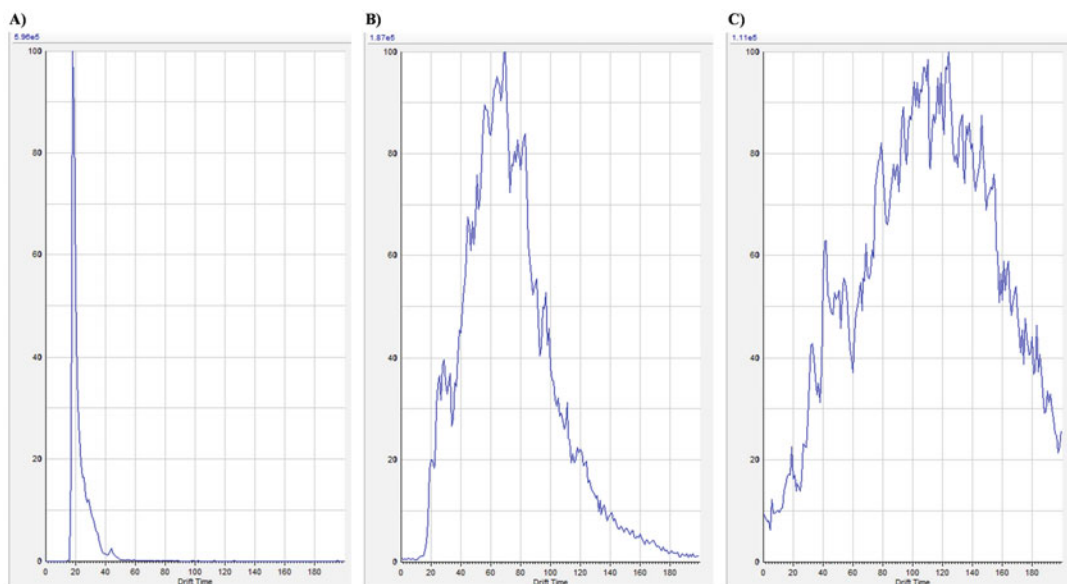


Fig. 7 Mobility spectra of the CCS Major Mix obtained using a wave velocity in the TWIM cell of 250 (a), 1000 (b) and 1750 m/s (c), respectively

13. Mass and CCS calibration are performed sequentially as part of this protocol. Instrument calibration is required to be done weekly. Mass accuracy is the limiting factor that indicates the need to calibrate the system. A mass accuracy deviation of up to 10 ppm can be accepted when working in “High Resolution” mode.
14. It is recommended to use CCS calibration mixtures with physicochemical properties similar to those of the analytes of interest. This ensures that TWIM-MS settings are optimal for the detection and analysis of the molecules either in the calibration mix or in the sample. Furthermore, calibrants with different physicochemical properties compared to the analytes of interest have been found to be unsuitable and can introduce a high bias between the measured CCS and the reference or expected CCS values for these molecules [26].
15. Automated calibration is based on the accumulation of total peak intensity, which can be detrimental to the detection of low intensity peaks if ions with a signal intensity several times higher are present. Therefore, calibrant ions with low intensity (e.g., m/z 1013.5379 in Fig. 2) are not detected with sufficient signal intensity to be used as calibration points in CCS calibration. In this context, it is recommended to perform a manual CCS calibration of the instrument rather than an automatic calibration. For manual calibration, infuse the CCS Major Mix at a flow rate of $10 \mu\text{L min}^{-1}$ and acquire the signal for at least 2 min (m/z range, 50–1200; scan time, 0.5 s). The

acquired data file must be loaded later in the “Calibration Reference Compound & Raw Data” option in the “Edit Manual Calibration” window when editing the calibration profile.

16. Use glassware and avoid the use of plastic receipts and materials when preparing formic acid solutions. Plasticizers are susceptible to cause unnecessary contamination of solutions and lead to complex mass spectra with unwanted m/z signals.
17. It is recommended to use the same “Tune Page” or “TWIM-MS tuning conditions file” for CCS calibration and CCS measurements to ensure that both processes are performed under the same TWIM-MS conditions.
18. A CCS calibration curve must be created in Driftscope to apply to the sample acquisition files and obtain the CCS values for analytes of interest.
19. Peak detection is time-consuming and computationally intensive, so it is suggested to select retention time and m/z ranges of interest to shorten this automated process.
20. Calibration curves can also be applied directly by replacing the “mob_cal.csv” file in the “samples”.raw data file with the one generated in the “CCS calibration”.raw data file after creating a CCS calibration curve in Driftscope. This is a faster way to apply the CCS calibration curve to a wide range of sample data files.
21. Other commercial software such as UNIFI [25] or freely available software such as Skyline [27] can be used for the visualization of TWIM-MS data, as well as for quantification purposes.
22. Separation can be improved by changing the gas in the mobility cell. However, CCS values are highly dependent on the buffer gas used in the mobility cell, so CCS measurements carried out on different neutral gases cannot be directly compared. In addition, it is worth noting the correlation that exists between m/z and CCS parameters (Fig. 8). Despite the correlation between both parameters, CCS has been shown to increase confidence in the determination of residues and contaminants in food products [28].
23. The Synapt G2-S HDMS instrument includes two fragmentation cells: the trap cell placed before the IMS cell and the transfer cell placed after it. Fragmentation in the transfer cell allows alignment during post-acquisition data processing of those ions that show the same drift time, indicating that they are likely related to the same parent ion.

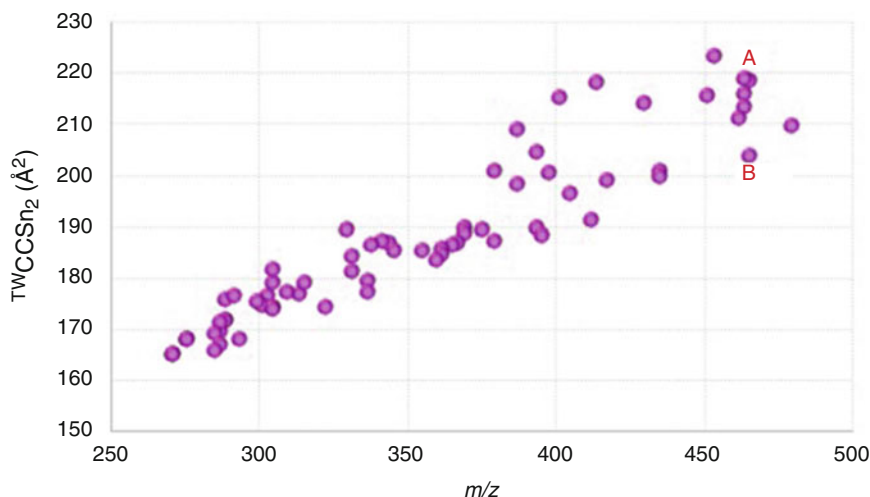


Fig. 8 Graphical representation of CCS vs m/z for protonated steroid ions. Data extracted from [14]. The differences that exist in the CCS of isomers of phase II steroid metabolites, such as testosterone glucuronide (m/z 465.2383; $TWCCSN_2 = 218.6 \text{ \AA}^2$) (a) and epitestosterone glucuronide (m/z 465.2383; $TWCCSN_2 = 203.8 \text{ \AA}^2$) (b), show how the CCS parameter provides additional information to m/z and retention indexes for identification

Acknowledgments

This project has received funding from the European Union's Horizon 2020 research and innovation program under the Marie Skłodowska-Curie grant agreement HAZARDOMics No 795946.

References

1. D'Atri V, Causon T, Hernandez-Alba O, Mutabazi A, Veuthey J-L, Cianferani S, Guillardarme D (2018) Adding a new separation dimension to MS and LC-MS: What is the utility of ion mobility spectrometry? *J. Sep. Sci.* 41:20–67. <https://doi.org/10.1002/jssc.201700919>
2. Hernández-Mesa M, Escorrou A, Monteau F, Le Bizec B, Dervilly-Pinel G (2017) Current applications and perspectives of ion mobility spectrometry to answer chemical food safety issues. *TrAC Trend. Anal. Chem.* 94:39–53. <https://doi.org/10.1016/j.trac.2017.07.006>
3. Hernández-Mesa M, Ropartz D, García-Campaña AM, Rogniaux H, Dervilly-Pinel G, Le Bizec B (2019) Ion mobility spectrometry in food analysis: principles, current applications and future trends. *Molecules* 24:2706. <https://doi.org/10.3390/molecules24152706>
4. Gabelica V, Shvartsburg AA, Afonso C et al (2019) Recommendations for reporting ion mobility Mass Spectrometry measurements. *Mass Spectrom Rev* 38:291–320. <https://doi.org/10.1002/mas.21585>
5. Paglia G, Smith AJ, Astarita G (2021) Ion mobility mass spectrometry in the omics era: challenges and opportunities for metabolomics and lipidomics. *Mass Spectrom Rev.* <https://doi.org/10.1002/mas.21686>
6. Lanucara F, Holman SW, Gray CJ, Evers CE (2014) The power of ion mobility-mass spectrometry for structural characterization and the study of conformational dynamics. *Nat Chem* 6:281–294. <https://doi.org/10.1038/nchem.1889>
7. Ridgeway ME, Lubeck M, Jordens J, Mann M, Park MA (2018) Trapped ion mobility spectrometry: a short review. *Int J Mass Spectrom*

- 425:22–35. <https://doi.org/10.1016/j.ijms.2018.01.006>
8. May JC, Morris CB, McLean JA (2017) Ion mobility collision cross section compendium. *Anal Chem* 89:1032–1044. <https://doi.org/10.1021/acs.analchem.6b04905>
 9. Regueiro J, Negreira N, Berntssen MHG (2016) Ion-mobility-derived collision cross section as an additional identification point for multiresidue screening of pesticides in fish feed. *Anal Chem* 88:11,169–11,177. <https://doi.org/10.1021/acs.analchem.6b03381>
 10. Righetti L, Bergmann A, Galaverna G, Rolfsson O, Paglia G, Dall'Asta C (2018) Ion mobility-derived collision cross section database: application to mycotoxin analysis. *Anal Chim Acta* 1014:50–57. <https://doi.org/10.1016/j.aca.2018.01.047>
 11. Tejada-Casado C, Hernández-Mesa M, Monteau F, Lara FJ, del Olmo-Iruela M, García-Campaña AM, Le Bizec B, Dervilly-Pinel G (2018) Collision cross section (CCS) as a complementary parameter to characterize human and veterinary drugs. *Anal Chim Acta* 1043: 52–63. <https://doi.org/10.1016/j.aca.2018.09.065>
 12. Picache JA, Rose BS, Balinski A, Leaprot KL, Sherrod SD, May JC, McLean JA (2019) Collision cross section compendium to annotate and predict multi-omic compound identities. *Chem Sci* 10:983–993. <https://doi.org/10.1039/C8SC04396E>
 13. Stow SM, Causon TJ, Zheng X, Kurulugama RT, Mairinger T, May JC, Rennie EE, Baker ES, Smith RD, McLean JA, Hann S, Fjeldsted JC (2017). An interlaboratory evaluation of drift tube ion mobility–mass spectrometry collision cross section measurements. *Anal Chem* 89:9048–9055. <https://doi.org/10.1021/acs.analchem.7b01729>
 14. Hernández-Mesa M, D'Atri V, Barknowitz G, Fanuel M, Pezzatti J, Dreolin N, Ropartz D, Monteau F, Vigneau E, Rudaz S, Stead S, Rogniaux H, Guillaume D, Dervilly G, Le Bizec B (2020) Interlaboratory and interplatform study of steroids collision cross section by traveling wave ion mobility spectrometry. *Anal Chem* 92:5013–5022. <https://doi.org/10.1021/acs.analchem.9b05247>
 15. Hinnenkamp V, Klein J, Meckelmann SW, Balsaa P, Schmidt TC, Schmitz OJ (2018) Comparison of CCS values determined by traveling wave ion mobility mass spectrometry and drift tube ion mobility mass spectrometry. *Anal Chem* 90:12,042–12,050. <https://doi.org/10.1021/acs.analchem.8b02711>
 16. Gabelica V, Marklund E (2018) Fundamentals of ion mobility spectrometry. *Curr Opin Chem Biol* 42:51–59. <https://doi.org/10.1016/j.cbpa.2017.10.022>
 17. Council Directive 96/22/EC of 29 April 1996 concerning the prohibition on the use in stock-farming of certain substances having a hormonal or thyrostatic action and of beta-agonists, and repealing Directives 81/602/EEC, 88/146/EEC and 88/299/EEC. *Off J Eur Communities* L125; 1996, pp. 3–9.
 18. Kaabia Z, Laparre J, Cesbron N, Le Bizec B, Dervilly-Pinel G (2018) Comprehensive steroid profiling by liquid chromatography coupled to high resolution mass spectrometry. *J Steroid Biochem Mol Biol* 183:106–115. <https://doi.org/10.1016/j.jsbmb.2018.06.003>
 19. Hernández-Mesa M, Monteau F, Le Bizec B, Dervilly-Pinel G (2019) Potential of ion mobility-mass spectrometry for both targeted and non-targeted analysis of phase II steroid metabolites in urine. *Anal Chim Acta X* 1: 100006. <https://doi.org/10.1016/j.acax.2019.100006>
 20. Hernández-Mesa M, Le Bizec B, Monteau F, García-Campaña AM, Dervilly-Pinel G (2018) Collision Cross Section (CCS) database: an additional measure to characterize steroids. *Anal Chem* 90:4616–4625. <https://doi.org/10.1021/acs.analchem.7b05117>
 21. Paglia G, Astarita G (eds) (2020) Ion mobility-mass spectrometry, *Methods in molecular biology*, vol 2084. Humana, New York, NY
 22. Paglia G, Astarita G (2017) Metabolomics and lipidomics using traveling-wave ion mobility mass spectrometry. *Nat Commun* 12: 797–813. <https://doi.org/10.1038/nprot.2017.013>
 23. Bush MF, Hall Z, Giles K, Hoyes J, Robinson CV, Ruotolo BT (2010) Collision cross sections of proteins and their complexes: a calibration framework and database for gas phase structural biology. *Anal Chem* 82:9557–9565. <https://doi.org/10.1021/ac1022953>
 24. Anizan S, Di Nardo D, Bichon E, Monteau F, Cesbron N, Antignac J-P, Le Bizec B (2011) Targeted phase II metabolites profiling as new screening strategy to investigate natural steroid abuse in animal breeding. *Anal Chim Acta* 700: 105–113. <https://doi.org/10.1016/j.aca.2010.12.009>
 25. Righetti L, Dall'Asta C (2020) A workflow for the identification of mycotoxin metabolites using liquid chromatography–ion mobility-mass spectrometry. In: Paglia G, Astarita G (eds) *Ion mobility-mass spectrometry, Methods in molecular biology*, vol 2084. Humana, New York, NY

26. Hines KM, May JC, McLean JA, Xu L (2016) Evaluation of collision cross section calibrants for structural analysis of lipids by traveling wave ion mobility-mass spectrometry. *Anal Chem* 88:7329–7336. <https://doi.org/10.1021/acs.analchem.6b01728>
27. Kino LK, Searle BC, Bollinger JG, Nunn B, MacLean B, MacCoss MJ (2020) The Skyline ecosystem: informatics for quantitative mass spectrometry proteomics. *Mass Spectrom Rev* 39:229–244. <https://doi.org/10.1002/mas.21540>
28. Goscinny S, McCullagh M, Far J, De Pauw E, Epe G (2019) Towards the use of ion mobility mass spectrometry derived collision cross section as a screening approach for unambiguous identification of targeted pesticides in food. *Rapid Commun Mass Spectrom* 33:34–48. <https://doi.org/10.1002/rcm.8395>



Determination Method of Acrylamide in Beverages and Foods by Supercritical Fluid Chromatography/Tandem Mass Spectrometry

Toshiaki Yoshioka, Yoshihiro Izumi, and Takeshi Bamba

Abstract

Acrylamide (AA) is important with regard to food safety, as it is a harmful chemical produced during the heating of food. Strategies for the reduction of AA in food are being sought after globally. AA is usually analyzed by gas chromatography/mass spectrometer and liquid chromatography/tandem mass spectrometer. However, rapid and accurate analysis of low-concentration AA is difficult. Therefore, we have developed a rapid and highly sensitive method using supercritical fluid chromatography/tandem mass spectrometer (SFC/MS/MS) for the determination of AA in beverages, grains, and confectioneries. By combining SFC/MS/MS and a pretreatment method that simplifies the QuEChERS method, trace amounts of AA (0.5 ng/g) can be quantified in beverages, and 60 samples can be analyzed in ~12 h. We expect this analytical method to be effective for food survey and quality control of AA in various beverages and foods.

Key words Supercritical fluid chromatography, Mass spectrometry, SFC/MS/MS, QuEChERS, High-throughput, High-sensitive, Coffee, Confectionery, Grain

1 Introduction

Acrylamide (AA) is a genotoxic carcinogen as well as a neurotoxin [1–3]. The presence of AA in various cooked foods has emerged as a global concern [4]. The mechanism of AA production in foods was studied, and it was suggested that AA was a by-product of the Maillard reaction generated by heating foods containing free asparagine and reducing sugars such as glucose above 120 °C [5–8]. JECFA concluded that AA is a genotoxic carcinogen with a small exposure margin and may affect the health adversely [9]. Because the toxicity threshold cannot be set for genotoxic carcinogens in food, it is required to reduce the content of such chemicals to the maximum possible extent, according to the ALARA (As Low As Reasonably Achievable) principle [10]. In

the EU, a benchmark level (90% of the highest value in AA monitoring results) is set for each food, and regular monitoring is conducted [11]. In addition, since foods and cooking methods are unique to each country, it is important to determine the AA content in various foods. Thus, for food surveys and quality control of AA in foods, it is necessary to have a simple, rapid, and quantitative method for determining the AA content in foods.

Gas chromatography/mass spectrometer (GC/MS) and liquid chromatography/tandem mass spectrometer (LC/MS/MS), which have excellent detection sensitivity and selectivity, are generally used for the quantitative analysis of AA [7, 10, 12, 13]. In the GC/MS method, AA is often derivatized to improve the detection sensitivity [14–18]. However, the derivatization of AA is a complex and time-consuming process, as it increases the number of steps. Thus, it is not suitable for the rapid analysis of many samples. In the LC/MS/MS method, direct analysis of AA is common. Although the QuEChERS (Quick, Easy, Cheap, Effective, Rugged, Safe) method is a simple pretreatment method, it is difficult to detect low concentrations, of the order of a few ng/g, of AA in foods such as coffee beverages and roasted barley tea [19–22]. With the existing methods using GC/MS and LC/MS/MS, achieving high throughput by shortening the pretreatment time and instrumental analysis time and high sensitivity required for precise quantitation of low-concentration AA are difficult.

Therefore, we focused on supercritical fluid chromatography (SFC) as a new separation technique for the rapid and highly sensitive quantitative analysis of AA. The latest SFC system developed employs ultra-high performance liquid chromatography (UHPLC) technology and a high upper limit of pressure; the retention time is highly reproducible, as for any analytical system [23]. SFC uses supercritical CO₂ (scCO₂) as the mobile phase. Since scCO₂ imparts low viscosity and high diffusivity to the analytes, their rate of migration is increased. As a result, the column efficiency improves even if the optimum flow rate of the mobile phase is high. Moreover, the analysis time can be shortened compared to UHPLC. In addition, SFC/tandem mass spectrometer (SFC/MS/MS), which combines SFC and mass spectrometer, can detect a compound with higher sensitivity than LC/MS/MS due to the improved efficiency of desolvation of the mobile phase by vaporizing CO₂ at the ion source [24–27]. Therefore, we developed a new method using SFC/MS/MS for the rapid and highly sensitive determination of AA. For high-speed separation, we investigated the conditions under which AA can be separated from food matrices in a short time, including column selection. For high sensitivity, we investigated a method to increase the amount of AA introduced into the mass spectrometer by increasing the pressure setting of the back-pressure regulator [28]. As a result, the

analysis time was shortened, and the sensitivity was significantly improved compared to the AA analysis by UHPLC/MS/MS [29].

The QuEChERS method is used for AA sample preparation. However, it is time-consuming as it involves several steps. Therefore, we developed a rapid pretreatment method by substituting solvent dilution, which is an easier step. In addition, if a membrane filter is used to remove fine substances in the extract, AA will elute from the membrane filter, rendering it difficult to quantify trace amounts of AA. Therefore, we substituted the filtration step with centrifugation, which facilitates the simultaneous processing of several samples [21, 29]. In other words, we developed a simple and high-throughput sample preparation method in which the surrogate of AA, salts for QuEChERS extraction, and ACN were added to the sample; the ACN extract was diluted with ACN and then centrifuged. Herein, the procedure for preparing each sample and the procedure for setting the SFC/MS/MS conditions are described.

The merits of the SFC/MS/MS-based AA analysis method developed in this study are the shortened analysis time, increased sensitivity, and the rapid pretreatment due to the reduction of food matrices by diluting the QuEChERS extract. It is applicable to beverages, their material grains, confectioneries, etc. and can be applied simply by changing the amount of sampling and diluting solvent according to the sample. The time required from sample pretreatment to obtaining analysis results is ~4 h for 20 samples and ~12 h for 60 samples. Because the throughput is significantly improved compared to that in the previous method, the merit of speed is appreciable even if there are many analytical samples. In addition, since this analysis method can accurately quantify low-concentration AA, even of the order of several ng/g, it is very effective for food survey in commercial foods, quality control of AA in products, and research on AA reduction methods by food manufacturers.

2 Materials

2.1 Chemicals

1. AA, $^{13}\text{C}_3$ -AA (*see Note 1*).
2. Acetonitrile (ACN, LC/MS grade), methanol (MeOH, LC/MS grade), formic acid (LC/MS grade), *n*-hexane (Hex, pesticide analytical grade).
3. Water (purified with a Milli-Q system (Merck Millipore, Billerica, MA)).

4. Magnesium sulfate (MgSO_4 , anhydrous, special grade), sodium chloride (NaCl , special grade), trisodium citrate dihydrate (special grade), disodium citrate sesquihydrate (special grade). (*see Note 2*).
5. CO_2 (99.5% grade).

2.2 Standard Solutions and Mobile Phase

1. AA stock solution: AA is dissolved in ACN to prepare a 500 $\mu\text{g}/\text{mL}$ stock solution. It can be stored in the freezer for 3 months.
2. AA working solution: The AA stock solution is diluted with ACN, and 5 and 500 ng/mL standard solutions are prepared for each analysis.
3. Surrogate stock solution: $^{13}\text{C}_3$ -AA is dissolved in ACN to prepare a 500 $\mu\text{g}/\text{mL}$ stock solution.
4. Surrogate working solution: The $^{13}\text{C}_3$ -AA solution is diluted with ACN to prepare 0.25 and 10 $\mu\text{g}/\text{mL}$ solutions. A mixture of 1 $\mu\text{g}/\text{mL}$ AA and $^{13}\text{C}_3$ -AA diluted with ACN was prepared for MRM transition optimization.
5. Mobile phase solvent (modifier): MeOH.
6. Strong wash solvent: 0.1% formic acid in MeOH/ H_2O (80/20, v/v).
7. Weak wash solvent: MeOH.
8. Seal wash solvent: MeOH.
9. Make-up solvent: MeOH/water (95/5, v/v).

2.3 SFC/MS/MS

1. SFC instrument: ACQUITY UltraPerformance Convergence Chromatography (UPC^2) system (Waters, Milford, MA) consisting of a pump (binary solvent manager), autosampler (sample manager—FL), column oven (column manager aux), back-pressure regulator (convergence manager), and make-up pump (515 HPLC pump).
2. MS instrument: Xevo TQ-S micro triple-quadrupole mass spectrometer (Waters) with ion source for electrospray ionization. A schematic diagram of the SFC/MS/MS system is shown in Fig. 1.
3. Column: ACQUITY UPC^2 Torus 1-aminoanthracene (1-AA, 150 mm \times 3.0 mm i.d., particle size 1.7 μm , Waters).
4. Data acquisition software: MassLynx version 4.1 SCN 909 (Waters).
5. Processing software: TargetLynx XS in MassLynx (Waters).

2.4 Samples

1. Beverages: coffee beverage and roasted barley tea, etc.
2. Confectioneries: biscuits, sables, cookies, etc. They are made into a uniform powder in a laboratory food processor (*see Note 3*).

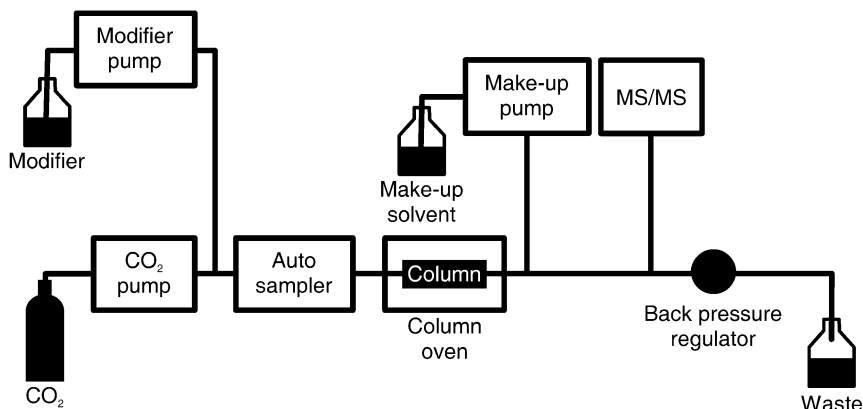


Fig. 1 Schematic diagram of the SFC/MS/MS system

3. Grains: coffee beans, roasted barley, etc. They are made into a uniform powder in a laboratory food processor (*see Note 3*).

3 Methods

3.1 MS/MS Parameter Optimization

1. A mixed solution (1 $\mu\text{g}/\text{mL}$) of AA and $^{13}\text{C}_3$ -AA is used for MRM transition optimization.
2. Mixed solution is injected into a mass spectrometer using a syringe pump (*see Note 4*).
3. m/z values of AA and $^{13}\text{C}_3$ -AA precursor/product ions are obtained in the ESI positive mode, and the cone voltage and collision energy are optimized to create the MRM analytical method. The optimized values obtained by Xevo TQ-S micro are listed in Table 1 (*see Note 5*).
4. The modifier (MeOH), strong wash solvent (0.1% formic acid in MeOH/ H_2O (80/20, v/v)), weak wash solvent (MeOH), seal wash solvent (MeOH), and Torus 1-AA column are set in the SFC, and the system is purged.
5. The SFC analytical method are set as listed in Table 2. The device is equilibrated for 30 min at a flow rate of 1 mL/min (*see Note 6*).
6. The mixed solution of AA and $^{13}\text{C}_3$ -AA is analyzed by SFC/MS/MS to confirm the retention time (*see Note 7*).
7. The capillary voltage and amount and temperature of the desolvation gas of the ESI probe are optimized for the SFC/MS/MS analysis of the AA solution to develop an MS method. The optimized values obtained by Xevo TQ-S micro are listed in Table 3 (*see Note 8*).

Table 1
MRM transitions of AA and ¹³C₃-AA

Transitions (precursor ion > product ion, <i>m/z</i>)	Cone voltage (V)	Collision energy (V)	Polarity
AA			
72 > 55 (Quantitative ion)	25	10	ESI+
72 > 44 (Identification ion)	25	8	ESI+
¹³ C ₃ -AA			
75 > 58 (Quantitative ion)	25	8	ESI+

Table 2
SFC parameters of UPC²

Parameters	
<i>SFC analytical method</i>	
Injection volume	3 μL
Strong wash volume	200 μL
Weak wash volume	600 μL
Flow rate	1 mL/min
Column temperature	40 °C
Gradient (A: CO ₂ , B: modifier)	0–1.0 min (5% B), 3.6 min (22% B), 4–5 min (47% B), 5.5–5.8 min (5% B)
Back-pressure gradient	0–3.2 min (2000 psi), 3.3–3.6 min (3000 psi), 3.65 min (2000 psi), 3.7–5.2 min (1800 psi), 5.25–5.8 min (2000 psi)
Make-up pump flow rate	0 mL/min
<i>SFC cleaning method</i>	
Flow rate	1 mL/min
Column temperature	40 °C
Isocratic (A: CO ₂ , B: modifier)	5.8–6.8 min (5% B)
Back-pressure setting	5.8–6.8 min (2000 psi)
Make-up pump flow rate	1 mL/min

8. The back-pressure gradient condition is set in the SFC analytical method according to the elution of AA. The optimized values are listed in Table 2 (*see Note 9*).

Table 3
MS parameters of Xevo TQ-S micro

	Parameters
Capillary voltage	1.6 kV
Desolvation temperature	400 °C
Desolvation gas flow	1000 L/h
Cone gas flow	50 L/h
Source temperature	150 °C

3.2 Sample Preparation

3.2.1 Beverage sample

1. Sample (2 g; $n = 3$) is weighed into a 50-mL PP centrifuge tube.
2. $^{13}\text{C}_3$ -AA surrogate solution (0.25 $\mu\text{g}/\text{mL}$; 200 μL) is added to all the samples (*see Note 10*).
3. ACN (9.8 mL) is added (*see Note 11*).
4. NaCl (1 g), 1 g of trisodium citrate dihydrate, 0.5 g of disodium citrate sesquihydrate, and 4 g of MgSO_4 are added, covered immediately, and shaken vigorously by hands (*see Notes 2 and 12*).
5. The mixture is shaken at 270 rpm for 15 min on a shaker and then centrifuged at $2380 \times g$ for 5 min.
6. Five hundred microliters of the upper layer and 500 μL of ACN are mixed in a vial and then analyzed by SFC/MS/MS.

3.2.2 Confectionery and Grain Samples

1. Powdered confectionery sample (1 g) is weighed in a 50-mL PP centrifuge tube at $n = 3$. Powdered grain sample (0.5 g) is weighed in the same way.
2. Twenty five microliters of 10 $\mu\text{g}/\text{mL}$ $^{13}\text{C}_3$ -AA surrogate solution is added to all the samples (*see Note 10*).
3. Water (5 mL) is added to all the sample, vortexed, and left for 15 min (*see Note 13*).
4. ACN (10 mL) and 2.5 mL of Hex are added to all the sample (*see Notes 11 and 14*).
5. NaCl (1 g), 1 g of trisodium citrate dihydrate, 0.5 g of disodium citrate sesquihydrate, and 4 g of MgSO_4 are added, covered immediately, and shaken vigorously by hands (*see Notes 2 and 12*).
6. The mixture is shaken at 270 rpm for 15 min on a shaker and then centrifuged at $2380 \times g$ for 5 min.
7. One hundred microliters of the upper layer and 0.9 mL of ACN are mixed in a 1.5-mL PP centrifuge tube.

8. The mixture is centrifuged at $15000 \times g$ for 3 min.
9. The supernatant is placed in a vial and analyzed by SFC/MS/MS.

3.3 Standard Preparation

1. AA standard solution (5 or 500 ng/mL), 0.25 $\mu\text{g/mL}$ or 10 $\mu\text{g/mL}$ $^{13}\text{C}_3$ -AA solution, and ACN are mixed in a vial to prepare 0.05–10 ng/mL solutions for preparing the calibration curve. The mixing ratios of these solutions are listed in Table 4.

3.4 SFC/MS/MS Analysis

1. The make-up solvent (MeOH/water (95/5, v/v)) is set and purged at 1 mL/min for 2 min.
2. The modifier (MeOH), strong wash solvent (0.1% formic acid in MeOH/H₂O (80/20, v/v)), weak wash solvent (MeOH), seal wash solvent (MeOH), and the Torus 1-AA column in the SFC/MS/MS system are set, and these solvents are purged (*see Note 15*).
3. The SFC cleaning method (Table 2) is set for the SFC/MS/MS system, and the system is equilibrated at 1 mL/min for 30 min.
4. The standard solutions for calibration and the sample extracts in the autosampler are set.
5. A batch file is created with the MRM analytical method, MS method, SFC analytical method, SFC cleaning method, and injection volume (3 μL), and the batch file is run for analysis (*see Note 16*).

3.5 Data Processing

1. The data analytical method is created using $^{13}\text{C}_3$ -AA as an internal standard for quantifying AA and $^{13}\text{C}_3$ -AA (*see Note 17*).
2. The data analysis method is run on the batch file that has been analyzed, and the concentration of AA in all the samples is determined (*see Note 18*).

4 Notes

1. d_3 -AA is less stable in solution as a surrogate; thus, it is better to use $^{13}\text{C}_3$ -AA. A commercially available surrogate standard solution can also be used.
2. A commercially available product containing 4 g of MgSO_4 , 1 g of NaCl, 1 g of trisodium citrate dihydrate, and 0.5 g of disodium citrate sesquihydrate may be used.
3. A food processor or a mill mixer for cooking can be used. The standard duration for powdering is 30–60 s for 50 g sample.

Table 4
Mixing ratios of calibration curve solution

STD concentration (ng/mL)	AA (μL)	$^{13}\text{C}_3\text{-AA}$ (μL)	ACN (μL)
0.05	10 ^a	10 ^b	980
0.1	20 ^a	10 ^b	970
0.5	100 ^a	10 ^b	890
2.5	500 ^a	10 ^b	490
12.5	25 ^c	10 ^b	965

^a5 ng/mL AA solution

^b250 ng/mL $^{13}\text{C}_3\text{-AA}$ solution. When analyzing grain and confectionery, the 10 $\mu\text{g/mL}$ $^{13}\text{C}_3\text{-AA}$ solution added to the sample is diluted with ACN to obtain 250 ng/mL $^{13}\text{C}_3\text{-AA}$ solution

^c500 ng/mL AA solution

4. A built-in syringe pump can be used with a mass spectrometer of the Waters. It is also possible to perform flow injection analysis with SFC/MS.
5. Because the optimum MS/MS parameters differ for each mass spectrometer, optimization of the parameters depending on the equipment is essential.
6. An SFC analytical method with the SFC conditions optimized for each company's equipment can be developed.
7. Under these analytical conditions, AA and $^{13}\text{C}_3\text{-AA}$ elute around 3.4 min.
8. Because the optimum values differ for each mass spectrometer, they must be optimized for the equipment used. If the optimum values of AA and $^{13}\text{C}_3\text{-AA}$ differ, those of AA are used. To optimize the MRM conditions, after acquiring the MRM transition of the highest intensity by infusion analysis, analysis is performed with the SFC/MS/MS system connected to the column, and ionization parameters for the conditions with the largest peak area are set.
9. Figure 1 shows a schematic diagram of the SFC/MS/MS system used in this study. Because there is branch to the waste in front of the mass spectrometer, the amount of AA introduced into the mass spectrometer by increasing the set pressure of the back-pressure regulator (back-pressure gradient actually increases the pressure with the gradient) contributes to higher sensitivity. For UPC², the back-pressure gradient is entered into the convergence manager tab of the inlet file. The back-pressure gradient is set to 3000 psi from 0.2 min before the elution of the AA until the completion of elution of AA, and then returned to 2000 psi. In addition, it is not necessary to set in a splitless system such as Shimadzu Nexera UC.

10. Stable quantification can be achieved by using the same $^{13}\text{C}_3$ -AA solution for the solution added to the sample and that added to the standard solution.

For the sample to be analyzed for the first time, a standard solution is added to it in order to perform the validation test of the analysis method. A standard solution of $n = 6$ is added to the validation sample at this time. Because most heated foods contain AA, it is necessary to analyze the non-additive sample with over $n = 2$ in order to determine the amount of AA added. The AA concentration added to a sample for validation is the same as the AA concentration in the sample.

11. Because AA in the environment dissolves in ACN, ACN is used from the reagent bottle each time instead of using the stored solution. In addition, SFC/MS/MS analysis of ACN is performed to confirm that AA contained in ACN is below the lower LOQ.
12. Because MgSO_4 absorbs water and hardens, MgSO_4 is added last and the subsequent shaking is done quickly.
13. By swelling the dried sample with water, the AA can be easily extracted, and the quantified value becomes stable. However, if there is excess water, the recovery rate decreases.
14. Hex defatting is used to remove oils and fats, which are impurities in confectionery and grains, from the ACN extract.
15. The auto purge function of each device is used. In UPC², the mobile phase solution is purged for 2 min, and the needle cleaning solution is purged five times.
16. Because the interior of the sample loop is not filled by purging the mobile phase, the area is not stable after several analyses. Therefore, after analyzing the blank for five times, the calibration solution and the sample solution are analyzed. By flowing MeOH/water (95/5, v/v) as a make-up solvent after sample analysis, clogging due to water-soluble salt remaining at the branch of the pipe can be prevented, thereby allowing stable quantitation. When creating a batch file with Waters SFC/MS/MS, file name, MS file (MRM analytical method), MS tune file (MS method), inlet file (SFC analytical method), vial position, injection volume, sample type, conc A, and inlet postrun (SFC cleaning method) are entered. Figure 2 shows the chromatogram of AA analysis in milk coffee.
17. The concentration can be calculated using a software such as Microsoft Excel by determining only the area of the AA peak, without using the analytical software of the equipment.
18. To obtain the accuracy and precision of the validation data, the added area obtained by subtracting the average of the non-added sample areas of over $n = 2$ from each area of the added sample of $n = 6$ is used for the calculation.

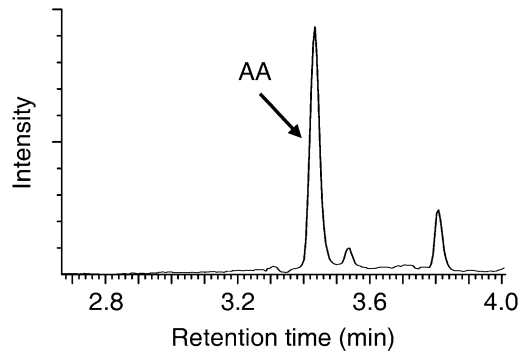


Fig. 2 Chromatogram of AA in milk coffee

References

- Erkekoglu P, Baydar T (2014) Acrylamide neurotoxicity. *Nutr Neurosci* 17:49–57
- Chevolleau S, Jacques C, Canlet C et al (2007) Analysis of hemoglobin adducts of acrylamide and glycidamide by liquid chromatography-electrospray ionization tandem mass spectrometry, as exposure biomarkers in French population. *J Chromatogr A* 1167:125–134. <https://doi.org/10.1016/j.chroma.2007.07.044>
- Bickers DR, Mukhtar H (1994) IARC monographs on the evaluation of carcinogenic risks to humans. In: International Agency for Research on Cancer, Lyon, France
- Rosén J, Hellenäs KE (2002) Analysis of acrylamide in cooked foods by liquid chromatography tandem mass spectrometry. *Analyst* 127: 880–882. <https://doi.org/10.1039/B204938D>
- Gökmen V, Palazoğlu TK (2008) Acrylamide formation in foods during thermal processing with a focus on frying. *Food Bioprocess Technol* 1:35–42. <https://doi.org/10.1007/s11947-007-0005-2>
- Pundir CS, Yadav N, Chhillar AK (2019) Occurrence, synthesis, toxicity and detection methods for acrylamide determination in processed foods with special reference to biosensors: a review. *Trends Food Sci Technol* 85: 211–225. <https://doi.org/10.1016/j.tifs.2019.01.003>
- Arvanitoyannis IS, Dionisopoulou N (2014) Acrylamide: formation, occurrence in food products, detection methods, and legislation. *Crit Rev Food Sci Nutr* 54:708–733. <https://doi.org/10.1080/10408398.2011.606378>
- Stadler RH, Blank I, Varga N et al (2002) Acrylamide from Maillard reaction products. *Nature* 419:449–450. <https://doi.org/10.1038/419449a>
- JECFA (2010) Summary and conclusions. In: Proceedings of the joint FAO/WHO expert Committee on food additives seventy-second meeting. JECFA, Rome, Italy, pp 1–16
- Food Safety Commission of Japan (2016) Acrylamide formed on heating. http://www.fsc.go.jp/osirase/acrylamide1.data/acrylamide_hyokasyo1.pdf. Accessed 22 Mar 2021
- Commission Regulation (EU) (2017) Establishing mitigation measures and benchmark levels for the reduction of the presence of acrylamide in food. <https://op.europa.eu/en/publication-detail/-/publication/1f3b45fb-ce6b-11e7-a5d5-01aa75ed71a1/language-en>. Accessed 22 Mar 2021
- Evrin Kepekci Tekkeli S, Önal C, Önal A (2012) A review of current methods for the determination of acrylamide in food products. *Food Anal Methods* 5:29–39. <https://doi.org/10.1007/s12161-011-9277-2>
- Keramat J, LeBail A, Prost C et al (2011) Acrylamide in foods: chemistry and analysis. a review. *Food Bioprocess Technol* 4:340–363. <https://doi.org/10.1007/s11947-010-0470-x>
- Andrawes F, Greenhouse S, Draney D (1987) Chemistry of acrylamide bromination for trace analysis by gas chromatography and gas chromatography-mass spectrometry. *J Chromatogr* 399:269–275. [https://doi.org/10.1016/S0021-9673\(00\)96129-6](https://doi.org/10.1016/S0021-9673(00)96129-6)
- Pittet A, Périsset A, Oberson JM (2004) Trace level determination of acrylamide in cereal-based foods by gas chromatography-mass spectrometry. *J Chromatogr A* 1035:123–130. <https://doi.org/10.1016/j.chroma.2004.02.037>
- Jezussek M, Schieberle P (2003) A new LC/MS-method for the quantitation of acrylamide

- based on a stable isotope dilution assay and derivatization with 2-mercaptobenzoic acid. Comparison with two GC/MS methods. *J Agric Food Chem* 51:7866–7871. <https://doi.org/10.1021/jf0349228>
17. Lim HH, Shin H (2013) Ultra trace level determinations of acrylamide in surface and drinking water by GC-MS after derivatization with xanthidol. *J Sep Sci* 36:3059–3066. <https://doi.org/10.1002/jssc.201300209>
 18. Zokaie M, Abedi AS, Kamankesh M et al (2017) Ultrasonic-assisted extraction and dispersive liquid-liquid microextraction combined with gas chromatography-mass spectrometry as an efficient and sensitive method for determining of acrylamide in potato chips samples. *Food Chem* 234:55–61. <https://doi.org/10.1039/C8AY02687D>
 19. De Paola EL, Montecchi G, Masino F et al (2017) Determination of acrylamide in dried fruits and edible seeds using QuEChERS extraction and LC separation with MS detection. *Food Chem* 217:191–195. <https://doi.org/10.1016/j.foodchem.2016.08.101>
 20. Huang Y, Li C, Hu H et al (2019) Simultaneous determination of acrylamide and 5-hydroxymethylfurfural in heat-processed foods employing enhanced matrix removal—lipid as a new dispersive solid-phase extraction sorbent followed by liquid chromatography-tandem mass spectrometry. *J Agric Food Chem* 67:5017–5025. <https://doi.org/10.1021/acs.jafc.8b05703>
 21. Mastovska K, Lehotay SJ (2006) Rapid sample preparation method for LC-MS/MS or GC-MS analysis of acrylamides in various food matrices. *J Agric Food Chem* 54:7001–7008. <https://doi.org/10.1021/jf061330r>
 22. Food Safety Commission of Japan (2016) Acrylamide in foods generated through heating. *Food Saf* 4:74–88
 23. Takeda H, Izumi Y, Takahashi M et al (2018) Widely-targeted quantitative lipidomics method by supercritical fluid chromatography triple quadrupole mass spectrometry. *J Lipid Res* 59:1283–1293. <https://doi.org/10.1194/jlr.D083014>
 24. Fujito Y, Hayakawa Y, Izumi Y et al (2017) Importance of optimizing chromatographic conditions and mass spectrometric parameters for supercritical fluid chromatography/mass spectrometry. *J Chromatogr A* 1508:138–147. <https://doi.org/10.1016/j.chroma.2017.05.071>
 25. Grand-Guillaume Perrenoud A, Veuthey JL, Guillaume D (2014) Coupling state-of-the-art supercritical fluid chromatography and mass spectrometry: from hyphenation interface optimization to high-sensitivity analysis of pharmaceutical compounds. *J Chromatogr A* 1339:174–184. <https://doi.org/10.1016/j.chroma.2014.03.006>
 26. Lesellier E, West C (2015) The many faces of packed column supercritical fluid chromatography—a critical review. *J Chromatogr A* 1382:2–46. <https://doi.org/10.1016/j.chroma.2014.12.083>
 27. Si-Hung L, Bamba T (2020) A review of retention mechanism studies for packed column supercritical fluid chromatography. *Anal Sci Adv* 2:47–67. <https://doi.org/10.1002/ansa.202000144>
 28. Yoshioka T, Nagatomi Y, Harayama K et al (2018) Development of an analytical method for polycyclic aromatic hydrocarbons in coffee beverages and dark beer using novel high-sensitivity technique of supercritical fluid chromatography/mass spectrometry. *J Biosci Bioeng* 126:126–130. <https://doi.org/10.1016/j.jbiosc.2018.01.014>
 29. Yoshioka T, Izumi Y, Nagatomi Y et al (2019) A highly sensitive determination method for acrylamide in beverages, grains, and confectioneries by supercritical fluid chromatography tandem mass spectrometry. *Food Chem* 294:486–492. <https://doi.org/10.1016/j.foodchem.2019.05.033>



Application of Bubbling Extraction Coupled to Gas Chromatography Mass Spectrometry in Food Analysis

Yuanji Gao, Lei He, Lijuan Zhao, and Quan He

Abstract

In recent years, occurrence of selective enrichment of organic matter and partial concentration of inorganic components by gaseous microbubbles in nature has necessitated development of various bubbling extraction systems. Particularly, bubbling extraction can promote transfer of solutes from a liquid to gas phase. Moreover, different carrier gases as well as coupling to mass spectrometer have allowed rapid analysis of solutes. Bubbling extraction is a versatile approach for efficient preconcentration of organic solutes in aqueous solutions. In this chapter, we describe use of bubbling extraction coupled to gas chromatography mass spectrometric for chromatographic separation and molecular characterization, as well as effective qualitative and quantitative analysis of food and environmental samples, targeting their chemical quality, safety, origin, and authentication. We summarize validation of the molecular masses of analytes within complex matrices using the electron impact mass spectrometry.

Key words Food analysis, Bubbling extraction, Carbon dioxide, Mass spectrometry (MS), Electron impact (EI)

1 Introduction

The current rapid development of economies, coupled with improvement in living standards, has gradually increased research in food quality. Generally, food analysis mainly focuses on assaying lipids, proteins, carbohydrates, preservatives, flavors, colorants, and texture modifiers, as well as vitamins, steroids, drugs, pesticide residues, and trace elements [1]. To date, considerable efforts have been devoted to developing rapid analytical methods for assessing food safety and quality [2]. For example, mass spectrometry (MS), an instrumental technique that measures the mass-to-charge (m/z) ratio of an ion, has been extensively applied in food analysis. The advantages of MS, including its high molecular sensitivity, throughput, precision, and accuracy, have made it an indispensable tool for food analysis. Consequently, liquid chromatography MS (LC-MS) and gas chromatography MS

(GC-MS) are now routinely and widely used for analysis of food and food-related samples. A typical MS analysis starts with sample pretreatment, especially for food samples with complex matrices and low analyte concentrations. This is because coexistence of matrices with analytes affects accuracy and efficiency of the detection results. Currently, the most widely used sample pretreatment techniques include solid phase extraction, liquid-liquid extraction, and microextraction techniques. However, these approaches require considerable analytical times as well as complex sample and reagent preparation steps.

The newly developed bubbling extraction (BE) technique, inspired by naturally occurring enrichment of organic solutes in sea spray aerosol [3–8], is a versatile and practical approach for preconcentrating and purifying analytical samples. In addition, the generated bubbles also play a crucial role in many Champagne or sparkling beverages and wines [9–11]. Previous studies have shown that BE can be combined with MS to realize real-time monitoring of food products, guaranteeing higher speeds, and less sample preparation procedures than conventional techniques [12–15]. Consequently, the BE-MS method is considered an important approach for food analysis [13, 16–20], where it facilitates direct, rapid, and high-throughput molecular analysis of different food and food-related samples with minimal or no sample preparation process. Therefore, the method offers an excellent alternative to LC-MS and GC-MS technologies that are generally applied in food analysis.

BE is a new method of sample pretreatment based on the interface characteristics of bubbles. Specifically, a carrier gas is dissolved in the sample solution, by applying pressure and stirring, followed by a sudden decompression or gas bubble operation, which results in formation of a large number of bubbles in the liquid sample that enrich the analytical material in the sample. Uninterrupted bubbles drag surfactants along their way through the liquid bulk phase, reach the gas-liquid interface, and finally burst to eject aerosol microdroplets into the atmosphere. Consequently, the released analytes are immediately transferred to the MS detector, as shown in Fig. 1. The BE principle is similar to that of adsorptive bubble separation in foaming systems [21]. The analytes ions then generate MS signals, which allow these compounds to be released in a very short time (a few seconds). Therefore, this method has a high signal-to-noise ratio [22]. Notably, this technique relies on the relationship between peak area and sample concentration to perform quantitative analysis. Here, the analytes are transferred to the ion source by gas-phase extraction, which causes minimal harm to the mass spectrometer. Existence of different ion sources allows BE to be combined with atmospheric pressure chemical ionization (APCI) [23, 24], electrospray ion source (ESI) [25, 26], electron ionization (EI) [22, 27, 28], and other ion sources coupled to MS, thereby increasing the range of detectable

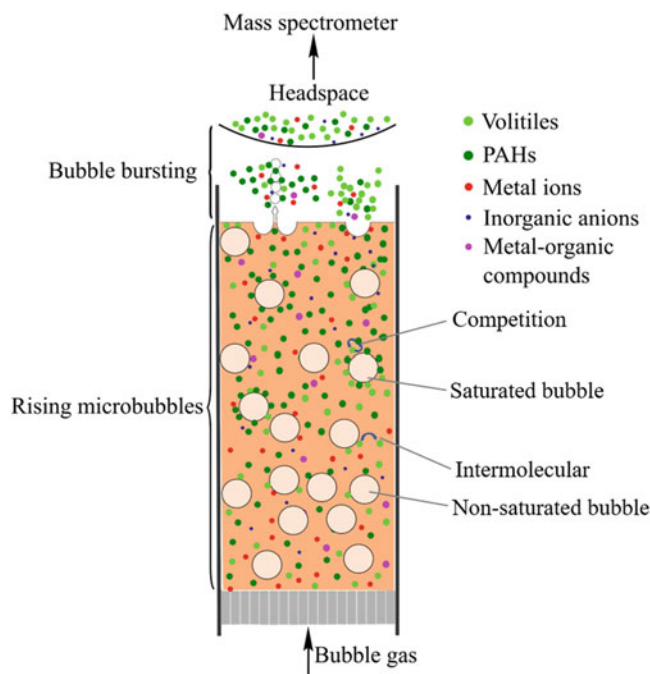


Fig. 1 Schematic representation of the proposed mechanism and bubble process of chemical enrichment in BE with liquid samples

analyte species. BE can also be coupled direct MS to create a simple, efficient, low-cost, and multi-purpose analytical strategy that can be widely used in food analysis. In fact, this strategy guarantees excellent identification and quantitative analysis of trace analytes in complex matrices. Coupling BE with MS allows combining of advantages from both techniques, thereby generating a technique that is very sensitive, and suitable for determination of ultra-trace levels of analytes that reaches down to pg/mL concentrations.

In this chapter, we describe coupling of BE and ionization methods used for MS measurements of foods samples using a suitable interface, then discuss the steps of sample preparation, optimization of spectrometric parameters, analysis, and quantification.

2 Materials

All solutions are prepared using HPLC-grade reagents and ultra-pure water with a resistivity of 18 M Ω cm at 25 °C. Unless otherwise specified, all reagents and prepared solutions are stored at room temperature. Follow all waste disposal regulations when disposing waste materials. As well, all experimental steps are performed in accordance with laboratory safety regulations.

2.1 Equipment and Supplies

1. Analytical balance.
2. Eppendorf pipettors of 1–10 μL , 20–200 μL , and 100–1000 μL .
3. Measuring cylinders of 10 mL and 50 mL.
4. Eppendorf tubes of 1.5 mL, 5 mL, and 10 mL.
5. Sample vials of 40 mL.
6. GC glass vials of 2 mL.
7. Water purification system (UPW-10NT).
8. BE system: an automated EST Analytical purge and trap unit (Centurion WS, LGX50, OH, USA) (*see Note 1*).
9. 7000C Triple Quadrupole GC-MS system (Agilent Technologies, Palo Alto, CA, USA) with electron ionization (EI) source (*see Note 2*).
10. BE system coupled with GC injector (*see Note 3* and Fig. 2).
11. 30 m DB-1MS GC column (0.32 mm ID, 0.25 μm film; J&W Scientific, Folsom, CA, USA) consisting of 100% dimethyl polysiloxane (Agilent Technologies) (*see Note 4*).
12. 50 mm Pac CS5A Anion column (4 mm DI).
13. Trapping device (*see Note 5*).
14. Split injection liner (Agilent Technologies, cat.no. 5190-3165) (*see Note 6*).
15. Syringe (CTC 10 μL , Combi/GC-Pal, cat.no. G6500-80116).
16. Inductively coupled plasma-mass spectrometry (ICP-MS) (Agilent, 8900) (*see Note 7*).
17. Ion chromatography (Thermo Scientific Dionex ICS-1100) (*see Note 7*).

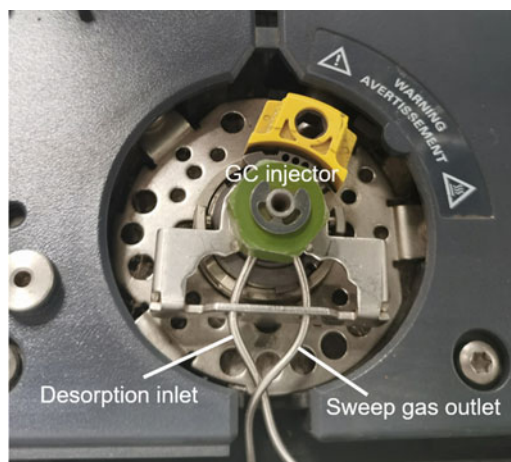


Fig. 2 Bubbling system coupled with GC injector

2.2 Solvents and Chemical Reagents

1. HPLC-grade methanol (Darmstadt, Germany). Store at room temperature.
2. HPLC-grade acetone (Darmstadt, Germany). Store at room temperature.
3. HPLC-grade dichloromethane (Darmstadt, Germany). Store at room temperature.
4. Extra-pure sodium chloride (NaCl).
5. Hydroxide eluent: 20 mM.
6. Stock standard solution: a dichloromethane solution containing 8 polycyclic aromatic hydrocarbons (PAHs) (2000 mg/L each), including naphthalene, acenaphthylene, acenaphthene, fluorene, phenanthrene, fluorine, pyrene, and chrysene. Dilute stock standard solution to 10 and 100 µg/mL with methanol/dichloromethane (1:1, v/v). Store them at -20 °C (*see Note 8*).
7. Stock internal standard (IS) solutions: three ISs, naphthalene-*d*₈, acenaphthylene-*d*₁₀, and fluorene-*d*₁₀ are used (1000 mg/L each, dissolved in acetone). Dilute stock IS solutions to 10 µg/mL with acetone. Store them at -20 °C (*see Note 8*).
8. Helium, nitrogen, argon, carbon dioxide (CO₂), and methane were used as BE carrier gases (*see Note 9*).
9. Metal ions, including ⁷Li, ⁹Be, ²³Na, ²⁴Mg, ³⁹K, ⁴³Ca, ⁴⁴Ca, ⁵¹V, ⁵²Cr, ⁵⁵Mn, ⁵⁹Co, ⁷¹Ga, ⁷⁵As, ⁷⁸Se, ⁸⁵Rb, ⁸⁸Sr, ¹⁰⁷Ag, ¹¹²Cd, ¹³³Cs, ¹³⁷Ba, ²⁰⁵Tl, ²⁰⁶Pb, ²⁰⁷Pb, ²⁰⁸Pb, and ²³⁸U in aqueous solutions (100 µg/mL). Store them at 4 °C.
10. Mixed inorganic anions including NO₃⁻, Br⁻, Cl⁻, SO₄²⁻, and F⁻: the stock standard solution is diluted to the concentration level of ng/mL. Store at 4 °C.
11. Intermediate standard solutions are prepared from the stock standard solutions and stored at 4 °C during the analysis week. The intermediate standard solutions are diluted to the required concentration before use.
12. Hops (*Humulus Lupulus L.*). Store it at -20 °C.
13. Lemonade bubble iced coffee. Store it at 4 °C.
14. Urine samples. Store at 4 °C.

2.3 Software

1. Agilent MSD ChemStation software (Agilent Technologies).
2. Agilent MassHunter GC/MS Acquisition version B.07.02.1938 or subsequent (Agilent Technologies).
3. Agilent MassHunter Qualitative Analysis version B.07.00 or subsequent (Agilent Technologies).

4. National Institute of Standards and Technology (NIST) mass spectra library 2011.
5. EST Analytical ENCON Evolution (Rev. 4.3).

3 Methods

A common strategy for analyzing volatile organic compounds (VOCs) is to trap them onto a sorbent material, then release them to again gas phase prior to detection. EI source, a hard ionization technique characterized by high sensitivity, is also widely used in mass spectrometers and has become the standard ionization source of GC-MS. It is widely applied in analysis of non-polar and volatile compounds. On the other hand, high-throughput GC-MS is a highly sensitive technique that is currently used in food sciences. EI-MS is often used in combination with GC, for determination of components in complex matrices, owing to its high selectivity and sensitivity. Therefore, the combination of BE and GC-MS is the ideal platform for analyzing VOCs in food.

All procedures are carried out at room temperature unless otherwise specified. Aerosols emitted into the atmosphere can be collected for laboratory analysis or in situ analyzed via different detectors. The MS analysis of aerosols can be readily achieved in both online (mainly for volatile and semi-volatile compounds) and offline (mainly for nonvolatile compounds and metal ions) systems.

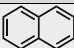
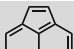
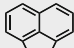
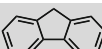
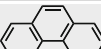
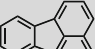
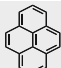
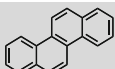
3.1 Prepare Apparatus

1. Perform the EI-MS tuning test.
2. Ensure the adequacy of water for cleaning the pipeline of bubbling system.
3. Establish the communication between automated EST Analytical purge and trap unit and GC-MS.
4. Introduce carbon dioxide as BE carrier gas.
5. Use the blank water to remove the organic compounds that may remain in the trap and clean the pipeline.
6. Two instruments are set on “Standby.”

3.2 PAHs Analysis

1. Using the bubbling system coupled with GC-MS, the 8 PAHs are analyzed by a high-sensitivity triple quadrupole mass spectrometer in selective ion monitoring (SIM) mode (*see Note 10*) and their GC retention times are recorded. The m/z values of the 8 PAHs are presented in Table 1.
2. Set the split ratio at 1:5.
3. Set the temperature gradient for the column oven: 0–2 min, 80 °C; 2–7 min, 80–180 °C; 7–12 min, 180 °C; 12–23 min, 180–290 °C; 23–31 min, 290 °C.
4. Set a constant flow rate of the carrier gas helium at 1.5 mL/min through the column.

Table 1
The quantification and confirmation ions of the 8 PAHs

Analytes	Structure	Quantitative ion (<i>m/z</i>)	Qualitative ion (<i>m/z</i>)	IS
Naphthalene		128	108, 154	Naphthalene- <i>d</i> ₈
Acenaphthylene		152	151, 153	Acenaphthylene- <i>d</i> ₁₀
Acenaphthene		154	153, 152	Acenaphthylene- <i>d</i> ₁₀
Fluorene		166	165, 167	Acenaphthylene- <i>d</i> ₁₀
Phenanthrene		178	179, 176	Fluorene- <i>d</i> ₁₀
Fluoranthene		202	200, 203	Fluorene- <i>d</i> ₁₀
Pyrene		202	200, 203	Fluorene- <i>d</i> ₁₀
Chrysene		228	226, 229	Fluorene- <i>d</i> ₁₀

5. Set injector and transfer line temperatures at 280 °C and 300 °C, respectively.
6. Filament source, 230 °C; electron ionization energy, 70 eV.
7. PAHs were detected using the triple quadruple mass spectrometer in SIM mode (Table 1).
8. Parameters are optimized using a single-factor method for detecting 8 PAHs. Optimized parameters: bubbling time, 15 min; CO₂ flow rate, 100 mL/min; extraction temperature, 50 °C; NaCl, 4.0 g.
9. Prepare the working standard solutions containing PAHs and ISs: the concentration of PAHs is set at a concentration range of 10–100 µg/L meanwhile the spiked ISs are set at a concentration of 20 µg/L. Store them at 4 °C.
10. Briefly, analytes extracted in microbubble are fully gasified at high-temperature GC inlet, and then introduced into an EI-MS for qualitative and quantitative analysis. A representative scheme of coupling BE with GC-EI-MS is shown in Fig. 3.
11. CO₂ (purity ≥ 99.999%) is used as BE carrier gas (*see Note 11*).
12. Eight PAHs in ultrapure water and 4–6 g NaCl were qualitatively and quantitatively analyzed (*see Note 12*).
13. A prepared water sample (5 mL) is transferred to the U-type chamber. Uninterrupted CO₂ bubbles are introduced through

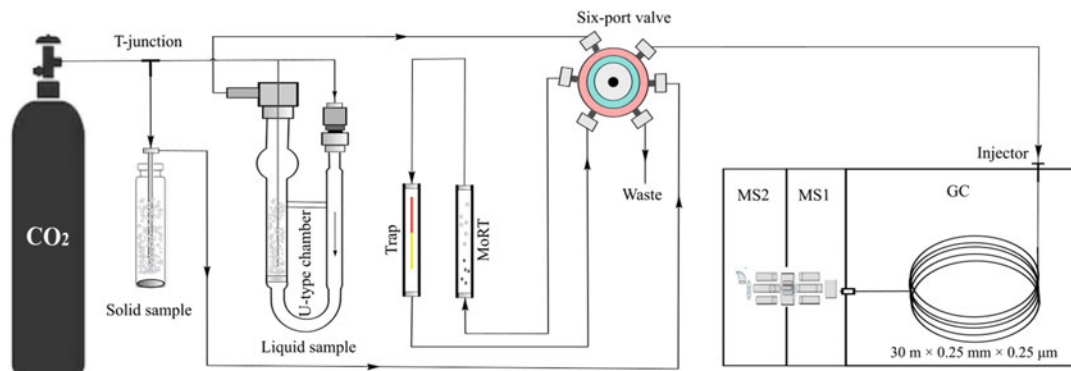


Fig. 3 A schematic representation of the entire experimental setup of carbon dioxide bubbling extraction system (CDBES). Arrows indicate direction of the gaseous flow. Reprinted with permission from [22]. Copyright (2020) American Chemical Society

100- μm micropores at the bottom of the sample solution. The bubbling time and temperature are iteratively optimized. After the extraction is completed, trace analytes in the water sample are desorbed and introduced into GC-MS for analysis (*see Note 13*).

14. Under the optimal BE conditions, the performance of the extraction method for 8 PAHs is evaluated by measuring linearity and precision (*see Note 14*). Analyze the working standard solution (50 $\mu\text{g}/\text{L}$) throughout the whole analysis cycle to evaluate the stability and performance of the system.
15. The analytical parameters, such as limits of detection (LODs) and limits of quantification (LOQs), are determined according to Knoll's definition [29] with the solutions of PAHs (*see Note 15*).
16. Add water sample to the U-type chamber, uninterrupted CO₂ microbubbles are introduced at the bottom of the sample solution (*see Note 16*). The ISs should be added to the water before BE to compensate for sample loss.
17. Before next use, U-type chamber is cleaned with hot ultrapure water for several times (*see Note 17*).
18. Add water-suspended soil sample to a sample vessel, continuous CO₂ bubbles are introduced from the probe tip for BE process (*see Note 18*). The ISs should be added to the soil before BE to compensate for sample loss.
19. Before next use, sample vessel and probe are cleaned with hot ultrapure water for several times (*see Note 17*).
20. Calibration curves are established using the regression analysis: $y = ax + b$, where y represents the ratio of the peak areas of PAH to IS while x represents the concentration of the investigated PAH.

3.3 Volatiles in Real Samples

1. The measurements are performed with helium in split mode using different split ratios: 1:50 for hops, 1:20 for lemonade bubble iced coffee, and 1:3 for urine samples.
2. Set the temperature gradient for the column oven: 0–2 min, 35 °C; 2–19 min, 35–290 °C.
3. Set injector and transfer line temperatures at 250 °C and 270 °C, respectively.
4. Set a constant flow rate of the carrier gas helium at 0.8 mL/min through the column.
5. Configure the electron impact ionization operating parameters as follows: 230 °C for the filament source and 70 eV of electron ionization energy.
6. Set the mass range window at 39–400 *m/z*.
7. Under the optimal experimental conditions except for the NaCl, urine sample is added into the U-type chamber, and CO₂-based bubbles are constantly introduced through 100- μ m micropores at the bottom of the sample solution (*see Note 19*).
8. Before next use, the sample chamber and probe are cleaned with hot ultrapure water for several times (*see Note 17*).
9. The lemonade bubble iced coffee is added into the sample vessel, continuous CO₂ microbubbles are introduced from the probe tip for the BE process (*see Note 20*).
10. Before next use, sample probe was cleaned with hot ultrapure water for several times (*see Note 17*).
11. Hops are pulverized, dissolved in distilled water, filtrated, and finally added into the sample vessel, and continuous CO₂ microbubbles are introduced from the probe tip for BE process (*see Note 21*).
12. Before next use, the sample vessel and probe are cleaned with hot ultrapure water for several times (*see Note 17*).
13. The 2011 National Institute of Standards and Technology (NIST11; National Institute of Standards and Technology, Gaithersburg, MD, United States) library is used to identify compounds, and only those with certainty greater than 55% are reported.

3.4 Metallic Element Analysis

Apart from organic analytes, the BE technique, coupled to ICP-MS, has also been applied in extraction of heavy metal ions.

1. Prepare heavy metal ion solution at the concentration level of ng/mL and transfer it into the U-type chamber.
2. Constant introduction of gas microbubbles through micropores at the bottom of the sample solution.

3. Recycling and filtration of sample solutions by a microporous membrane.
4. Analysis of the recycled solutions via ICP-MS.
5. Compare the measured concentration with the original concentration. Removal efficiency (RE) of heavy metal ions concentrations can be obtained by the Eq. 1:

$$RE = \frac{C_{\text{sample}} - C_{\text{residual}}}{C_{\text{sample}}} \times 100\% \quad (1)$$

where C_{sample} represents the origin sample concentration, while C_{residual} means residual sample concentration after BE process (see **Note 22**).

6. The trace metal ions remaining in the inner wall of the pipe and U-type chamber were cleaned with hot ultrapure water for several times.

3.5 Inorganic Anion Capture

The BE technique coupled to IC can also be applied in the extraction of inorganic anion.

1. Preparation of inorganic anion solution at ng/mL concentration level and transfer it in the U-type chamber.
2. Constant introduction of gas microbubbles through micropores at the bottom of the sample solution.
3. Recycling and filtration of sample solutions by a microporous membrane.
4. Set parameters as follows: Flow rate, 1.3 mL/min; sample volume, 25 μ L; current, 50 mA.
5. Analysis of the recycled solutions via IC.
6. Compare the measured concentration with the original concentration. Removal efficiency (RE) of inorganic anion can be obtained by the Eq. 1.
7. The trace metal ions remaining in the inner wall of the pipe and U-type chamber were cleaned with hot ultrapure water for several times.

4 Notes

1. Other models are also acceptable as long as they are compatible with GC-MS.
2. The mass spectrometer operated in the EI mode is set as follows: quadrupole temperature, 150 $^{\circ}$ C; injector temperature, 230–280 $^{\circ}$ C; transfer line temperature, 250–300 $^{\circ}$ C; electron beam energy, 70 eV; and ion source temperature, 200–250 $^{\circ}$ C. Suitable split ratios are chosen and adjusted

according to the sample concentration. Either a full scan mode or selected ion monitoring modes can be used. The monitoring interval is selected according to the target analytes. The temperature of transfer line is generally 10–20 °C higher than that of GC injector.

3. The desorption outlet of bubbling system should be connected to the GC injector via a stainless-steel tube (*see* Fig. 2).
4. The column size should match GC-MS. Columns with different filling materials are selected according to the type of the compounds to be analyzed. To select an appropriate GC column, it is important to consider both the polarity and types of analytes. Generally, the maximum oven temperature generally should not exceed the maximum tolerated temperature of the column.
5. Trapping materials can take a variety of forms depending on analytes type.
6. The injection liner with glass hairs to ensure full ionization of analytes.
7. The ICP-MS and IC instruments are performed according to common conditions.
8. The configuration steps should be performed in a chemical fume hood. In addition, standard solutions should also be configured in regular volumetric flasks.
9. Other inert gases can also be used as carrier gases for BE.
10. The 8 PAHs can also be analyzed using a full scan mode.
11. The corresponding standard solution is prepared at different concentrations ranging from 1.0 to 50 µM.
12. The online system requires a carrier gas that has >99.999% purity, whereas the offline system has no purity requirements. The BE carrier gas is set at a flow rate and pressure of 10–100 mL/min and 20–100 psi pressure, respectively.
13. The volatile/semivolatile analytes are extracted by CO₂ micro-bubbles from aqueous solution at 40–90 °C for 0.1–30 min and then absorbed onto the Trap through a moisture removal trap (MoRT). The trapped components are desorbed at 240–265 °C for 3.0 min and transferred online to GC-MS for analysis. In addition, blank samples are analyzed likewise to identify false positives as well as chemical contamination. During the validation process for food samples, several analytical parameters, such as stability, recovery, LOD, LOQ, relative standard deviation, and linear relationship, are evaluated.
14. The method precision is measured using the concentrations within the linear range for sextuplicated tests.

15. The LODs are based on a signal-to-noise ratio (SNR) of 3, and the LOQs are based on an SNR of 10.
16. All water samples should be filtered through 0.22 μm micro-porous membrane.
17. During each GC-MS measurement cycle, the sampling needle, loop, and U-type chamber should be cleaned with hot water (90 $^{\circ}\text{C}$). The trap is also heated at 250 $^{\circ}\text{C}$ for 8.0 min. These procedures are sufficient to clean the purge system for subsequent measurements. The dry purge step is set to 2.0 min to remove water trapped on the sorbent.
18. Soil samples need to be crushed and suspended in water, and the amount should be less than 1.0 g to protect the probe from contamination.
19. Urine samples are collected from healthy/diseased volunteers and should be analyzed within 12 h after collection to avoid biodegradation. Urine contains numerous inorganic salt ions, which are harmful to chromatographic column and mass spectrometer. In addition, the content of organic components is low. Therefore, the experiments should be conducted at low split ratios. In addition, the analysis of urine sample can be achieved using an offline process: (1) generation of bursting bubbles in urine sample by feeding gas through an air diffuser; (2) collection of the bursting bubble aerosol droplets; and (3) analysis of the collected aerosols and bulk solutions by direct-infusion EI-MS.
20. The lemonade bubble iced coffee can be obtained from a local Kentucky Fried Chicken shop.

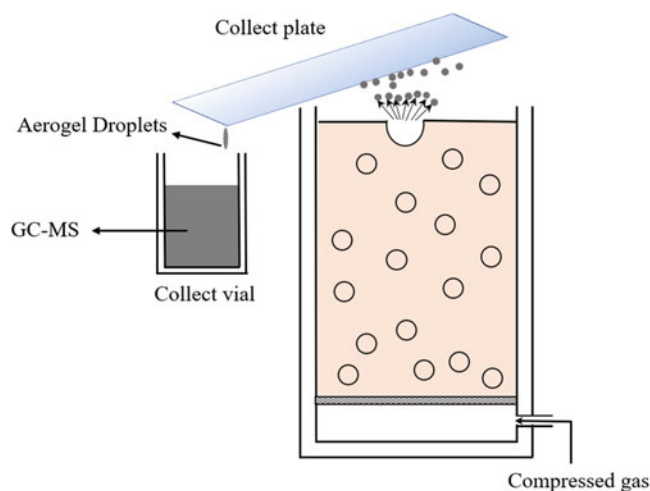


Fig. 4 Profile of the apparatus used for generation and collection of aerogel droplets. Gas is fed through the porous surface at the bottom of the aqueous analyte solution

21. The hops can be purchased from the local market.
22. Microbubbles can also be produced in solution by passing gas through an air diffuser, as shown in Fig. 4. The metal ions in solution can be identified by collecting aerosol droplets.

Acknowledgments

Authors want to express their gratitude to the financial support received from the National Natural Science Foundation of China (No. 51873133) and the Zhejiang Post-Doctoral Preferential Fund Project (ZJ2021144).

References

1. Basha M (2020) Chromatography. In: Analytical techniques in biochemistry. Springer US, New York, NY, pp 39–59
2. Black C, Chevallier OP, Elliott CT (2016) The current and potential applications of ambient mass spectrometry in detecting food fraud. *Trac-Trends in Anal Chem* 82:268–278. <https://doi.org/10.1016/j.trac.2016.06.005>
3. Pham DQ, O'Brien R, Fraund M et al (2017) Biological impacts on carbon speciation and morphology of sea spray aerosol. *ACS Earth Space Chem* 1:551–561. <https://doi.org/10.1021/acsearthspacechem.7b00069>
4. Russell LM, Hawkins LN, Frossard AA et al (2010) Carbohydrate-like composition of sub-micron atmospheric particles and their production from ocean bubble bursting. *Proc Natl Acad Sci U S A* 107:6652–6657. <https://doi.org/10.1073/pnas.0908905107>
5. Wolf MJ, Coe A, Dove LA et al (2019) Investigating the heterogeneous ice nucleation of sea spray aerosols using prochlorococcus as a model source of marine organic matter. *Environ Sci Technol* 53:1139–1149. <https://doi.org/10.1021/acs.est.8b05150>
6. Axson JL, May NW, Colón-Bernal ID et al (2016) Lake spray aerosol: a chemical signature from individual ambient particles. *Environ Sci Technol* 50:9835–9845. <https://doi.org/10.1021/acs.est.6b01661>
7. Bertram TH, Cochran RE, Grassian VH et al (2018) Sea spray aerosol chemical composition: elemental and molecular mimics for laboratory studies of heterogeneous and multiphase reactions. *Chem Soc Rev* 47:2374–2400. <https://doi.org/10.1039/C7CS00008A>
8. Gantt B, Meskhidze N (2013) The physical and chemical characteristics of marine primary organic aerosol: a review. *Atmos Chem Phys* 13:3979–3996. <https://doi.org/10.5194/acp-13-3979-2013>
9. Liger-Belair G, Parmentier M, Cilindre C (2012) More on the losses of dissolved CO₂ during champagne serving: toward a multiparameter modeling. *J Agric Food Chem* 60:11777–11786. <https://doi.org/10.1021/jf104675s>
10. Liger-Belair G, Polidori G, Jeandet P (2008) Recent advances in the science of champagne bubbles. *Chem Soc Rev* 37:2490–2511. <https://doi.org/10.1039/B717798B>
11. Liger-Belair G (2012) The physics behind the fizz in champagne and sparkling wines. *Eur Phys J Special Topics* 201:1–88. <https://doi.org/10.1140/epjst/e2012-01528-0>
12. Vallebona G, Banchini G, Borra Cc Ini A et al (1988) Bubble extraction as a preconcentration step in trace elemental analysis: a preliminary study. *Fres Zeit Anal Chem* 331:584–587. <https://doi.org/10.1007/BF01032529>
13. Sun Y, Yang K, Cao Q et al (2017) Homogenate-assisted vacuum-powered bubble extraction of moso bamboo flavonoids for on-line scavenging free radical capacity analysis. *Molecules* 22:1–13. <https://doi.org/10.3390/molecules22071156>
14. An SZ, Ranaweera R, Luo L (2020) Harnessing bubble behaviors for developing new analytical strategies. *Analyst* 145:7782–7795. <https://doi.org/10.1039/D0AN01497D>
15. Davis JJ, Foster SW, Grinias JP (1638) Low-cost and open-source strategies for chemical separations. *J Chromatogr A* 2021. <https://doi.org/10.1016/j.chroma.2020.461820>
16. Ryu J, Kim M-J, Lee J (2019) Extraction of green tea phenolics using water bubbled with

- gases. *J Food Sci* 84:1308–1314. <https://doi.org/10.1111/1750-3841.14606>
17. Devine CE, Bennett P, Synowiec K et al (2014) Development and testing of a field screening method based on bubbling extraction and photoionization detection for measurement of benzene and total VOCs. *Groundwater Monit Rem* 34:95–104. <https://doi.org/10.1111/gwmr.12070>
 18. Ongaratto RS, do Nascimento Silva MM, da Cunha Lage PL et al (2015) Extraction of aroma compounds of fruit juices by air stripping using a bubble column operating with antifoam and its effect on juice properties. *J Food Eng* 159:1–8. <https://doi.org/10.5194/acp-13-3979-2013>
 19. Zhao C, Zu Y, Li C (2009) Extraction of solanesol from tobacco (*Nicotiana tobaccum* L.) leaves by bubble column. *Chem Eng Process* 48:203–208. <https://doi.org/10.1016/j.cep.2008.03.005>
 20. Chang C-H, Urban PL (2016) Fizzy extraction of volatile and semivolatile compounds into the gas phase. *Anal Chem* 88: 8735–8740. <https://doi.org/10.1021/acs.analchem.6b02074>
 21. Backleth-Sohrt M, Ekici P, Leupold G et al (2005) Efficiency of foam fractionation for the enrichment of nonpolar compounds from aqueous extracts of plant materials. *J Nat Prod* 68:1386–1389. <https://doi.org/10.1021/np049743e>
 22. Gao YJ, Xia B, Qin YN et al (2020) Online scavenging of trace analytes in complex matrices for fast analysis by carbon dioxide bubbling extraction coupled with gas chromatography-mass spectrometry. *J Agric Food Chem* 68: 5732–5740. <https://doi.org/10.1021/acs.jafc.0c01663>
 23. Elpa DP, Wu S-P, Urban PL (2020) Rapid extraction and analysis of volatile solutes with an effervescent tablet. *Anal Chem* 92: 2756–2763. <https://doi.org/10.1021/acs.analchem.9b05009>
 24. Yang H-C, Chang C-H, Urban PL (2017) Fizzy extraction of volatile organic compounds combined with atmospheric pressure chemical ionization quadrupole mass spectrometry. *J Vis Exp*:1–9. <https://doi.org/10.3791/56008>
 25. Chingin K, Cai YF, Chagovets V et al (2016) Preconcentration of organic solutes in urine by bubble bursting. *Metabolomics* 12:171. <https://doi.org/10.1007/s11306-016-1122-6>
 26. Chingin K, Cai Y, Liang J et al (2016) Simultaneous preconcentration and desalting of organic solutes in aqueous solutions by bubble bursting. *Anal Chem* 88:5033–5036. <https://doi.org/10.1021/acs.analchem.6b00582>
 27. Yang H-C, Urban PL (2019) On-line coupling of fizzy extraction with gas chromatography. *Anal Bioanal Chem* 411:2511–2520. <https://doi.org/10.1007/s00216-019-01755-9>
 28. Zarejousheghani M, Walte A, Borsdorf H (2018) Sprayed liquid–gas extraction of semi-volatile organophosphate malathion from air and contaminated surfaces. *Anal Methods* 10: 2503–2511. <https://doi.org/10.1039/C8AY00636A>
 29. Knoll JE (1985) Estimation of the limit of detection in chromatography. *J Chromatogr Sci* 23:422–425. <https://doi.org/10.1093/chromsci/23.9.422>



Aroma Analysis by Proton Transfer Reaction-Mass Spectrometry

Jonathan Beauchamp, Franco Biasioli, and Patrick Silcock

Abstract

Proton transfer reaction-mass spectrometry (PTR-MS) is a quantitative analytical technique for the online detection of gas-phase volatile organic compounds (VOCs), among them aroma compounds, over a broad dynamic range and down to ultra-trace concentrations. Its rapid detection capabilities and high sensitivity make it an ideal tool in food science for various applications, ranging from flavor release studies (in vivo and in vitro), characterizing food spoilage, maturation and/or processing via volatile markers, or for high-throughput mass spectral fingerprinting of food headspace. This protocol describes the general use of PTR-MS for food flavor analysis, with three highlighted applications: dynamic headspace analysis, high-throughput static headspace analysis by use of an autosampler, and nosespace analysis for in vivo aroma release during food consumption.

Key words Headspace analysis, Nosespace analysis, In vivo, Aroma release, Chemical ionization mass spectrometry, Online analysis, Volatile organic compounds, High-throughput, Autosampler, Fingerprinting

1 Introduction

The flavor of foods and beverages is characterized by the composition of their constituent aroma compounds and taste components. While the latter elicit the five taste impressions—sweet, salty, bitter, sour, and umami—via receptors on the tongue, the volatile fraction imparts the characteristic aroma through their detection by olfactory receptors located in the nasal epithelium. These aroma compounds transition from the food or beverage into the gas-phase and are subsequently directed to the olfactory cleft via either the ortho-nasal (through the nostrils) or retronasal (via the oronasopharynx) routes. Foods readily release these volatile compounds, which impart their distinctive aroma, and are further liberated during food oral processing to elicit characteristic flavor impressions [1].

Elucidating the chemical identity of an aroma-active compound can be achieved by analytical means. This can be undertaken

through use of gas chromatography-mass spectrometry/olfactometry (GC-MS/O), which offers a comprehensive deconstruction of the volatile fraction of a food matrix (*see* Chap. 13). Due to the dynamic and transient nature of flavor release processes, however, their analytical characterization requires a tool that allows for continuous analysis with a high time resolution. Proton transfer reaction-mass spectrometry (PTR-MS) is a direct injection technique that exhibits sufficient technical features to allow the real-time analysis of aroma compound release from food, i.e., online measurements with high temporal resolution, low detection limits, and a broad dynamic range. The technique was developed in the mid-1990s [2] and has been used extensively in food science for various applications, including mass spectral fingerprinting, online analysis of dynamic flavor release processes, and linking *in vivo* flavor release to sensory perception, among other topics [3–5].

There is an abundance of technical papers that present and discuss the operating principles of PTR-MS [2, 3, 6], but a brief overview is given here. In short, the technique utilizes soft chemical ionization of volatile organic compounds (VOCs) by proton transfer reactions from protonated water ($\text{H}_2\text{O}\cdot\text{H}^+$). Due to the relatively low ionization energy (1–2 eV, compared to 70 eV commonly established in electron ionization, as used in GC-MS), the degree of fragmentation of the target analyte (aroma compound) is typically low, often with the protonated molecule ($\text{M}\cdot\text{H}^+$) representing the most abundant product ion. Accordingly, the detection of that individual product provides quantitative information of its abundance in a sample gas. The generation of the protonated water primary ions takes place in an ion source (typically a hollow cathode discharge), and these are continuously injected into a reaction chamber (drift tube). Sample gas containing VOCs for analysis is fed into the drift tube and proton transfer reactions occur upon collision between the primary ions and the neutral VOCs, leading to the protonation of the VOCs (generation of $\text{M}\cdot\text{H}^+$ and potentially some fragments and/or clusters, depending on the molecule and PTR-MS operating conditions). A prerequisite of this reaction is that the proton affinity of the VOC is higher than that of water (165 kcal/mol) [2], which is true for most aroma compounds. Upon ionization, the (protonated) VOCs are directed along the drift tube towards the mass spectrometer, where they are subsequently separated according to the ratio of their mass-to-charge (m/z) and detected.

As with other technologies, PTR-MS has evolved since its early days and now boast detection limits of the single-digit ppt, levels or lower, and high sensitivities of several thousand counts-per-second per ppb_v [7]. Notably, the original quadrupole mass filter (PTR-QMS instruments) has been replaced with a time-of-flight mass spectrometer (TOF-MS), leading to a remarkable improvement in m/z detection rates and previously impossible isobaric

compound separation capability [8]. Further, peripheral equipment, such as fast gas chromatography (fastGC) [9], a calibration system for use with bespoke solutions [10] and the coupling to an autosampler [11, 12] have opened up new possibilities for food flavor studies using PTR-TOF-MS [13, 14]. This protocol paper will center on PTR-TOF-MS although notes on PTR-QMS are included for completeness. Three focal applications are described here: dynamic headspace analysis [15–17], high-throughput static headspace analysis using an autosampler [11], and nose-space analysis for in vivo aroma release during food consumption [18–20]. Data processing is an essential and complex part of PTR-MS analysis but is beyond the scope of this protocol and is therefore not included; the reader is referred to the literature for further insights on this aspect of PTR-MS analysis [21, 22].

2 Materials

The materials required for the analysis of aroma release from a food sample will vary according to the food or beverage, analytical configuration, and the target of the research. The following protocol centers on three representative cases of analyzing aroma release.

2.1 Laboratory Equipment

The chosen sampling receptacle(s) must meet the requirements of dynamic or static headspace analysis. In dynamic headspace analysis, the receptacle must have two sampling ports for the purge gas and sampling connection, respectively; further, it should be inert to minimize adsorption of VOCs to the inner surfaces (*see Note 1*). Examples are perfluoroalkoxy alkane (PFA) beakers (e.g., from Savillex, Eden Prairie, MN), glass bottles (e.g., from Schott AG, Mainz, Germany), or large passivated stainless steel beakers (e.g., DHS L containers, Gerstel, Mülheim an der Ruhr, Germany). Sampling lines to the PTR-MS instrument should be similarly inert, either PFA, polyether ether ketone (PEEK), or passivated stainless steel (e.g., Silcosteel or Sulfinert, Restek, Bellefonte, PA) (*see Note 1*). In static headspace analysis, the implementation of an autosampler typically requires the use of glass vials, as are used in gas chromatography (e.g., for low-volume processed or liquid samples), typically 20 mL or larger, equipped with pierceable septa. The autosampler is equipped with a gas-tight syringe, typically heated, for transferring the sample gas in the vial headspace to the PTR-MS instrument.

In static headspace analysis, it is important that a reproducible equilibrium in the headspace is reached. This might require that the sample is heated prior to and/or during analysis. This can be achieved by various means, for example, a laboratory oven or incubator with access ports for sampling, a water bath, or hotplate,

or bespoke autosampler heating systems for sample vials. Sample agitators and/or stirrers might also be of use, depending on the application. Further, achieving equilibrium between the food sample and its headspace gas in the receptacle takes time, the duration of which depends on their respective volumes (as well as temperature, and the nature of the sample) (*see Note 2*).

2.2 Gas Supplies

Dynamic headspace analysis requires a constant supply of gas into the sampling receptacle for continuous sampling by PTR-MS. Synthetic air or nitrogen are suitable for most applications. Ideally, the gas should be scrubbed/purified before being purged through the sampling receptacle, which is referred to as zero-air. This can be achieved by use of a charcoal filter or a catalytic VOC scrubber (e.g., that utilizes Pt/Pd at high temperature) (*see Note 3*). Vials used in static headspace analysis can be similarly purged with zero-air.

2.3 Instrumentation

Several commercial PTR-MS instruments are available on the market. Although different instruments have common and similar operating parameters, this protocol paper will be based on the implementation of a PTR-TOF 8000 model instrument (IONICON Analytik, Innsbruck, Austria).

2.3.1 Operating Requirements and Maintenance

The operating requirements of a PTR-TOF-MS instrument (or PTR-QMS) are low, comprising only a mains electricity supply (*see Note 4*) and ultra-pure water (*see Note 5*). No additional carrier or make-up gases are required (with the exception of when operating in switchable reagent ion mode; *see Note 6*). Routine maintenance (*see Note 7*) is mostly limited to occasionally cleaning the hollow cathode ion source (once or twice per year, depending on use).

2.3.2 Operating Parameters

The PTR-MS operating parameters should be set according to the application and/or target analytes (aroma compounds) of interest. The drift tube (reaction chamber) settings determine the reaction energies, thus they have a direct influence on the degree of fragmentation or cluster generation during the proton transfer reaction (*see Notes 8 and 9*). Other instrument settings can influence the abundance of primary ions in the ion source and their distribution in the drift tube (*see Notes 10–12*). For comparability of datasets, it is important that drift voltage (U_d), drift temperature (T_d), and drift pressure (p_d) remain consistent across all measurements. Similarly, if the instrument has been calibrated for the target analytes [23], then sensitivity values derived from these calibrations can only be applied to subsequent measurements if the operating parameters are kept identical for the calibration and the measurements. An alternative to calibration is to use empirically- or theoretically-derived reaction rate coefficients [24].

2.3.3 Measurement Parameters

Once the PTR-MS operating parameters are set according to the application and/or target analytes, the parameters for data acquisition can be established. PTR-TOF-MS offers the advantage (over PTR-QMS) of detecting all ion signals within the specified mass spectral (m/z) range, without the need for a priori selection of individual signals, providing more comprehensive datasets with shorter measurement intervals. An important aspect of PTR-TOF-MS analysis is that the mass scale is calibrated at regular intervals (*see Note 13*). Further technical details of data acquisition rates and settings, as well as dead-time correction and other nuances relating to PTR-TOF-MS, are treated in the literature [25–27].

Choosing an appropriate cycle time for measurements depends on the application (*see Note 14*). Further, in dynamic headspace analysis, e.g., of aroma release, the gas exchange time in the sampling receptacle should be taken into account (*see Note 15*).

2.4 Optional Equipment

Some optional equipment might be useful, depending on the application, for instance a sensor/data logger for relative humidity and/or temperature. Peripheral equipment that is particularly useful are the systems that generate reference mixtures of volatile compounds for calibration or comparison [9, 23] and, in general, gas handling or dilution systems.

3 Methods

The procedures described in the following focus on three applications: dynamic headspace analysis of aroma release from a food sample, high-throughput static headspace analysis using an auto-sampler, and nosepace analysis of *in vivo* aroma release.

3.1 Sample Preparation

Sample pretreatment, if necessary, is unique to the application, thus no guidelines can be given here. Sample pretreatment might include mechanical processing, e.g., grinding, cutting, scoring (*see Note 16*), or matrix modification, e.g., creating a suspension in (purified) water or adding NaCl to promote salting out. It is worthy of mention that a homogenous preparation of all samples is crucial in headspace experiments because contaminations and different processing can lead to artifacts.

3.2 Dynamic Headspace Analysis

1. Connect the purge gas and the PTR-MS sampling inlet to the gas ports of the (empty) sampling receptacle.
2. Analyze the empty receptacle prior to adding the (food) sample; this provides important quantitative data on the background levels of VOCs (and target analytes) (*see Note 17*).
3. Add the sample to the receptacle and close the receptacle.

4. Commence analysis by PTR-MS; quantitative and qualitative changes in VOCs can be directly monitored (in real-time) via the PTR-MS data acquisition viewer software.
5. Continue PTR-MS dynamic headspace analysis for the required duration, according to the application and research target.
6. Repeat with further samples, as necessary.

3.3 High-Throughput Static Headspace Analysis

1. Connect the PTR-MS sampling inlet to the autosampler sampling interface (typically a gas-tight syringe controlled by the autosampler).
2. Connect the electrical input/output interface of the autosampler to the PTR-MS to trigger the acquisition when a sample is ready.
3. Load the samples (vials) onto the autosampler trays at controlled temperature (typically the sample storage temperature before analysis, e.g., 4 °C). Randomization of sample order and addition of blank and reference samples is recommended to minimize systematic bias and account for variability.
4. Set the autosampler procedure as follows: (i) trigger PTR-MS acquisition; (ii) load a sample for a given time on a heated tray (e.g., the heated tray could be at 37 °C and the loading time could be 30 min) (*see Note 18*); (iii) move the sample to the measuring station; (iv) pierce the septum on the vial cap with the syringe connected to the PTR-MS (alternative configurations exist; *see Note 19*); (v) purge the headspace for a given short time, e.g., 30 s; (vi) disconnect the syringe; (vii) stop PTR-MS data acquisition; wait for a short period (typically a few min) to avoid memory effects.
5. Run the autosampler procedure for all samples.
6. Based on the autosampler generated log file, generate for each sample a data matrix of the concentrations of all detected peaks and proceed with data analysis (*see Note 20*).

3.4 Nosespace Analysis

1. Connect an appropriate nosepiece interface to the PTR-MS sampling inlet. Depending on the compounds of interest, a passive glass nosepiece will suffice, but a heated nosepiece constructed from passivated materials will minimize losses and carry-over effects, which is beneficial for characterizing the fast changes occurring at a breath-by-breath frequency (*see Notes 1 and 21*).
2. Start PTR-MS acquisition at a suitable rate (e.g., 2 spectra/s, *see Note 14*): ambient (laboratory) air will be sampled and represents the background (baseline). Due to the high concentration of carbon dioxide (CO₂) in exhaled breath (~5%), this

elicits a signal in PTR-MS (*see Note 22*), which can be used to trace the exhalation profiles; endogenous acetone (detected at m/z 59.049) can be similarly used as an alternative or additional breath tracker.

3. The panelist should insert the nosepiece into the nostrils, assume a comfortable (sedentary) position, and breathe normally through the nose; the aroma compounds in the panelist's exhaled breath will be sampled by PTR-MS (this is termed *nosespace*).
4. The volunteer should then take the food or beverage sample into their mouth and consume it according to a free or fixed oral processing (e.g., specified breathing, chewing, and/or swallowing procedure) protocol, with the nosepiece sampling interface still in position at their nostrils: the nosespace will be sampled and analyzed, as in **step 3**. After sample mastication, the panelist can either expectorate or swallow the sample, depending on the needs of the analysis and/or the nature of the sample.
5. Record the times of all relevant phases/events: sample in mouth, partial swallows, final swallow or expectoration, etc.
6. Stop the measurement at a suitable duration after swallowing/expectoration.
7. The release curves can be evaluated directly or, more commonly, after extracting release parameters, such as area under the curve (AUC), maximum concentration (I_{\max}), time to reach maximum concentration (t_{\max}), as well as others. (Nosespace analyses using PTR-MS are often accompanied by sensory perception methods, e.g., time intensity or temporal dominance of sensation (TDS), allowing for correlations between quantitative and dynamic *in vivo* aroma release data from PTR-MS and sensory impressions reported by the panelists [28–30].
8. Proceed with data analysis.

4 Notes

1. Choosing a sampling receptacle made from inert materials, such as perfluoroalkoxy alkane (PFA) or glass, is essential to minimize adsorption of VOCs on the inner surfaces and reduce memory effects and carry-over between samples. Sampling receptacles may be baked at >120 °C (depending on the properties of the material) for up to 12 h (e.g., overnight) to reduce the concentration of adsorbed VOCs. Further, it is important that sampling lines and connections downstream of the sample receptacle are inert to avoid similar problems with adsorption

and memory effects. Use of metal fittings (stainless steel or brass) are not recommended, unless these have been specially treated (e.g., passivated). Appropriate choices for sampling lines are Silcosteel™ (Restek, Bellefonte, PA), polyether ether ketone (PEEK), or PFA (the former two are preferable to the latter).

2. Optimum equilibration times for static headspace analysis are best ascertained in pre-trials in which the duration is varied for sample replicates and the target compounds are quantified and compared between the conditions. A typical equilibration time for a 20 mL vial held at room temperature is around 15–20 min.
3. When purifying the supply/purge gas, it is important to note that use of a charcoal filter will also remove water vapor (to a degree), thus the purge gas will be drier (i.e., will have a lower relative humidity) downstream of the filter than upstream. This is not the case when using a Pt/Pd scrubber, whereby water vapor passes through the device and the sample gas humidity remains unaffected.
4. Due to the high vacuum in the detection system, it is recommended that the PTR-MS instrument is connected to an uninterruptable power supply (UPS). This avoids instrument downtime (and damage) in power failure events and has the additional advantage of smoothing the alternating current (AC) supply (suppression of peaks that might damage sensitive electronic circuitry).
5. Ultra-pure water is supplied via an internal reservoir as water vapor to the hollow cathode ion source for the generation of hydronium primary ions; the reservoir has a fill capacity of 0.5–1 L and, depending on operating time, typically requires refilling only once or twice per year.
6. The switchable reagent ion (SRI) configuration allows PTR-MS to operate with alternative primary ions to protonated water, for instance, O_2^+ or NO^+ , among others [31]. Reactions proceed via electron transfer, and this offers the ability to detect some compounds that do not undergo proton transfer reactions with hydronium, such as many alkanes and alkenes, but also compounds whose proton affinity is close to that of water (e.g., formaldehyde). In the case of SRI configuration, an external gas supply (high purity O_2 , either 5.0 or 6.0, for O_2^+ or a mixture of high purity O_2 and N_2 for NO^+ mode) is required for the hollow cathode ion source, in order to generate the respective primary ions.
7. Other less-frequent maintenance is common to all mass spectrometers: replacement of membranes on the backing pump, lubricant reservoir replacement for the turbo molecular pumps,

replacement of the detector (multi-channel plate, MCP, in PTR-TOF-MS; secondary electron multiplier, SEM, in PTR-QMS).

8. Proton transfer reactions in the PTR-MS drift tube are controlled by three parameters: the drift voltage (U_d), drift temperature (T_d), and drift pressure (p_d). These determine the electric field (E) to buffer gas number density (N) in the reaction chamber, represented by the term E/N and quantified by the unit Townsend (Td), whereby $1 \text{ Td} = 10^{-21} \text{ V m}^2$. Typical settings are: $U_d = 400\text{--}600 \text{ V}$; $T_d = 60\text{--}100 \text{ }^\circ\text{C}$; $p_d = 2.0\text{--}2.4 \text{ mbar}$, which establish an E/N range of 81–163 Td. Values beyond these ranges may also be implemented under some circumstances. Common settings for flavor applications are $U_d = 600 \text{ V}$, $T_d = 60 \text{ }^\circ\text{C}$, $p_d = 2.2 \text{ mbar}$. In PTR-TOF-MS, the extraction voltage, U_{dx} , influences the efficiency of extraction of protonated analytes into the detection region of the instrument. U_{dx} is typically set to around 35 V.
9. The E/N conditions of the drift tube (see previous note) determine the suprathreshold energy of the proton transfer reactions in the drift tube. Low E/N conditions suppress fragmentation but promote (water) clustering; conversely, high E/N suppresses clustering but leads to a higher degree of fragmentation; settings should be chosen according to application and target analytes. It is important to note that the degree of clustering and/or fragmentation can vary for the same E/N set via different U_d , T_d , and p_d configurations. For example, although the settings $U_d = 400 \text{ V}$, $T_d = 70 \text{ }^\circ\text{C}$, and $p_d = 2.3 \text{ mbar}$, and $U_d = 500 \text{ V}$, $T_d = 60 \text{ }^\circ\text{C}$, and $p_d = 2.0 \text{ mbar}$ similarly establish an E/N of 108 Td, a target analyte might fragment to different degrees between these two conditions.
10. The source and source-out voltages of the hollow cathode ion source, U_s and U_{so} , respectively, can be varied to increase the abundance of hydronium and suppress the generation of O_2^+ (see next note). Further, increasing the hollow cathode current (I_{HC}) (typical range: 3–7 mA), increasing the flow of water vapor through the ion source (typical range: 5–8 standard cubic centimeters per minute; sccm), or altering the source valve (typical range: 40–60%) affects the abundance and distribution of primary ions.
11. O_2^+ ions are produced in the hollow cathode ion source from oxygen due to a small backflow of air (sample gas) from the drift tube. The backflow is caused by differential pumping of the ion source. (Note that use of nitrogen as a sample carrier gas does not lead to the production of O_2^+ due to the absence of oxygen in the backflow.) Due to higher energies of electron transfer reactions via O_2^+ to the target analytes and a

corresponding higher degree of fragmentation, the abundance of O_2^+ should be kept minimal: a rule of thumb is to maintain O_2^+ at a level of <2% of the abundance of H_3O^+ , as can be monitored via their respective signals (*see* next note). Note that changing the ion source voltages (U_s and U_{s0}) does not affect the ionization of analytes in the drift tube, apart from yielding more or fewer analyte ions due to an increase or decrease of primary ions generated.

12. Due to a high abundance of primary ions (and O_2^+ from the hollow cathode) in the drift tube, their intensities are typically monitored via their ^{18}O isotopes to avoid detector saturation (i.e., achieve accurate quantitation) and extend the lifetime of the detector. Oxygen atoms contain eight protons and have two isotopes: one with eight neutrons (^{16}O); the other with ten neutrons (^{18}O). These have the exact masses 15.9949 Da and 17.9992 Da, respectively (note that the exact mass of ^{16}O is not 16.0 Da due to the associated mass defect [32]). The ratio of natural abundances of these isotopes is 0.9976:0.0020 (^{16}O : ^{18}O); correspondingly, the abundance of ^{16}O is approximately 500 times (more precisely, 498.8) greater than that of the ^{18}O isotope. Taking H_3O^+ and O_2^+ as examples, their most abundant isotopes elicit signals at m/z 19.018 and m/z 31.990, respectively. Due to the aforementioned issues, their detection at their respective ^{18}O isotopes is necessary; these are m/z 21.022 and m/z 33.994, respectively. Note that the isotopic distribution of O_2^+ is altered due to the presence of two oxygen atoms, i.e., 0.9952:0.0040, or a factor 248.8. Accordingly, the signals at m/z 21.022 (H_3O^+) and m/z 33.994 (O_2^+) are multiplied by 500 (or 498.8) and 250 (or 248.8), respectively, to attain their corresponding isotope-corrected abundances.
13. Minor physical changes in the TOF chamber (minute expansion or contraction of the metal flight chamber due to thermal changes) affect the flight distance of ions; this correspondingly has an impact on the time of flight of ions through the chamber, which is directly observable through a shift in the ion signal position over the mass scale (shift to the left or the right). This phenomenon can be corrected for by anchoring the scale to the positions of two or three known ions that span the entire mass scale (from low to high m/z). To achieve this, it is important to select ions that are always present (at clearly detectable and consistent abundances). An obvious choice is the H_3O^+ primary ion at m/z 21.022 (*see* previous note) for the low-scale end anchor point. At the upper end of the scale, the use of a reference compound is helpful, such as achieved in the commercial PerMaSCal system (IONICON Analytik, Innsbruck, Austria), which provides a continuous feed of

1,3-diiodobenzene ($C_6H_4I_2$) into the reaction chamber to elicit a stable signal at m/z 203.943 [33].

14. Rapid data acquisition over a long period generates large data-sets, which can compromise the processor speed of the data acquisition computer, and quickly fill up data storage drives. The data acquisition rate should be chosen to suit the application. Characterizing fast processes, such as breath-by-breath nosespace analysis of aroma release, requires sufficiently rapid data acquisition to allow reliable measurement of maximum m/z concentration per breath, i.e., at least several times per second [21, 30, 34], yet longer measurement intervals are adequate when less rapid changes are expected, for instance when monitoring volatile food spoilage markers [35, 36]. Further, the data acquisition rate need not be faster than the gas exchange rate in the sampling receptacle (*see* next note).
15. When a closed receptacle is flushed with a gas, the gas exchange rate within the receptacle is directly proportional to the flow rate of the purge gas. Considering a receptacle of volume V that is purged with a gas at a flow rate F , then one gas exchange will be completed within a time $\tau = V/F$. However, due to admixing between the purge gas and the headspace gas, a complete gas exchange within the sample receptacle is achieved only after approximately 5τ . Accordingly, it is sufficient to set the PTR-MS data acquisition rate (cycle time) to 5τ . As an example, consider a 250 mL sample receptacle that is purged at a rate of 500 mL/min (assuming the receptacles is empty; if it contains a food sample, the headspace volume will be reduced by the equivalent volume of the food sample). One gas exchange takes 0.5 min ($=\tau$) and a complete exchange of gas within the receptacle takes 2.5 min (5τ). Accordingly, it is sufficient to choose a cycle time to match this, i.e., 2.5 min (although shorter cycle times can nevertheless be used).
16. If a sample is to be ground into coarse or fine particles, this can be achieved using a laboratory blender. However, high temperature of the blades during grinding can affect the food sample and its aroma compound composition, including thermal-induced changes, changes of state, or protein denaturation. In some cases, this can be overcome by rapidly freezing the food sample using liquid nitrogen prior to mechanical processing.
17. Chemical background can arise from adsorption of VOCs to the wetted surfaces of the receptacle and/or sampling lines from previous samples, as well as VOC traces in the purge gas. Data from these background measurements can be used to calculate the limit of detection (LOD) of the system.

18. Selection of holding time and temperatures are sample and analyte specific. These can be selected based on general principles used for selection of static headspace gas chromatography [37].
19. The sampling interface between the autosampler syringe and the PTR-MS inlet can have different configurations. In some systems, the inlet is connected to a modified syringe that allows for direct analysis of the vial headspace once the syringe pierces the vial septum. In other systems, the gas-tight syringe extracts a specified volume of headspace gas from the vial and subsequently injects this into a carrier gas flow being sampled by PTR-MS. The former system avoids dilution of the sample but limits the sampling time due to continuous extraction of the limited volume of headspace gas in the 20 mL vial. The latter system has the advantage of extending the analysis time and permits repeated sampling, yet dilutes the headspace gas, thereby effectively increasing the LOD of the system.
20. Compounds may be filtered from the background using a t-test against each sample or average background plus three standard deviations for each m/z . Data complexity can be further reduced by analysis of variance (ANOVA). Due to the high dimensionality of these datasets multivariate data analysis is recommended to aid data interpretation.
21. The nosespace sampling interface should also be designed so that ideally it is comfortable for the panelist, especially when they are required to participate in lengthy sessions consisting of multiple measurements. Further, the sampling flow rate of the PTR-MS inlet should be set high to account for the rapid changes during breath-by-breath analysis.
22. Despite CO_2 having a lower proton affinity than water, when it is present at high abundance in the PTR-MS drift tube, as is the case when sampling exhaled breath, the drift tube extraction lens in PTR-TOF-MS (or nosecone in PTR-QMS), leads to its protonation and its subsequent detection at m/z 44.998 ($\text{CO}_2\cdot\text{H}^+$).

References

1. Buettner A, Beauchamp J (2010) Chemical input—sensory output: diverse modes of physiology-flavour interaction. *Food Qual Prefer* 21(8):915–924. <https://doi.org/10.1016/j.foodqual.2010.01.008>
2. Hansel A, Jordan A, Holzinger R, Prazeller P, Vogel W, Lindinger W (1995) Proton-transfer reaction mass-spectrometry—online trace gas-analysis at the ppb level. *Int J Mass Spectrom Ion Proc* 149(150):609–619. [https://doi.org/10.1016/0168-1176\(95\)04294-U](https://doi.org/10.1016/0168-1176(95)04294-U)
3. Biasioli F, Gasperi F, Yeretzian C, Märk TD (2011) PTR-MS monitoring of VOCs and BVOCs in food science and technology. *TrAC Trend Anal Chem* 30(7):968–977. <https://doi.org/10.1016/j.trac.2011.03.009>
4. Beauchamp J, Zardin E (2017) Odorant detection by on-line chemical ionization mass

- spectrometry. In: Buettner A (ed) Springer handbook of odor. Springer Nature, Cham, Switzerland, pp 355–408
5. Beauchamp JD (2021) Dynamic Flavor: Capturing Aroma Using Real-Time Mass Spectrometry. American Chemical Society: Vol. 1402
 6. Ellis AM, Mayhew CA (2014) PTR-MS: principles and applications, 1st edn. Wiley, Chichester, UK
 7. Sulzer P, Hartungen E, Hanel G, Feil S, Winkler K, Mutschlechner P, Haidacher S, Schottkowsky R, Gunsch D, Seehauser H, Striednig M, Jürschik S, Breiev K, Lanza M, Herbig J, Märk L, Märk TD, Jordan A (2014) A proton transfer reaction-quadrupole interface time-of-flight mass spectrometer (PTR-QiTOF): high speed due to extreme sensitivity. *Int J Mass Spectrom* 368:1–5. <https://doi.org/10.1016/j.ijms.2014.05.004>
 8. Graus M, Müller M, Hansel A (2010) High resolution PTR-TOF: quantification and formula confirmation of VOC in real time. *J Am Soc Mass Spectr* 21(6):1037–1044. <https://doi.org/10.1016/j.jasms.2010.02.006>
 9. Romano A, Fischer L, Herbig J, Campbell-Sills H, Coulon J, Lucas P, Cappellin L, Biasioli F (2014) Wine analysis by FastGC proton-transfer reaction-time-of-flight-mass spectrometry. *Int J Mass Spectrom* 369:81–86. <https://doi.org/10.1016/j.ijms.2014.06.006>
 10. Fischer L, Klinger A, Herbig J, Winkler K, Gutmann R, Hansel A (2013) The LCU: versatile trace gas calibration. In: Hansel A, Dunkl J (eds) 6th international conference on proton transfer reaction mass spectrometry and its applications, Obergurgl, Austria. Innsbruck University Press, pp 192–195
 11. Capozzi V, Yener S, Khomenko I, Farneti B, Cappellin L, Gasperi F, Scampicchio M, Biasioli F (2017) PTR-ToF-MS coupled with an automated sampling system and tailored data analysis for food studies: bioprocess monitoring, screening and nose-space analysis. *JoVE* 123:e54075. <https://doi.org/10.3791/54075>
 12. Li M, Cappellin L, Xu J, Biasioli F, Varotto C (2020) High-throughput screening for in planta characterization of VOC biosynthetic genes by PTR-ToF-MS. *J Plant Res* 133(1): 123–131. <https://doi.org/10.1007/s10265-019-01149-z>
 13. Beauchamp J, Biberacher S, Gao S (2019) Rapid quantitation of phenolic compounds in Islay Single Malt Scotch Whiskies by direct injection mass spectrometry. In: Guthrie B, Beauchamp JD, Buettner A, Toth S, Qian MC (eds) Sex, smoke, and spirits: the role of chemistry, ACS Symposium Series, vol 1321. American Chemical Society, Washington, DC, pp 117–124
 14. Beauchamp J, Herbig J (2015) Proton-transfer-reaction time-of-flight mass spectrometry (PTR-TOFMS) for aroma compound detection in real-time: technology, developments, and applications. In: Guthrie B, Beauchamp J, Buettner A, Lavine BK (eds) The chemical sensory informatics of food: measurement, analysis, integration, ACS Symposium Series, vol 1191. American Chemical Society, Washington, DC, pp 235–251
 15. Siefarth C, Tyapkova O, Beauchamp J, Schweiggert U, Buettner A, Bader S (2011) Influence of polyols and bulking agents on flavour release from low-viscosity solutions. *Food Chem* 129(4):1462–1468. <https://doi.org/10.1016/j.foodchem.2011.05.115>
 16. Beauchamp J, Zardin E, Silcock P, Bremer PJ (2014) Monitoring photooxidation-induced dynamic changes in the volatile composition of extended shelf life bovine milk by PTR-MS. *J Mass Spectrom* 49(9):952–958. <https://doi.org/10.1002/jms.3430>
 17. Soukoulis C, Aprea E, Biasioli F, Cappellin L, Schuhfried E, Märk TD, Gasperi F (2010) Proton transfer reaction time-of-flight mass spectrometry monitoring of the evolution of volatile compounds during lactic acid fermentation of milk. *Rapid Commun Mass Spectrom* 24(14):2127–2134. <https://doi.org/10.1002/rcm.4617>
 18. Heenan S, Soukoulis C, Silcock P, Fabris A, Aprea E, Cappellin L, Märk TD, Gasperi F, Biasioli F (2012) PTR-TOF-MS monitoring of in vitro and in vivo flavour release in cereal bars with varying sugar composition. *Food Chem* 131(2):477–484. <https://doi.org/10.1016/j.foodchem.2011.09.010>
 19. Menghi L, Khomenko I, Pedrotti M, Clicerì D, Aprea E, Endrizzi I, Cavazzana A, Biasioli F, Giacalone D, Gasperi F (2020) Arousal influences olfactory abilities in adults with different degree of food neophobia. *Sci Rep* 10(1): 20,538. <https://doi.org/10.1038/s41598-020-77428-w>
 20. Pedrotti M, Spaccasassi A, Biasioli F, Fogliano V (2019) Ethnicity, gender and physiological parameters: Their effect on in vivo flavour release and perception during chewing gum consumption. *Food Res Int* 116:57–70. <https://doi.org/10.1016/j.foodres.2018.12.019>
 21. Romano A, Cappellin L, Ting V, Aprea E, Navarini L, Gasperi F, Biasioli F (2014) Nose-space analysis by PTR-ToF-MS for the characterization of food and tasters: the case study of

- coffee. *Int J Mass Spectrom* 365–366:20–27. <https://doi.org/10.1016/j.ijms.2013.12.001>
22. Cappellin L, Soukoulis C, Aprea E, Granitto P, Dallabetta N, Costa F, Viola R, Märk TD, Gasperi F, Biasioli F (2012) PTR-ToF-MS and data mining methods: a new tool for fruit metabolomics. *Metabolomics* 8(5):761–770. <https://doi.org/10.1007/s11306-012-0405-9>
 23. Beauchamp J, Herbig J, Dunkl J, Singer W, Hansel A (2013) On the performance of proton-transfer-reaction mass spectrometry for breath-relevant gas matrices. *Meas Sci Technol* 24(12):125,003
 24. Cappellin L, Probst M, Limtrakul J, Biasioli F, Schuhfried E, Soukoulis C, Märk TD, Gasperi F (2010) Proton transfer reaction rate coefficients between H₃O⁺ and some sulphur compounds. *Int J Mass Spectrom* 295(1–2):43–48. <https://doi.org/10.1016/j.ijms.2010.06.023>
 25. Müller M, Mikoviny T, Jud W, D'Anna B, Wisthaler A (2013) A new software tool for the analysis of high resolution PTR-TOF mass spectra. *Chemometr Intell Lab Syst* 127: 158–165. <https://doi.org/10.1016/j.chemolab.2013.06.011>
 26. Cappellin L, Biasioli F, Fabris A, Schuhfried E, Soukoulis C, Märk TD, Gasperi F (2010) Improved mass accuracy in PTR-TOF-MS: another step towards better compound identification in PTR-MS. *Int J Mass Spectrom* 290(1):60–63. <https://doi.org/10.1016/j.ijms.2009.11.007>
 27. Cappellin L, Biasioli F, Schuhfried E, Soukoulis C, Märk TD, Gasperi F (2011) Extending the dynamic range of proton transfer reaction time-of-flight mass spectrometers by a novel dead time correction. *Rapid Commun Mass Spectrom* 25(1):179–183. <https://doi.org/10.1002/rcm.4819>
 28. Frank D, Appelqvist I, Piyasiri U, Wooster TJ, Delahunty C (2011) Proton transfer reaction mass spectrometry and time intensity perceptual measurement of flavor release from lipid emulsions using trained human subjects. *J Agric Food Chem* 59(9):4891–4903. <https://doi.org/10.1021/jf104376b>
 29. Délérís I, Saint-Eve A, Dakowski F, Sémon E, Le Quéré J-L, Guillemin H, Souchon I (2011) The dynamics of aroma release during consumption of candies of different structures, and relationship with temporal perception. *Food Chem* 127(4):1615–1624. <https://doi.org/10.1016/j.foodchem.2011.02.028>
 30. Charles M, Romano A, Yener S, Barnabà M, Navarini L, Märk TD, Biasoli F, Gasperi F (2015) Understanding flavour perception of espresso coffee by the combination of a dynamic sensory method and in-vivo nosespace analysis. *Food Res Int* 69:9–20. <https://doi.org/10.1016/j.foodres.2014.11.036>
 31. Jordan A, Haidacher S, Hanel G, Hartungen E, Herbig J, Märk L, Schottkowsky R, Seehauser H, Sulzer P, Märk TD (2009) An online ultra-high sensitivity proton-transfer-reaction mass-spectrometer combined with switchable reagent ion capability (PTR+SRI-MS). *Int J Mass Spectrom* 286(1):32–38. <https://doi.org/10.1016/j.ijms.2009.06.006>
 32. Pleil JD, Isaacs KK (2016) High-resolution mass spectrometry: basic principles for using exact mass and mass defect for discovery analysis of organic molecules in blood, breath, urine and environmental media. *J Breath Res* 10(1): 012001
 33. Kramshøj M, Albers CN, Holst T, Holzinger R, Elberling B, Rinnan R (2018) Biogenic volatile release from permafrost thaw is determined by the soil microbial sink. *Nat Commun* 9(1):3412. <https://doi.org/10.1038/s41467-018-05824-y>
 34. Deuscher Z, Andriot I, Sémon E, Repoux M, Preys S, Roger J-M, Boulanger R, Labouré H, Le Quéré J-L (2019) Volatile compounds profiling by using proton transfer reaction-time of flight-mass spectrometry (PTR-ToF-MS). The case study of dark chocolates organoleptic differences. *J Mass Spectrom* 54(1): 92–119. <https://doi.org/10.1002/jms.4317>
 35. Zardin E, Silcock P, Siefarth C, Bremer PJ, Beauchamp J (2016) Dynamic changes in the volatiles and sensory properties of chilled milk during exposure to light. *Int Dairy J* 62:35–38. <https://doi.org/10.1016/j.idairyj.2016.07.005>
 36. Zareian M, Böhner N, Loos HM, Silcock P, Bremer P, Beauchamp J (2018) Evaluation of volatile organic compound release in modified atmosphere-packaged minced raw pork in relation to shelf-life. *Food Packaging Shelf Life* 18: 51–61. <https://doi.org/10.1016/j.foodpsl.2018.08.001>
 37. Kolb B, Ettre LS (2006) *Static headspace–gas chromatography*, 2nd edn. Wiley, Hoboken, NJ

INDEX

A

Acetylcholinesterase 213, 214
Acheta domesticus 134, 136–138, 142
Acrylamides 281–290
 α -glucosidase 213–218
Alkaloids 246
Amazon 219, 220
Analytical methods 44, 72, 123, 124,
146, 154, 225, 260, 285, 286, 288–290, 293
Animal's protein v
Antifoaming agent 89
Apples 18–20
Aroma extract dilution analysis (AEDA) 158, 160,
163–165, 168
Aroma quantification 159

B

Beer v
Berries 219–224
 β -casomorphins (β -CMs) 109–118
Beverages 72, 85, 122,
281–291, 294, 307, 309, 313
Bioactive compounds 43, 44, 61, 194, 219
Bubbling extraction 293–305

C

Calibration curves 46, 48, 50–53,
55, 58, 66, 69, 94, 95, 117, 118, 125, 152, 261,
267, 272, 277, 288, 289, 300
Carbon dioxide 67, 297, 298, 312
Cheese 24, 26, 27,
185, 193, 195, 196, 207
Chemical characterizations 245–249,
251, 253, 255
Coffees 5, 8, 9, 71–86,
176–178, 180, 184–187, 282, 284, 285, 290,
291, 297, 301, 304
Collision cross section (CCS) 260–262, 264–268,
271–273, 275–277
Complex data 308
Comprehensive characterization 33, 245
Crickets 134, 136

D

Database searches 122, 131,
134, 138, 197
Data visualization 4
De novo sequencing 122, 125, 131
Deprotonated molecule ($[M-H]^-$) 150
Design of experiments (DoE) 175, 189
Drift time 261, 269,
272, 273, 275, 277
Dry-cured ham 225–242

E

Effect-directed analysis (EDA) 213–218
Electron ionization (EI) 165, 177, 180,
294, 296, 298, 299, 301, 302, 308
Electrospray ionization (ESI) 4, 7, 13, 33,
45, 49, 52, 55, 72, 75, 82–84, 90, 96, 98, 115,
116, 147, 217, 222, 247, 264–267, 272,
284–286, 294
Emulsifier 89
Espresso coffees 72

F

Fermented foods 194–196, 207
Fingerprints 5, 10, 18, 62
Fish 18, 24, 146, 148–150, 153, 154
Flame ionization detector (FID) 158–161,
164–166, 169
Flavonoids 31, 44–46,
54, 56, 57, 219
Flavor dilution (FD) 159, 163, 165, 168
Flavors 72, 122, 193, 293, 307–309, 315
Food 3–14, 17–21, 23, 24,
43, 44, 50, 62, 89–98, 122, 133–140, 145, 146,
157–170, 173–190, 193–207, 214, 224–242,
245–255, 259–277, 281–290, 293–305,
307–311, 313, 317
Food authenticity 3–14
Food fraud 24
Foodomics 225, 226
Food safety 90, 133,
214, 260, 262, 293

Hector Koolen (ed.), *Mass Spectrometry for Food Analysis*.

Methods and Protocols in Food Science, <https://doi.org/10.1007/978-1-0716-2107-3>,

© The Editor(s) (if applicable) and The Author(s), under exclusive license to Springer Science+Business Media, LLC, part of Springer Nature 2022

G

- Gas chromatography-olfactometry
(GC-O) 158–161, 164–166, 169
Glazing agent 89
Global Natural Product Social Molecular Networking
(GNPS) 39, 246–253, 255
Grains 5, 7, 13, 283, 285, 287–290

H

- Headspace (HS) 166, 173–175,
178, 180, 183, 184, 189, 309–312, 314, 317, 318
High performance thin-layer chromatography
(HPTLC) 213–218
High-resolution mass spectrometry
(HRMS) 33, 72, 110, 225, 226
Hydrophilic interaction chromatography 145–154

I

- Imaging mass spectrometry (IMS) 225–242,
259–263, 267, 275, 277
Imazalil 19, 20
Inductively coupled plasma mass spectrometer
(ICP-MS) 296, 301–303
Inhibitors 122, 130, 213–217
Ion mobility-mass spectrometry
(IM-MS) 259–262, 266, 275
Ion trap 5–7, 207

L

- Lactic acid bacteria 193–207
Lactobacillus 195, 196, 198
Leaf spray ionization mass spectrometry
(LS-MS) 223
Limit of detection (LOD) 169, 303, 317, 318
Limit of quantification (LOQ) 290, 303
Lipidomics 12, 78, 145, 146, 154
Liquid chromatography coupled to mass spectrometry
(LC-MS) 12, 17, 24,
31–41, 44, 45, 73, 76, 85, 92, 109, 122, 131, 134,
135, 147, 195–198, 201, 204, 206, 220, 224,
248, 249, 260, 262, 263, 293, 294
Liquid-introduction electrospray ionization
(DLI-ESI) 4–10
Lipids 4, 71–85, 145–150,
152–154, 226, 229, 232, 233, 235, 241, 293
Low-temperature plasma (LTP) 4, 6, 8

M

- Mass spectrometry (MS) 3–6, 8–10,
13, 17, 23–29, 32, 35, 43–58, 62, 89–98,
121–131, 133, 135, 145–154, 176, 194, 201,
207, 213–218, 225–242, 245–255, 259–277,
281–290, 293–305

- Mass spectrometry-based proteomics 133
Mass spectrometry fingerprinting method
(MSF) 3–5, 10, 203
Mass to charge ratio (m/z) 133, 228, 265
Matrix-assisted laser desorption mass spectrometry
(MALDI) 6, 9, 18–20, 24, 25, 28, 90, 195,
225–242
Matrix effects 57, 110
Meat 18, 23–29, 205
Methyl *tert*-butyl ether 73, 237, 239
Milk 18, 23–29,
109–119, 195, 290, 291
Molecular networking 245–249, 251, 253, 255

N

- National Center for Biotechnology Information
Nonredundant Database
(NCBI) 131, 134,
135, 137–139, 141, 142
Novel food sources 134

O

- Odor detection port (ODP) 158–161,
164–166, 169
Oligopeptides 121–131
Olive oils 61–69
Open-source software 5, 33, 72, 247
Opioid peptides 109
Organic acids 219–221, 223, 224

P

- Paper spray ionization (PS) 73, 90,
147, 150, 151, 219–224
Peptides 4, 24, 109, 115, 121,
122, 125, 127, 129–131, 133, 140–142, 194,
196, 198–204, 207, 225–242
Phenolic compounds 31–34, 39, 44,
45, 50, 55–57, 61, 246
Phospholipids 71, 72, 83, 146,
147, 149, 150, 152–154
Phytosterols 61
Polyethylene glycol (PEG) 89–108
Polymers 89, 90, 92, 98, 235, 240
Polyphenols 31–41, 220, 221, 223, 224
Polyunsaturated fatty acids (PUFAs) 146
Principal component analysis (PCA) 5, 11, 13, 154
Probiotics 193, 194, 196, 197, 205, 246
Protonated molecules ($[M+H]^+$) 4, 308

Q

- Quadrupole 64, 131, 177,
180, 226, 302, 308
Quadrupole-orbitrap 121–132

Quality control3–14, 75, 80,
 85, 114, 163, 241, 263, 266, 267, 282, 283
 Quantification 17, 32, 44, 45, 50, 53, 57, 110, 117, 125,
 129–131, 145, 152, 159, 196, 197, 220, 226,
 254, 255, 272, 277, 290, 295, 299, 300
 QuEChERS (Quick, Easy, Cheap, Effective, Rugged, and
 Safe) method 282, 283

R

Retention times40, 44, 49,
 52, 56, 76, 79, 80, 85, 99, 106, 117, 118, 129,
 149, 150, 153, 154, 158, 164, 176, 179, 188,
 189, 218, 249, 260, 277, 282, 285, 298
 Ribosomal proteins 194, 195,
 198, 200, 202, 204, 206

S

Sample preparation4–9, 18, 19,
 23–29, 45, 50–51, 73, 160–164, 166, 194, 198,
 206, 220, 221, 225–242, 246, 247, 262, 264,
 265, 283, 287, 288, 294, 295, 311
 Saponification62, 64
 Selected reaction monitoring
 (SRM) 45, 48,
 49, 253
 Solanaceae 245–255
 Solid phase extraction (SPE)45, 46, 50,
 54, 57, 110, 114, 116, 294
 Solid phase microextraction (SPME) 173–180,
 183, 184, 188, 189
 Solvent-assisted flavor evaporation
 (SAFE) 158–160, 162,
 163, 167, 168, 282
 Species identification 23
 Steroidal glycosides 250–252
 Sterols61–69, 71, 77
 Supercritical fluid chromatography/tandem mass
 spectrometry (SFC/MS/MS) 282–285,
 287–290

T

Tandem mass spectrometry
 (MS/MS) 32, 39–41, 43–58,
 77, 79–81, 83, 125, 201, 228, 234, 235, 246,
 248, 250, 251, 253–255
 Tea 122, 123, 125, 127, 131, 282, 284
 Thin-layer chromatography (TLC) 63, 65, 68, 69,
 214–216
 Time of flight (TOF) 265, 266, 316
 Traveling Wave Ion Mobility-Mass Spectrometry (TWIM-
 MS) 261, 262,
 264–269, 271, 273, 275–277
 Triacylglycerol (TAG) 71, 77, 78, 81, 82, 146
 Triple quadrupole 44, 45,
 220, 223, 284, 296, 298
 Two-dimensional gas chromatography-mass
 spectrometry/olfactometry
 (2D-GC-MS/O) 158

U

Ultrahigh-performance liquid chromatography
 (UHPLC) 33, 39,
 40, 73, 115–117, 123, 130, 200, 201, 282, 283
 Ultra-high resolution mass spectrometry
 (UHRMS) 121–132
 Ultraperformance liquid chromatography coupled to
 mass spectrometry
 (UPLC-MS)62–64, 66, 67
 UniProt Knowledgebase
 (UniProt-KB) 134, 136, 140, 141

V

Volatile organic compounds
 (VOCs) 176, 184–186,
 188, 298, 308, 309, 311–313, 317

W

White tea 122